ESTUDIO METABOLÓMICO POR RESONANCIA MAGNÉTICA NUCLEAR DE INDIVIDUOS EXPUESTOS AL VIH-1 ORIENTADO A LA BÚSQUEDA DE BIOMARCADORES Y RUTAS METABÓLICAS ASOCIADAS A LA RESISTENCIA NATURAL Y A LA PROGRESIÓN DE LA INFECCIÓN

León Gabriel Gómez Archila

Tesis para optar al título de:

Doctor en Ciencias Farmacéuticas y Alimentarias con énfasis en Biorgánica

Avalado por el comité tutorial compuesto por:

Dr. Elkin Galeano Jaramillo. Grupo de Investigación en Sustancias Bioactivas, Universidad de Antioquia, Medellín (Colombia)

Dra. Martina Palomino S. Centro de Investigación Príncipe Felipe, Valencia (España)

Dr. Wildeman Zapata Builes. Grupo Infettare, Universidad Cooperativa de Colombia, Medellín (Colombia)

Universidad de Antioquia

Facultad de Ciencias Farmacéuticas y Alimentarias

Doctorado en Ciencias Farmacéuticas y Alimentarias con énfasis en Biorgánica

Medellín, Antioquia, Colombia

2024

DEDICATORIA

A mi esposa Laura María, quien ha sido mi pilar y mi motivación para ser cada día mejor persona durante 15 años. Amor, este logro es tan tuyo como mío, los sueños si se hacen realidad, te amo.

A mi madre Olga Lucía, quien me enseñó los valores y la ética de trabajo que me han permitido nunca claudicar en busca de este sueño. Mamá, espero que sientas el mismo orgullo que yo por este logro.

AGRADECIMIENTOS

Al Doctor Edison Osorio director del Grupo de Investigación en Sustancias Bioactivas, por permitirme pertenecer a su grupo de investigación y realizar esta tesis con su apoyo.

A mi co-director de tesis, el Doctor Elkin Galeano, por creer en mí aun cuando me había alejado del mundo de la investigación y confiarme este hermoso proyecto.

A mi co-director de tesis, el Doctor Wildeman Zapata y el grupo de investigación Inmunovirología, por suministrar las muestras de los pacientes indispensables para el cumplimiento de los objetivos planteados en el proyecto, además de brindarme su asesoría y conocimiento en los momentos de dificultad.

A mi co-directora de tesis, la Doctora Martina Palomino por ser un apoyo incondicional durante estos 6 años de proceso. Martina, sus palabras de aliento, su confianza en mí, su disposición y paciencia inagotable fueron indispensables para llegar a este punto. Puedo decir sin temor a equivocarme que si Dios no la hubiese puesto en mi camino no habría llegado hasta aquí. Siempre le estaré agradecido.

TABLA DE CONTENIDO

LISTA DE TABLAS

LISTA DE FIGURAS

SIGLAS, ACRÓNIMOS Y ABREVIATURAS

ANOVA	Análisis de varianza
CE	Electroforesis capilar
CMSP	Células mononucleares de sangre periférica
CV	Coeficiente de variación
FDR	Tasa de descubrimiento falso
GC	Cromatografía de gases
HESN	Expuestos al VIH-1 seronegativos
HPLC	Cromatografía Líquida de Alta Eficiencia
IFN-ɣ	Interferón gama
IgA	Inmunoglobulina A
LC	Cromatografía Líquida
LTNP	No progresores a largo plazo
MS	Espectrometría de masas
OPLS-DA	Análisis discriminante de Mínimos cuadrados parciales Ortogonal
PCA	Análisis de componentes principales
PLHIV-ART	Personas que viven con VIH-1 en terapia antiretroviral
PLS-DA	Análisis discriminante de Mínimos cuadrados parciales
RMN	Espectroscopia de resonancia magnética nuclear
TAR	Terapia antirretroviral
VIH-1	Virus de Inmunodeficiencia Humana 1
VIP	Proyección de importancia variable

RESUMEN

La infección por el Virus de Inmunodeficiencia Humana 1 (VIH-1) y el desarrollo del Síndrome de Inmunodeficiencia Adquirida (SIDA) continúa siendo uno de los principales problemas de salud pública mundial. De manera frecuente la exposición al VIH-1 provoca una infección; sin embargo, algunas personas muestran una resistencia natural a la infección; estos individuos se conocen como expuestos al VIH-1 pero seronegativos (HESN). Adicionalmente, algunos individuos infectados logran controlar la replicación del VIH-1 y la progresión a SIDA de manera natural y en ausencia de terapia antirretroviral (TAR); denominados controladores. Los mecanismos biológicos que explican estos fenómenos no se conocen de forma precisa. En este contexto, la metabolómica surge como un método para identificar metabolitos en respuesta a estímulos fisiopatológicos, que pueden ayudar a establecer mecanismos de resistencia natural a la infección y progresión del VIH-1. El VIH-1 infecta específicamente a linfocitos T CD4+, monocitos y células dendríticas, en conjunto denominadas células mononucleares de sangre periférica (CMSP), causando hiperactivación y agotamiento del sistema inmune, lo cual conduce al desarrollo del SIDA; por lo tanto, el estudio de las CMSP a través de la metabolómica podría ayudar a explicar este fenómeno. En esta investigación realizamos un estudio transversal con 88 muestras de plasma (30 HESN, 14 controladores, 14 progresores y 30 controles sanos) y 48 muestras de CMSP (20 personas que viven con el VIH-1 en TAR (PLHIV-ART), 8 HESN y 20 controles sanos). En cada matriz biológica, se identificaron potenciales biomarcadores de cada grupo de estudio. En plasma; la creatinina, tirosina y lipoproteínas están diferencialmente expresadas en progresores; el glutamato, piruvato y acetato son marcadores metabólicos de los controladores, y el lactato y fosfocolina son biomarcadores de la resistencia natural en HESN. En CMSP, la fenilalanina, carnitina y glicina son potenciales biomarcadores de la respuesta efectiva de los voluntarios a la TAR en forma de reconstitución inmunológica en términos de disminución de la carga viral y aumento del recuento de linfocitos T CD4+; alanina, AMP, inosina y leucina al estatus de HESN. Adicionalmente, la valina es un metabolito importante en el control de la infección dada su expresión diferencial en controladores y progresores. Identificamos una serie de rutas metabólicas alteradas en mayor proporción en PLHIV-ART y progresores que en HESN. Dentro de las vías alteradas, las que presentan un mayor impacto en el análisis de enriquecimiento de rutas de Metaboanalyst® son las de biosíntesis de fenilalanina, tirosina y triptófano, aminoácidos aromáticos implicados en la síntesis de proteínas. En conclusión, nuestro estudio muestra que los mecanismos de resistencia natural a la infección por el VIH-1 y a la progresión hacia el SIDA están estrechamente relacionados con el metabolismo de los individuos expuestos y/o infectados,

y que cambios en la expresión de metabolitos específicos pueden generar desenlaces positivos o negativos en una persona que se expone y/o infecta con el VIH-1. Esperamos que nuestros resultados tengan un impacto sobre el conocimiento y el descubrimiento de mecanismos de resistencia a la enfermedad y que con este trabajo se abran nuevos horizontes de investigación de otras enfermedades infecciosas a través de la plataforma de metabolómica por Resonancia Magnética Nuclear (RMN).

Palabras clave: Resonancia magnética nuclear -RMN, Metabolómica, virus de inmunodeficiencia humana VIH-1, Biomarcadores, Rutas de señalización.

ABSTRACT

Infection with Human Immunodeficiency Virus 1 (HIV-1) and the development of Acquired Immune Deficiency Syndrome (AIDS) is one of the leading global public health problems. Exposure to HIV-1 frequently causes infection; however, some people show a natural resistance to infection; these individuals are known as HIV-1 exposed but seronegative (HESN). Additionally, some infected individuals control HIV-1 replication and progression to AIDS naturally in the absence of antiretroviral therapy (ART), called controllers. The biological mechanisms that explain these phenomena are not known precisely. In this context, metabolomics emerges as a method to identify metabolites in response to pathophysiological stimuli, which can help establish mechanisms of natural resistance to HIV-1 infection and progression. HIV-1 infects CD4+ T lymphocytes, monocytes and dendritic cells, together called peripheral blood mononuclear cells (PBMC), causing hyperactivation and exhaustion of the immune system, which leads to the development of AIDS. Therefore, the study of PBMCs through metabolomics could help explain this phenomenon. In this research, we carried out a cross-sectional study with 88 plasma samples (30 HESN, 14 controllers, 14 progressors, and 30 healthy controls) and 48 PBMC samples (20 people living with HIV-1 on ART (PLHIV-ART), 8 HESN, and 20 healthy controls). In each biological matrix, potential biomarkers for each study group were identified. In plasma, creatinine, tyrosine, and lipoproteins are differentially expressed in progressors; glutamate, pyruvate, and acetate are metabolic markers of controllers, and lactate and phosphocholine are biomarkers of natural resistance in HESN. In PBMC, phenylalanine, carnitine and glycine are potential biomarkers of the effective response of volunteers to ART in the form of immunological

reconstitution in terms of decreased viral load and increased CD4+ T lymphocyte count; alanine, AMP, inosine and leucine to HESN status.

Additionally, valine is an important metabolite in the control of infection given its differential expression in controllers and progressors. We identified a series of metabolic pathways altered to a significant extent in PLHIV-ART and progressors than in HESN. Among the altered pathways, those that had the highest impact in the Metaboanalyst® pathway enrichment analysis are those of the biosynthesis of phenylalanine, tyrosine and tryptophan, aromatic amino acids involved in protein synthesis. In conclusion, our study shows that the mechanisms of natural resistance to HIV-1 infection and progression toward AIDS are closely related to the metabolism of exposed and/or infected individuals and that changes in the expression of specific metabolites can generate positive or negative outcomes in a person who is exposed and/or infected with HIV-1. We hope that our results will have an impact on the knowledge and discovery of disease resistance mechanisms and that this work will open new research horizons for other infectious diseases through the Nuclear Magnetic Resonance (NMR) metabolomics platform.

Keywords: NMR, Metabolomics, HIV-1, Biomarkers, Pathways.

CAPÍTULO 1:
Introducción

1. Introducción

En 1983 se descubrió que el VIH-1 era el agente causal del síndrome de la inmunodeficiencia adquirida -SIDA en humanos (Barré-Sinoussi et al., 1983; Gallo et al., 1983). En la actualidad, 39 millones de personas viven con VIH-1 en el mundo y 630.000 personas fallecieron a causa de enfermedades relacionadas con el SIDA. En Colombia, 190.000 personas viven con el VIH-1 y 1.500 personas fallecieron en 2022 según cifras de ONUSIDA (ONUSIDA, 2023). Desde que se llevan registros de la pandemia del SIDA, 85,6 millones de personas contrajeron la infección y 40,4 millones de personas fallecieron (ONUSIDA 2023). Entre todas las personas que vivían con el VIH-1, el 86% [73- >98%] conocía su estado serológico, el 76% [65-89%] recibía tratamiento y el 71% [60-83%] tenía supresión viral en 2022 (De Lay, 2021). Por lo tanto, se puede afirmar que el VIH-1 es un problema de salud pública mundial que genera una alta mortalidad entre los infectados, y a su vez un alto costo para el sistema de salud.

Durante la infección por el VIH-1, diferentes factores genéticos, inmunológicos y virológicos interactúan entre sí para determinar el tiempo de progresión a SIDA de las personas infectadas en ausencia de tratamiento (Ver Figura 1.1.) (Zhang et al., 2013; McLaren and Carrington 2015). Por esta razón, algunas personas progresan de manera rápida en menos de 5 años (10-15%), la mayoría progresan de manera típica, entre 7 y 10 años (80%) y un 5% progresan de manera lenta (>10 años), conocidos como no progresores a largo plazo (del inglés, Long-Term Non Progressors) (Passaes et al., 2014; Teixeira et al., 2014). Además, existen individuos que pueden controlar de forma natural la replicación del VIH-1, mantener niveles bajos de carga viral y un adecuado recuento de linfocitos T CD4+, en ausencia de TAR (Walker, 2007; Cao et al., 1995), conocidos como controladores (élite o virémicos). La existencia de LTNP y de controladores sugiere la presencia de mecanismos de resistencia a la progresión.

Estos mecanismos de resistencia a la progresión están relacionados con la capacidad de ciertas personas infectadas de generar una respuesta inmune particularmente vigorosa y eficaz que es capaz de controlar la infección (Rugeles et al., 2011). Por ejemplo, la expresión de ciertos alelos del HLA (antígeno leucocitario humano) se han asociado con resistencia/susceptibilidad a la infección por el VIH-1. La heterocigosidad de los alelos HLA clase I se asocia con un retraso en la progresión de la infección (Hendel et al., 1999; O'Brien et al., 2001) y la presencia de los alelos HLA B27 y B57 con un retraso en el desarrollo del SIDA (Kaslow et al., 1996; Migueles et al., 2000; Gillespie et al., 2002). Así mismo, se ha logrado identificar que 1 de cada 300 individuos infectados es capaz de mantener la viremia por debajo de los umbrales asociados con la

transmisión y la progresión de la enfermedad sin necesidad de TAR, gracias a una respuesta efectiva de linfocitos T CD8+ específicos del VIH-1, los cuales se denominaron controladores espontáneos de viremia infectados con el VIH-1 (Collins et al., 2020).

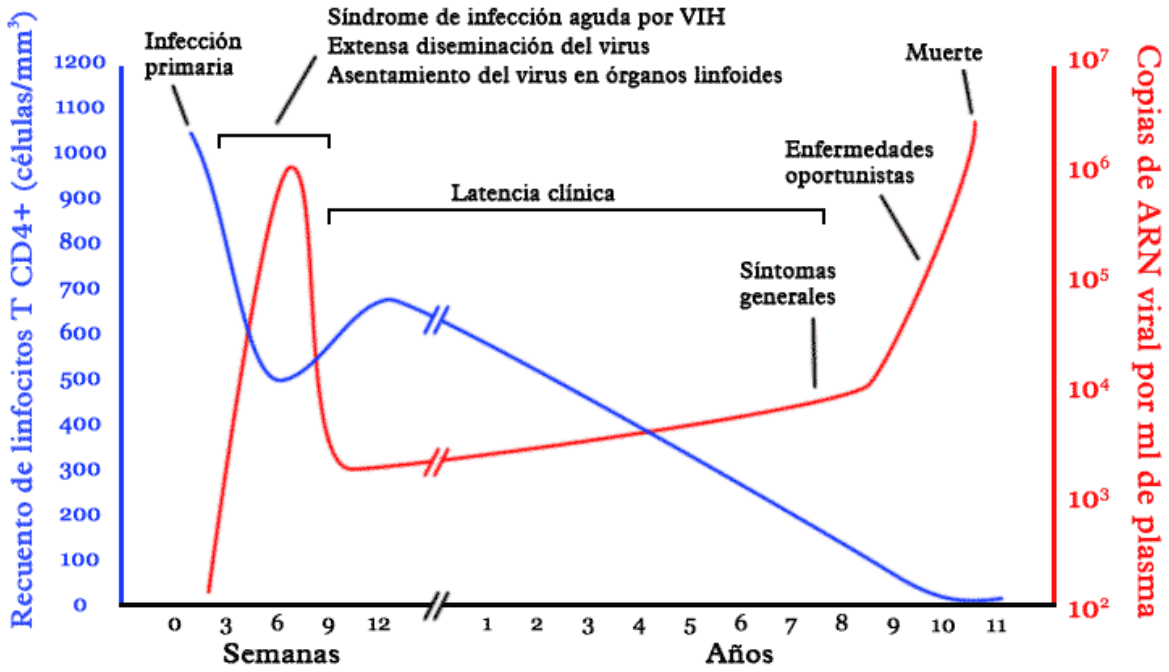

Figura 1.1. Curso natural de la infección por el VIH. Los detalles varían ampliamente en cada individuo. En azul, evolución del recuento de linfocitos T CD4+ y en rojo, la carga viral. La historia natural de la infección se divide en tres fases. **1ª Síndrome retroviral o infección aguda:** después de 2-4 semanas de infección las personas infectadas experimentan algunos síntomas parecidos a los de la gripe, como fiebre, dolor de cabeza y sarpullido. En esta fase ocurre una amplificación de la población viral en el microambiente linfático; esta replicación ocurre con activa pero insuficiente oposición del sistema inmunológico y muerte de los linfocitos T CD4+, células diana del virus. Luego, aparece una respuesta inmune específica, que provoca un descenso de la población viral plasmática a niveles variables y una recuperación parcial del recuento de linfocitos T CD4+. **2ª Fase crónica (latencia clínica):** el individuo infectado no presenta signos ni síntomas asociados a la infección, el virus se sigue propagando, pero en bajos niveles, con permanente infección de nuevas células, cuya vida media se ve acortada, generando así la liberación de nuevas partículas virales que infectan células susceptibles sanas. En respuesta a la continua destrucción de linfocitos CD4+ se producen nuevas células, por lo que, durante esta etapa, el recuento permanece relativamente estable mientras se pueda compensar el déficit. Luego, la hiperactivación y el agotamiento inmunológico lleva a la caída del recuento de linfocitos T CD4+ y el aumento en la susceptibilidad a distintos patógenos oportunistas, lo cual marca el ingreso a la fase de SIDA. **3ª SIDA (Enfermedades oportunistas):** La caída del recuento de linfocitos CD4+ es el marcador del debilitamiento inmunológico, lo cual trae como consecuencia la aparición de un número creciente de infecciones oportunistas. Las personas infectadas con el VIH, con recuentos de linfocitos T CD4+ menores de 200 células/mm3, y presencia de algunas infecciones oportunistas son diagnosticadas con el SIDA; además, si no reciben TAR pueden morir en un promedio de 3 años. Fuente: Dra. García Mónica Epidemiologia molecular de enfermedades infecciosas, cuantificación de carga viral.

Mientras que, en No progresores a largo plazo (LTNP) se han evidenciado dos tipos factores asociados con su resistencia a la progresión. Por un lado, factores relacionados con el virus, debido a la presencia de una serie de defectos genéticos que causan una atenuación del virus,

específicamente, mutaciones con deleción de *nef*; gen regulador crucial del VIH-1 (Ahmad and Venkatesan, 1988; Baur et al., 1994). Por el otro lado, factores relacionados con el huésped, dado que estos individuos tienen respuestas inmunes que son cuantitativa y cualitativamente más potentes y efectivas para controlar la infección por VIH-1, en términos de vigorosas respuestas inmunitarias humorales y celulares específicas de virus, así como títulos elevados de anticuerpos neutralizantes contra un amplio espectro de aislados de VIH (Fernández-Cruz et al., 1990).

De manera interesante, algunos individuos se exponen al virus por diferentes vías, especialmente la sexual, pero no tienen evidencia clínica ni serológica de la infección, conocidos como HESN (del inglés HIV-exposed but seronegatives) (Meyers y Fowke, 2010; Young et al., 2011). Hasta la fecha, solo la mutación Δ32 en estado homocigoto en el gen CCR5, principal correceptor de entrada del virus, se ha asociado de manera consistente con la resistencia del hospedador al VIH-1 (Huang et al., 1996), mientras que otros mecanismos de resistencia genética e inmunológica a la infección por el VIH-1, sólo explican de manera parcial este fenómeno (Lederman et al., 2010; Taborda et al., 2011). Particularmente, los individuos heterocigotos para esta mutación no son totalmente resistentes a la infección, pero si han mostrado una progresión lenta hacia el desarrollo de SIDA (Stewart et al., 1997; Meyer et al., 1997).

Al mismo tiempo, existen otros mecanismos inmunológicos de resistencia a la infección por VIH-1, entre los que se destaca: la apoptosis de células diana del VIH-1 que podría jugar un papel importante para evitar el establecimiento de la infección por VIH-1 en HESN (Velilla et al., 2005), la producción de citocinas tipo Interferón gama (IFN-ɣ) por células de la inmunidad innata (Roff et al., 2014), la inmunidad humoral mediada por Inmunoglobulina A (IgA) anti VIH-1 (Mazzoli et al., 1997), la producción de factores solubles tipo α y β defensinas (Zapata et al., 2008; Pace et al., 2017) y la inmunidad celular mediada por linfocitos (Brenna et al., 2022). Por lo tanto, la resistencia a la infección o a la progresión, podría ser el resultado de un evento multifactorial, donde mecanismos inmunológicos y genéticos podrían conjugarse con aspectos metabólicos para potenciar el control de la infección por el VIH.

Con el fin de poder evaluar el impacto de la infección o exposición al VIH-1 en el cuerpo humano se analizan diferentes tipos de muestras, entre las cuales destacan las muestras de sangre y sus diferentes componentes (Constantine et al., 2005). La sangre transporta hacia los tejidos del cuerpo nutrientes, electrólitos, hormonas, vitaminas, anticuerpos, oxígeno y células del sistema inmune que luchan contra las infecciones, como el VIH-1. Además, la sangre transporta desde los tejidos del cuerpo desperdicios y dióxido de carbono (Mathew et al., 2023). Por lo tanto, la sangre es un reflejo de la homeostasis del cuerpo y responde a cualquier perturbación externa

(Modell et al., 2015). La sangre está compuesta por plasma, glóbulos rojos (eritrocitos), glóbulos blancos (leucocitos): linfocitos, monocitos, células dendríticas, eosinófilos, basófilos, neutrófilos y plaquetas (trombocitos) (Dean., 2005). Analizar el plasma o fracción acelular de la sangre, permite determinar el estado metabólico de una persona, dado que es reflejo en tiempo de real de su estado de salud. Por otra parte, analizar los linfocitos, monocitos y células dendríticas (en conjunto denominadas CMSP) es crucial para medir el impacto directo de la infección, dado que estas células (en especial los linfocitos T CD4+) son las células diana de la infección por el VIH-1 (Caputo et al., 2023), y las principales células inmunológicas que responden frente a la infección (Vidya et al., 2017).

Para realizar el análisis de este tipo de muestras biológicas y conocer su estado metabólico es indispensable conocer su Metaboloma. Metaboloma es una palabra que fue acuñada en 1998 por Oliver y et al. (1998) como el conjunto de compuestos de baja masa molecular sintetizados por un organismo (metabolitos). Más adelante, Nicholson et al. (1999) introdujeron el término metabonómica, como el análisis de los cambios en el metaboloma de un organismo debido a agentes externos, como; enfermedades y su tratamiento con medicamentos, factores ambientales, alimentación, estilos de vida, efectos genéticos, exposición tóxica, etc. (Martin et al., 2011). Se desconoce el número exacto de metabolitos (<1.500 Da) de los humanos, pero se ha estimado que es alrededor de 20.000 con amplios rangos de concentración (Giovane et al., 2008). En conjunto, estos números hacen que el análisis completo del metaboloma humano sea un desafío. En este contexto, la metabolómica, entendida como la identificación y cuantificación imparcial de pequeñas moléculas en fluidos biológicos (Nicholson et al., 1999), puede servir como un camino para la comprensión del estado bioquímico de un organismo y ayudar en el descubrimiento de biomarcadores.

La metabolómica se ha utilizado en animales (Liu y Locasale., 2017), plantas (Tenenboim y Brotman., 2016) y alimentos (Kim et al., 2016). Así mismo de manera multidisciplinaria; en investigación biomédica (Kim et al., 2016), nutrición (Astarita y Langridge 2013), medicina de precisión (Beger et al., 2016), ecología (Macel et al., 2010) y agricultura (Nadella et al., 2012). Dentro de la metabolómica, se encuentra la lipidómica, dedicada al estudio y caracterización de los lípidos celulares, las moléculas con que interactúan y sus funciones en el organismo (Audano et al., 2018). El metaboloma representa la huella de la regulación de genes, proteínas y la interacción con el medio ambiente. Su rama lipídica, el lipidoma, aporta información crítica para su análisis funcional. Por tanto, el metaboloma y el lipidoma se puede emplear para monitorizar

cambios temporales en respuesta a un estímulo o con la evolución de una enfermedad (Ochoa, 2006).

Debido a que los virus como el VIH-1, utilizan íntimamente y a menudo reconectan el metabolismo del huésped (Eisenreich et al., 2019), la metabolómica es una excelente opción para estudiar los cambios inducidos por la infección o la exposición (Nicholson et al., 1999). En la actualidad, los datos provenientes de estudios de metabolómica, muestran que el VIH-1 y la TAR influyen en el metabolismo de carbohidratos (Dickens et al., 2015) y lípidos (Swanson et al., 2009), por lo que se podría inferir que los portadores de la infección son susceptibles a complicaciones metabólicas específicas. Estudios metabolómicos por RMN han logrado proponer modelos estadísticos multivariados basados en perfiles metabólicos de muestras biológicas que son capaces de distinguir entre individuos; VIH-1 negativo, VIH-1 positivo sin y con TAR (Calza et al., 2003; Philippeos et al., 2009), así como predecir la aparición de dislipidemia en pacientes que reciben TAR (Rodríguez-Gallego, E et al., 2018); sin embargo, no se han estudiado biomarcadores específicos en sangre asociados a la resistencia natural a la infección en HESN, el tiempo de progresión a SIDA en individuos progresores, la respuesta al tratamiento antirretroviral y el control espontáneo de la replicación viral en individuos controladores.

El desarrollo de la metabolómica fue posible gracias al crecimiento significativo de plataformas analíticas como RMN y la espectrometría de masas (MS). La RMN y la MS tienen ventajas y desventajas. Las ventajas de la RMN son la detección no sesgada de metabolitos, robustez de la técnica, reproducibilidad y mínima preparación de muestra; mientras que las desventajas incluyen la baja sensibilidad y que el análisis de biofluidos se complica por la supresión del agua (Crook et al., 2020). En RMN, la sensibilidad ha sido la cuestión de interés general. Los avances tecnológicos y metodológicos en la mejora de la sensibilidad realizados hasta el momento han permitido revelar información estructural hasta ahora inaccesible, fortaleciendo la espectroscopia de RMN como medio para el análisis químico. Es por eso que la RMN de sensibilidad mejorada continúa y seguirá siendo un tema de investigación activo en la comunidad (Lvee et al., 2014).

En contraste, la MS es muy sensible, posee alta eficiencia de separación y elevada resolución espectral, mientras que las desventajas son la destrucción de muestras, una menor reproducibilidad, y una compleja preparación de muestras, además de un mayor tiempo de análisis por muestra (Scalbert et al., 2009). Ambas técnicas proporcionan información que contribuye a la elucidación e identificación de compuestos desconocidos. La principal razón por la que en el trabajo se utilizó la RMN reside en la facilidad de interpretación y análisis de los datos

espectrales, y su elevada reproducibilidad, que permite obtener resultados significativos también a partir de tamaños muestrales relativamente pequeños (Sitole et al., 2013).

La espectroscopia de resonancia magnética nuclear puede ser utilizada para determinar las estructuras de los compuestos orgánicos. Esta técnica espectroscópica puede utilizarse sólo para estudiar núcleos atómicos con un número impar de protones o neutrones (o de ambos). Esta situación se da en los átomos de ^{1}H, ^{13}C, ^{19}F y ^{31}P. Este tipo de núcleos son magnéticamente activos, es decir poseen espín, igual que los electrones, ya que los núcleos poseen carga positiva y poseen un movimiento de rotación sobre un eje que hace que se comporten como si fueran pequeños imanes. En ausencia de campo magnético, los espines nucleares se orientan al azar. Sin embargo, cuando una muestra se coloca en un campo magnético, los núcleos con espín positivo se orientan en la misma dirección del campo, en un estado de mínima energía denominado estado de espín α, mientras que los núcleos con espín negativo se orientan en dirección opuesta a la del campo magnético, en un estado de mayor energía denominado estado de espín β. Existen más núcleos en el estado de espín α que en el β pero aunque la diferencia de población no es enorme sí que es suficiente para establecer las bases de la espectroscopia de RMN. La diferencia de energía entre los dos estados de espín α y β, depende de la fuerza del campo magnético aplicado H0 (Hodgkinson y Emsley, 2000). Cuanto mayor sea el campo magnético, mayor diferencia energética habrá entre los dos estados de espín. Cuando una muestra que contiene un compuesto orgánico es irradiada brevemente por un pulso intenso de radiación, los núcleos en el estado de espín α son promovidos al estado de espín β. Esta radiación se encuentra en la región de las radiofrecuencias (rf) del espectro electromagnético por eso se le denomina radiación rf (Pykett et al., 1982). Cuando los núcleos vuelven a su estado inicial emiten señales cuya frecuencia depende de la diferencia de energía (ΔE) entre los estados de espín α y β. El espectrómetro de RMN detecta estas señales y las registra como una gráfica de frecuencias frente a intensidad, que es el llamado espectro de RMN. El término resonancia magnética nuclear procede del hecho de que los núcleos están en resonancia con la radiofrecuencia o la radiación rf. Es decir, los núcleos pasan de un estado de espín a otro como respuesta a la radiación rf a la que son sometidos. Para obtener un espectro de RMN, se coloca una pequeña cantidad del compuesto orgánico disuelto en medio mililitro de disolvente en un tubo de vidrio largo que se sitúa dentro del campo magnético del aparato. El tubo con la muestra se hace girar alrededor de su eje vertical. El campo magnético se mantiene constante mientras un breve pulso de radiación rf excita a todos los núcleos simultáneamente. Como el corto pulso de radiofrecuencia cubre un amplio rango de frecuencias los protones individualmente absorben la radiación de frecuencia necesaria para entrar en resonancia (cambiar de estado de espín). A medida que dichos núcleos

vuelven a su posición inicial emiten una radiación de frecuencia igual a la diferencia de energía entre estados de espín. La intensidad de esta frecuencia disminuye con el tiempo a medida que todos los núcleos vuelven a su estado inicial. Un ordenador recoge la intensidad respecto al tiempo y convierte dichos datos en intensidad respecto a frecuencia, esto es lo que se conoce con el nombre de transformada de Fourier (FT-RMN) (Johnson y Schmidt-Rohr, 2014).

Es importante resaltar que el protio o protón (^{1}H) es el isótopo de hidrógeno más adecuado para la mayoría de los estudios de metabolómica, debido a que los espectros de RMN de protones unidimensionales (1D) (^{1}H-RMN) de alta resolución son: abundantes, cuantitativos, altamente reproducibles y no destructivos (Rolin et al., 2013). Además, los espectros ^{1}H-RMN contienen una gran cantidad de información (desplazamiento químico, intensidad, propiedades de relajación magnética) sobre la identidad de las moléculas de la muestra, por lo que pueden utilizarse para identificar y cuantificar metabolitos. Adicionalmente, la toma de espectros ^{1}H-NMR es rápida, conveniente y muy efectiva para discriminar entre grupos mediante la variación del patrón espectral (Mocco, 2022). Dependiendo de los grupos moleculares de interés, se pueden seleccionar adquisiciones de RMN adecuadas de una variedad de experimentos. Los experimentos más comunes para aplicaciones metabolómicas en espectrómetros son: 1D-NOESY y 1D-CPMG (Kruk et al., 2017).

El compuesto más abundante en la metabolómica de RMN es el agua, el componente principal de los biofluidos y tejidos. Por lo tanto, la supresión de agua es crucial para obtener espectros interpretables y existen numerosas técnicas de supresión de agua y presaturación de agua. La secuencia de pulsos 1D-NOESY (espectroscopia de efecto Overhauser nuclear, tren de pulsos con presaturación durante la relajación y el tiempo de mezcla) permite obtener una gran supresión de agua con alta reproducibilidad. Vale la pena mencionar que la técnica NOESY es la más popular y permite la optimización del proceso. Actualmente, debido a la variabilidad en la calidad de la supresión de agua, los picos de agua están presentes en los espectros y, por lo tanto, la región de resonancia del agua no se incluye en el análisis metabolómico (aproximadamente 4,50–5,00 ppm) (Araníbar et al., 2006). El 1D NOESY es útil para biofluidos como la orina y mezclas de metabolitos extraídos que carecen de macromoléculas. La principal desventaja de este experimento es como se afectan los espectros por las señales de las macromoléculas y las lipoproteinas, lo que causa que no se puedan identificar ni cuantificar estos compuestos.

Los espectros 1D también se adquieren con la secuencia de pulsos Carr–Purcell–Meiboom–Gill (CPMG) para disminuir las señales amplias de las proteínas y lipoproteínas debido a sus tiempos de relajación transversal relativamente largos (Ye et al., 2011). De este modo, las señales de los

compuestos con bajo peso molecular no se ven eclipsadas por las señales de las macromoléculas (Zhang et al., 2013). El experimento CPMG se utiliza a menudo para muestras como suero/plasma sanguíneo que tienen altas concentraciones de macromoléculas como proteínas y lípidos. La principal desventaja de este experimiento en su naturaleza no cuantatitativa.

En conjunto con técnicas de alineación espectral, seguidas de análisis estadísticos multivariables se identifican regiones espectrales o patrones espectrales de interés, para finalmente identificar y posiblemente cuantificar los compuestos de interés de las regiones espectrales discriminantes (Enwas et al., 2019).

Específicamente hablando, en el análisis de muestras biológicas, las señales en los espectros de RMN se pueden asignar de manera confiable a metabolitos específicos y las intensidades de las señales son directamente proporcionales al número de núcleos contribuyentes. Por tanto, la RMN proporciona una gran cantidad de información tanto sobre la identidad como sobre la cantidad de metabolitos en paralelo (Nagana Gowda et al., 2015). Por ello, la espectroscopia de RMN es un método analítico importante utilizado en metabolómica en aplicaciones que abarcan una amplia gama de disciplinas, la mayoría se ha centrado en comprender, prevenir, diagnosticar y gestionar enfermedades humanas (Nagana Gowda et al., 2021). Estas fueron las razones que nos llevaron a realizar nuestro estudio metabolómico usando RMN.

Un estudio metabolómico suele consistir en una serie de pasos definidos (Ver Figura 1.2). Comienza por el diseño experimental que debe concretar el tipo y número de muestras que se van a analizar. También debe definir el tipo de estudio (prospectivo, retrospectivo, longitudinal, etc) que se va analizar y la estrategia. Para ello existen dos tipos de estrategias; la metabolómica no dirigida (o huella digital metabólica) y la metabolómica dirigida (o perfil metabolómico). En el primer caso, el objetivo es identificar la mayor cantidad de metabolitos en una muestra dada en una sola ejecución; mientras que la segunda estrategia es un enfoque específico que se centra en el análisis de metabolitos preseleccionados y, en particular, se usa ampliamente para obtener datos cuantitativos de compuestos específicos (Astarita y Langridge, 2013). Nuestro estudio consistió en un estudio de tipo transversal descriptivo; debido a que las muestras de los voluntarios se tomaron en un solo momento y en un único tiempo, y fue un estudio tipo casos (Controladores, progresores, PLHIV-ART y HESN) y controles (Sanos). Así mismo, podríamos afirmar que utilizamos una estrategia de metabolómica no dirigida, dado que queríamos identificar la mayor cantidad de metabolitos para luego usarlas como variables de estudio en búsqueda de diferencias entre casos y controles.

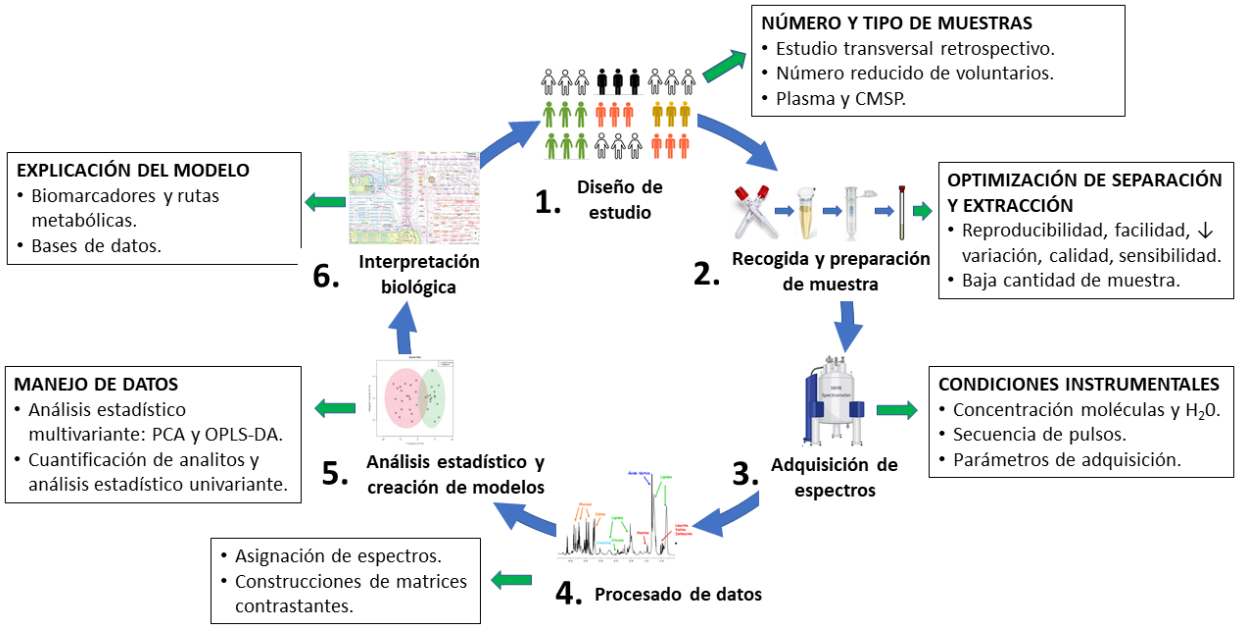

Figura 1.2 Pasos de un estudio metabolómico. Detalle del paso a paso necesario para la realización de un estudio metabolómico por RMN. Un estudio metabolómico por RMN comprende en general 6 pasos o etapas. **1. El diseño del estudio:** en el que se define el tipo de estudio a realizar, así como el tipo de muestras y voluntarios a incluir en el mismo. **2. Recogida y preparación de muestras:** etapa en la que se determina el(los) protocolo(s) de tratamiento a utilizar para extraer los metabolitos de intereses de la(s) matriz(ces) biológica(s) seleccionada(s) previamente, todo en función de si se trata de un estudio de huella metabolómica o perfil metabolómico. **3. Adquisición de espectros:** en la que se definen los parámetros analíticos y/o instrumentales que se configuraran en el equipo de RMN para obtener los espectros de mejor calidad y relación señal/ruido. **4. Procesado de datos:** los espectros son separados en secciones o señal a señal con el fin de identificar la mayor cantidad de metabolitos que sea posible. Luego, se crean matrices de datos que contienen las integrales (área bajo la curva) de cada señal de interés (asignación de un metabolito) de cada espectro (muestra de voluntarios) del estudio. **5. Análisis estadístico y creación de modelos:** Se realizan análisis multivariados y univariados de las matrices con el fin de establecer las diferencias y similitudes entre los grupos de estudio, así como determinar cuáles son los metabolitos que determinan estas diferencias. **6. Explicación del modelo:** finalmente se realiza una interpretación biológica coherente de los resultados, estableciendo una relación de los metabolitos alterados con las rutas biológicas y el objetivo del estudio.

Luego, se realiza la toma u obtención, el transporte, el almacenamiento y la preparación de las muestras, donde la optimización de los procedimientos de separación y extracción, en el caso de

las células sanguíneas, garantiza la reproducibilidad y la calidad del análisis. El método de extracción debe elegirse dependiendo del tipo de enfoque metabolómico que se aplicará posteriormente, es decir, huella digital metabólica (preparación de muestra mínima o nula para evitar la pérdida de metabolitos de las muestras biológicas) o perfil metabólico (método de extracción y purificación orientado de los metabolitos seleccionados) (Astarita y Langridge, 2013). Cabe resaltar, que nuestro estudio abordó de manera independiente las matrices biológicas analizadas (plasma y CMSP). En el caso del plasma, aplicamos dos protocolos de procesamiento independientes para analizar la misma muestra (dos fracciones separadas de plasma del mismo voluntario). Un primer método de tratamiento se basó en el análisis directo del plasma, estrategia que permite conocer el perfil metabolómico completo de las muestras con lípidos, proteínas y metabolitos, y un segundo método, se fundamentó en el desproteinizado del plasma, esto permite visualizar los metabolitos libres de las interferencias espectrales propias de lípidos de gran peso molecular o lipoproteínas y proteínas. Por otro lado, para el análisis de las CMSP, fue necesario el desarrollo y estandarización de un protocolo de procesamiento específico para este tipo de células. El método se fundamentó en utilizar ultrasonido de alta intensidad para realizar *quenching* estructural antes de realizar la extracción de los metabolitos constituyentes de las muestras de CMSP.

El siguiente paso es la adquisición de datos, en el cual el objetivo es procesar un conjunto relativamente importante de muestras para la construcción de matrices contrastantes. Diferentes tecnologías analíticas se han utilizado en estudios de metabolómica y lipidómica. Cómo ya se han mencionado anteriormente, las principales técnicas para el análisis metabolómico son la MS y la RMN (Barnes et al., 2016). En todos los casos, es importante asegurarse ante cada serie de medidas que el equipo cumpla una serie de requisitos de calidad en relación a sensibilidad/resolución de los datos, la temperatura, etc. Específicamente, para garantizar la calidad mencionada, nuestro grupo realizaba una serie de ajustes en el equipo de RMN antes de medir las muestras, entre ellos: estabilizar el campo magnético utilizando la frecuencia de absorción de la resonancia de deuterio del disolvente (la señal de bloqueo), sintonizar la sonda a la radiofrecuencia de la muestra, realizar pequeños ajustes en el campo magnético a través de shimming, calibrar el pulso de 90°, suprimir la señal del solvente y ajustar la ganancia del receptor de RMN para maximizar la relación señal/ruido.

A continuación, se debe proceder con el procesado de los datos adquiridos en el equipo de RMN. Los datos de RMN sin procesar se transforman en Fourier utilizando funciones de apodización adecuadas, se corrige la fase y la línea base. MestReNova es el Software mas recomendado.

MestReNova tiene la ventaja de proporcionar una serie de características específicas para el análisis posterior de los datos de metabolómica (por ejemplo, binning/bucketing, deconvolución máxima y cuantificación de la señal). Se debe considerar, al seleccionar un paquete de software para estudios de metabolómica de RMN, la posibilidad de reducir el número de herramientas involucradas en el análisis de los datos de metabolómica de RMN. Por ejemplo, la selección de paquetes de software que integran herramientas para el procesamiento de espectros y la identificación y cuantificación de compuestos, como Chenomx. Dependiendo de las propiedades fisicoquímicas de la muestra (es decir, pH, contenido de proteína, fuerza iónica, etc.), a veces se requiere realizar una alineación espectral para compensar pequeñas variaciones en las posiciones de los picos entre los diferentes espectros. Este proceso generalmente se aplica en todo el espectro y se realiza mediante la referencia de todos los espectros a un compuesto externo o un metabolito interno.

Una vez que los espectros de RMN se han transformado y alineado, los datos generalmente se organizan en una matriz en la que cada fila corresponde a una muestra particular y cada columna a la intensidad de la señal en un cambio químico particular. El análisis estadístico de los datos requiere la fragmentación de los espectros completos en segmentos más pequeños, un proceso denominado binning o bucketing, que se puede realizar utilizando diferentes enfoques. El ancho del bucket generalmente se fija a 0.04 ppm, lo que resulta en la reducción de un espectro de RMN típico a un promedio de 250 buckets, pero esta metodología puede ocasionar la separación de un pico específico en varios compartimientos. Por el contrario, la distribución variable, que generalmente requiere la intervención manual del usuario, está diseñada específicamente para tener en cuenta la región espectral precisa cubierta por picos individuales.

La normalización de la matriz de datos obtenida después del binning o bucketing de los espectros de RMN es un paso importante para mejorar el rendimiento del análisis estadístico posterior. Normalmente se llevan a cabo dos procesos de normalización diferentes, una normalización por filas y por columnas. Primero la normalización propiamente dicha, es una operación de fila que se aplica a los datos de cada muestra y comprende métodos para hacer que los datos de todas las muestras sean directamente comparables entre sí. Se ha intentado la normalización de un metabolito de "limpieza", por lo general utilizando un área de pico de creatinina como referencia. Un método común de normalización consiste en configurar cada observación (espectro) para que tenga una unidad de intensidad total al expresar cada punto de datos como una fracción de la integral espectral total (normalización a una suma constante (CS)). En segundo lugar, se encuentra el escalado, esta operación se realiza en las columnas de datos (es decir, en cada

intensidad espectral en todas las muestras). A cada columna de la tabla se le puede dar una media de cero al restar la media de la columna de cada valor de la columna (centrado de la media). Esto se hace normalmente para que todos los componentes encontrados por PCA tengan como origen el centroide de los datos, lo que resulta en un modelo parsimonioso. En segundo lugar, cada columna de la tabla se puede escalar para que tenga una varianza unitaria, dividiendo cada valor en la columna por la desviación estándar de la columna. Si los datos están centrados en la media, la ponderación refleja la covarianza de las variables, mientras que en la escala de varianza unitaria, la ponderación refleja su correlación. Otras formas de escalado son la escala de Pareto, donde cada variable se divide por la raíz cuadrada de la desviación estándar de los valores de columna, o escala logarítmica, cuando se desean valores relacionados con las puntuaciones de orden de magnitud.

El análisis de datos es el quinto paso; la variabilidad entre muestras es muy difícil de detectar mediante la observación directa de los espectros de RMN y hace necesaria la introducción de técnicas estadísticas que permitan evaluar esas diferencias en relación a las variables que se conocen de cada muestra, entre las que se encuentran desde los datos clínicos del individuo hasta los parámetros instrumentales de adquisición del experimento de RMN. Allí, el análisis estadístico multivariante es una parte esencial del manejo de datos en metabolómica (Barnes et al., 2016). Combina métodos matemáticos, estadísticos y de computación que permiten obtener información diversa del análisis de datos con un gran número de variables y muestras. Se puede dividir en métodos "no supervisados" y "supervisados". El análisis de componentes principales (PCA) es el método no supervisado más común utilizado para agrupar los datos dentro de cada matriz, mietras que el análisis discriminante por mínimos cuadrados (PLS-DA) es el método supervisado más común usado en metabolómica.

El PCA es un método no supervisado, es decir, no requiere conocimiento previo de las muestras, que resulta de gran utilidad para la identificación de patrones y/o tendencias dentro de los grupos de muestras. Consiste en la reducción de la dimensionalidad de los datos de manera que las múltiples variaciones quedan agrupadas en distintos componentes (primero, segundo, etc.), de acuerdo a su importancia en la interpretación de la variable observada (Halouska & Powers, 2006). Como resultado de este análisis, los datos extraídos de una matriz (X) con k-dimensiones, donde k corresponde al número de variables, son reducidos a un espacio definido por unos pocos componentes principales (PCs), capaces de explicar la mayor variabilidad entre las muestras (n). Una particularidad de este método es que los PCs son ortogonales entre ellos, de manera que la representación gráfica de los datos en el espacio bidimensional definido por los dos primeros PCs

(t1 y t2) proporciona una proyección de los datos multidimensionales conocido como gráfico de puntuaciones de las muestras en función de los componentes principales (score plot), en el que puedenapreciarse las agrupaciones y tendencias entre las muestras (n). De manera análoga, en el gráfico de las puntuaciones de las variables en función de los componentes principales (loading plot), p1 y p2 definen la relación entre las k variables que integran la matriz de datos original (X) con las mismas direcciones que las del score plot, lo que permite identificar fácilmente, de forma gráfica, cuáles son las variables (buckets) responsables de las tendencias observadas entre las distintas muestras. El PCA es el método de elección para obtener una visión global de la variabilidad entre muestras, y su correspondiente score plot es el gráfico generalmente utilizado para la identificación de posibles tendencias o agrupaciones que se den dentro de los grupos de muestras y que sean debidas a otras variables, distintas de la variable de estudio (p. ej., edad, sexo, estilo de vida, etc.). Este tipo de análisis es también de gran utilidad para la identificación de outliers, muestras que se desvían significativamente del perfil que muestran, de forma global, el resto de muestras incluidas dentro de los grupos del estudio. Otro gráfico muy utilizado para la identificación de outliers dentro de los grupos incuidos en el estudio es el gráfico T2 de Hotelling. En este tipo de gráficos se pueden identificar todas las muestras que se encuentran fuera del intervalo de confianza del 95% en el modelo no supervisado (Zhang et al., 2012).

El PLS-DA es una herramienta multivariada de reducción de dimensionalidad (Ståhle and Wold,, 1987; Barker and Rayens,, 2003) popular en el campo de la quimiometría y ampliamente recomendado para su uso en el análisis de datos -ómicos, especialmente en metabolómica (Worley and Powers., 2013), donde los conjuntos de datos (como los de nuestro estudio) se caracterizan por poseer un volumen extenso y una cantidad elevada de características (Eriksson et al., 2014); además, de que suelen tener muchas menos observaciones que variables (Ruiz-Perez et al., 2020). El PLS-DA es una versión supervisada del PCA, dado que reduce la dimensionalidad, pero con pleno conocimiento de las etiquetas de clase, además sirve en la selección de características (Christin et al., 2013) y en clasificación de muestras (Nguyen and Rocke., 2002). Por estas razones, el PLS-DA es el método supervisado más empleado para identificar potenciales candidatos a biomarcadores, dado que arroja las variables y/o características de la muestra; para nuestro caso metabolitos, que explican la diferencia entre los grupos de estudio. Definidos estos potenciales candidatos a biomarcadores, se realizan la cuantificación de los analitos y el análisis estadístico univariante para definir las diferencias estadísticamente significativas entre las variables candidatas para cada grupo de estudio.

En este tipo de modelos supervisados, basados en un conocimiento previo de las propiedades de las muestras, es muy importante evaluar la calidad de los análisis realizados y la fiabilidad de los modelos obtenidos (Westerhuis et al., 2008). Existen distintas aproximaciones para la validación de los modelos de clasificación, una de ellas es el test de permutación, que consiste en el cálculo de nuevos modelos de clasificación obtenidos tras una asignación aleatoria de las variables de clasificación entre las distintas muestras del modelo. A partir de los datos obtenidos, se calcula la bondad de ajuste (R^2) y la capacidad predictiva (Q^2) de los modelos generados de forma aleatoria, siendo el resultado esperado que la capacidad predictiva de los modelos aleatorios sea significativamente inferior a la obtenida para el modelo original. Para el análisis de los resultados del test de permutación, se representan los valores de R^2 y Q^2 obtenidos en los modelos de permutación y los valores de R^2 y Q^2 del modelo original, y se calcula la recta de regresión.

Otra aproximación consiste en la denominada validación cruzada, en la que se vuelve a construir el mismo modelo, pero esta vez dejando fuera un porcentaje determinado del conjunto de muestras original. Posteriormente se calcula el error de la predicción del modelo para el grupo de muestras inicialmente excluido del modelo. Este procedimiento se repite hasta que todas las muestras han sido excluidas del modelo al menos una vez. Los parámetros obtenidos, utilizados para evaluar la fiabilidad del modelo, son los estadísticos R^2 y Q^2. R^2 es una medida del grado de ajuste del modelo a los datos originales y Q^2, obtenido como resultado de la validación cruzada, da idea de la capacidad predictiva del modelo. De manera análoga, en aquellos casos en los que el número de muestras disponibles para el estudio lo permite, es posible realizar un test de validación más robusto a través de la predicción sobre un conjunto de muestras de validación, obtenidas y medidas de manera independiente. En general, un modelo de clasificación en metabolómica se considera significativo cuando se obtienen valores de Q^2 superiores a 0.5, siempre y cuando la diferencia entre R^2 y Q^2 sea de al menos 0.2.

Una vez identificadas las señales más relevantes en la discriminación entre grupos y los metabolitos responsables de las diferencias gracias al PLS-DA, se realiza de nuevo una integración de los espectros de RMN, pero esta vez dirigida específicamente a las señales identificadas. A partir de las intensidades obtenidas para cada señal se comprueba, mediante la prueba de Kolmogorov-Smirnov, si la mayoría de las variables siguen una distribución normal. En caso positivo, y para confirmar la importancia estadística univariante de las variables identificadas, se utiliza la prueba paramétrica Student para la comparación de dos medias independientes. En los casos en los que la mayoría de las variables no sigan una distribución

normal, se emplea una prueba no paramétrica para la comparación de dos medias independientes, la prueba de Wilcoxon. El objetivo de este análisis es poder descartar cualquier variable que, de manera individual, no contribuya de manera significativa a la discriminación entre grupos.

Finalmente, se realiza la interpretación biológica de las variaciones encontradas entre los distintos perfiles metabólicos. Los metabolitos seleccionados se vinculan a su contexto biológico mediante dos tipos de análisis: de rutas metabólicas y de enriquecimiento. El análisis de enriquecimiento explora el perfil de metabolitos para determinar el vínculo entre los cambios en la expresión de los metabolitos y el contexto biológico permitiendo sugerir rutas metabólicas. El análisis de rutas metabólicas identifica las que tienen un impacto significativo en un proceso biológico específico (Chen et al., 2022). Existen diversas bases de datos con información sobre rutas metabólicas relevantes, en las que se detallan los metabolitos que intervienen en ellas, la HMDB, la ConsensusPathDB-human (Kamburov et al., 2009, 2011), y la KEGG pathway analysis database (Kanehisa, 2013). De forma complementaria, también es necesaria la búsqueda en la literatura de información relacionada que permita situar los metabolitos encontrados en el contexto adecuado. Por lo tanto, la combinación de metabolómica con análisis de datos multivariantes permite estudiar alteraciones en las vías metabólicas.

También, es posible dentro del proceso de interpretación biológica realizar inferencias a otras ciencias ómicas, específicamente a la genómica. En este estudio, por ejemplo, los biomarcadores específicos de cada grupo se asociaron con genes y proteínas relacionadas con el VIH-1 a través de MetaboAnalyst®, usando el Metabolite-Gene-Disease Interaction Network analysis, así se obtuvo una lista de genes conectados a los biomarcadores y al VIH-1, luego la revisión bibliográfica permitió inferir una potencial expresión diferencial de algunos genes entre grupos que podría explicar las características de cada grupo. Cabe resaltar, que se identificaron genes relacionados con más de un grupo y/o con más de un metabolito, sin embargo, estas relaciones son responsabilidad de diferentes metabolitos para cada grupo o diferentes niveles entre los grupos para el mismo metabolito.

1.1. Planteamiento del problema

La epidemia por el VIH-1 es un problema de salud pública que afecta a Colombia y al mundo. A pesar de las campañas de autocuidado y la educación a las poblaciones susceptibles, las personas que viven con VIH-1 continúa en aumento, llegando a 166.496 casos reportados en el periodo 2023 en Colombia; con el agravante de que solo el 43,5% de los casos incidentes se detectaron de forma temprana, con todas las implicaciones que tiene este fenómeno dentro de la progresión de la infección (Rutstein et al., 2017). Además, según cifras de Cuenta de Alto Costo (CAC), para el 2023 el 82,68% de las personas viviendo con el VIH-1 recibían TAR y de estos solo el 68,35% alcanzó el objetivo de indetectabilidad de la carga viral (< 50 copias/ml) luego de completar 48 o más semanas desde el inicio de su primera TAR; estas cifras se alejan de las metas fijadas para el 2030 por parte de ONUSIDA (De Lay et al., 2021).

La forma en la que el organismo y el sistema inmune del individuo reacciona frente a la exposición y la infección del VIH-1 determinará la transmisión, el pronóstico y la expectativa de vida de este, la cual está directamente relacionada con la progresión a SIDA. Cabe destacar que, existen 3 poblaciones de individuos que han sido expuestos a la infección que generan gran interés; los expuestos seronegativos (HESN), que no presentan evidencia clínica ni serológica de la infección a pesar de la continua exposición (Montoya et al., 2006); los LTNP que permanecen asintomáticos e inmunológicamente estables durante 10 años o más de infección sin TAR e incluso algunos no progresan a SIDA (Walker, 2007) y los controladores, con la capacidad de controlar la replicación viral, presentando cargas virales bajas o indetectables en ausencia de TAR (Walker, 2007).

Hasta ahora no ha sido posible demostrar qué mecanismos biológicos determinan que una persona sea resistente a la infección por el VIH-1 o a la progresión hacia SIDA. Por lo que la investigación científica ha buscado nuevas formas de explicar estos fenómenos. Dentro de las opciones a considerar, surge la metabolómica, que se define como la medición cuantitativa de la respuesta metabólica dinámica multiparamétrica de los sistemas vivos a estímulos fisiopatológicos o modificaciones genéticas (Nicholson et al., 1999). La resonancia magnética nuclear (RMN) y la espectroscopía de masas (MS), son tecnologías instrumentales utilizadas en metabolómica, para la identificación y cuantificación de múltiples metabolitos en paralelo; por lo tanto, pueden ser usadas para lograr una aproximación de los cambios metabólicos inducidos por el VIH-1 durante la exposición o la infección.

La metabolómica es una herramienta que puede usarse junto con la genómica, la transcriptómica y la proteómica para comprender las interacciones huésped-patógeno a niveles de moléculas pequeñas (Mayer et al., 2019; Kimhofer et al., 2020; Overmyer et al., 2021). La aplicación más común de la metabolómica es con fines de pronóstico (Weiner et al., 2018) y diagnóstico (Isa et al., 2018), específicamente la detección de biomarcadores específicos de enfermedades mediante metabolómica basada en RMN o espectrometría de masas. Además, la metabolómica es de gran importancia para el descubrimiento de enzimas metabólicas y/o reguladores metabólicos farmacológicos mediante el uso de análisis de flujo más modernos, por ejemplo, mediante la elucidación de mecanismos metabólicos (Tounta et al., 2021).

Los estudios del efecto del VIH-1 sobre el metabolismo celular durante la replicación *in vitro* y la infección en modelos animales o humanos, han proporcionado nuevos conocimientos, así como nuevos objetivos para la terapia y la identificación de biomarcadores (Valle-Casuso et al., 2019). Los estudios previos comprenden grupos generales de personas infectadas y controles de sanos, sin indagar de manera exhaustiva en los grupos de personas especiales como los controladores, progresores y HESN; grupos de especial interés en la comunidad científica por su respuesta diferencial a la infección o exposición. Del mismo modo, la identificación de las rutas metabólicas utilizadas por el VIH-1 tiene el potencial de revelar información esencial de la enfermedad y su seguimiento. En estudios previos se han descrito desequilibrios en el metabolismo de los aminoácidos, lípidos, ácidos orgánicos y la glucosa en personas infectadas por el VIH-1, durante la evolución de la infección y relacionados con la introducción de la TAR (Hewer et al., 2006; Philippeos et al., 2009; Munshi et al., 2013; Rodríguez-Gallego et al., 2018); sin embargo, hasta ahora no hay investigaciones ni evidencia sobre las particularidades metabólicas de las personas que han sido expuestos al virus, pero continúan sin infectarse (HESN); además, tampoco se ha realizado una comparación metabólica en plasma y CMSP entre los controladores y los progresores crónicos. Lo cual daría información clave para definir cuales metabolitos o rutas metabólicas pueden explicar la resistencia natural a la infección o a la progresión.

En el estudio actual, planteamos la hipótesis de que el fenotipo diferente entre los individuos infectados (progresores, controladores y PLHIV-ART) ó expuestos (HESN) al VIH-1 y controles sanos, mostrará a su vez un perfil metabolómico distinto. Por lo tanto, el propósito del estudio fue identificar niveles metabólicos de las personas VIH-1 positivas que ayuden a diferenciar los grupos de progresores, controladores y PLHIV-ART, así como a los HESN y controles sanos, e identificar biomarcadores que se relacionen con la progresión del VIH-1, la resistencia natural a la infección y la respuesta a la TAR mediante

un estudio metabolómico por RMN de protones (^{1}H-RMN), con el fin de obtener conocimientos sobre la patogénesis de la infección por el VIH-1. Por lo cual, surge la pregunta de investigación: ¿Es posible a través de metabolómica por ^{1}H-RMN establecer qué mecanismos biológicos (biomarcadores y rutas metabólicas) determinan que una persona presente resistencia natural a la infección (HESN), progresión del VIH-1 diferencial (progresores y controladores) o una respuesta efectiva a la TAR?

1.2. Objetivos

1.2.1. General:

Identificar biomarcadores específicos en plasma sanguíneo y células mononucleares de sangre periférica (CMSP) mediante RMN asociados a la resistencia natural a la infección por el VIH-1 en HESN y al tiempo de progresión a SIDA en individuos controladores y progresores.

1.2.2. Específicos:

1. Desarrollar un protocolo optimizado para la determinación del perfil metabolómico de muestras de CMSP de voluntarios mediante RMN.
2. Construir matrices metabolómicas para el plasma sanguíneo y las CMSP que permitan comparar los grupos de individuos del estudio.
3. Determinar, mediante análisis multivariado dependiente e interdependiente, los metabolitos que se puedan identificar como biomarcadores diferenciadores de los grupos del estudio.
4. Proponer las rutas metabólicas que ayuden a explicar las diferencias metabolómicas que se encuentren entre los grupos del estudio.

1.3. Referencias

Aguilar-Jiménez, W., Zapata, W., Caruz, A., and Rugeles, M. T. (2013). High transcript levels of vitamin D receptor are correlated with higher mRNA expression of human beta defensins and IL-10 in mucosa of HIV-1-Exposed seronegative individuals. PLoS One [Internet 8 (12), e82717. Available from. doi:10.1371/journal.pone.0082717

Ahmad N, Venkatesan S. Nef protein of HIV-1 is a transcriptional repressor of HIV-1 LTR. Science. 1988 Sep 16;241(4872):1481-5. doi: 10.1126/science.3262235. Erratum in: Science 1988 Oct 7;242(4875):242. PMID: 3262235.

Araníbar N, Ott KH, Roongta V, Mueller L. Metabolomic analysis using optimized NMR and statistical methods. Anal Biochem. 2006 Aug 1;355(1):62-70. doi: 10.1016/j.ab.2006.04.014. Epub 2006 May 22. PMID: 16762305.

Astarita, G., Langridge, J. (2013). An emerging role for metabolomics in nutrition science. J Nutrigenet Nutrigenomics, 6(4-5), 181-200. DOI: 10.1159/000354403.

Audano, M., Maldini, M., De Fabiani, E., Mitro, N., Caruso, D. (2018). Gender-related metabolomics and lipidomics: From experimental animal models to clinical evidence. J Proteomics, 178, 82-91. DOI: 10.1016/j.jprot.2017.11.001.

Barker, M. and Rayens, W. (2003), Partial least squares for discrimination. J. Chemometrics, 17: 166-173. https://doi.org/10.1002/cem.785

Barré-Sinoussi, F., Chermann, J. C., Reym F., Nugeyre, M. T., Chamaret, S., Gruest, J., Dauguet, C., Axler-Blin, C., Vézinet-Brun, F., Rouzioux, C., Rozenbaum, W., Montagnier, L. (1983). Isolation of a T-lymphotropic retrovirus from a patient at risk for acquired immune deficiency syndrome (AIDS). Science, 220(4599), 868-71.

Barnes, S., Benton, H. P., Casazza, K., Cooper, S. J., Cui, X., Du, X., Engler, J. A., Kabarowski, J. H., Li, S., Pathmasiri, W., Prasain, J. K., Renfrow, M. B., Tiwari, H. K. (2016). Training in metabolomics research. I. Designing the experiment, collecting and extracting samples and generating metabolomics data. J Mass Spectrom. 51(7), ii-iii. DOI: 10.1002/jms.3672.

Baur AS, Sawai ET, Dazin P, Fantl WJ, Cheng-Mayer C, Peterlin BM. HIV-1 Nef leads to inhibition or activation of T cells depending on its intracellular localization. Immunity. 1994 Aug;1(5):373-84. doi: 10.1016/1074-7613(94)90068-x. PMID: 7882168.

Beckonert, O., Keun, H. C., Ebbels, T. M. D., Bundy, J., Holmes, E., Lindon, J. C., & Nicholson, J. K. Metabolic profiling, metabolomic and metabonomic procedures for NMR spectroscopy of urine, plasma, serum and tissue extracts. Nature Protocols. 2007; 2(11): 2692–703.

Beger RD, Dunn W, Schmidt MA, Gross SS, Kirwan JA, Cascante M, Brennan L, Wishart DS, Oresic M, Hankemeier T, Broadhurst DI, Lane AN, Suhre K, Kastenmüller G, Sumner SJ, Thiele I, Fiehn O, Kaddurah-Daouk R; for “Precision Medicine and Pharmacometabolomics Task Group”-Metabolomics Society Initiative. Metabolomics enables precision medicine: "A White Paper, Community Perspective". Metabolomics. 2016;12(10):149. doi: 10.1007/s11306-016-1094-6. Epub 2016 Sep 2. PMID: 27642271; PMCID: PMC5009152.

Bertini I., Cacciatore S., Jensen B. V., et al. Metabolomic NMR fingerprinting to identify and predict survival of patients with metastatic colorectal cancer. Cancer Research. 2012;72(1):356–364. doi: 10.1158/0008-5472.CAN-11-1543.

Brenna E, McMichael AJ. The Importance of Cellular Immune Response to HIV: Implications for Antibody Production and Vaccine Design. DNA Cell Biol. 2022 Jan;41(1):38-42. doi: 10.1089/dna.2021.0520. Epub 2021 Oct 18. PMID: 34664991; PMCID: PMC8787704.

Cao Y, Qin L, Zhang L, Safrit J, Ho DD. Virologic and immunologic characterization of long-term survivors of human immunodeficiency virus type 1 infection. N. Engl. J. Med. 1995 Ene 26;332(4):201-208.

Caputo V, Libera M, Sisti S, Giuliani B, Diotti RA, Criscuolo E. The initial interplay between HIV and mucosal innate immunity. Front Immunol. 2023 Jan 30;14:1104423. doi: 10.3389/fimmu.2023.1104423. PMID: 36798134; PMCID: PMC9927018.

Calza, L., Manfredi, R., Chiodo, F. (2003). Hyperlipidaemia in patients with HIV-1 infection receiving highly active antiretroviral therapy: epidemiology, pathogenesis, clinical course and management. Int J Antimicrob Agents, 22(2), 89-99. DOI: https://doi.org/10.1016/S0924-8579(03)00115-8

Chen Y, Li EM, Xu LY. Guide to Metabolomics Analysis: A Bioinformatics Workflow. Metabolites. 2022 Apr 15;12(4):357. doi: 10.3390/metabo12040357. PMID: 35448542; PMCID: PMC9032224.

Collins DR, Gaiha GD, Walker BD. CD8+ T cells in HIV control, cure and prevention. Nat Rev Immunol. 2020 Aug;20(8):471-482. doi: 10.1038/s41577-020-0274-9. Epub 2020 Feb 12. PMID: 32051540; PMCID: PMC7222980.

Constantine NT, Kabat W, Zhao RY. 2005. Update on the laboratory diagnosis and monitoring of HIV infection. Cell Res 15:870–876. doi: 10.1038/sj.cr.7290361.

Christin C, Hoefsloot HC, Smilde AK, Hoekman B, Suits F, Bischoff R, Horvatovich P. A critical assessment of feature selection methods for biomarker discovery in clinical proteomics. Mol Cell Proteomics. 2013 Jan;12(1):263-76. doi: 10.1074/mcp.M112.022566. Epub 2012 Oct 31. PMID: 23115301; PMCID: PMC3536906.

Crook AA, Powers R. Quantitative NMR-Based Biomedical Metabolomics: Current Status and Applications. Molecules. 2020 Nov 4;25(21):5128. doi: 10.3390/molecules25215128. PMID: 33158172; PMCID: PMC7662776.

De Lay PR, Benzaken A, Karim QA, Aliyu S, Amole C, Ayala G, Chalkidou K, Chang J, Clayton M, Couto A, Dieffenbach C, Dybul M, El Sadr W, Gorgens M, Low-Beer D, Mesbah S, Saveedra J, Sirinirund P, Stover J, Syarif O, Taslim A, Thiam S, Njenga LW, Ghys PD, Izazola-Licea JA, Frescura L, Lamontagne E, Godfrey-Faussett P, Fontaine C, Semini I, Hader S. Ending AIDS as a public health threat by 2030: Time to reset targets for 2025. PLoS Med. 2021 Jun 8;18(6):e1003649. doi: 10.1371/journal.pmed.1003649. PMID: 34101728; PMCID: PMC8219148.

Dean L. Blood Groups and Red Cell Antigens [Internet]. Bethesda (MD): National Center for Biotechnology Information (US); 2005. Chapter 1, Blood and the cells it contains. Available from: https://www.ncbi.nlm.nih.gov/books/NBK2263/

Dickens, A.M., Anthony, D.C., Deutsch, R., Mielke, M.M., Claridge, T.D., Grant, I., Franklin, D., Rosario, D., Marcotte. T., Letendre, S., McArthur, J.C., Haughey, N.J. (2015). Cerebrospinal fluid metabolomics implicate bioenergetic adaptation as a neural mechanism regulating shifts in cognitive states of HIV-infected patients. AIDS, 29(5), 559-69. DOI: 10.1097/QAD.0000000000000580

Eisenreich W, Rudel T, Heesemann J and Goebel W (2019) How Viral and Intracellular Bacterial Pathogens Reprogram the Metabolism of Host Cells to Allow Their Intracellular Replication. Front. Cell. Infect. Microbiol. 9:42. doi: 10.3389/fcimb.2019.00042

Emwas AH, Roy R, McKay RT, Tenori L, Saccenti E, Gowda GAN, Raftery D, Alahmari F, Jaremko L, Jaremko M, Wishart DS. NMR Spectroscopy for Metabolomics Research. Metabolites. 2019 Jun 27;9(7):123. doi: 10.3390/metabo9070123. PMID: 31252628; PMCID: PMC6680826.

Eriksson L, Antti H, Gottfries J, Holmes E, Johansson E, Lindgren F, Long I, Lundstedt T, Trygg J, Wold S. Using chemometrics for navigating in the large data sets of genomics, proteomics, and

metabonomics (gpm). Anal Bioanal Chem. 2004 Oct;380(3):419-29. doi: 10.1007/s00216-004-2783-y. Epub 2004 Sep 22. PMID: 15448969.

Fernández-Cruz E, Desco M, Garcia Montes M, Longo N, Gonzalez B, Zabay JM. Immunological and serological markers predictive of progression to AIDS in a cohort of HIV-infected drug users. AIDS. 1990 Oct;4(10):987-94. doi: 10.1097/00002030-199010000-00007. PMID: 1979743.

Fiehn, O. (2002). Metabolomics - the link between genotypes and phenotypes. Plant Molecular Biology, 48(1–2), 155–171. DOI: https://doi.org/10.1023/A:1013713905833

Fisher, M. J., Dickson, A. J., and Pogson, C. I. (1987). The role of insulin in the modulation of glucagon-dependent control of phenylalanine hydroxylation in isolated liver cells. Biochem. J. [Internet 242 (3), 655–660. Available at:. doi:10.1042/bj2420655

Folch J, Lees M, Stanley GHS. A simple method for the isolation and purification of total lipides from animal tissues. J Biol Chem. 1957 May 1;226(1):497–509.

Gallo, R. C., Sliski, A., Wong-Staal, F. (1983). Origin of human T-cell leukaemia- lymphoma virus. Lancet, 2(8356), 962-963.

Gillespie GM, Kaul R, Dong T, Yang HB, Rostron T, Bwayo JJ, Kiama P, Peto T, Plummer FA, McMichael AJ, Rowland-Jones SL. Cross-reactive cytotoxic T lymphocytes against a HIV-1 p24 epitope in slow progressors with B*57. AIDS. 2002 May 3;16(7):961-72. doi: 10.1097/00002030-200205030-00002. PMID: 11953462.

Giovane, A., Balestrieri, A., & Napoli, C. (2008). New Insights Into Cardiovascular and Lipid Metabolomics. Journal of Cellular Biochemistry, 105(3), 648–654. DOI: 10.1002/jcb.21875

Gowda, G. A., Zhang, S., Gu, H., Asiago, V., Shanaiah, N., Raftery, D. (2008). Metabolomics-based methods for early disease diagnostics. Expert Rev Mol Diagn, 8(5), 617-33. DOI: 10.1586/14737159.8.5.617.

Halouska, S., & Powers, R. Negative impact of noise on the principal component analysis of NMR data. Journal of Magnetic Resonance (San Diego, Calif. : 1997). 2006; 178(1): 88–95.

Hendel H, Caillat-Zucman S, Lebuanec H, Carrington M, O'Brien S, Andrieu JM, Schächter F, Zagury D, Rappaport J, Winkler C, Nelson GW, Zagury JF. New class I and II HLA alleles strongly associated with opposite patterns of progression to AIDS. J Immunol. 1999 Jun 1;162(11):6942-6. PMID: 10352317.

Hewer, R., Vorster, J., Steffens, F.E., Meyer, D. (2006). Applying biofluid 1H NMR-based metabonomic techniques to distinguish between HIV-1 positive/AIDS patients on antiretroviral treatment and HIV-1 negative individuals. J Pharm Biomed Anal, 41(4), 1442–6. DOI: 10.1016/j.jpba.2006.03.006

Hodgkinson P. and Emsley L. Numerical simulation of solid-state NMR experiments, Progress in Nuclear Magnetic Resonance Spectroscopy, Volume 36, Issue 3, 2000, Pages 201-239, ISSN 0079-6565, https://doi.org/10.1016/S0079-6565(99)00019-9.

Holz, M., Heil SR. and Sacco A. (2000). Temperature-dependent Self-diffusion Coefficients of Water and Six Selected Molecular Liquids for Calibration in Accurate 1H NMR PFG Measurements. Physical Chemistry Chemical Physics. 2. 10.1039/B005319H. DOI: https://doi.org/10.1039/B005319H

Huang Y, Paxton WA, Wolinsky SM, et al. The role of a mutant CCR5 allele in HIV-1 transmission and disease progression, Nat Med, 1996, vol. 2 (pg. 1240-3)

Isa F, Collins S, Lee MH, Decome D, Dorvil N, Joseph P, Smith L, Salerno S, Wells MT, Fischer S, Bean JM, Pape JW, Johnson WD, Fitzgerald DW, Rhee KY. Mass Spectrometric Identification of Urinary Biomarkers of Pulmonary Tuberculosis. EBioMedicine. 2018 May;31:157-165. doi: 10.1016/j.ebiom.2018.04.014. Epub 2018 Apr 22. PMID: 29752217; PMCID: PMC6013777.

Johnson RL, Schmidt-Rohr K. Quantitative solid-state 13C NMR with signal enhancement by multiple cross polarization. J Magn Reson. 2014 Feb;239:44-9. doi: 10.1016/j.jmr.2013.11.009. Epub 2013 Nov 27. PMID: 24374751.

Kamburov A, Wierling C, Lehrach H, Herwig R. ConsensusPathDB--a database for integrating human functional interaction networks. Nucleic Acids Res. 2009 Jan;37(Database issue):D623-8. doi: 10.1093/nar/gkn698. Epub 2008 Oct 21. PMID: 18940869; PMCID: PMC2686562.

Kamburov A, Pentchev K, Galicka H, Wierling C, Lehrach H, Herwig R. ConsensusPathDB: toward a more complete picture of cell biology. Nucleic Acids Res. 2011 Jan;39(Database issue):D712-7. doi: 10.1093/nar/gkq1156. Epub 2010 Nov 11. PMID: 21071422; PMCID: PMC3013724.

Kanehisa M. Molecular network analysis of diseases and drugs in KEGG. Methods Mol Biol. 2013;939:263-75. doi: 10.1007/978-1-62703-107-3_17. PMID: 23192552.

Kaslow RA, Carrington M, Apple R, Park L, Muñoz A, Saah AJ, Goedert JJ, Winkler C, O'Brien SJ, Rinaldo C, Detels R, Blattner W, Phair J, Erlich H, Mann DL. Influence of combinations of

human major histocompatibility complex genes on the course of HIV-1 infection. Nat Med. 1996 Apr;2(4):405-11. doi: 10.1038/nm0496-405. PMID: 8597949.

Kim, S., Kim, J. Yun, E. J., Kim, K.H. (2016). Food metabolomics: from farm to human. Curr Opin Biotechnol, 37, 16-23. DOI: 10.1016/j.copbio.2015.09.004.

Kimhofer T, Lodge S, Whiley L, Gray N, Loo RL, Lawler NG, Nitschke P, Bong SH, Morrison DL, Begum S, Richards T, Yeap BB, Smith C, Smith KGC, Holmes E, Nicholson JK. Integrative Modeling of Quantitative Plasma Lipoprotein, Metabolic, and Amino Acid Data Reveals a Multiorgan Pathological Signature of SARS-CoV-2 Infection. J Proteome Res. 2020 Nov 6;19(11):4442-4454. doi: 10.1021/acs.jproteome.0c00519. Epub 2020 Sep 14. Erratum in: J Proteome Res. 2021 Jun 4;20(6):3400. PMID: 32806897.

Koshani R., Jafari SM, van de Ven TGM, Going deep inside bioactive-loaded nanocarriers through Nuclear Magnetic Resonance (NMR) spectroscopy, Trends in Food Science & Technology, Volume 101, 2020, Pages 198-212, ISSN 0924-2244, https://doi.org/10.1016/j.tifs.2020.05.010. (https://www.sciencedirect.com/science/article/pii/S0924224420304714)

Kostidis, S, Addie RD, Morreau H, Mayboroda OA, Giera M. Quantitative NMR analysis of intra- and extracellular metabolism of mammalian cells: A tutorial. Analytica Chimica Acta 980 (2017) 1-24. http://dx.doi.org/10.1016/j.aca.2017.05.011

Kruk J, Doskocz M, Jodłowska E, Zacharzewska A, Łakomiec J, Czaja K, Kujawski J. NMR Techniques in Metabolomic Studies: A Quick Overview on Examples of Utilization. Appl Magn Reson. 2017;48(1):1-21. doi: 10.1007/s00723-016-0846-9. Epub 2016 Nov 2. PMID: 28111499; PMCID: PMC5222922.

Le Gall, G. Sample Collection and Preparation of Biofluids and Extracts for NMR Spectroscopy. Jacob T. Bjerrum (ed.), Metabonomics: Methods and Protocols, Methods in Molecular Biology, vol. 1277, DOI 10.1007/978-1-4939-2377-9_2.

Lee JH, Okuno Y, Cavagnero S. Sensitivity enhancement in solution NMR: emerging ideas and new frontiers. J Magn Reson. 2014 Apr;241:18-31. doi: 10.1016/j.jmr.2014.01.005. PMID: 24656077; PMCID: PMC3967054.

Lederman MM, Alter G, Daskalakis DC, et al. Determinants of protection among HIV-exposed seronegative persons: an overview, J Infect Dis, 2010, vol. 202 Suppl(pg. S333-8)

Liu, X. and Locasale, J. W. (2017). Metabolomics: A Primer. Trends in Biochemical Sciences, 42(4), 274-284. DOI: http://dx.doi.org/10.1016/j.tibs.2017.01.004

Liu R, Paxton WA, Choe S, Ceradini D, Martin SR, Horuk R, MacDonald ME, Stuhlmann H, Koup RA, Landau NR. Homozygous defect in HIV-1 coreceptor accounts for resistance of some multiply-exposed individuals to HIV-1 infection. Cell. 1996 Aug 9;86(3):367-77. doi: 10.1016/s0092-8674(00)80110-5. PMID: 8756719.

Macel, M., Van Dam, N.M. and Keurentjes, J.J.B. (2010). Metabolomics: the chemistry between ecology and genetics. Molecular ecology resources, 10(4), 583-593. DOI: https://doi.org/10.1111/j.1755-0998.2010.02854.

Martin, F. P. J., Collino, S., & Rezzi, S. (2011). 1H NMR-based metabonomic applications to decipher gut microbial metabolic influence on mammalian health. Magnetic Resonance in Chemistry, 49, S47–S54. DOI: 10.1002/mrc.2810

Mathew J, Sankar P, Varacallo M. Physiology, Blood Plasma. [Updated 2023 Apr 24]. In: StatPearls [Internet]. Treasure Island (FL): StatPearls Publishing; 2024 Jan-. Available from: https://www.ncbi.nlm.nih.gov/books/NBK531504/

Mayer KA, Stöckl J, Zlabinger GJ, Gualdoni GA. Hijacking the Supplies: Metabolism as a Novel Facet of Virus-Host Interaction. Front Immunol. 2019 Jul 3;10:1533. doi: 10.3389/fimmu.2019.01533. PMID: 31333664; PMCID: PMC6617997.

Mazzoli S, Trabattoni D, Lo Caputo S, Piconi S, Blé C, Meacci F, Ruzzante S, Salvi A, Semplici F, Longhi R, Fusi ML, Tofani N, Biasin M, Villa ML, Mazzotta F, Clerici M. HIV-specific mucosal and cellular immunity in HIV-seronegative partners of HIV-seropositive individuals. Nat Med. 1997 Nov;3(11):1250-7. doi: 10.1038/nm1197-1250. PMID: 9359700.

McLaren PJ, Carrington M. The Impact of Host Genetic Variation on Infection With HIV-1. Nat Immunol (2015) 16(6):577–83. 10.1038/ni.3147

Meyer L, Magierowska M, Hubert JB, Rouzioux C, Deveau C, Sanson F, Debre P, Delfraissy JF, Theodorou I. Early protective effect of CCR-5 delta 32 heterozygosity on HIV-1 disease progression: relationship with viral load. The SEROCO Study Group. AIDS. 1997 Sep;11(11):F73-8. doi: 10.1097/00002030-199711000-00001. PMID: 9302436.

Meyers AFA, Fowke KR. International symposium on natural immunity to HIV: a gathering of the HIV-exposed seronegative clan, J Infect Dis, 2010, vol. 202 Suppl(pg. S327-8)

Migueles SA, Sabbaghian MS, Shupert WL, Bettinotti MP, Marincola FM, Martino L, Hallahan CW, Selig SM, Schwartz D, Sullivan J, Connors M. HLA B*5701 is highly associated with restriction of virus replication in a subgroup of HIV-infected long term nonprogressors. Proc Natl Acad Sci U S A. 2000 Mar 14;97(6):2709-14. doi: 10.1073/pnas.050567397. PMID: 10694578; PMCID: PMC15994.

Moco S. Studying Metabolism by NMR-Based Metabolomics. Front Mol Biosci. 2022 Apr 27;9:882487. doi: 10.3389/fmolb.2022.882487. PMID: 35573745; PMCID: PMC9094115.

Modell H, Cliff W, Michael J, McFarland J, Wenderoth MP, Wright A. A physiologist's view of homeostasis. Adv Physiol Educ. 2015 Dec;39(4):259-66. doi: 10.1152/advan.00107.2015. PMID: 26628646; PMCID: PMC4669363.

Montoya, C. J., Velilla, P. A., Chougnet, C., Landay, A. L., Rugeles, M. T. (2006). Increased IFN-gamma production by NK and CD3+/CD56+ cells in sexually HIV-1-exposed but uninfected individuals. Clin Immunol, 120(2), 138–46. DOI: 10.1016/j.clim.2006.02.008

Munshi, S.U., Rewari, B.B., Bhavesh, N.S., Jameel, S. (2013). Nuclear magnetic resonance based profiling of biofluids reveals metabolic dysregulation in HIV-infected persons and those on antiretroviral therapy. PLoS One, 8(5), e64298. DOI: https://doi.org/10.1371/journal.pone.0064298

Nadella, K. D., Marla, S. S. and Kumar, P. A. (2012). Metabolomics in Agriculture. OMICS: A Journal of Integrative Biology, 16(4). DOI: http://doi.org/10.1089/omi.2011.0067

Nagana Gowda GA, Gowda YN, Raftery D. Expanding the limits of human blood metabolite quantitation using NMR spectroscopy. Anal Chem. 2015 Jan 6;87(1):706-15. doi: 10.1021/ac503651e. Epub 2014 Dec 8. PMID: 25485990; PMCID: PMC4287831.

Nagana Gowda GA, Raftery D. NMR-Based Metabolomics. Adv Exp Med Biol. 2021;1280:19-37. doi: 10.1007/978-3-030-51652-9_2. PMID: 33791972; PMCID: PMC8816450.

Nguyen, D.V., Rocke, D.M. (2002). Classification of Acute Leukemia Based on DNA Microarray Gene Expressions Using Partial Least Squares. In: Lin, S.M., Johnson, K.F. (eds) Methods of Microarray Data Analysis. Springer, Boston, MA. https://doi.org/10.1007/978-1-4615-0873-1_9

Nicholson, J. K., Lindon, J. C., & Holmes, E. (1999). 'Metabonomics': Understanding the metabolic responses of living systems to pathophysiological stimuli via multivariate statistical analysis of

biological NMR spectroscopic data. Xenobiotica, 29(11), 1181–1189. DOI: 10.1080/004982599238047

Ochoa, B. (2006). La lipidómica, una nueva herramienta al servicio de la salud. The lipidomic, a new tool to the service of the health. Gac Med Bilbao, 103, 101-2. DOI: 10.1016/S0304-4858(06)74534-6

Oliver, S. G., Winson, M. K., Kell, D. B., & Baganz, F. (1998). Systematic functional analysis of the yeast genome. Trends in Biotechnology, 16(9), 373–378. DOI: 10.1016/S0167-7799(98)01214-1

ONUSIDA, Comunicaciones y Promoción Mundial (2023). HOJA INFORMATIVA 2023. Estadísticas mundiales sobre el VIH. Available at: https://www.unaids.org/sites/default/files/media_asset/UNAIDS_FactSheet_es.pdf

O'Brien SJ, Gao X, Carrington M. HLA and AIDS: a cautionary tale. Trends Mol Med. 2001 Sep;7(9):379-81. doi: 10.1016/s1471-4914(01)02131-1. PMID: 11530315.

Overmyer KA, Shishkova E, Miller IJ, Balnis J, Bernstein MN, Peters-Clarke TM, Meyer JG, Quan Q, Muehlbauer LK, Trujillo EA, He Y, Chopra A, Chieng HC, Tiwari A, Judson MA, Paulson B, Brademan DR, Zhu Y, Serrano LR, Linke V, Drake LA, Adam AP, Schwartz BS, Singer HA, Swanson S, Mosher DF, Stewart R, Coon JJ, Jaitovich A. Large-Scale Multi-omic Analysis of COVID-19 Severity. Cell Syst. 2021 Jan 20;12(1):23-40.e7. doi: 10.1016/j.cels.2020.10.003. Epub 2020 Oct 8. PMID: 33096026; PMCID: PMC7543711.

Pace BT, Lackner AA, Porter E, Pahar B. The Role of Defensins in HIV Pathogenesis. Mediators Inflamm. 2017;2017:5186904. doi: 10.1155/2017/5186904. Epub 2017 Aug 3. PMID: 28839349; PMCID: PMC5559915.

Palomino-Schtzlein M, García H, Gutiérrez-Carcedo P, Pineda-Lucena A, Herance JR. Assessment of gold nanoparticles on human peripheral blood cells by metabolic profiling with 1H-NMR spectroscopy, a novel translational approach on a patient-specific basis. PLoS One. 2017;12(8):e0182985.

Passaes CP, Cardoso CC, Caetano DG, Teixeira SL, Guimarães ML, Campos DP, et al.. Association of Single Nucleotide Polymorphisms in the Lens Epithelium-Derived Growth Factor (LEDGF/p75) With HIV-1 Infection Outcomes in Brazilian HIV-1+ Individuals. PloS One (2014) 9(7):e101780. 10.1371/journal.pone.0101780

Pereyra, F., Addo, M. M., Kaufmann, D. E., Liu, Y., Miura, T., Rathod, A., et al. (2008). Genetic and immunologic heterogeneity among persons who control HIV infection in the absence of therapy. J. Infect. Dis. 197 (4), 563–571. doi:10.1086/526786

Philippeos, C., Steffens, F.E., Meyer, D. (2009). Comparative 1H NMR-based metabonomic analysis of HIV-1 sera. J Biomol NMR, 44(3), 127-37. DOI: 10.1007/s10858-009-9329-8

Pykett IL, Newhouse JH, Buonanno FS, Brady TJ, Goldman MR, Kistler JP, Pohost GM. Principles of nuclear magnetic resonance imaging. Radiology. 1982 Apr;143(1):157-68. doi: 10.1148/radiology.143.1.7038763. PMID: 7038763.

Puchades-Carrasco, L., Pineda-Lucena, A. (2015). Metabolomics in pharmaceutical research and development. Curr Opin Biotechnol, 35, 73-7. DOI: 10.1016/j.copbio.2015.04.004.

Rodríguez-Gallego, E., Gómez, J., Domingo, P., Ferrando-Martínez, S., Peraire, J., Viladés, C., Veloso, S., López-Dupla, M., Beltrán-Debón, R., Alba, V., Vargas, M., Castellano, A.J., Leal, M., Pacheco, Y. M., Ruiz-Mateos, E., Gutiérrez, F., Vidal, F., Rull, A., on behalf of the CORIS-NADES events Study Group. (2018). Circulating metabolomic profile can predict dyslipidemia in HIV patients undergoing antiretroviral therapy, Atherosclerosis. DOI: 10.1016/j.atherosclerosis.2018.04.008

Roff SR, Noon-Song EN, Yamamoto JK. The Significance of Interferon-γ in HIV-1 Pathogenesis, Therapy, and Prophylaxis. Front Immunol. 2014 Jan 13;4:498. doi: 10.3389/fimmu.2013.00498. PMID: 24454311; PMCID: PMC3888948.

Rolin D., Deborde C., Maucourt M., Cabasson C., Fauvelle F., Jacob D., Canlet C., Moing A., Chapter One - High-Resolution 1H-NMR Spectroscopy and Beyond to Explore Plant Metabolome, Editor(s): Dominique Rolin, Advances in Botanical Research, Academic Press, Volume 67, 2013, Pages 1-66, ISSN 0065-2296, ISBN 9780123979223, https://doi.org/10.1016/B978-0-12-397922-3.00001-0.

Rugeles MT, Velilla PA, Montoya CJ. Mechanisms of human natural resistance to HIV: a summary of ten years of research in the Colombian population. Biomedica. 2011 Jun;31(2):269-80. doi: 10.1590/S0120-41572011000200016. PMID: 22159545.

Ruiz-Perez D, Guan H, Madhivanan P, Mathee K, Narasimhan G. So you think you can PLS-DA? BMC Bioinformatics. 2020 Dec 9;21(Suppl 1):2. doi: 10.1186/s12859-019-3310-7. PMID: 33297937; PMCID: PMC7724830.

Rutstein SE, Ananworanich J, Fidler S, Johnson C, Sanders EJ, Sued O, Saez-Cirion A, Pilcher CD, Fraser C, Cohen MS, Vitoria M, Doherty M, Tucker JD. Clinical and public health implications of acute and early HIV detection and treatment: a scoping review. J Int AIDS Soc. 2017 Jun 28;20(1):21579. doi: 10.7448/IAS.20.1.21579. PMID: 28691435; PMCID: PMC5515019.

Samson M, Libert F, Doranz BJ, Rucker J, Liesnard C, Farber CM, Saragosti S, Lapoumeroulie C, Cognaux J, Forceille C, Muyldermans G, Verhofstede C, Burtonboy G, Georges M, Imai T, Rana S, Yi Y, Smyth RJ, Collman RG, Doms RW, Vassart G, Parmentier M. Resistance to HIV-1 infection in caucasian individuals bearing mutant alleles of the CCR-5 chemokine receptor gene. Nature. 1996 Aug 22;382(6593):722-5. doi: 10.1038/382722a0. PMID: 8751444.

Scalbert A, Brennan L, Fiehn O, Hankemeier T, Kristal BS, van Ommen B, Pujos-Guillot E, Verheij E, Wishart D, Wopereis S. Mass-spectrometry-based metabolomics: limitations and recommendations for future progress with particular focus on nutrition research. Metabolomics. 2009 Dec;5(4):435-458. doi: 10.1007/s11306-009-0168-0. Epub 2009 Jun 12. PMID: 20046865; PMCID: PMC2794347.

Shen Y, Wang J, Wang Z, Shen J, Qi T, Song W, et al. A cross-sectional study of leukopenia and thrombocytopenia among Chinese adults with newly diagnosed HIV/AIDS. Biosci Trends. 2015;9(2):91–6.

Ståhle, L. and Wold, S. (1987), Partial least squares analysis with cross-validation for the two-class problem: A Monte Carlo study. J. Chemometrics, 1: 185-196. https://doi.org/10.1002/cem.1180010306

Sitole, L. J., Williams, A. A., Meyer, D. (2013). Metabonomic analysis of HIV-infected biofluids. Mol Biosyst, 9(1), 18-28. doi: 10.1039/c2mb25318f.

Stewart GJ, Ashton LJ, Biti RA, Ffrench RA, Bennetts BH, Newcombe NR, Benson EM, Carr A, Cooper DA, Kaldor JM. Increased frequency of CCR-5 delta 32 heterozygotes among long-term non-progressors with HIV-1 infection. The Australian Long-Term Non-Progressor Study Group. AIDS. 1997 Dec;11(15):1833-8. doi: 10.1097/00002030-199715000-00007. PMID: 9412701.

Swanson, B., Sha, B.E., Keithley, J.K., Fogg, L., Nerad, J., Novak, R., Adeyemi, O. (2009). Lipoprotein Particle Profiles by Nuclear Magnetic Resonance Spectroscopy in Medically-Underserved HIV-Infected Persons. J Clin Lipidol, 3(6), 379-384. DOI: 10.1016/j.jacl.2009.10.005

Taborda-Vanegas, N., Zapata, W., and Rugeles, M. T. (2011). Genetic and immunological factors involved in natural resistance to HIV-1 infection. Open Virol. J. 5, 35–43. doi:10.2174/1874357901105010035

Tenenboim, H. and Brotman, Y. (2016). Omic Relief for the Biotically Stressed: Metabolomics of Plant Biotic Interactions. Trends in Plant Science, 21(9), 781-791. DOI: http://dx.doi.org/10.1016/j.tplants.2016.04.009

Teixeira SL, de Sá NB, Campos DP, Coelho AB, Guimarães ML, Leite TC, et al.. Association of the HLA-B*52 Allele With Non-Progression to AIDS in Brazilian Hiv-1-infected Individuals. Genes Immun (2014) 15(4):256–62. 10.1038/gene.2014.14

Tounta V, Liu Y, Cheyne A, Larrouy-Maumus G. Metabolomics in infectious diseases and drug discovery. Mol Omics. 2021 Jun 14;17(3):376-393. doi: 10.1039/d1mo00017a. PMID: 34125125; PMCID: PMC8202295.

UNAIDS, 2023 Global AIDS Update: The Path That Ends AIDS; July 2023. UNAIDS, AIDSinfo website; accessed July 2023, available at: http://aidsinfo.unaids.org/. UNAIDS, 2023 Core epidemiology slides; July 2023.

Valle-Casuso JC, Angin M, Volant S, Passaes C, Monceaux V, Mikhailova A, Bourdic K, Avettand-Fenoel V, Boufassa F, Sitbon M, Lambotte O, Thoulouze MI, Müller-Trutwin M, Chomont N, Sáez-Cirión A. Cellular Metabolism Is a Major Determinant of HIV-1 Reservoir Seeding in CD4+ T Cells and Offers an Opportunity to Tackle Infection. Cell Metab. 2019 Mar 5;29(3):611-626.e5. doi: 10.1016/j.cmet.2018.11.015. Epub 2018 Dec 20. PMID: 30581119.

Velilla PA, Hoyos A, Rojas M, Patiño PJ, Vélez LA, Rugeles MT. Apoptosis as a mechanism of natural resistance to HIV-1 infection in an exposed but uninfected population. J Clin Virol. 2005 Apr;32(4):329-35. doi: 10.1016/j.jcv.2004.08.018. PMID: 15780814.

Vergis EN, Mellors JW. Natural history of HIV-1 infection. Infect Dis Clin North Am. 2000;14(4):809–25, v-vi. Epub 2001/01/06. pmid:11144640

Vidya Vijayan KK, Karthigeyan KP, Tripathi SP, Hanna LE. Pathophysiology of CD4+ T-Cell Depletion in HIV-1 and HIV-2 Infections. Front Immunol. 2017 May 23;8:580. doi: 10.3389/fimmu.2017.00580. PMID: 28588579; PMCID: PMC5440548.

Walker, B. D. (2007). Elite control of HIV infection: Implications for vaccines and treatment. *Top HIV Med, 15*(4),134–6.

Weiner J 3rd, Maertzdorf J, Sutherland JS, Duffy FJ, Thompson E, Suliman S, McEwen G, Thiel B, Parida SK, Zyla J, Hanekom WA, Mohney RP, Boom WH, Mayanja-Kizza H, Howe R, Dockrell HM, Ottenhoff THM, Scriba TJ, Zak DE, Walzl G, Kaufmann SHE; GC6-74 consortium. Metabolite changes in blood predict the onset of tuberculosis. Nat Commun. 2018 Dec 6;9(1):5208. doi: 10.1038/s41467-018-07635-7. PMID: 30523338; PMCID: PMC6283869.

Westerhuis, J. a., Hoefsloot, H. C. J., Smit, S., Vis, D. J., Smilde, A. K., Velzen, E. J. J., Duijnhoven, J. P. M., & Dorsten, F. a. Assessment of PLSDA cross validation. Metabolomics. 2008; 4(1): 81–89.

Worley B, Powers R. Multivariate Analysis in Metabolomics. Curr Metabolomics. 2013;1(1):92-107. doi: 10.2174/2213235X11301010092. PMID: 26078916; PMCID: PMC4465187.

Ye T, Zheng C, Zhang S, Gowda GA, Vitek O, Raftery D. "Add to subtract": a simple method to remove complex background signals from the 1H nuclear magnetic resonance spectra of mixtures. Anal Chem. 2012 Jan 17;84(2):994-1002. doi: 10.1021/ac202548n. Epub 2011 Dec 30. PMID: 22221170; PMCID: PMC3282557.

Young JM, Turpin JA, Musib R, Sharma OK. Outcomes of a national institute of allergy and infectious diseases workshop on understanding HIV-exposed but seronegative individuals, AIDS Res Hum Retroviruses, 2011, vol. 27 (pg. 737-43)

Zapata, W., Rodriguez, B., Weber, J., Estrada, H., Quiñones-Mateu, M. E., Zimermman, P. A., et al. (2008). Increased levels of human beta-defensins mRNA in sexually HIV-1 exposed but uninfected individuals. Curr. HIV Res. 6 (6), 531–538. doi:10.2174/157016208786501463

Zhang, A., Sun, H., Wang, X. (2012). Recent highlights of metabolomics for traditional Chinese medicine. Pharmazie, 67(8), 667-75.

Zhang X, Xu L, Shen J, Cao B, Cheng T, Zhao T, Liu X, Zhang H. Metabolic signatures of esophageal cancer: NMR-based metabolomics and UHPLC-based focused metabolomics of blood serum. Biochim Biophys Acta. 2013 Aug;1832(8):1207-16. doi: 10.1016/j.bbadis.2013.03.009. Epub 2013 Mar 20. PMID: 23524237.

Zhang ZN, Xu JJ, Fu YJ, Liu J, Jiang YJ, Cui HL, et al.. Transcriptomic Analysis of Peripheral Blood Mononuclear Cells in Rapid Progressors in Early HIV Infection Identifies a Signature Closely Correlated With Disease Progression. Clin Chem (2013) 59(8):1175–86. 10.1373/clinchem.2012.197335

CAPÍTULO 2:

Development of an optimized method for processing Peripheral Blood Mononuclear Cells for ^{1}H-Nuclear Magnetic Resonance-based metabolomic profiling

PLoS ONE 16(2): e0247668. 20 pag, 2021

Development of an optimized method for processing Peripheral Blood Mononuclear Cells for ^{1}H-Nuclear Magnetic Resonance-based metabolomic profiling

2.1. Abstract

Human peripheral blood mononuclear cells (PBMCs) are part of the innate and adaptive immune system, and form a critical interface between both systems. Studying the metabolic profile of PBMC could provide valuable information about the response to pathogens, toxins or cancer, the detection of drug toxicity, in drug discovery and cell replacement therapy. The primary purpose of this study was to develop an improved processing method for PBMCs metabolomic profiling with nuclear magnetic resonance (NMR) spectroscopy. To this end, an experimental design was applied to develop an alternative method to process PBMCs at low concentrations. The design included the isolation of PBMCs from the whole blood of four different volunteers, of whom 27 cell samples were processed by two different techniques for quenching and extraction of metabolites: a traditional one using organic solvents and an alternative one employing a high-intensity ultrasound probe, the latter with a variation that includes the use of deproteinizing filters. Finally, all the samples were characterized by ^{1}H-NMR and the metabolomic profiles were compared by the method. As a result, two new methods for PBMCs processing, called Ultrasound Method (UM) and Ultrasound and Ultrafiltration Method (UUM), are described and compared to the Folch Method (FM), which is the standard protocol for extracting metabolites from cell samples. We found that UM and UUM were superior to FM in terms of sensitivity, processing time, spectrum quality, amount of identifiable, quantifiable metabolites and reproducibility.

2.2. Introduction

A peripheral blood mononuclear cell (PBMC) is any blood cell with a round nucleus, such as lymphocyte, monocyte or macrophage [1]. PBMC are composed of three types of cells: lymphocytes, dendritic cells and monocytes. The abundance or frequency of each type has a characteristic distribution in humans as follows: most PBMC correspond to lymphocytes with an abundance of between 70% and 90%, while dendritic cells are rare with only between 1% and 2% of the total population, and monocytes are in the middle with an abundance ranging from 10% to 20%. There are different types of cells in the lymphocyte family, including $CD3^{+}$ T cells (70-85%),

B-cells (5-10%), and NK cells (5-20%). Specifically, $CD3^+$ lymphocytes are composed of $CD4^+$ and $CD8^+$ T cells with an approximate 2:1 ratio. Furthermore, the activation process of $CD4^+$ T-cells causes a conversion phenomenon in various subsets of effector cells, including Th1, Th2, Th17, Th9, Th22 cells, follicular helpers (Tfh) and different types of regulatory cells [2–5].

In the immune system, PBMCs stand out as an essential component as they are responsible for generating a response to the external agents that enter the body. [6,7] and to the cells that have transformed into a cancerous cell type [8,9]. This has led to medical and research interest being shown in studying PBMC in diverse areas such as immunology [10–13], toxicology [14,15], infectious disease [16–18], allergic diseases [19,20], cardiovascular diseases [21,22], hematological malignancies [23], transplant therapy [24], vaccine development [25,26] and personalized medicine [27]. It is possible to find fundamental information on the function of different types of cells [28], to identify biomarkers and metabolic pathways associated with different medical conditions [29], and to perform disease modeling [30] through *in vitro* studies of PBMCs.

Metabolomic profiling can gain insight into changes in the metabolic state of cells due to external agents, such as diseases and their treatment with medications, environmental factors, diet, lifestyles, genetic effects, toxic exposure, etc. [31–35]. For this purpose, nuclear magnetic resonance (NMR) spectroscopy provides the unbiased detection of metabolites, robustness, reproducibility, minimal sample preparation, easy interpretation and analysis of spectral data, and quantitative information about the metabolome of cells [36,37].

Previous protocols for the metabolomics profiling of PBMCs by NMR were performed, starting from 20 mL blood and 20 million PBMCs [38]. However, the blood volume available for extracting PBMCs in clinical studies is limited, and the amount of PBMCs in the blood depends on the patient's condition. For instance, immunosuppressive diseases such as HIV-1 infection [39], cancer [40], and primary immunodeficiencies, characterized by low PBMC counts. Therefore, it would be optimal to work with smaller blood and cell samples by optimizing different metabolite extraction method steps, including the cell disruption method, the amount and type of solvents, and the processing time. [41–45].

Accordingly, this study aimed to develop an improved method to process PBMCs for metabolomic profiling by NMR spectroscopy. We wished to obtain reproducible and robust high-quality data from PBMC samples of 12.5 million cells or fewer, with minimal sample handling and a short processing time. Our approach is based on using high-intensity ultrasound, as previously

described for other types of cells and tissues [46–49], and to compare it to the Folch method, the international standard for processing these biological samples [50,51]. The method developed for analyzing the metabolic profile of PBMCs by ^{1}H-NMR could be a tool for the biomarker identifications associated with disease diagnosis, evaluations of the effects of new treatments on patients, among other approaches [34,35,52].

2.3. Materials and Methods

2.3.1. Chemicals and materials

Solvents and reagents were Ficoll-Paque Plus, Phosphate-Buffered Saline (PBS), sodium phosphate dibasic dehydrate and sodium azide, methanol, chloroform, deuterated water and deuterated trimethylsilyl propanoic acid (TSP-D4) were supplied by Merck (Germany). The ultrapure water was obtained in a Milli-Q purification system of Merck Millipore. The Vivaspin® 500 3,000K MWCO Centrifugal Concentrators were provided by Sartorius.

In order to develop the high-intensity ultrasound process, an LSP-500 ultrasonic liquid processor (Sonomechanics, New York, USA), equipped with an ultrasonic generator of 500 W, an air-cooled piezoelectric transducer (ACT-500), a full-wave Barbell Horn™ (FBH, 21-mm tip diameter) and a reactor chamber (jacketed beaker refrigerated), was used for all the experimental runs.

2.3.2. Human subjects

This study was approved by the Bioethical Committee, Universidad de Antioquia; and all the individuals signed informed consent, prepared according to Colombian Legislation, Resolution 008430/1993. Healthy controls were 59, 34, 25, and 40 year-old male individuals, recruited through the blood bank from the IPS Universitaria, Universidad de Antioquia. These individuals fulfilled the donor eligibility requirements; their hemoglobin levels equaled or exceeded 13g/dL, or the hematocrit value equaled or was over 39 percent; they were negative for several infectious diseases and the blood samples donation protocol did not require eitherfasting or a nonfasting status. For whole blood, a donation of 450 mL (60-70ml of Citrate Phosphate Dextrose anticoagulant) was obtained from each individual. Four volunteers were analyzed. From the first volunteer, a total of nine samples were processed, a triplicate for each evaluated method (FM, UM, UUM). For the three remaining volunteers, a duplicate of each volunteer was analyzed by

each method on two different evaluation days; that is, a total of 27 measurements were made, nine for each evaluated method.

2.3.3. Human peripheral blood mononuclear cells isolation

The isolation of PBMCs leukocytes was carried out by a Ficoll-Paque gradient method [53]. Peripheral blood, freshly extracted from healthy volunteers, was carefully poured into a tube with Ficoll at the blood/Ficoll 1:4 proportion, and allowed to stand for approximately 20 min, centrifuged at 591 g for 30 minutes at room temperature with brake off to ensure that deceleration did not disrupt the density gradient. Three phases were obtained. At the bottom of the tube, red blood cells (RBCs) and granulocytes concentrated. Likewise, a white fraction of the mononuclear in the middle (PBMCs) and an upper phase corresponding to plasma and platelets formed. The PBMCs phase was carefully transferred to a separate tube and washed with PBS 1X at the 1:10 PBMCs/PBS 1X proportion. Subsequently, PBMC were centrifuged at 1000 g for 5 min at 4ºC.

The supernatant was discarded, and the pellet containing PBMCs was resuspended in 1 mL of PBS 1X for cell counting and viability tests. Cells were diluted within a range between 250000 cells/mL and 500000 cells/mL to be counted with the Neubauer chamber. Later an aliquot (50 µL) of the cell suspension was diluted 1:1 (v/v) with 0.4% trypan blue dye (Trypan Blue should be sterile-filtered before using it to do away with the particles in solution that would disturb the counting process). After carefully the hemocytometer chamber was filled with 20 µL of cell suspension. Then it was incubated for 1–2 min at room temperature (incubations exceeding 30 min may cause decreased cell viability due to Trypan toxicity). Nonviable cells are blue and viable cells are unstained. Next, viable cells were counted under the microscope in four 1 x 1 mm squares of the Neubauer chamber and the average number of cells per square was determined (Neubauer hemocytometer consists of two chambers, each divided into 9 mm^2 squares) [54–57]. Finally, cells were diluted in PBS 1X to obtain individual portions of 12.5 million viable cells in 100 µL. PBMC were frozen at -80°C until processed.

2.3.4. Extraction of metabolites for the ^{1}H-NMR experiments

Frozen samples were placed on ice for 5 min, and then subjected to the first extraction procedures, the Folch Method (FM) [58,59]. Briefly, 160 µL of methanol and 80 µL of chloroform at 4ºC were added per tube (12.5 million cells). Samples were then homogenized by vortexing and left to stand for 15 min. For uniform cell breakage, samples were submitted to three freeze-thaw cycles with

liquid nitrogen. Then 125 µL of distilled water and 125 µL of chloroform were added to each sample, which were later vortexed. Samples were then centrifuged at 15000 g for 30 min at 4ºC to separate phases. The solution was separated into an upper water/methanol phase (with polar metabolites, aqueous phase), an interphase containing mainly proteins, DNA/RNA, cell membranes, and a lower chloroform/methanol phase (with lipophilic compounds, organic phase). The aqueous phase was lyophilized overnight to obtain dry extracts. Extracts were stored at -80˚C until sample preparation for the ^{1}H-NMR experiments.

The second procedure was the Ultrasound Method (UM), in which 650 µL of phosphate buffer (50 mM Na_2HPO_4 pH 7.4, in D_2O with 0.1 mM of deuterated trimethylsilyl propanoic acid (TSP-D4)) were added per sample with 12.5 million cells. Cells were resuspended with a micropipette and homogenized with a vortex. Then for cell breakage, samples were submitted to a cycle described as follows: First cells were frozen with liquid nitrogen (1 min). Then the sample was immersed in a refrigerated bath (4˚C) equipped with a high-intensity ultrasound probe set at a frequency of 20050 Hz and a 100% amplitude for 5 min. This cycle was run six times. Samples were then centrifuged at 12000 g for 120 min at 4ºC to separate phases. The solution was separated into an upper phase (with metabolites) and a lower phase (containing mainly proteins, DNA/RNA, and cell membranes). The supernatant was stored at -80ºC until the sample analysis for the ^{1}H-NMR experiments.

The third procedure was called the Ultrasound and Ultrafiltration Method (UUM). It involves taking the supernatant obtained from the second method and filtered with a ultrafilter previously washed with phosphate buffer (10X with phosphate buffer, pH 7.4). Samples were then centrifuged at 12000 g for 120 min at 4ºC and the filtered solution was stored at -80ºC until the sample analysis for the ^{1}H-NMR experiments.

2.3.5. ^{1}H-NMR experiments

The freeze-dried powder from FM was solubilized in 650 µL of phosphate buffer (50 mM Na_2HPO_4, pH 7.4, in D2O) containing 0.1 mM of deuterated trimethylsilyl propanoic acid (TSP-D4) as a reference standard and 550 µL were transferred to a 5 mm NMR tube. Likewise, 550 µL of supernatant, or filtered from UM and UUM, were transferred to independent 5 mm NMR tubes. All the samples (FM, UM, or UUM method) were stored at 4ºC, equilibrated at room temperature for 15 min before analyzing, which took place on the same day. The ^{1}H-NMR spectra of extracts were recorded at 300K by a Bruker AVANCE III 600.13 MHz spectrometer, equipped with 5 mm triple-

resonance z-gradient cryoprobe (Prodigy® TCI, 1H-13C/15N-2H). TopSpin, version 3.6.2 (Bruker GmbH, Karlsruhe, Germany), was used for spectrometer control purposes. ^{1}H 1D Nuclear Overhauser Effect Spectroscopy (NOESY) NMR spectra, with water presaturation and spoil gradients (*noesygppr1d* pulse sequence), were acquired with 256 free induction decays (FIDs), 64k data points, a spectral width of 30 ppm, and a relaxation delay of 60 s. Total Correlation Spectroscopy (TOCSY) and multiplicity Heteronuclear Single Quantum Correlation (HSQC) were performed on representative samples with 256–512 t1 increments, 32–96 transients and a relaxation delay of 1.5 s. The TOCSY spectra were recorded by a standard MLEV-17 pulse sequence with mixing times (spin-lock) of 65 ms.

2.3.6. Data analysis and statistics

NMR spectra processing: ^{1}H-NMR spectra were transformed with a 0.5 line-broadening, and manually baseline- and phase-corrected with Topspin 4.0.9. NMR signals of TSP-D4 were referenced to 0 ppm. For metabolite identification purposes, the ^{1}H and chemical shift values and multiplicity of signals were compared with the reference data from the Chenomx® software (Chenomx NMR Suite 8.4, Chenomx Inc., Edmonton, Canada) in combination with spectral databases Human Metabolome Database and the Biological Magnetic Resonance Bank and several literature reports [33,60]. Optimal integration regions were defined for each metabolite in an attempt to select signals without overlapping. Integration was performed with MestreNova 14 (Mestrelab Research, SL, Santiago de Compostela, Spain) by performing a manual integration of the previously identified signals. With these regions, an integration matrix (Integral Regions) was built, which was later applied to the 27 acquired spectra and a matrix of integrals was built for all the spectra (Integral series). This matrix of integrals was normalized by the sum of the total signals of the spectrum using Excel® (Microsoft, USA).

Quantification and comparison of Metabolic Profiles: An analysis of the areas of every variable (metabolite) was carried out for each method (FM, UM and UUM) in the 27 spectra analyzed as follows: measures of central tendency (mean or median) were determined with Excel®, and statistical assumptions of normality (Shapiro-Wilk Normality Test) and homoskedasticity (Levene test) were evaluated with RStudio. To determine the difference in the measures of central tendency between the methods, a comparison of the gold standard for the processing of biological samples (FM) with the developed methods (UM and UUM) was made. Resulting in two comparisons, FM versus UM and FM versus UUM. The difference in measures of central tendency was determined as appropriate; mean difference using t-Test for paired

samples (if the variable in both methods had normal distribution and homoskedasticity) or median difference using Wilcoxon Test for k paired samples (if the variable in one of the methods had non normal distribution and/or heteroskedasticity). For tests with a p value less than 0.05 ($p<0.05$), a statistically significant difference between the means (mean or median as appropriate) is assumed for the variable evaluated. This last statistical test was performed with the RStudio software.

Analysis of repeatability and reproducibility: The *Six Sigma Gage R&R Measure* (Part of the Six Sigma package of the R software) was applied to evaluate repeatability and reproducibility of three methods. The analysis was performed with the three patient samples analyzed on different days and by different analysts. A total of 18 samples were analyzed, 1 sample per patient, per day and per method, in 2 evaluation days. The input data were the variables that presented statistically significant changes ($p<0.05$) in the central (measures of central tendency) difference test (t-Test or Wilcoxon Test as applicable). The coefficient of variation (CV) per variable of each method was compared. The repeatability of the methods was analyzed by determining the CV between replicates of the same patient, analyzed by NMR on the same day and processed by the same analyst. On the other hand, for the reproducibility analysis, the CV was determined between samples from the same patient, analyzed by NMR but processed in two days and by different analysts. Results were represented graphically.

Determination of limit of detection and limit of quantitation: Three regions were selected in the NMR spectrum (0.5 ppm, 6.5 ppm, 9.5 ppm) and had the lowest possible noise or interference level. The integration process of these regions was carried out (in the same way as with the other metabolites in the samples) in the 27 spectra analyzed, and the limit of detection (LOD) and the limit of quantification (LOQ) of all three methods (FM, UM and UUM) were determined. All the statistical analyses were performed with the RStudio and Excel software.

2.4. Results

2.4.1. Optimization of the pretreatment of samples and metabolite extraction

Equal amounts of isolated PBMCs were processed by the new protocols (Figure 2.1) and the results were compared to the Folch method (FM) [50,51], which is widely used in mammalian cell metabolomics and has been previously applied to PBMCs [38]. In the new methods, cells were mixed with an aqueous buffer, and not with toxic solvents, such as methanol and chloroform in FM. Then cycles of freezing and cell disruption with a high-intensity sonicator were applied to the

cell suspension, and the resulting supernatant was transferred directly to an NMR tube to be analyzed (in the UM method).

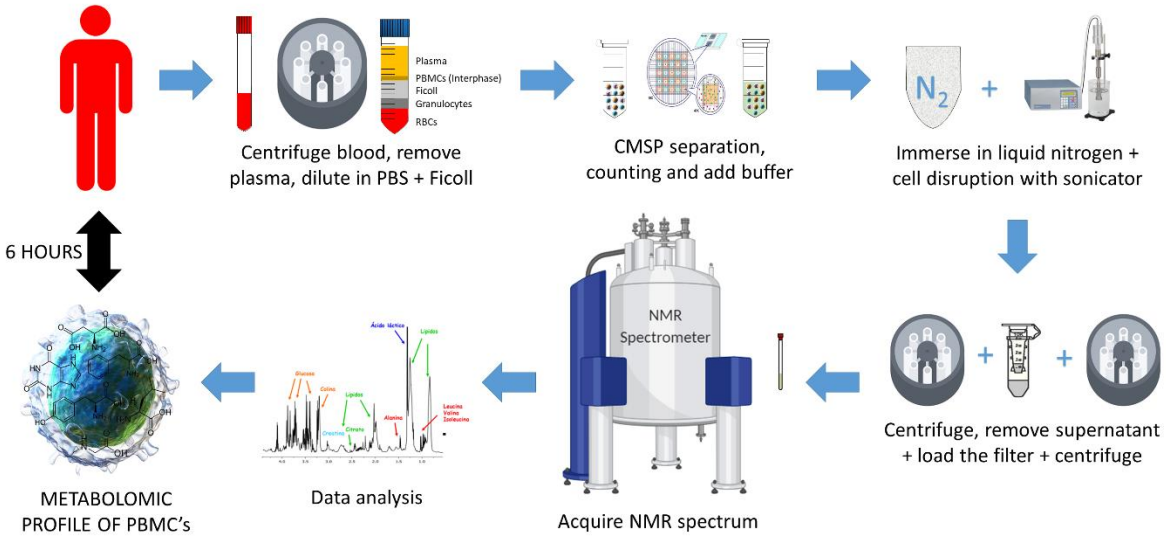

Figure 2.1. Step by step UUM method. Schematic explanation of PBMC processing by the UUM method (Ultrasound and Ultrafiltration Method). Using these methods, it is possible to obtain the metabolomic profile in 6 h starting from whole blood. The PBMC samples were isolated from the peripheral blood of healthy human individuals. Samples were split into an aliquot (12.5 million cells) for characterization. Finally, PBMC were extracted and the ^{1}H-NMR metabolic profiles were determined.

The cell freezing and disruption processes were optimized as follows: starting with a simple cycle to immerse the sample into liquid nitrogen (1 min), combined with high-intensity ultrasound at 20,050 Hz, and 50% amplitude for 5 min (in a cold bath at 4ºC). However, under these conditions, the necessary cell disruption was not achieved as verified by visual inspection and a microscope. Therefore, the parameters of the ultrasound equipment were increased from 50% to 100% of the amplitude for the same period time. The number of cycles (freezing + cell disruption by ultrasound) was increased one by one until six cycles, which was the amount required to achieve a successful quenching and extracting process with the sample. For the UM centrifugation process, we based our work on previous cell disruption and metabolite isolation protocols [46,47]. However, we had to apply more time and more power during centrifugation to eliminate membranes and cell debris as the volume of PBMC cells is much smaller than most other cells (e.g., HeLa cells have an average volume of 3000 µm3, while the volume of PBMCs is only 130 µm3). We determined that a cycle of 12000 g for 120 min at 4ºC would be required to separate the pellet from the solution.

An increase in centrifugation force or time did not improve the subsequent NMR results, and shorter centrifugation times did not achieve optimal cell pellet separation. When analyzing the UM ^{1}H-NMR spectra results, we detected the presence of proteins in the spectrum, which is a generally undesirable characteristic for metabolomic profiling. Therefore, as a second option, the suspension was first transferred to a centrifugal filter to eliminate proteins, re-centrifuged and then moved to an NMR tube (for the UUM method). In both cases (methods UM and UUM), an NMR spectrum was obtained for PBMCs in less than 6 h, while FM required several hours for solvent elimination by freeze-drying and evaporation.

2.4.2. Metabolic profile of PBMCs

The representative ^{1}H-NMR spectra resulting from the three tested methods are shown in Figure 2.2. An assignment of the different signals in the spectra was performed with the help of 2D-NMR spectra, and with information available from public databases, the software Chenomx 8.6 (Alberta, Canada) and existing literature about the metabolic content of PBMCs [38]. As a result, it was possible to identify more than 40 different metabolites (Figure 2.3). The primary metabolites were organic acids, amino acids and nucleotides.

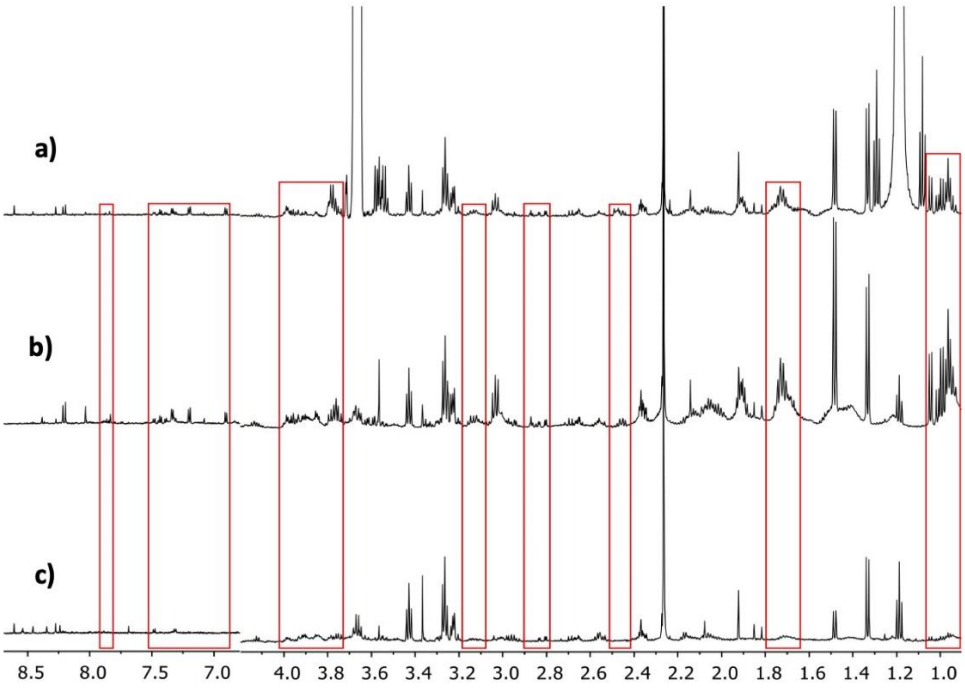

Figure 2.2. Comparison of the spectra obtained from the three different PBMC processing methods evaluated for metabolomic profiling. a) Ultrasound and Ultrafiltration Method, b) Ultrasound Method, c) Folch Method. The differences in specter regions between methods are seen in red boxes.

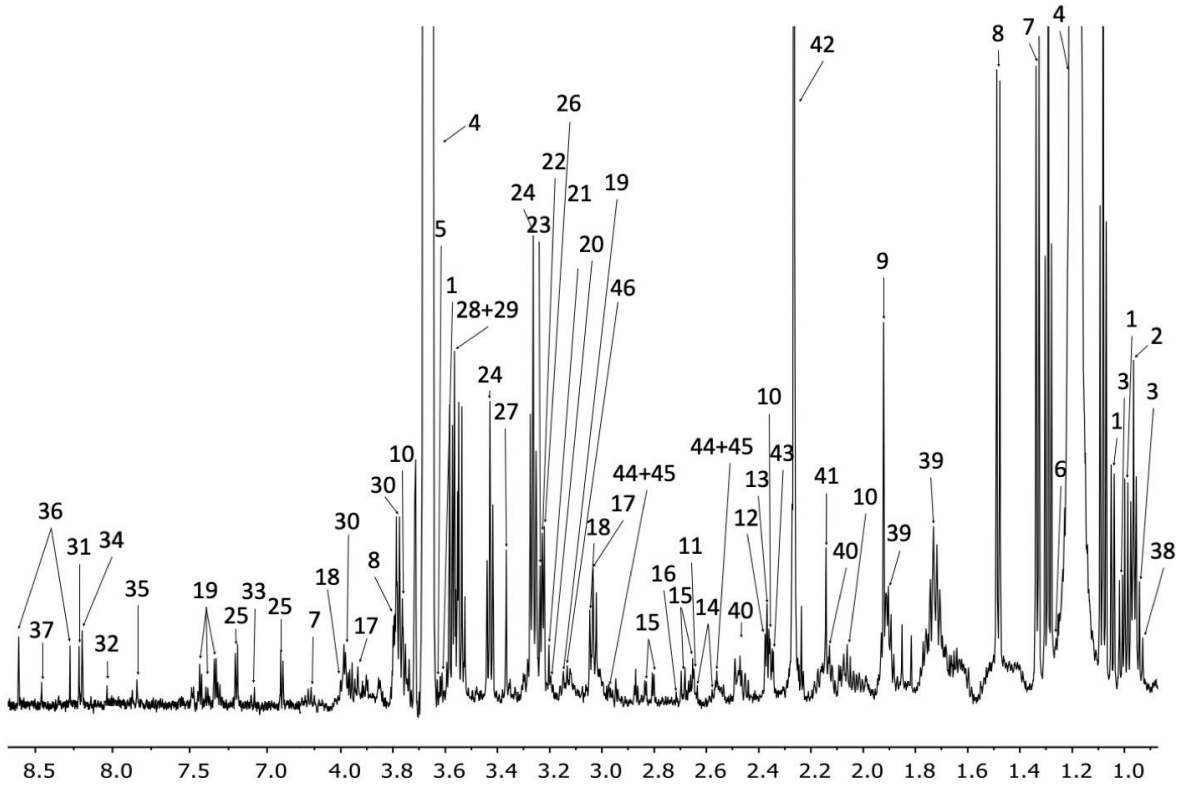

Figure 2.3. The assigned UUM ^{1}H-NMR spectrum of PBMCs. Metabolite assignments are indicated by the numbers 1. Valine, 2. Leucine, 3. Isoleucine, 4. Ethanol, 5. Threonine, 6. 3-Hydroxyisovalerate, 7. Lactate, 8. Alanine, 9. Acetate, 10. Glutamate, 11. Methionine, 12. Pyruvate, 13. Succinate, 14. Citrate, 15. Aspartate, 16. Sarcosine, 17. Creatine, 18. Creatinine, 19. Phenylalanine, 20. Choline, 21. O-Phosphocoline, 22. Carnitine, 23. Betaine, 24. Taurine, 25. Tyrosine, 26. Trimethylamine N-oxide, 27. Methanol, 28. Glycine, 29. Glycerol, 30. Serine, 31. Inosine, 32. GTP, 33. Xanthurenate, 34. Oxypurinol, 35. Xanthine, 36. AMP, 37. Formiate, 38. 2-hydroxybutyrate, 39. Lysine, 40. Glutamine, 41. Hydroxyacetone, 42. Acetoacetate, 43. Methylacetoacetate, 44. Reduced glutathione (GSH), 45. Oxidized glutathione (GSSG), 46. Malonate, 47. Trimethylamine.

A comparison of the metabolites that could be quantified and identified in the spectra resulting from each extraction method is found in Table 1. For FM, 37 metabolites, consisting in 17 organic acids, 18 amino acids and two nucleotides, were identified. For UM and UUM, 43 metabolites consisting in 19 organic acids, 19 amino acids and five nucleotides, were identified.

Table 2.1. List and detail of the metabolites assigned in the different evaluated methods evaluated

METABOLITE	δ in ppm (Multiplicity)	CT	GA (Visual)			FO (%)		
			FM	UM	UUM	FM	UM	UUM
2-hydroxybutyrate	0,89 (t), 1.61 (m), 1.65 (m),	OA	+	+	+	100	100	100
3-Hydroxyisovalerate	1.25 (s)	OA	+	+	+	100	100	100
Acetate	1.92 (s)	OA	+	+	+	100	100	100
Acetoacetate	2.26 (s)	OA	+	+	+	100	100	100
Alanine	1.48 (d), 3.80 (q)	AA	+	+ +	+ +	100	100	100
AMP	8.27 (s), 8.61 (s)	N	+	+	+	100	100	100
Aspartate	2.67 (m), 2.81 (m)	OA	+	+	+	100	100	100
Betaine	3.24 (s), 3.89 (s)	AA	+	+ +	+ +	100	100	100
Carnitine	3.23 (s)	AA	+	+	+	100	100	100
Choline	3.20 (s), 4.04 (m)	OA	+	+	+	100	100	100
Citrate	2.56 (d), 2.63 (d)	OA	+	+	+	100	100	100
Creatine	3.03 (s), 3.92 (s)	AA	+	+ +	+	100	100	100
Creatinine	3.05 (s), 4.01 (s)	AA	+	+ +	+ +	89	100	100
Formiate	8.46 (s)	OA	-	+	+	33	100	100
Glutamate	2.05 (m), 2.36 (m), 3.76 (m)	OA	+	+	+	100	100	100
Glutamine	2.12 (m), 2.48 (m)	AA	-	+	+	44	100	100
Glycine	3.57 (s)	AA	+	+ +	+ +	100	100	100
GSH+GSSG	2.53-2.58 (m), 2.96 (dd)	AA	+	+	+	100	100	100
GTP	8.03 (s)	N	O	+ +	+	33	100	89
Hydroxyacetone	2.14 (s)	OA	+	+ +	+ +	100	100	100
Inosine	6.14 (d), 8.19 (s), 8.22 (s)	N	+	+	+	78	100	100
Isoleucine	0.94 (t), 1.01 (d)	AA	+	+	+	100	100	100
Lactate	1.33 (d), 4.11 (q), 4.12 (q), 4.13 (q)	OA	+	+	+	100	100	100
Leucine	0.96 (t)	AA	+	+ +	+ +	100	100	100
Lysine	1.72 (m), 1.91 (m)	AA	+	+ +	+ +	100	100	100
Malonate	3.13 (s)	OA	-	+	+	89	100	100
Methionine	2.17 (m), 2.65 (t), 3.85 (dd)	AA	+	+	+	100	100	100

Methylacetoacetate	2.34 (s)	OA	+	+	+	100	100	100
O-Phosphocoline	3.21 (s)	AA	+	+	+	100	100	100
Oxypurinol	8.38 (s)	N	O	+	+	33	100	78
Phenylalanine	3.14 (m), 3.30 (m), 7.34 (d), 7.38 (d), 7.43 (t)	AA	-	+	+	44	100	100
Pyruvate	2.38 (s)	OA	+	+	+	100	100	100
Sarcosine	2.72 (s)	AA	-	+	-	56	100	44
Serine	3.79 (dd), 3.99 (m)	AA	-	+	+	100	100	100
Succinate	2.37 (s)	OA	+	+	+	100	100	100
Taurine	3.26 (t), 3.43 (t)	OA	+	+	+	100	100	100
Treonine	3.59 (d), 4.22 (m)	AA	+	+	+	78	100	56
Trimethylamine	2.87 (s)	OA	O	+ +	+	56	100	100
Trimethylamine N-oxide	3.22 (s)	OA	+	+	+	100	100	100
Tyrosine	3.96 (dd), 6.90 (d), 7.20 (d)	AA	O	+ +	+	22	100	100
Valine	0.99 (d), 1.04 (d), 2.29 (m), 3.62 (d)	AA	+	+ +	+ +	100	100	100
Xanthine	7.83 (s)	N	O	+ +	+	33	100	100
Xanthurenate	7.08 (dd)	OA	O	+ +	+	33	100	100

FM: Folch Method, UM: Ultrasound Method, UUM: Ultrasound and Ultrafiltration Method, δ: chemical shift, (s): singlet, (d): duplet, (dd): double doublet, (t): triplet; (q): quartet, (m): multiplet, CT: Compound Type, OA: Organic Acid, AA: Amino Acid, N: Nucleotide, GA: Graphical Analysis, +: Present, ++: Increased presence O: Absent, -: Unquantifiable, FO: frequency of occurrence. For FO less than or equal to 33%, the individual integration values were evaluated to define presence or absence. If the integration mean was less than 0, it was determined as absent in the method samples.

It should also be noted that not all the metabolites identified in spectra had an optimal quantification quality for the later metabolomics analysis. In Table 1, the quality of the signals from each metabolite in all the methods is classified (present, increased presence, absent, unquantifiable). The most noteworthy case was FM, for which 37 metabolites were identified, but only 31 were quantifiable (Table 1).

2.4.3. Quantitative comparison of the PBMCs Metabolomic Profiles

The normalized concentration values of the all metabolites, See **Supplementary Table 1 and Supplementary Table 2 (Anexo 2)** were compared by applying a Student's t-Test (normal

distribution and homoscedasticity) or a Wilcoxon Test (non normal distribution and/or heteroskedasticity). From this analysis, the number of metabolites lowered to 20, for which statistically significant differences were found for both comparisons. The results presented in Table 2 show the differences obtained between the means of the two established comparisons FM vs. UM and FM vs. UUM.

Table 2.2. Metabolites significant for the comparisons between FM vs. UM and FM vs. UUM.

Metabolite	FM		UM		UUM		FM	UM	UUM	LT	FM vs UM	FM vs UUM	Variation	
	Mean	Med	Mean	Med	Mean	Med	S-W p-Value	S-W p-Value	S-W p-Value	p-Value	Mean Comparison	Mean Comparison	FM vs UM	FM vs UUM
2-hydroxybutyrate	5.50	4.76	13.88	14.85	16.15	17.87	0.615	0.105	0.113	0.066	1.75.E-04	7.39.E-04	↓	↓
Alanine	18.87	16.30	43.88	38.92	35.39	29.71	0.141	0.070	0.106	0.260	4.64.E-06	6.85.E-04	↓	↓
AMP	4.87	4.86	1.60	1.44	2.03	1.89	0.483	0.545	0.748	0.171	1.53.E-05	5.73.E-05	↑	↑
Carnitine	15.18	15.88	8.44	8.39	10.98	11.15	0.085	0.848	0.120	0.099	4.06.E-06	6.97.E-04	↑	↑
Choline	7.12	6.01	4.67	4.96	5.83	5.14	0.225	0.207	0.283	0.161	2.32.E-02	4.90.E-02	↑	↑
Citrate	12.43	12.45	9.25	9.10	4.58	4.71	0.839	0.600	0.319	0.038	1.95.E-02	3.91.E-03	↑	↑
Creatine	2.20	1.79	9.97	10.09	6.02	7.06	0.047	0.032	0.281	0.197	3.91.E-03	3.91.E-03	↓	↓
Creatinine	1.80	1.43	6.21	6.38	4.19	4.53	0.057	0.166	0.133	0.083	2.85.E-06	3.25.E-05	↓	↓
Glutamate	36.55	33.61	64.27	63.90	18.37	17.75	0.119	0.065	0.804	0.318	1.38.E-06	9.07.E-07	↓	↑
GSH+GSSG	6.11	6.09	10.22	10.44	1.91	2.30	0.983	0.467	0.473	0.542	2.50.E-03	5.40.E-04	↓	↑
Hydroxyacetone	5.16	5.09	8.18	8.12	6.87	6.83	0.444	0.445	0.583	0.069	4.13.E-08	1.33.E-04	↓	↓
Inosine	1.07	0.94	3.10	3.17	3.42	3.33	0.590	0.120	0.481	0.029	3.91.E-03	3.91.E-03	↓	↓
Isoleucine	2.88	2.52	9.10	8.44	7.07	4.52	0.282	0.014	0.006	0.145	3.91.E-03	3.91.E-03	↓	↓
Leucine	14.67	12.12	42.93	40.20	28.11	22.97	0.007	0.131	0.039	0.686	3.91.E-03	3.91.E-03	↓	↓
Lysine	32.74	27.16	94.86	90.05	60.29	55.44	0.010	0.090	0.445	0.589	3.91.E-03	3.91.E-03	↓	↓
Methionine	13.39	12.55	11.04	10.56	7.70	7.61	0.745	0.006	0.183	0.198	7.81.E-03	1.28.E-05	↑	↑
Methylacetoacetate	1.19	1.00	2.61	2.67	0.73	0.66	0.050	0.328	0.149	0.445	7.81.E-03	2.73.E-02	↓	↑
Taurine	51.04	50.39	21.06	19.64	40.21	38.88	0.570	0.018	0.179	0.154	3.91.E-03	1.10.E-03	↑	↑

Trimethylamine N-oxide	13.04	13.57	7.26	6.56	8.27	8.51	0.061	0.029	0.533	0.000	3.91.E-03	3.91.E-03	↑	↑
Valine	3.69	3.08	12.08	10.46	11.16	7.35	0.027	0.182	0.004	0.155	3.91.E-03	3.91.E-03	↓	↓

FM: Folch Method, UM: Ultrasound Method, UUM: Ultrasound and Ultrafiltration, Med: Median, S-W p-Value: Shapiro-Wilk (Normality Test) p-Value, LT: Levene test (Homoskedasticity test), Mean comparison: using t-test or Wilcoxon test, Variation: ↓ (Smaller area or relative concentration in the reference method) ↑ (Bigger area or relative concentration in the reference method).

For a more detailed analysis, eight representative metabolites with isolated well-defined signals in all the spectra were selected (Valine, Alanine, Hydroxyacetone, Creatine, Creatinine, Choline, Taurine, Inosine). A repeatability and reproducibility analysis of each method was carried out by the Six Sigma Gage R&R Measure command. The results of this analysis are shown in Figure 2.4 and **Supplemetary Figures 1-8 (Anexo 3)**.

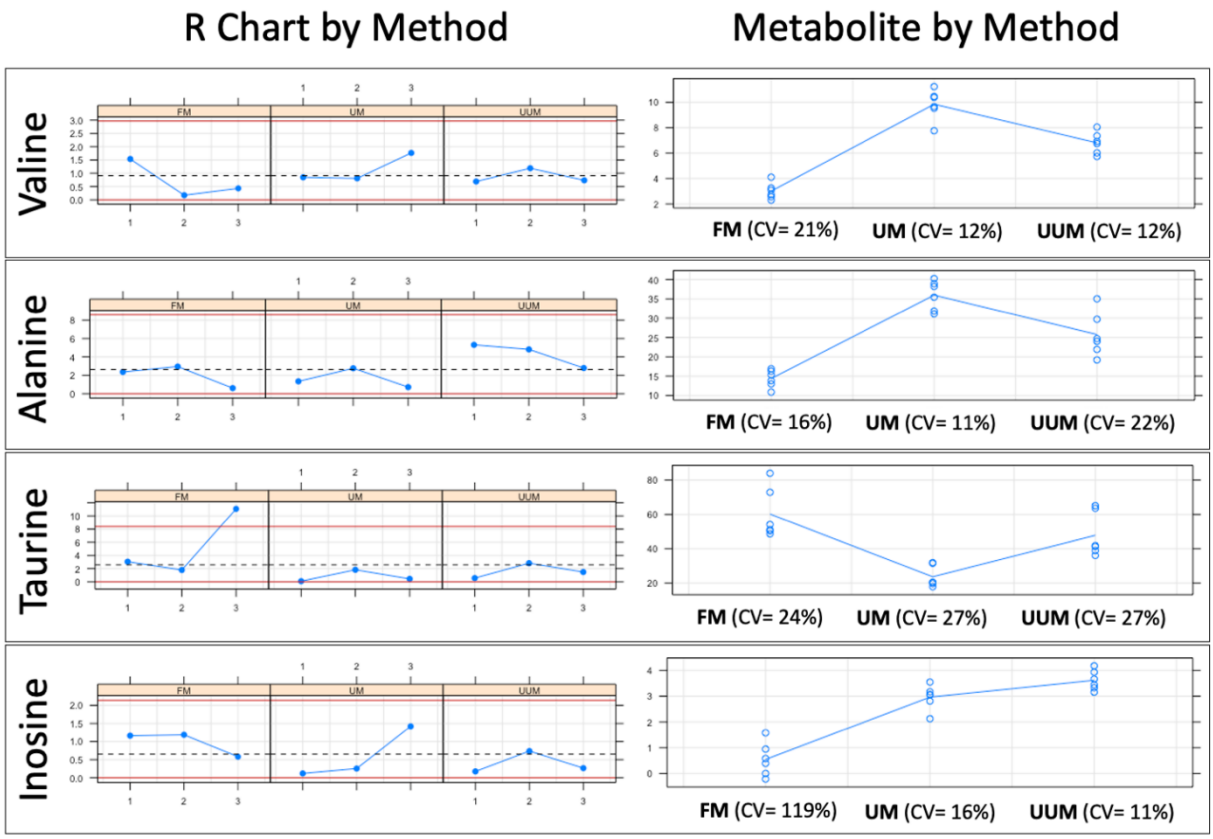

Figure 2.4. Six Sigma Gage R&R Measure. A comparative repeatability and reproducibility analysis (FM vs. UM vs. UUM) for metabolites Valine, Alanine, Taurine and Inosine was carried out using the Six Sigma tool from RStudio. FM: Folch Method, UM: Ultrasound Method, UUM: Ultrasound and Ultrafiltration Method, R Chart by Method: Range chart by method (Numbers 1, 2, and 3 on the x-axis: Patients evaluated; Differences in normalized concentration values on the y-axis), Metabolite by Method: Metabolite concentration of samples by method (Methods evaluated on the x-axis; Normalized concentration values on the y-axis), CV: coefficient of variation as a percent.

In Figure 2.4, the graphs on the left represent the range control chart evaluated per metabolite with their corresponding control limits adapted for R&R studies. In a method or process with good repeatability, all the points should lie within the control limits. For the FM method, a point (Taurine concentration range of patient 3) is observed outside the upper control limit. In addition, FM has ranges and, therefore, the dispersion of the values between the replicates for the same patient are wider than those presented in methods UM and UUM. For this reason, we can affirm that UM and UUM are methods with greater repeatability than FM.

The graphs on the right show all the measurement points (Concentration of each metabolite) by method (x-axis). The tracer line represents the mean of each one. These graphs allow an analysis of the methods' reproducibility as the dispersion of the data between patients can be observed on different days for each method. The graphs show how data dispersion (scattered points on the y-axis of each inflection point of the tracer line) for FM is generally wider compared to UM and UUM. This was confirmed by comparing the coefficients of variation (CV) for each method, which are observed at the bottom of each graph per evaluated metabolite. Once again, FM has higher CVs for most of the metabolites evaluated against UM and UUM, with an average CV of 45%, compared to 16% and 18% for UM and UUM, respectively. To further complete this numerical comparison, we also made a graphical comparison by overlapping the zoomed signals of the selected metabolites, as depicted in Figure 2.5 and Figure 2.6.

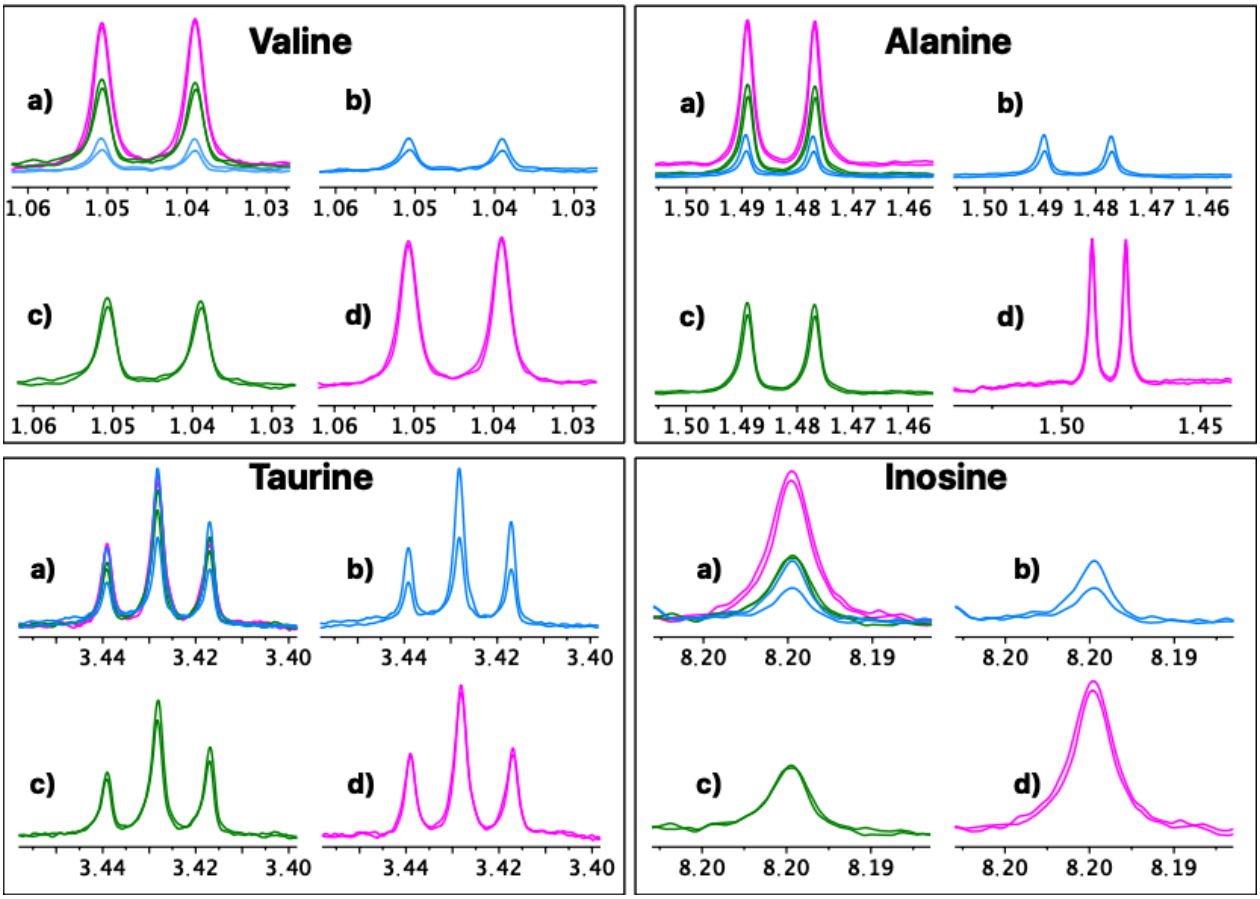

Figure 2.5. Comparative repeatability graphical analysis (FM vs. UM vs. UUM) for metabolites Valine, Alanine, Taurine and Inosine. a) Three overlapping methods, b) Folch method, c) Ultrasound and ultrafiltration method, d) Ultrasound method. A duplicate spectrum, acquired for the same patient and on the same day, is shown for each method.

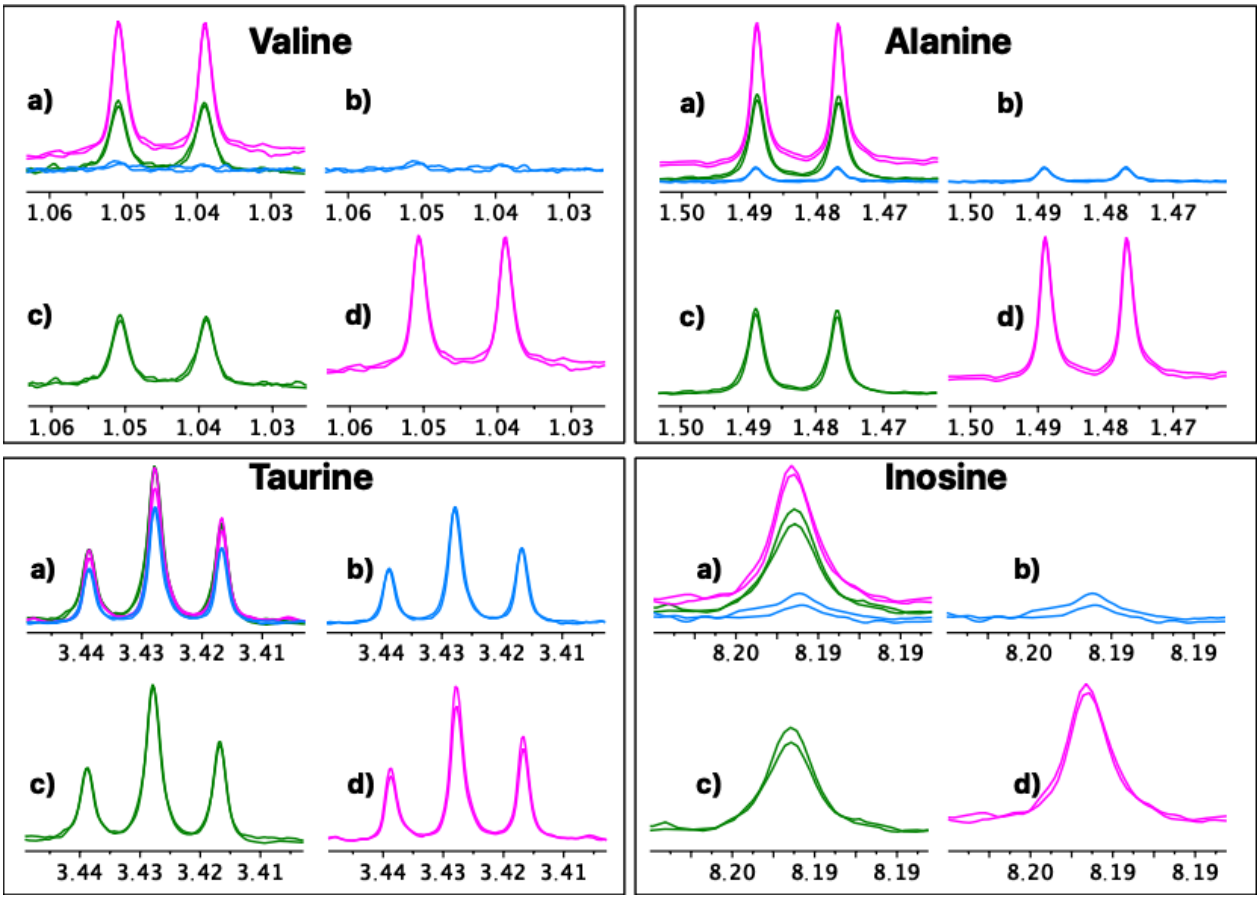

Figure 2.6. Comparative reproducibility graphical analysis (FM vs. UM vs. UUM) for metabolites Valine, Alanine, Taurine and Inosine. a) Three overlapping methods, b) Folch method, c) Ultrasound and ultrafiltration method, d) Ultrasound method. For each method a duplicate spectrum is shown for the same patient but processed on different days.

Finally, we also calculated the LOD and LOQ of the three methods, as presented in Figure 2.7. Once again, we obtained better results for UUM and UM than for FM, and slightly better results for UUM than for UM. This result was expected as we were able to identify and quantify more metabolites with methods UUM and UM.

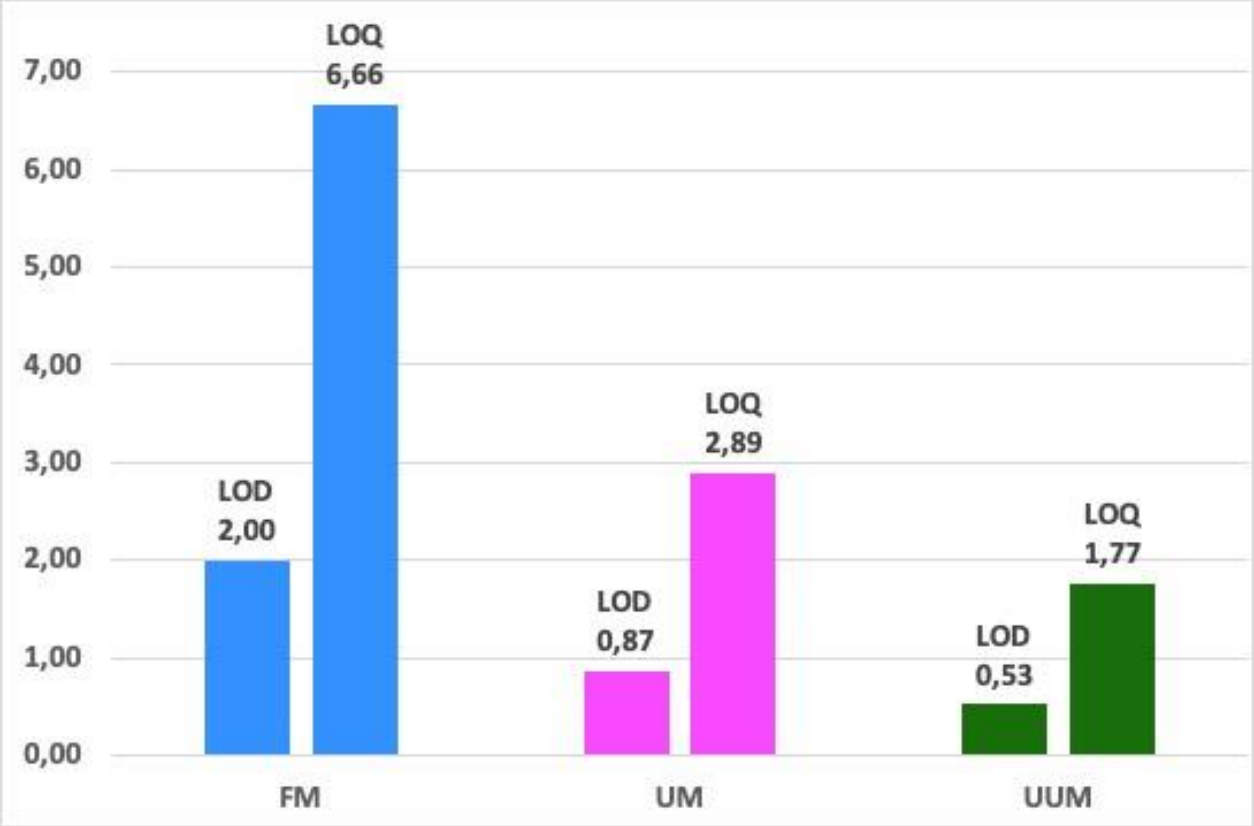

Figure 2.7. Sensitivity comparison of the FM, UM and UUM methods with the limit of detection and limit of quantification. Calculated by the standard deviation (LOD=3xSD and LOQ=10xSD) of the integrals of the three selected noise regions of the spectrum (0.5 ppm, 6.5 ppm and 9.5 ppm) for all the spectra of each method. Normalized concentration values on the y-axis.

2.5. Discussion

In this work, we present two new methods for determining the metabolic profile of PBMCs by NMR, which were compared with the FM method by evaluating processing and quality parameters. As a quantitative comparison proved (Table 2), significant differences in the normalized metabolite concentration between the new methods (UM and UUM) and the FM method existed. It is worth mentioning that these analyzes were performed with a small sample size, which may affect the power of the statistical tests performed. For example, the normality test (Shapiro-Wilk test) was used as a means to select whether to take a parametric or non-parametric approach to testing the hypothesis and contrast the methods and its metabolites. In these case, normality and t test have

little power to reject the null hypothesis because small samples most often pass normality tests. But, both tests are designed to achieve reliable results with small sample sizes. (n<30) [61].

In Table 3, we present a comparison of the main parameters of the three methods (FM, UM, UUM). Our results suggest that the best method to analyze PBMCs for NMR metabolomic profiling was UUM for sensitivity, repeatability and reproducibility, but also processing time and robustness (related to the number of steps to be performed).

Table 2.3. General comparison of the three methods tested for the metabolomics profiling of PBMCs by NMR.

FEATURE	Method		
	FM	**UM**	**UUM**
Number of cells	12.5 million cells	12.5 million cells	12.5 million cells
Processing time	16 hours	4 hours	6 hours
Processing steps	7	4	5
Lyophilization	Yes	No	No
Presence of Protein	No	Yes	No
Solvents	Methanol, H_2O, $CHCl_3$	H_2O	H_2O
Amount of metabolites (detected–quantifiable)	37 - 31	43 - 43	43 - 42
R&R test[1]	36%	15%	23%
Repeatability[2]	10%	3%	3%
Reproducibility[3]	30%	5%	10%
Limit of detection[4]	2.00	0.87	0.53
Limit of quantification[4]	6.66	2.89	1.77

FM: Folch Method, UM: Ultrasound Method, UUM: Ultrasound and Ultrafiltration Method, +: Acceptable, ++: Good, +++: Very good. [1]Overall Coefficient of Variation for the R&R test for the eight evaluated metabolites. [2]Coefficient of variation between replicates of the same patient (processed on the same day) for the concentration of the eight evaluated metabolites (as an average of individual CVs), [3]Coefficient of variation between replicates of the same patient (processed on two different days) for the concentration of eight evaluated metabolites (as an average of individual CVs), Calculated with the standard deviation (LOD=3xSD and LOQ=10xSD) of the integrals of the three selected noise regions of the spectrum (0.5 ppm, 6.5 ppm, 9.5 ppm) for all the spectra from each method.

Of the advantages that the new method offers, it is worth highlighting the fewer PBMCs required to obtain quantifiable results. A previous work has employed 20 million cells [38], which is twice the number of cells herein used, but with similar spectral quality. When working with 12.5 million of PBMCs, we obtained a better LOQ and LOD with the new methods UM and UUM *versu*s FM, which identified more metabolites (43, 43 and 37, respectively), and, most importantly, many more quantifiable metabolites (43, 42 and 31, respectively). This increase in the number of metabolites means more variables to be analyzed in a metabolomic study and, therefore, an increased probability of identifying a biomarker and metabolic pathway associated with a biological process or medical condition, which summarizes the goal of metabolomics. However, it should be noted that the use of centrifugal filters caused two unwanted signals to appear in the spectrum that resulted from the filter's own composition (Glycerol at 3.56 ppm) or the washing solution (Ethanol at 3.67 ppm), as seen in the UUM spectrum in Figure 2.2. Fortunately, these signals did not overlap the signals of the other metabolites detected in the spectrum from UUM.

Furthermore, FM is very efficient in removing metabolites that could interfere with the analysis and are present in the biological matrix (proteins, lipids, and other interferences). Therefore, it has an advantage over the UM method, where it was still possible to observe wide bands of protein and lipoprotein signals (see the red boxes in the spectrum, panels b, and c of Figure 2.2) that markedly overlap the metabolite signals in the ^{1}H-NMR spectrum. This overlapping could hinder a correct integration of the signals of the individual metabolites, requiring a deconvolution process for a correct quantification. However, this advantage was not present compared to the UUM method, where the additional filtration process in the centrifugal filters eliminated all interferences with a superior quality spectrum and better line base (see the red boxes in the spectrum, panels a and c of Figure 2.2). Moreover, the increased additional signal-to-noise ratio of the spectra obtained with the UUM method compared with FM, enhances a correct integration and quantification of the signals.

It is also interesting to focus on the extraction and lysis processes required to obtain samples for NMR-based metabolomic profiling. These workups are often the most laborious and rate-limiting steps in metabolomics because they require accuracy, repeatability and reproducibility, as well as robustness. To date, several rigorous studies recommend the use of the methanol–chloroform–water mixture (FM) to extract the largest number of metabolites with repeatability [62,63]. However, following FM is associated with many sequential manipulations (i.e., quenching, multiple lysis, centrifugation, solvent elimination, sample drying, etc.) that significantly increase the risk of experimental errors or the introduction of variability. Instead, the methods herein developed (UM and UUM) involve fewer steps (i.e., simultaneous quenching-lysis-extracting cycles, centrifugation and ultrafiltration), which take place in the same container and minimize the risk of sample loss. Both UM and UUM provided higher reproducibility and repeatability of the results compared to FM, as represented in Figures 2.4-2.6.

Moreover, the processing time is another crucial variable. Table 3 denotes how FM takes 2-5-fold longer than UUM and takes 4-fold longer than UM; this is translated into higher sample handling costs and fewer samples analyzed per day. The latter is perhaps the most critical variable in clinics where many samples have to be evaluated, and the results need to be obtained in the shortest possible time. In addition, the need to use toxic solvents (methanol and chloroform) and disposable materials increases the cost of FM. While processing a sample by FM, water, methanol, chloroform, buffer, and at least three centrifuge tubes, are required. With UM, only buffer and one centrifugal tube are needed. UUM requires an additional centrifugal filter, which slightly increases the price of this process compared to UM. FM involves using a freeze dryer, an instrument with a relatively high cost compared to the ultrasound probe required for UM and UUM. The metabolites detected from PBMCs can provide valuable information to diagnose and manage diseases given their nature and function in the human body. The immune system involves two fundamental types of responses in which PBMCs perform functions: the humoral response (Humoral Immunity) and the cell-mediated one (Cellular immunity). These responses are related to the activation of T- and B-lymphocytes. Likewise, in immune defense lines (the innate and adaptive immune systems), PBMCs also play a role. In the innate system, in which cells perform an effector function without requiring specific antigen recognition, NK cells perform related functions, whereas dendritic cells (a type of PBMCs) form a critical interface between both innate and adaptive systems. It should be noted that the medical and therapeutic interest in PBMCs, which has led to state-of-the-art developments in the field of stem cells using a fraction of PBMCs from a single donor, lies in the generation of induced pluripotent stem cells (iPSC), which is extremely relevant in personalized medicine. Moreover, there have been more recent

developments, which aim to treat human cancers without a compatible donor by using genome editing technology, such as CRISPR / Cas9, to transform T-cells into CAR-T cells [64]. When the aim is to acquire information about changes in the metabolic state of cells, as is the case of PBMCs, metabolomic profiling by NMR is an analysis method that allows the non-targeted characterization of a large number of different metabolites in a single analysis. This metabolomic technique provides data that can be used in combination with other omics data, such as those obtained by genomics and proteomics. Taken together, these data have been applied to a wide range of *in vitro* models and have helped to better understand the metabolism of a healthy and a diseased individual [65]. Although we know that some studies exist on the metabolomic profiling of blood cells, most of them have been carried out on red blood cells (RBC) and polymorphonuclear cells (PMNs) [66–74], and very limited data about analyzing PBMCs by NMR spectroscopy from patients are available [38,75].

In future works, this method can be directly applied to perform high-throughput metabolomics analyses in clinical studies, especially for studying diseases in which the immune system plays an important role. In particular, we intend to apply it to research about the human immunodeficiency virus (HIV), to identify biomarkers and metabolic pathways associated with AIDS development.

2.6. Conclusions

This work presents a new processing method of PBMCs for metabolomic profiling by NMR spectroscopy. High quality, robust and reproducible data can be obtained from PBMC samples of 12.5 million cells (half the amount previously reported) by combining high-intensity ultrasound and centrifugal filtration. The resulting ultrasound and ultrafiltration method (UUM) is characterized by minimum sample handling (the whole process can be done in the same vial) and a short processing time (6 h vs. 16 h that the traditional method lasts). In combination with the easy availability of PBMC samples from patients, methods open up new avenues for the application of ^{1}H-NMR-based PBMC metabolomics profiling for disease diagnosis and management.

2.7. Author Contributions

Conceptualization: León Gabriel Gómez-Archila, Martina Palomino-Schätzlein, Elkin Galeano.

Data curation: León Gabriel Gómez-Archila, Martina Palomino-Schätzlein, Elkin Galeano.

Formal analysis: León Gabriel Gómez-Archila, Martina Palomino-Schätzlein.

Funding acquisition: Martina Palomino-Schätzlein, Wildeman Zapata-Builes, Elkin Galeano.

Investigation: León Gabriel Gómez-Archila.

Methodology: León Gabriel Gómez-Archila, Martina Palomino-Schätzlein, Elkin Galeano.

Project administration: León Gabriel Gómez-Archila, Elkin Galeano, Wildeman Zapata-Builes.

Resources: Wildeman Zapata-Builes, Elkin Galeano.

Supervision: Elkin Galeano.

Validation: Martina Palomino-Schätzlein.

Visualization: León Gabriel Gómez-Archila, Martina Palomino-Schätzlein

Writing - original draft preparation: León Gabriel Gómez-Archila, Martina Palomino-Schätzlein, Wildeman Zapata-Builes, Elkin Galeano.

Writing - review & editing: León Gabriel Gómez-Archila, Martina Palomino-Schätzlein, Wildeman Zapata-Builes, Elkin Galeano.

2.8. References

1. Delves PJ, Martin SJ, Burton DR, Roitt IM. Roitt's essential immunology. 2017.
2. Kleiveland CR. Peripheral Blood Mononuclear Cells BT - The Impact of Food Bioactives on Health: in vitro and ex vivo models. In: Verhoeckx K, Cotter P, López-Expósito I, Kleiveland C, Lea T, Mackie A, et al., editors. Cham: Springer International Publishing; 2015. p. 161–7.
3. Autissier P, Soulas C, Burdo TH, Williams KC. Evaluation of a 12-color flow cytometry panel to study lymphocyte, monocyte, and dendritic cell subsets in humans. Cytom Part A. 2010;77A(5):410–9.
4. Gulati P. Janeway's Immunobiology, 7th Edition by Kenneth Murphy, Paul Travers, and Mark Walport. Biochem Mol Biol Educ. 2009 Mar 1;37(2):134.

5. Corkum CP, Ings DP, Burgess C, Karwowska S, Kroll W, Michalak TI. Immune cell subsets and their gene expression profiles from human PBMC isolated by Vacutainer Cell Preparation Tube (CPT™) and standard density gradient. BMC Immunol. 2015;16(1):1–18.

6. Von Andrian UH, Mackay CR. T-Cell fuction and migration Two sides of the same coin. N Engl J Med. 2000;(10–11):338–9.

7. Delves PJ, Roitt IM. The Immune System. N Engl J Med. 2000 Jul 13;343(2):108–17.

8. Templeton AJ, McNamara MG, Šeruga B, Vera-Badillo FE, Aneja P, Ocaña A, et al. Prognostic Role of Neutrophil-to-Lymphocyte Ratio in Solid Tumors: A Systematic Review and Meta-Analysis. JNCI J Natl Cancer Inst. 2014 May 29;106(6).

9. Li M-X, Liu X-M, Zhang X-F, Zhang J-F, Wang W-L, Zhu Y, et al. Prognostic role of neutrophil-to-lymphocyte ratio in colorectal cancer: A systematic review and meta-analysis. Int J Cancer. 2014 May 15;134(10):2403–13.

10. Baine MJ, Chakraborty S, Smith LM, Mallya K, Sasson AR, Brand RE, et al. Transcriptional Profiling of Peripheral Blood Mononuclear Cells in Pancreatic Cancer Patients Identifies Novel Genes with Potential Diagnostic Utility. PLoS One. 2011 Feb 10;6(2):e17014.

11. Herazo-Maya JD, Noth I, Duncan SR, Kim S, Ma S-F, Tseng GC, et al. Peripheral blood mononuclear cell gene expression profiles predict poor outcome in idiopathic pulmonary fibrosis. Sci Transl Med. 2013 Oct 2;5(205):205ra136-205ra136.

12. Srivastava S, Macaubas C, Deshpande C, Alexander HC, Chang S-Y, Sun Y, et al. Monocytes are resistant to apoptosis in systemic juvenile idiopathic arthritis. Clin Immunol. 2010;136(2):257–68.

13. Miao Y-L, Xiao Y-L, Du Y, Duan L-P. Gene expression profiles in peripheral blood mononuclear cells of ulcerative colitis patients. World J Gastroenterol. 2013 Jun 7;19(21):3339–46.

14. Pourahmad J, Salimi A. Isolated Human Peripheral Blood Mononuclear Cell (PBMC), a Cost Effective Tool for Predicting Immunosuppressive Effects of Drugs and Xenobiotics. Iran J Pharm Res IJPR. 2015;14(4):979.

15. Steuer AE, Brockbals L, Kraemer T. Metabolomic Strategies in Biomarker Research–New Approach for Indirect Identification of Drug Consumption and Sample Manipulation in Clinical and Forensic Toxicology? . Vol. 7, Frontiers in Chemistry . 2019. p. 319.

16. Rasmussen AL, Wang I-M, Shuhart MC, Proll SC, He Y, Cristescu R, et al. Chronic immune activation is a distinguishing feature of liver and PBMC gene signatures from HCV/HIV coinfected patients and may contribute to hepatic fibrogenesis. Virology. 2012/05/16. 2012 Aug 15;430(1):43–52.

17. Sidharthan S, Kim C-W, Murphy AA, Zhang X, Yang J, Lempicki RA, et al. Hepatitis C-associated mixed cryoglobulinemic vasculitis induces differential gene expression in peripheral mononuclear cells. Front Immunol. 2014 May 27;5:248.

18. Rallon NI, Lopez-Fernandez LA, Garcia MI, Benguria A, Fiorante S, Soriano V, et al. Interferon-stimulated genes are associated with peginterferon/ribavirin treatment response regardless of IL28B alleles in hepatitis C virus/HIV-coinfected patients. AIDS. 2013;27(5).

19. Neunkirchner A, Schmetterer KG, Pickl WF. Lymphocyte-Based Model Systems for Allergy Research: A Historic Overview. Int Arch Allergy Immunol. 2014;163(4):259–91.

20. Wang X, Zhao H, Andersson R. Proteomics and Leukocytes: An Approach to Understanding Potential Molecular Mechanisms of Inflammatory Responses. J Proteome Res. 2004 Oct 1;3(5):921–9.

21. Wigren M, Nilsson J, Kolbus D. Lymphocytes in atherosclerosis. Clin Chim Acta. 2012;413(19):1562–8.

22. Bhat T, Teli S, Rijal J, Bhat H, Raza M, Khoueiry G, et al. Neutrophil to lymphocyte ratio and cardiovascular diseases: a review. Expert Rev Cardiovasc Ther. 2013 Jan 1;11(1):55–9.

23. Ishimura M, Yamamoto H, Mizuno Y, Takada H, Goto M, Doi T, et al. A Non-invasive Diagnosis of Histiocytic Necrotizing Lymphadenitis by Means of Gene Expression Profile Analysis of Peripheral Blood Mononuclear Cells. J Clin Immunol. 2013;33(5):1018–26.

24. Grigoryev YA, Kurian SM, Avnur Z, Borie D, Deng J, Campbell D, et al. Deconvoluting Post-Transplant Immunity: Cell Subset-Specific Mapping Reveals Pathways for Activation and Expansion of Memory T, Monocytes and B Cells. PLoS One. 2010 Oct 14;5(10):e13358.

25. Tan Y, Tamayo P, Nakaya H, Pulendran B, Mesirov JP, Haining WN. Gene signatures related to B-cell proliferation predict influenza vaccine-induced antibody response. Eur J Immunol. 2014 Jan 1;44(1):285–95.

26. Komatsu N, Matsueda S, Tashiro K, Ioji T, Shichijo S, Noguchi M, et al. Gene expression

profiles in peripheral blood as a biomarker in cancer patients receiving peptide vaccination. Cancer. 2012 Jun 15;118(12):3208–21.

27. Gardeux V, Bosco A, Li J, Halonen MJ, Jackson D, Martinez FD, et al. Towards a PBMC “virogram assay” for precision medicine: Concordance between ex vivo and in vivo viral infection transcriptomes. J Biomed Inform. 2015;55:94–103.

28. Kammula US, Lee K-H, Riker AI, Wang E, Ohnmacht GA, Rosenberg SA, et al. Functional Analysis of Antigen-Specific T Lymphocytes by Serial Measurement of Gene Expression in Peripheral Blood Mononuclear Cells and Tumor Specimens. J Immunol. 1999 Dec 15;163(12):6867 LP – 6875.

29. Davis JM, Knutson KL, Strausbauch MA, Crowson CS, Therneau TM, Wettstein PJ, et al. Analysis of Complex Biomarkers for Human Immune-Mediated Disorders Based on Cytokine Responsiveness of Peripheral Blood Cells. J Immunol. 2010 May 21;ji_0904180.

30. Hokayem J El, Cukier HN, Dykxhoorn DM. Blood Derived Induced Pluripotent Stem Cells (iPSCs): Benefits, Challenges and the Road Ahead. J Alzheimer’s Dis Park. 2016;6(5):5–7.

31. Martin F-PJ, Collino S, Rezzi S. 1H NMR-based metabonomic applications to decipher gut microbial metabolic influence on mammalian health. Magn Reson Chem. 2011 Dec 1;49(S1):S47–54.

32. Blow N. Biochemistry’s new look. Nature. 2008;455(7213):697–8.

33. Wishart DS, Feunang YD, Marcu A, Guo AC, Liang K, Vázquez-Fresno R, et al. HMDB 4.0: the human metabolome database for 2018. Nucleic Acids Res. 2018 Jan 4;46(D1):D608–17.

34. Yang Z. Pharmacometabolomics in Drug Discovery & Development: Applications and Challenges. J Postgenomics Drug Biomark Dev. 2012;02(05):2–4.

35. Robertson DG, Frevert U. Metabolomics in Drug Discovery and Development. Clin Pharmacol Ther. 2013 Nov 1;94(5):559–61.

36. Sitole LJ, Williams AA, Meyer D. Metabonomic analysis of HIV-infected biofluids. Mol Biosyst. 2013;9(1):18–28.

37. Aranibar N, Borys M, Mackin NA, Ly V, Abu-Absi N, Abu-Absi S, et al. NMR-based

metabolomics of mammalian cell and tissue cultures. J Biomol NMR. 2011;49(3):195–206.

38. Palomino-Schtzlein M, García H, Gutiérrez-Carcedo P, Pineda-Lucena A, Herance JR. Assessment of gold nanoparticles on human peripheral blood cells by metabolic profiling with 1H-NMR spectroscopy, a novel translational approach on a patient-specific basis. PLoS One. 2017;12(8):e0182985.

39. Shen Y, Wang J, Wang Z, Shen J, Qi T, Song W, et al. A cross-sectional study of leukopenia and thrombocytopenia among Chinese adults with newly diagnosed HIV/AIDS. Biosci Trends. 2015;9(2):91–6.

40. Zhou J-G, Tian X, Cheng L, Zhou Q, Liu Y, Zhang Y, et al. The Risk of Neutropenia and Leukopenia in Advanced Non-Small Cell Lung Cancer Patients Treated With Erlotinib: A Prisma-Compliant Systematic Review and Meta-Analysis. Medicine (Baltimore). 2015;94(40).

41. Posevitz-Fejfár A, Posevitz V, Gross CC, Bhatia U, Kurth F, Schütte V, et al. Effects of Blood Transportation on Human Peripheral Mononuclear Cell Yield, Phenotype and Function: Implications for Immune Cell Biobanking. PLoS One. 2014 Dec 26;9(12):e115920.

42. Schlenke P, Klüter H, Müller-Steinhardt M, Hammers HJ, Borchert K, Bein G. Evaluation of a novel mononuclear cell isolation procedure for serological HLA typing. Clin Diagn Lab Immunol. 1998 Nov;5(6):808–13.

43. Mckenna K, Beatty K, Vicetti Miguel R, Bilonick R. Delayed processing of blood increases the frequency of activated CD11b+ CD15+ granulocytes which inhibit T cell function. J Immunol Methods. 2008 Dec 1;341:68–75.

44. Reimann KA, Chernoff M, Wilkening CL, Nickerson CE, Landay AL. Preservation of Lymphocyte Immunophenotype and Proliferative Responses in Cryopreserved Peripheral Blood Mononuclear Cells from Human Immunodeficiency Virus Type 1-Infected Donors: Implications for Multicenter Clinical Trials. Clin Diagn Lab Immunol. 2000 May 1;7(3):352 LP – 359.

45. Brown LM, Clark JW, Neuland CY, Mann DL, Pankiw-Trost LK, Blattner WA, et al. Cryopreservation and long-term liquid nitrogen storage of peripheral blood mononuclear cells for flow cytometry analysis effects on cell subset proportions and fluorescence intensity. J Clin Lab Anal. 1991 Jan 1;5(4):255–61.

46. Matheus N, Hansen S, Rozet E, Peixoto P, Maquoi E, Lambert V, et al. An easy, convenient cell and tissue extraction protocol for nuclear magnetic resonance metabolomics. Phytochem Anal. 2014;25(4):342–9.

47. Lauri I, Savorani F, Iaccarino N, Zizza P, Pavone LM, Novellino E, et al. Development of an optimized protocol for NMR metabolomics studies of human colon cancer cell lines and first insight from testing of the protocol using DNA G-quadruplex ligands as novel anti-cancer drugs. Metabolites. 2016;6(1):1–14.

48. Kostidis S, Addie RD, Morreau H, Mayboroda OA, Giera M. Quantitative NMR analysis of intra- and extracellular metabolism of mammalian cells: A tutorial. Anal Chim Acta. 2017;980:1–24.

49. Lari Z, Ahmadzadeh H, Hosseini M. Chapter 2 - Cell Wall Disruption: A Critical Upstream Process for Biofuel Production. In: Hosseini MBT-A in FCT for AF and B, editor. Woodhead Publishing Series in Energy. Woodhead Publishing; 2019. p. 21–35.

50. Folch J, Lees M, Stanley GHS. A SIMPLE METHOD FOR THE ISOLATION AND PURIFICATION OF TOTAL LIPIDES FROM ANIMAL TISSUES. J Biol Chem . 1957 May 1;226(1):497–509.

51. Van Noorden R, Maher B, Nuzzo R. The top 100 papers. Nature. 2014;514(7524):550–3.

52. Wishart DS. Emerging applications of metabolomics in drug discovery and precision medicine. Nat Rev Drug Discov. 2016;15(7):473–84.

53. NOBLE PB, CUTTS JH, CARROLL KK. Ficoll Flotation for the Separation of Blood Leukocyte Types. Blood. 1968 Jan 1;31(1):66–73.

54. Strober W. Trypan Blue Exclusion Test of Cell Viability. Curr Protoc Immunol. 1997 Mar 1;21(1):A.3B.1-A.3B.2.

55. Strober W. Trypan Blue Exclusion Test of Cell Viability. Curr Protoc Immunol. 2015 Nov 2;111:A3.B.1-A3.B.3.

56. Louis KS, Siegel AC. Cell Viability Analysis Using Trypan Blue: Manual and Automated Methods BT - Mammalian Cell Viability: Methods and Protocols. In: Stoddart MJ, editor. Totowa, NJ: Humana Press; 2011. p. 7–12.

57. Kim JS, Nam MH, An SSA, Lim CS, Hur DS, Chung C, et al. Comparison of the automated

fluorescence microscopic viability test with the conventional and flow cytometry methods. J Clin Lab Anal. 2011 Jan 1;25(2):90–4.

58. Eggers LF, Schwudke D. Liquid Extraction: Folch BT - Encyclopedia of Lipidomics. In: Wenk MR, editor. Dordrecht: Springer Netherlands; 2016. p. 1–6.

59. Eggers LF, Schwudke D. Encyclopedia of Lipidomics. Encycl Lipidomics. 2019;3:1–6.

60. Ulrich EL, Akutsu H, Doreleijers JF, Harano Y, Ioannidis YE, Lin J, et al. BioMagResBank. Nucleic Acids Res. 2007 Nov 4;36(suppl_1):D402–8.

61. Kim TK, Park JH. More about the basic assumptions of t-test: normality and sample size. Korean J Anesthesiol. 2019/04/01. 2019 Aug;72(4):331–5.

62. Lin CY, Wu H, Tjeerdema RS, Viant MR. Evaluation of metabolite extraction strategies from tissue samples using NMR metabolomics. Metabolomics. 2007;3(1):55–67.

63. Martineau E, Tea I, Loaëc G, Giraudeau P, Akoka S. Strategy for choosing extraction procedures for NMR-based metabolomic analysis of mammalian cells. Anal Bioanal Chem. 2011;401(7):2133.

64. Cooper ML, Choi J, Staser K, Ritchey JK, Devenport JM, Eckardt K, et al. An “off-the-shelf” fratricide-resistant CAR-T for the treatment of T cell hematologic malignancies. Leukemia. 2018;32(9):1970–83.

65. Mülleder M, Calvani E, Alam MT, Wang RK, Eckerstorfer F, Zelezniak A, et al. Functional Metabolomics Describes the Yeast Biosynthetic Regulome. Cell. 2016 Oct 6;167(2):553-565.e12.

66. D’Alessandro A, Blasi B, D’Amici GM, Marrocco C, Zolla L. Red blood cell subpopulations in freshly drawn blood: Application of proteomics and metabolomics to a decades-long biological issue. Blood Transfus. 2013;11(1):75–87.

67. Catalán Ú, Rodríguez M-Á, Ras M-R, Maciá A, Mallol R, Vinaixa M, et al. Biomarkers of food intake and metabolite differences between plasma and red blood cell matrices; a human metabolomic profile approach. Mol Biosyst. 2013;9(6):1411–22.

68. Sana TR, Gordon DB, Fischer SM, Tichy SE, Kitagawa N, Lai C, et al. Global Mass Spectrometry Based Metabolomics Profiling of Erythrocytes Infected with Plasmodium falciparum. PLoS One. 2013 Apr 9;8(4):e60840.

69. D'Alessandro A, Nemkov T, Kelher M, West FB, Schwindt RK, Banerjee A, et al. Routine storage of red blood cell (RBC) units in additive solution-3: a comprehensive investigation of the RBC metabolome. Transfusion. 2015 Jun 1;55(6):1155–68.

70. Otiko G, Razi MT, Sadler PJ, Isab AA, Rabenstein DL. A 1H nmr study of the interaction of aurothiomalate ("Myocrisin") with human red blood cells in vitro. J Inorg Biochem. 1983;19(3):227–35.

71. Humpfer E, Spraul M, Nicholls AW, Nicholson JK, Lindon JC. Direct observation of resolved intracellular and extracellular water signals in intact human red blood cells using 1H MAS NMR spectroscopy. Magn Reson Med. 1997 Aug 1;38(2):334–6.

72. Brindle KM, Campbell ID, Simpson RJ. A 1H n.m.r. study of the kinetic properties expressed by glyceraldehyde phosphate dehydrogenase in the intact human erythrocyte. Biochem J. 1982 Dec 15;208(3):583–92.

73. Freikman I, Amer J, Cohen JS, Ringel I, Fibach E. Oxidative stress causes membrane phospholipid rearrangement and shedding from RBC membranes—An NMR study. Biochim Biophys Acta - Biomembr. 2008;1778(10):2388–94.

74. Wright LC, Obbink KLG, Delikatny EJ, Santangelo RT, Sorrell TC. The origin of 1H NMR-visible triacylglycerol in human neutrophils. Eur J Biochem. 2000 Jan 1;267(1):68–78.

75. Palomino-Schätzlein M, Simó R, Hernández C, Ciudin A, Mateos-Gregorio P, Hernández-Mijares A, et al. Metabolic fingerprint of insulin resistance in human polymorphonuclear leucocytes. PLoS One. 2018;13(7):1–15.

CAPÍTULO 3:

Identification of Biomarkers and metabolic pathways associated with HIV-1 infection through ^{1}H-Nuclear Magnetic Resonance metabolomics of Peripheral Blood Mononuclear Cells

Identification of Biomarkers and metabolic pathways associated with HIV-1 infection through ^{1}H-Nuclear Magnetic Resonance metabolomics of Peripheral Blood Mononuclear Cells

3.1. Abstract

HIV-1 chronically attacks the immune system, specifically targeting CD4+ T lymphocytes, monocytes and dendritic cells, which are part of Peripheral Blood Mononuclear cells (PBMC), which collectively play a crucial role in controlling infections. Therefore, HIV infection and exposure could alter cellular metabolites due to the viral pathophysiology. Metabolomics studies on these cells during HIV infection and exposure have been poorly explored. Therefore, metabolomics could explain how HIV infection leads to immunological exhaustion or cellular senescence, which leads to AIDS; likewise, metabolomics could help to find mechanisms of natural resistance to HIV infection during sexual exposure. We conducted a cross-sectional study involving 20 people living with HIV on anti-retroviral therapy (PLHIV-ART), 8 HIV-exposed but seronegative individuals (HESN) who were sexually-exposed and 20 healthy controls (HC). PBMC were isolated from the whole blood of the volunteers. Using a novel method developed in our laboratory, which employs high-intensity ultrasound for the quenching and extraction process and deproteinizing filters for the purification of the constituent metabolites of the sample, we performed metabolic profiling of the groups. As a result, we identified potential biomarkers and metabolic pathways associated with infection in PLHIV-ART and natural resistance to HIV in HESN. In PLHIV-ART, a decrease in the expression of phenylalanine and carnitine, and an increase in the expression of glycine are proposed as biomarkers of the effective response to ART. In HESN, a decreased expression of adenosine monophosphate (AMP), leucine and inosine are established as potential biomarkers of resistance to HIV-1 infection. In the PLHIV-ART group, changes in metabolic pathways had a higher impact factor and higher statistical significance than those observed in the HESN group. The phenylalanine, tyrosine and tryptophan biosynthesis pathway stands out in both groups. This is the first published research that analyzes PBMC's in these groups, and opens the door for new studies of diseases that affect the immune system using NMR metabolomics.

3.2. Introduction

The history of Human immunodeficiency virus type 1 (HIV-1) spans over 40 years, with the first case of acquired immunodeficiency syndrome (AIDS) in humans described in 1983 (Barré-

Sinoussi et al., 1983; Gallo et al., 1983). Despite extensive research, and the availability of effective treatments controlling the infection and prolonging the life expectancy of infected people (Günthard et al., 2016) a cure has not yet been found (Sankaranantham, 2019), and AIDS associated mortality continues to be a significant public health issue. HIV-1 infection occurs mainly through anal or vaginal sex or sharing needles and syringes (DeHaan et al., 2022). Regardless of the transmission route, viral particles are found in the bloodstream and they use CD4+ T lymphocytes to carry out their biological cycle, leading to viral replication, the establishment of reservoirs, and the progression of the infection (Pan et al., 2013). T lymphocytes, which regulate the adaptative response against HIV-1, belong to the Peripheral Blood Mononuclear cells (PBMC), which also includes dendritic cells and monocytes, potential targets for HIV-1 infection as well (Wu et al., 2023).

PBMC are activated in defense against HIV-1, and their response to the virus determines the progression of the disease and contribute with the natural resistance to the HIV-1 infection (Woodham et al., 2016). Repeated contact with HIV-1 would suppose an infection; however, some individuals remain uninfected despite multiple high-risk sexual exposures; they are known as HIV-exposed but seronegative individuals (HESN) and represent the existence of potential factors mediating natural resistance to HIV-1 infection (Miyazawa et al., 2009 ; Alarcón-Uribe et al., 2023; Ossa-Giraldo et al., 2022). Therefore, studying PBMC can provide valuable insights into the pathophysiology of the virus and the biological mechanisms involved in controlling this infection. To date, studies on PBMC during HIV infection and exposure have focused on evaluating immunological function by measure activation markers, proliferation, effector activity and determining their morphology and physiology (Mazzoli et al., 1997; Stranford et al., 1999; Bégaud et al., 2006). However, as of the time of writing this article, there were no studies evaluating the changes occurring in the metabolome of PBMC exposed to or infected by HIV-1. The metabolome is the complete set of metabolites (amino acids, nucleotides, carbohydrates, and lipids) present in an organism or a biological sample, which serve as substrates, intermediates, and products of metabolism within cells (Qiu et al., 2023). The study of changes in the metabolome provides a biochemical synopsis of the physiological impact of a disease, and this is typically performed through metabolomics (Qiu et al., 2023). This study includes the application of an protocol optimized by our research team for the analysis of PBMC, which uses high-intensity ultrasound for the quenching and extraction process, avoiding the use of solvents and maximizing the use of the sample with less treatment time and sample handling (Gómez-Archila et al, 2021).

Previous metabolomics studies using nuclear magnetic resonance (NMR) spectroscopy have been carried out to evaluate the effects of HIV-1 on the human body. These investigations have primarily focused on biological fluids such as serum, plasma, urine and cerebrospinal fluid (Bertini et al., 2012; Li and Deng, 2016; Paris et al., 2018). However, to our knowledge, no studies have examined PBMC from exposed to, or HIV-1 infected individuals.

3.3. Materials and Methods

3.3.1. Chemicals and materials

All solvents and reagents used were of analytical grade. Sodium phosphate dibasic dihydrate, sodium azide, deuterium oxide, and 3-(Trimethylsilyl) propionic-2,2,3,3-d4 acid sodium salt (TSP-d4) were supplied by Merck (Darmstadt, Germany). Phosphate buffered saline (PBS) 1X pH 7.4 is composed of 137 mM NaCl, 2.7 mM KCl, 4.3 mM Na2HPO and 1.47 mM KH2PO were supplied by Gibco® Ultrapure water was obtained using a Milli-Q purification system of Merck Millipore. Vivaspin® 500 3000 K MWCO Centrifugal Concentrators were provided by Sartorius® (Göttingen, Germany).

To develop the high-intensity ultrasound process, an LSP-500 ultrasonic liquid processor (Sonomechanics, New York, USA) equipped with a 500 W ultrasonic generator, an air-cooled piezoelectric transducer (ACT-500), a full-wave Barbell Horn™ (FBH) with a 21-mm tip diameter, and a reactor chamber (jacketed beaker refrigerated) was used for all experimental runs.

3.3.2. Human subjects

A retrospective study was developed. The study used a defined database of volunteers to establish case-control relationships. PBMC samples from 48 volunteers were evaluated and distributed as follows:

- PLHIV-ART: This group included twenty individuals who had been diagnosed with HIV-1 infection for more than one year. The median CD4+ T cell count was 466 cells/uL (range 353-769 cells/uL) and the median viral load was 20757 copies/mL (range 97-96900 copies/mL). All individuals in this group were receiving ART.
- HESN: This group included eight HIV-negative individuals from serodiscordant couples which are defined as follow: one individual is HIV-positive and its partner is HIV-negative

(clinically and serologically). The individuals of HESN group reported multiple unprotected sexual episodes for more than 2 years at the time of enrollment. They reported at least 5 episodes of high-risk intercourse within 6 months before study entry. Their partners were HIV-positive with a detectable viral load (Zapata et al., 2008). No Δ32-homozygous subjects were included in this group.

- Healthy controls: This group involved twenty individuals. They had negative serological tests for HIV-1 and reported nonsexual risk behaviors.

Study Approval: This study was approved by the Bioethical Committee at the Universidad de Antioquia. All individuals participating in the study signed an informed consent form. This form was prepared according to the Colombian Legislation Resolution 008430/1993.

Exclusion criteria: Individuals with hemoglobin ≤8.0 g/dl; neutrophil count ≤1,000/mm3; individuals under immunosuppressive treatment; pregnant or lactating women; volunteers with cancer or with an active infection or disease that require hospitalization.

3.3.3. Human peripheral blood mononuclear cells isolation

The isolation of PBMC was carried out through a density gradient using the Ficoll-Histopaque (Sigma-Aldrich, St. Louis, MO, USA). Peripheral blood from healthy volunteers was carefully poured into a tube with Ficoll at the blood/Ficoll ratio 1:4. Let the mixture rest for 20 minutes and subjected to 591 g by centrifugation at room temperature for 30 minutes. Three phases are obtained; red blood cells (RBC) and granulocytes at the bottom of the tube; the white mononuclear cell (PBMC) fraction in the medium; and plasma and platelets in the upper one. The PBMC phase was separated and washed with 1X PBS (PBMC/PBS ratio of 1:10). Subsequently, the PBMC were centrifuged at 1000 g for 5 min at 4ºC, the supernatant was discarded and the cells were resuspended in 1X PBS for cell counting (Neubauer chamber) and viability tests (0.4% trypan blue). (Strober, 1997; Strober 2015; Louis and Siegel, 2011; Kim et al., 2011). Finally, cells were diluted in 1X PBS to obtain individual portions of 10 million viable cells in 100 µL. PBMC were frozen at −80°C until processing.

3.3.4. Extraction of metabolites for the ^{1}H-NMR experiments

The cells are thawed on ice for 5 minutes and 650 µL of phosphate buffer (50 mM Na2HPO4, pH 7.4, in D2O with 0.1 mM deuterated trimethylsilylpropanoic acid (TSP-D4)) are added per sample with 10 million PBMC. The samples were resuspended and homogenized. Then, to break the

cells, the following cycle was applied to the samples: First cells were frozen with liquid nitrogen (1 min). Then the sample was immersed in a refrigerated bath (4˚C) equipped with a high-intensity ultrasound probe set at a frequency of 20050 Hz and a 100% amplitude for 5 min. This cycle was run six times. Samples were centrifuged at 12000 g for 120 min at 4ºC to separate phases. The solution separated into an upper phase (containing metabolites) and a lower phase (mainly proteins, DNA/RNA, and cell membranes). The supernatant was filtered with an ultrafilter previously washed with phosphate buffer (10X with phosphate buffer, pH 7.4). The samples were then centrifuged at 12000 g for 120 min at 4ºC. The filtered solution was stored at -80ºC until ^{1}H-NMR analysis.

3.3.5. ^{1}H-NMR experiments

550 µL of the filtered solution was transferred to separate 5 mm NMR tubes. All the samples were stored at 4ºC, then equilibrated at room temperature for 15 min before analysis, which was conducted on the same day. The ^{1}H-NMR spectra of the extracts were recorded at 300K using a Bruker AVANCE III 600.13 MHz spectrometer, equipped with a 5 mm triple-resonance z-gradient cryoprobe (Prodigy® TCI, 1H-13C/15N-2H). The spectrometer was controlled using TopSpin, version 3.6.2 (Bruker GmbH, Karlsruhe, Germany). ^{1}H 1D Nuclear Overhauser Effect Spectroscopy (NOESY) NMR spectra were acquired using water presaturation and spoil gradients (*noesygppr1d* pulse sequence) with 256 free induction decays (FIDs), 64k data points, a spectral width of 30 ppm, and a relaxation delay of 60 s. Total Correlation Spectroscopy (TOCSY) and multiplicity Heteronuclear Single Quantum Correlation (HSQC) were performed on representative samples with 256–512 t1 increments, 32–96 transients and a relaxation delay of 1.5 s. The TOCSY spectra were recorded by a standard MLEV-17 pulse sequence with mixing times (spin-lock) of 65 ms.

3.3.6. Data analysis and statistics

NMR spectra processing: ^{1}H-NMR spectra were transformed with a 0.5 line-broadening and manually baseline- and phase-corrected with Topspin 4.0.9. NMR signals of TSP-D4 were referenced to 0 ppm. For metabolite identification purposes, the ^{1}H and chemical shift values and multiplicity of signals were compared with the reference data from the Chenomx software (Chenomx NMR Suite 8.4, Chenomx Inc., Edmonton, Canada) in combination with spectral databases Human Metabolome Database and the Biological Magnetic Resonance Bank and

several literature reports. Optimal integration regions were defined for each metabolite to select signals without overlapping. Integration was performed with MestreNova 14 (Mestrelab Research, SL, Santiago de Compostela, Spain) by manually integrating the previously identified signals. An integration matrix (Integral Regions) was built with these regions, which was later applied to the 48 acquired spectra. A matrix of integrals was built for all the spectra (Integral series). This matrix of integrals was normalized by the sum of the total signals of the spectrum using Excel® (Microsoft, United States of America).

Multivariate and univariate analysis of Metabolomic Profiles: The previously normalized matrix of integrals was processed using MetaboAnalyst 5.0. A principal component analysis (PCA) was first performed to identify groups of samples with a similar metabolic pattern and/or segment with a different metabolome.

Two case-control relationships were established: healthy controls versus PLHIV-ART and healthy controls versus HESN. These relationships were evaluated by Partial Least Squares Discriminant Analysis (PLS-DA), which links two data matrices and enhances the separation between different groups of samples. The quality of the PLS-DA was assessed by carrying out a permutation test to calculate the goodness of fit (R2) and the predictive capacity (Q2) of the randomly generated models. The PLS-DA results (VIP scores) were analyzed to identify the metabolites significantly contributing to the separation of the groups. Variables with a VIP score greater than 1.0 were considered significant for the model.

The selected variables were then subjected to a Univariate analysis using a difference of means test (Wilcoxon Test). In cases where more than one significant signal was obtained for a given metabolite, the signal with less overlap was selected for graphical representation.

Partial Least Squares (PLS) regression was done to correlate the metabolomic profile with the viral load of PLHIV-ART individuals using the software SIMCA® 17 (Sartorius). VIP scores identified significant metabolites and a 100-fold permutation test validated the model.

Finally, metabolites differentially expressed in the groups were subjected to Pathway Analysis using MetaboAnalyst 5.0.

3.4. Results

3.4.1. Human subjects and analysis of metabolic PBMC profiles

The main characteristics of the individuals used in the study are shown in Figure 3.1. The two case-control relationships analyzed in the study were carried out by selecting the group of volunteers with the best age-sex balance.

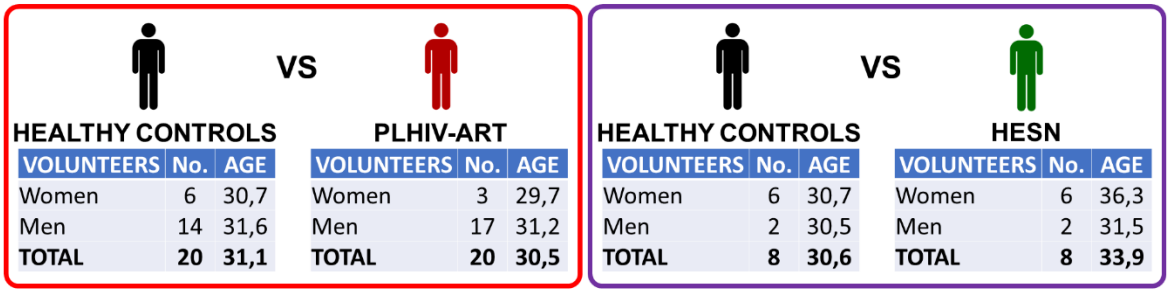

FIGURE 3.1. Case-control relationships. Detail of each of the two relationships built to analyze PBMC samples. Healthy controls are in black, HESN in green and PLHIV-ART in red. HC: Healthy control, HESN: HIV-exposed seronegative, PLHIV-ART: PLHIV with Antiretroviral Therapy. AGE: average age.

It is important to note that this is a retrospective longitudinal study, and the number of samples is limited. In addition, cells obtained from whole blood contain limited PBMC. From 10 mL of whole blood the amount of PBMCs recovered from each volunteer oscilated between 15 and 20 million PBMC in healthy controls, however, this amount decreases significantly in PLHIV, where the lymphocyte count is declining due to the HIV-1 infection, representing a challenge for the research since previous studies in which NMR analyzed PBMC samples used 20 million cells per volunteer (Palomino-Schätzlein et al., 2017). To address this issue, we had previously developed a new method for PBMC processing that, using 10 million cells or fewer, yields better data for metabolomic profiling in terms of quality, robustness and reproducibility (Gómez-Archila et al., 2021).

We used this method to perform metabolomic analysis by ^{1}H-NMR in the PBMCs samples of the volunteers. From the analysis of the obtained spectra, we identified 43 metabolites in the PBMC samples: 19 organic acids, 19 amino acids, and five nucleotides. To know the details of the metabolites identified in the plasma samples, see **Supplementary Table 1 (Anexo 4)**. Each identified metabolite became an evaluation variable to define the metabolomic profile of the study groups; after the spectra assignment, the normalized integration tables were used for multivariate analysis, see **Supplementary Table 2 (Anexo 5)**.

3.4.2. Multivariate comparison of PBMC metabolomic profiles of the PLHIV-ART and HESN groups versus healthy controls

To define the similarities and differences between samples and groups, we performed two multivariate analyses: unsupervised (PCA) and supervised (PLS-DA). Figure 3.2 shows the PCA results, which show cluster formation among the study groups (healthy controls, PLHIV-ART and HESN). Notably, healthy controls exhibited less data dispersion than PLHIV-ART and HESN. The HESN group displayed the highest data dispersion, possibly due to the small number of samples analyzed and the nature of HESN individuals. The HESN phenomenon has been widely studied, but a common origin for this condition has not been established due to its multifactorial causes that vary among exposed individuals. This is also reflected in our study as a dispersed metabolic variation.

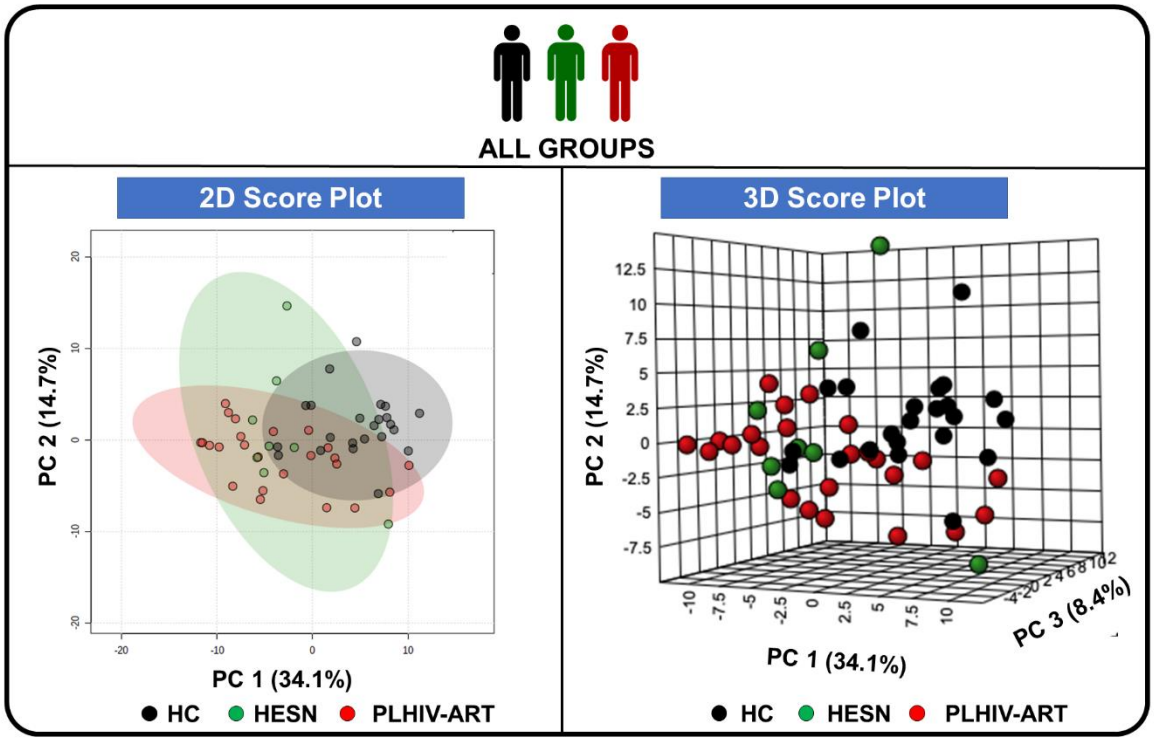

FIGURE 3.2. Principal component analysis (PCA) of the study groups. 2D and 3D score plot charts of the PCA analysis of the volunteers. Each of the three axes of the graph represents a principal component. The values that each of the axes takes are related to the fact that there is a score value for each observation (row) in the data set; therefore, there are score values for each of the three componentsd. The score value for an observation, say the first component, is the distance from the origin, along the direction (load vector) of the first component, to the point where that observation projects onto the direction vector. Healthy controls are in black, HESN is in green and PLHIV-ART is in red. PC: Principal component, HC: Healthy control, HESN: HIV-exposed seronegative, PLHIV-ART: PLHIV with Antiretroviral Therapy.

To specifically observe the metabolic differences between the study groups, a PLS-DA analysis was performed (See Figure 3.3).

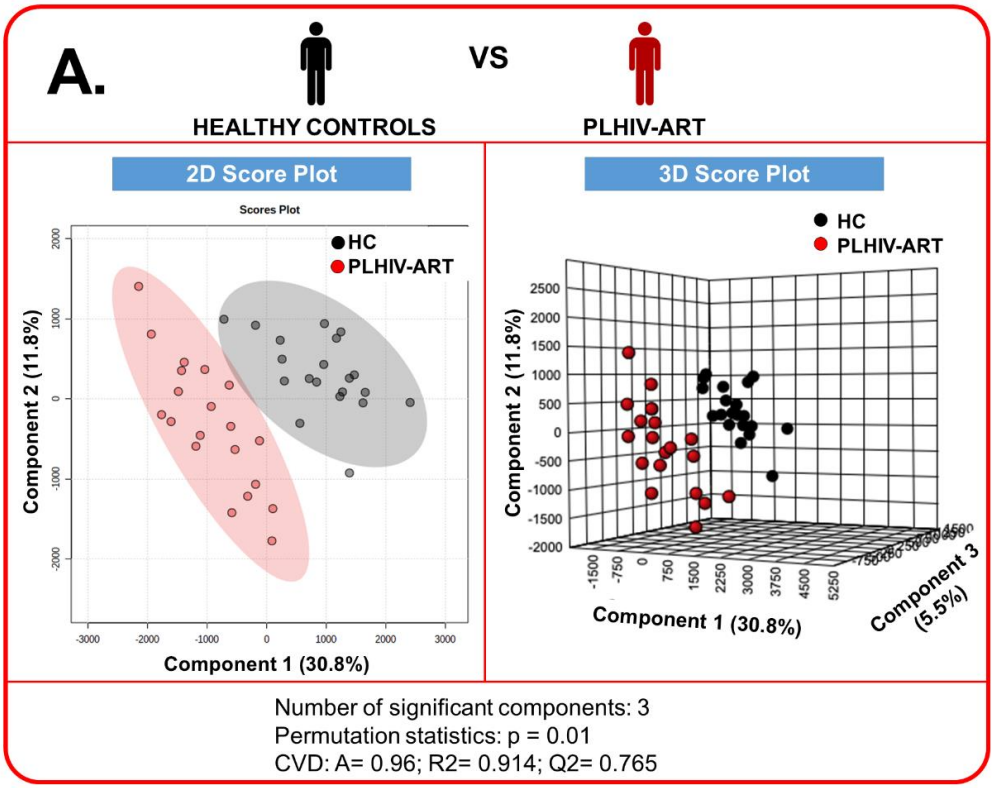

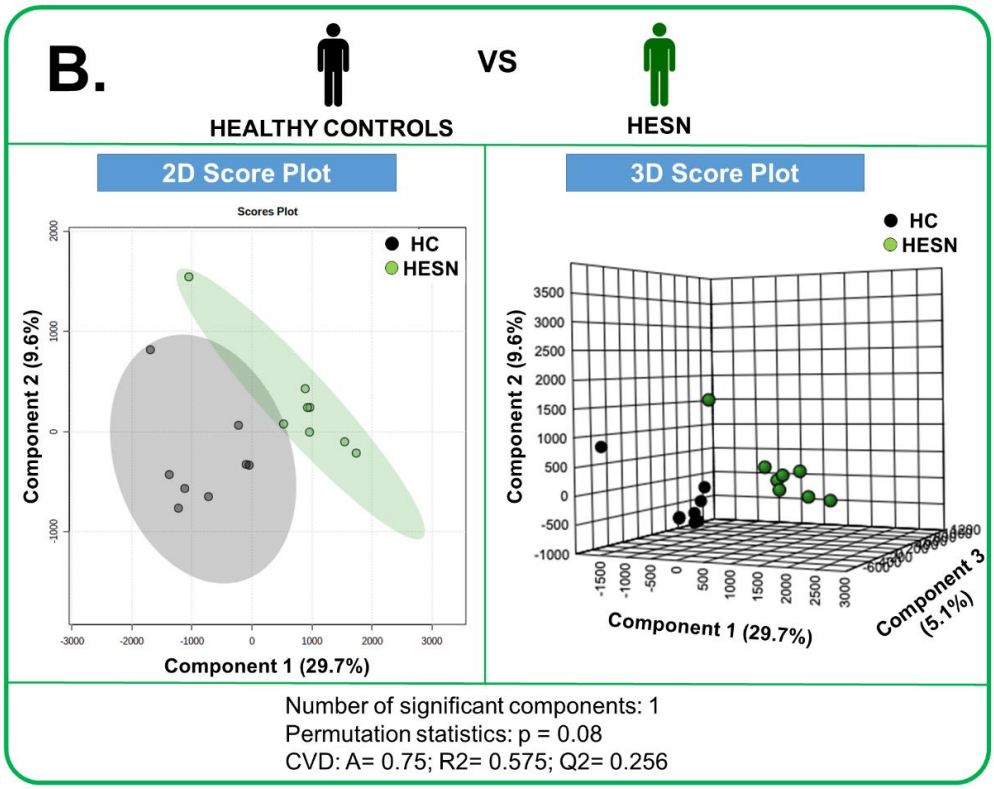

FIGURE 3.3. Partial Least Squares Discriminant Analysis (PLS-DA). Score plot charts of the PLS-DA of the two case-control relationships established. **Panel A.** Healthy control versus PLHIV-ART ; on the left side, the 2D score plot and on the right side the 3D score plot. **Panel B.** Healthy control versus HESN; on the left side, the 2D score plot and on the right side the 3D score plot. Each of the three axes of the graph represents a principal component. The values that each of the axes takes are related to the fact that there is a score value for each observation (row) in the data set; therefore, there are score values for the first component, another for the second component, and one for the third. The score value for an observation, say the first component, is the distance from the origin, along the direction (load vector) of the first component, to the point where that observation projects onto the direction vector. HC: Healthy control, HESN: HIV-exposed seronegative, PLHIV-ART: PLHIV with Antiretroviral Therapy. CVD: Cross-validation details, A: Accuracy, R2: goodness of fit, Q2: predictive capacity. Healthy controls are in black, HESN is in green and PLHIV-ART is in red.

A statistically significant model was obtained from the PLS-DA comparing healthy controls and PLHIV-ART. In contrast, the PLS-DA result of healthy controls vs HESN is relatively weak, despite the clear group separation. This result may be due to the low number of HESN samples (n=8), and it should also be noted that HESN volunteers only differ from healthy controls by their level of sexual exposure to HIV-1 infection, but both are seronegative. Based on the statistical PLS-DA results, we identified the relevant variables (metabolites) that explain the difference between the groups through the result of the VIP score. Thirty-two variables were identified, comparing healthy controls versus PLHIV-ART, and for healthy controls versus HESN, 46 variables were found.

All the relevant variables explaining the differences between the groups, according to the PLS-DA VIP score, were then subjected to a mean difference analysis (Wilcoxon Test) to determine if there was a statistically significant difference in their expression in each group. It should be noted that although a more significant number of variables (With VIP>1) were identified in comparing healthy controls versus HESN (46 variables) than in healthy controls versus PLHIV-ART (32 variables), in both cases, fourteen (14) metabolites were identified as responsible for the differences in each case-control relationship. For the details of the PLS-DA statistics see **Supplementary Table 3 (Anexo 6)**.

The 14 metabolites of the healthy controls versus PLHIV-ART comparison correspond to 5 organic acids (aspartate, taurine, trimethylamine N-oxide, acetoacetate and glutamate) and 9 amino acids (betaine, carnitine, glycine, lysine, methionine, phenylalanine, serine, tyrosine and sarcosine). Meanwhile, the 14 in the comparison healthy controls versus HESN correspond to two nucleotides (AMP and inosine), three organic acids (formiate, taurine and glutamate) and 9 amino acids (alanine, betaine, isoleucine, leucine, lysine, methionine, serine, tyrosine and valine). A visual comparison of the spectral intensities as well as a quantitative comparison in form of boxplots of the significant metabolites is shown in Figure 3.4.

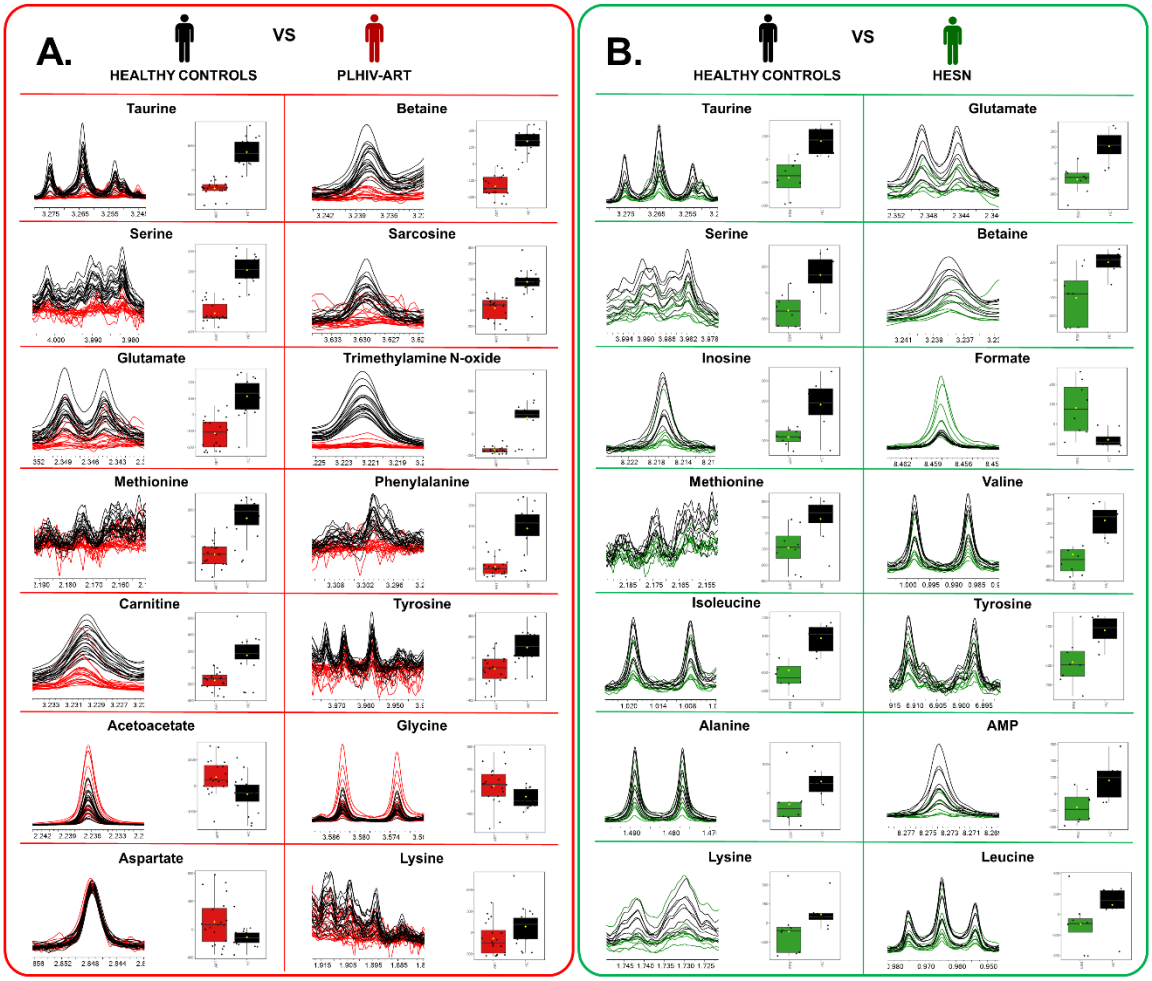

FIGURE 3.4. Metabolites explaining group differences. Results of the Wilcoxon test for the significant variables (metabolites) for each proposed PLS-DA model. **Panel A.** (main red box), there is a comparison between healthy controls and PLHIV-ART. **Panel B.** (main green box), the comparison of healthy controls and HESN is shown. Within each small individual box: the left side shows the region of the spectrum (metabolite signal) ^{1}H-NMR superimposed of all the samples analyzed in each comparison. On the right side is the box-and-whisker plot for the normalized concentration and the statistical significance of each test. Healthy controls are shown in black, HESN in green and PLHIV-ART in red.

It should be noted that there are similarities and differences in the identified metabolites, with 7 metabolites that were altered in both groups (HESN and PLHIV-ART) (Figure 3.5.). Interestingly, the direction of the variation in both groups was the same; betaine, glutamate, lysine, methionine, serine, taurine, and tyrosine showed decreased expression compared to healthy controls. On the other hand, specific metabolomic alterations were identified for each group (Figure 3.5.). In the PLHIV-ART group, carnitine, phenylalanine, sarcosine and trimethylamine N-oxide were reduced,

while aspartate, acetoacetate, and glycine were increased. In the HESN group, alanine, AMP, inosine, isoleucine, leucine, and valine differentially decreased, and only formiate increased in this group.

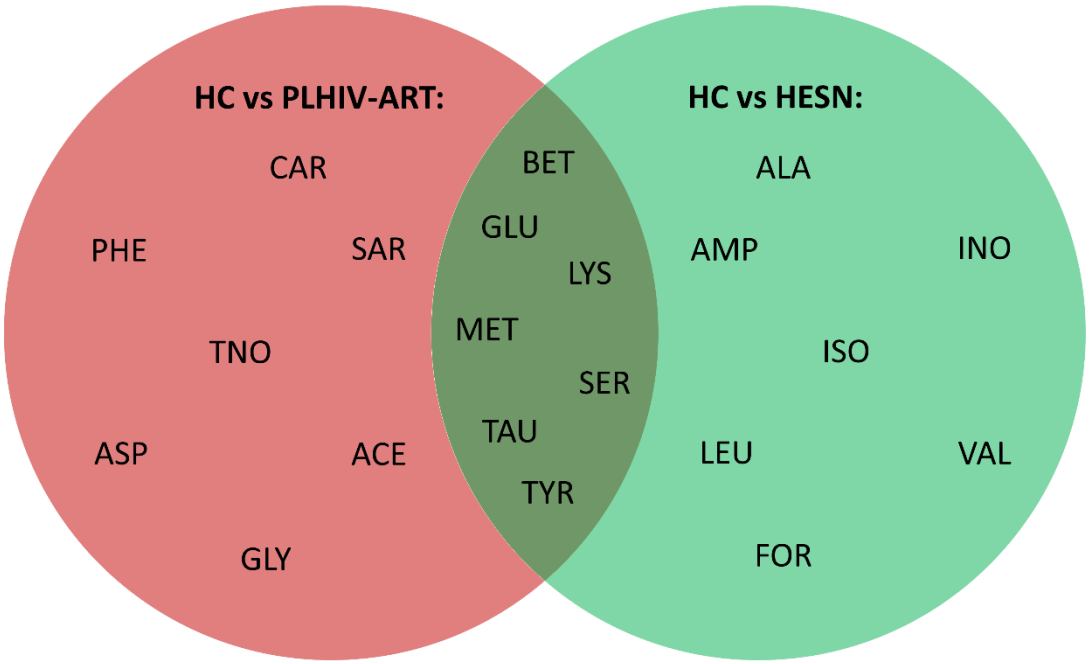

FIGURE 3.5. Venn diagram of metabolites explaining differences among groups. Set Analysis showing the metabolites related to differences and similarities among HESN and PLHIV-ART metabolomic profiles. In the main part of each set, the metabolites related only to one study group are shown, and in the intercept, the metabolites related to two groups (central intercept). HESN: HIV-exposed seronegative (In green color set), PLHIV-ART: PLHIV with ART (In red color set). HC: Healthy controls, BET: Betaine, GLU: Glutamate, LYS: Lysine, MET: Methionine, SER: Serine, TAU: Taurine, TYR: Tyrosine, CAR: Carnitine, PHE: Phenylalanine, SAR: Sarcosine, TNO: Trimethylamine N-oxide, ASP: Aspartate, ACE: Acetoacetate, GLY: Glycine, ALA: Alanine, INO: Inosine, ISO: Isoleucine, LEU: Leucine, VAL: Valine, FOR: Formiate

3.4.3. Multivariate correlation between the metabolomic profile and CD4+ T lymphocytes in PLHIV-ART

We evaluate the relationship between the metabolomic profile of the PLHIV-ART group and the CD4+ T Lymphocyte count. Using SIMCA, we obtained, through a PLS analysis, an interesting model that correlates the percentage of CD4+ T lymphocytes present in the volunteers and their metabolomic profile (See Figure 3.6). A total of 3 correlations were evaluated: metabolomic profile versus CD4+ T lymphocyte count, metabolomic profile versus viral load, and metabolomic profile versus percentage of CD4+ T lymphocytes. Only the relationship with the percentage of CD4+ T

lymphocytes presented significant results. The other two relationships were not significant (data not shown).

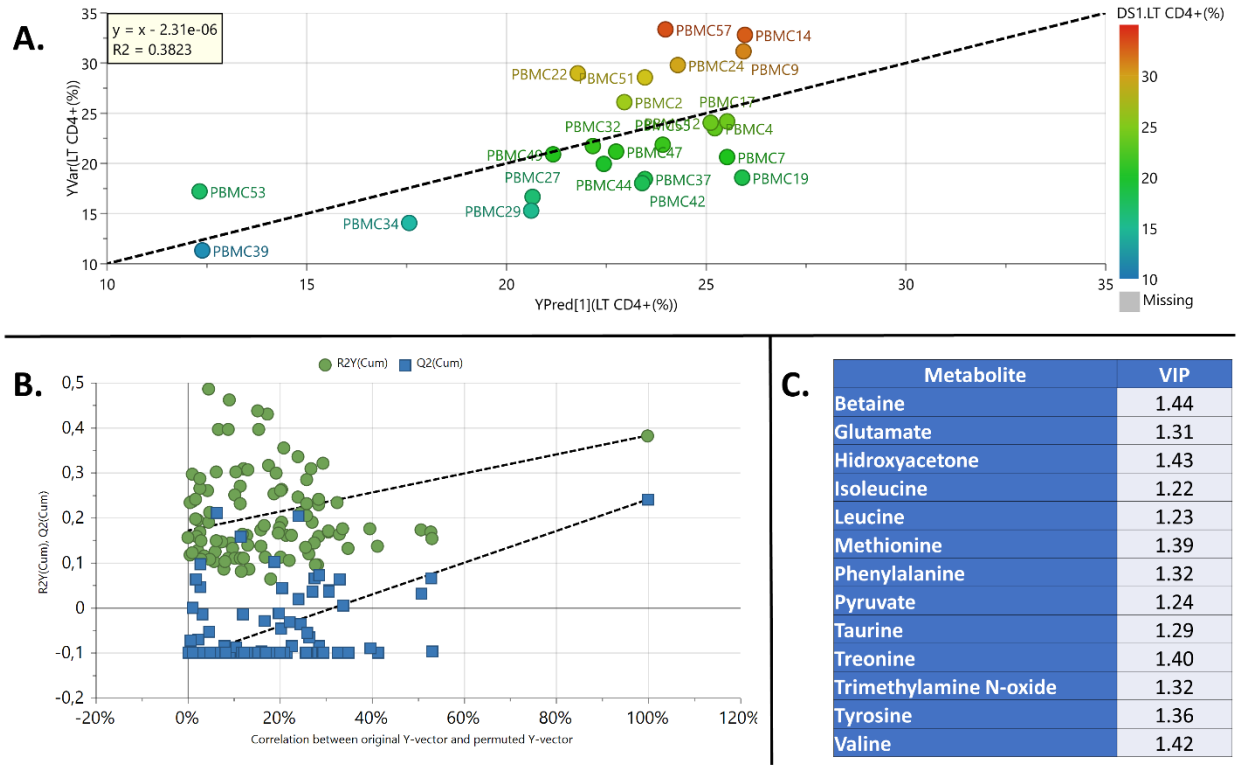

Metabolite	VIP
Betaine	1.44
Glutamate	1.31
Hidroxyacetone	1.43
Isoleucine	1.22
Leucine	1.23
Methionine	1.39
Phenylalanine	1.32
Pyruvate	1.24
Taurine	1.29
Treonine	1.40
Trimethylamine N-oxide	1.32
Tyrosine	1.36
Valine	1.42

Figure 3.6. Partial Least Squares regression (PLS) of the PLHIV-ART group. A. Observed versus predicted plot of a partial least squares (PLS) regression model for the percentage of CD4+ T lymphocytes present in PBMC samples from PLHIV-ART using their metabolomic profile obtained by ^{1}H-NMR. UV scalding, R2Y(cum) = 0.38, Q(cum) = 0.24. **B.** Permutation test results of the PLS model for the percentage of CD4+ T lymphocytes in PBMC samples from PLHIV-ART. The R2Y value represents the goodness of fit of the model. The Q2 value represents the predictability of the models. Most R2Y and Q2 values to the left were lower than the original points to the right of the blue regression line of the Q2 points, which intersects the vertical axis (on the left) at or below zero, showing that the PLS model was valid. Permutation test plot for the PLS model (number of permutations, 100, R2 = (0.0, 0.17), Q2 = (0.0, -0.112). **C.** Significant metabolites for the PLS model with a VIP value greater than 1.2

Figure 3.6 shows the correlation between, the percentage of the primary target cells of HIV-1 (CD4+ T lymphocytes) and the PLHIV-ART metabolomic profile. Metabolites change their expression directly proportional depending on the cell count. That is, as the percentage of CD4+ T lymphocytes in the PBMC sample increases, the levels of the metabolites in the sample increase. It should be noted that a maximum of 60% of the total PBMC are CD4+ T cells, so this correlation is very representative, given that there are other types of cells in the PBMC and CD4+ T lymphocytes have a significant weight in the correlation with the metabolomic profile. The permutation test allows us to validate the model. In the graph (See Figure 3.6B), the predicted

model (Q2) does not exceed the random model (R2Y). Therefore, it can be stated that the model was valid and was unlikely to be constructed by chance.

When the metabolites that were significant for the PLS model are observed in detail (See Figure 3.6C), the majority were found to be differentially expressed in the PLHIV-ART group compared to the healthy controls. betaine, glutamate, methionine, taurine, and tyrosine were found differentially expressed in PLHIV-ART and HESN groups (See Figure 3.4). However, phenylalanine and trimethylamine N-oxide were found only in the PLHIV-ART group (See Figure 3.5).

3.4.4. Metabolomic pathway analysis

We performed a metabolic pathway analysis to further relate these metabolic changes with more complex metabolic processes. The results of this analysis can be seen in Figure 3.7.

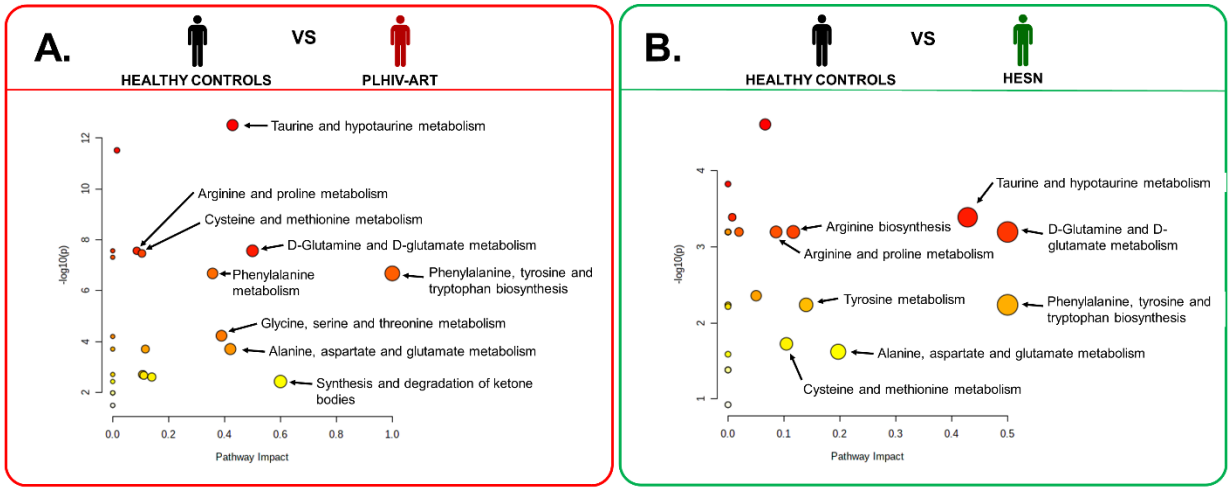

Figure 3.7. Metabolic pathway analysis of HESN and PLHIV-ART. Panel A. (main red box) shows the pathway analysis of PLHIV-ART. **Panel B.** (main green box) shows the pathway analysis of HESN. The X-axis of the graph measures the impact on the metabolic pathway. The Y-axis of the graph measures the level of statistical significance in the test. As the significance level increases, the point becomes redder, turning from white to yellow, until reaching intense red. As the impact of the route increases, the point becomes larger.

Interestingly, several pathways appear altered in both groups, PLHIV-ART and HESN, in coherence with the 7 metabolites altered similarly in both groups. The metabolic pathways that are significantly altered in both groups are phenylalanine, tyrosine and tryptophan biosynthesis

and D-Glutamine and D-glutamate metabolism. While, in the PLHIV-ART group, a differentially affected metabolic pathway stands out, the Synthesis and degradation of ketone bodies pathway. However, the PLHIV-ART group has more affected pathways and higher impacts on the metabolic pathway than the HESN group. It is enough to observe the axes of the graph of each group; in the case of the HESN group, the pathways with the highest impact (X-axis of the graph) are around 0.5, while the HESN group presents pathways with an impact of 1.0. Also, the level of significance (Y-axis of the graph) of the routes impacting PLHIV-ART is higher than in the HESN group.

3.5. Discussion

This article presents the results of the analysis of PBMC samples from patients infected (PLHIV-ART) and/or exposed (HESN) to HIV-1 using the sample processing protocol that we previously developed and standardized (Gomez-Archila et al., 2021). The use of this protocol allowed us, starting from a limited number of PBMC, know the metabolomic profile of the study groups, as well to contrast them through multivariate and univariate statistical analyses, in order to identify the metabolites that explain the differences between the study groups. Analyzing the metabolites that change exclusively in each group (HESN or PLHIV-ART) makes it possible to relate their variation to altered routes and signaling pathways in HIV-1.

The analysis of the metabolites that change significantly in the PLHIV-ART group reflects the effects generated by HIV-1 and antiretroviral treatment in the PBMC. For instance, phenylalanine was found to be significantly decreased in PBMC in the PLHIV-ART group, contrary to the previously documented elevated blood levels of phenylalanine during HIV-1 infection in the absence of treatment (Gostner et al., 2015). Phenylalanine is important for the biosynthesis of neurotransmitters; therefore, it is related to neuropsychiatric symptoms during AIDS, such as the development of depression, fatigue and cognitive impairment. Increased phenylalanine/tyrosine ratios are associated with immune activation in persons with HIV-1 infection and decrease with effective antiretroviral therapy (Zangerle et al., 2010). Previous NMR studies identified tyrosine downregulation in untreated HIV-infected patients (Sitole et al., 2019). We identified that tyrosine decreased in PBMC of HESN and PLHIV-ART groups, but phenylalanine only decreased in PLHIV-ART, which could be an indicator of the effectiveness of the treatment in this group.

Another example of treatment effectiveness in the PLHIV-ART group could be decreased sarcosine and trimethylamine N-oxide levels in PBMC. Previous plasma studies identified

elevated levels of sarcosine in persons with HIV/AIDS, which decreased with treatment, although not below the levels in healthy controls (Munshi et al., 2013). We also observed increased glycine levels, which could be related to the decrease in sarcosine, since it is a metabolite downstream of choline and is converted into glycine; thus the decrease in sarcosine could increase glycine in PBMC of the PLHIV-ART group.

In the case of trimethylamine N-oxide, high levels have been associated with carotid plaques, endothelial dysfunction, and silent cardiac ischemia in HIV-positive subjects (Montrucchio et al., 2020). PLHIV-ART group showed low levels of trimethylamine N-oxide; therefore, we could suggest that they present a lower cardiovascular risk.

In the HESN group, the amino acid alanine was decreased. It has been identified the relationship of alanine with Viral Protein U (Vpu), an accessory protein of HIV that acts by degrading the viral receptor molecule CD4 in the endoplasmic reticulum and the release of virions from the cell surface (Bour et al., 1995). Stimulation of CD4+ T cells with mitogenic molecules results in high surface expression of the alanine transporter SNAT1, which increases the intracellular alanine pool and, thus, increases mitogenesis in the absence of Vpu. In contrast, the presence of Vpu negatively regulates SNAT1 from the cell surface by binding to SNAT1 to induce its ubiquitination and degradation, which results in decreased alanine uptake, reducing the mitogenic capacity of CD4+ T cells (Sudgen and Cohen, 2015); therefore, this mechanism is part of the immune evasion and viral alteration of immunometabolism in HIV-1 infection.

The previous model was described in HIV-infected cells. However, it should be noted that HESN did not show evidence of quantifiable viral infection, which leads us to presume that the potential decrease in T cell activation mediated by alanine in HESN is due to a phenomenon called immune quiescence (Card et al., 2013; Su et al., 2015). This protection model against infection is based on a low basal immune activation phenotype, in which unactivated CD4+ T cells are less susceptible to HIV infection, limiting HIV target cell availability (Card et al., 2013; Ossa-Giraldo et al., 2022). Evidence from HIV transmission studies in HESN implicates elevated immune activation as a risk factor for acquiring HIV (Card et al., 2013). Our previous study in plasma identified decreased alanine in progressors and HESN (Gomez-Archila et al., 2023). In the case of progressors, it could indicate immunological activation, while in HESNs, may suggest a process of immune quiescence.

Another evidence of T cell activation suppression in HESN is the decreased expression of adenosine monophosphate (AMP) observed in the PLS-DA model. Regulatory T cells (Tregs)

suppress T cell activation in HESN, in the Pumwan cohort, Tregs were elevated in HESN relative to high-risk HIV-negative controls (Card et al., 2009). Tregs can directly suppress HIV replication through cyclic adenosine monophosphate (cAMP) activity, negatively regulating HIV replication (Moreno-Fernandez et al., 2011; Moreno-Fernandez et al., 2012). Therefore, the decreased levels of AMP in HESN would be related to an elevated consumption of Tregs.

Additionally, it should be highlighted that HIV causes chronic inflammation and immune activation despite viral suppression with ART (Cai and Sereti., 2021; Elvstam et al., 2021). The adenosine pathway regulates persistent inflammation, limiting tissue damage associated with inflammatory conditions. However, HIV infection is associated with disorders in the adenosine pathway that limit its ability to control HIV-associated inflammation (Hixson et al., 2021). AMP is a fundamental part of purinergic metabolism and is converted to adenosine by the action of ecto-5'-nucleotidase (CD73) (Zimmermann, 2000). Adenosine activates purinergic receptors with an anti-inflammatory role (Panther et al., 2003). Extracellular adenosine can be metabolized to inosine, a pro-inflammatory substrate, through adenosine deaminase (Alam et al., 2015). It should be noted that, in our HESN group, inosine was found to be decreased. The significant decrease in the expression of AMP and inosine in HESN PBMC is likely related to the production of adenosine and demonstrates the anti-inflammatory profile of this group.

In HESN, the activation and function of natural killer (NK) cells have been linked to protection against HIV. A recent study found that NK cells from HESN sex workers had higher expression of the Fc receptor CD16, and NK cells with higher CD16 expression tended toward higher antibody-dependent cellular cytotoxicity (ADCC) activity (Zhao et al. al., 2020). In addition, $CD56^{dim}CD16^{+}$ NK cells were more frequent in men who have sex with men with a high risk of HIV infection but seronegative, compared to low-risk individuals, suggesting the NK cell role during HIV exposure (Flórez-Alvarez et al., 2020; Rincón et al., 2023).

CD16 expression and ADCC activity may vary due to a polymorphism at residue 158 of the CD16 protein; possessing at least one valine in this residue instead of phenylalanine, leads to increased expression of CD16 on the cell surface (Hatjiharissi et al., 2007). We suggest that valine may play an important role in the NK cell function of HESNs, then its decreased expression in PBMC is related to that event. Therefore, decreased Valine levels in HESN PBMC would be related to increased CD16 expression.

In plasma we identified decreased valine in HIV controllers and increased in progressors (Gomez-Archila et al., 2023). It should be noted that previous studies demonstrated that an increase in

valine expression is related to the loss of controller status in transient elite controllers (Tarancon-Diez et al., 2019). Likewise, it may suggests that the intracellular valine levels in HESN PBMC would be related to their ability to control infection.

Similarly, leucine has been closely associated with the Negative Regulatory Factor (NEF) protein of HIV, Nef interacts with the endosomal sorting machinery via a leucine-based motif. Nef proteins containing leucine motifs down-regulated CD4 from the cell surface and enhanced viral replication (Coleman et al., 2005). Thus, the decrease in leucine concentration in HESN could be related to the functioning of viral proteins such as NEF.

Furthermore, we also identified the carnitine metabolite that links the metabolism of HESN and PLHIV-ART groups. Carnitine is synthesized through lysine and methionine (Steiber et al., 2004); which decreased in HESN and PLHIV-ART groups. However, carnitine levels were altered in PLHIV-ART, where they decreased. carnitine is a conditionally essential amino acid that is fundamental to energy metabolism. It intervenes in the transport of long-chain fatty acids from the cytosol to the interior of the mitochondria, where the beta-oxidation process takes place and adenosine triphosphate (ATP) is produced, leaving acetyl-coenzyme A as the final product of the fatty acid degradation. During this process, acetyl-coenzyme A forms beta-hydroxybutyrate and acetoacetate, used as an energy source by the brain and other tissues (Flanagan et al., 2010). In summary, the decrease in lysine and methionine in both groups is related to the production of carnitine and energy for the PBMC. Carnitine is significantly decreased in the PLHIV-ART group due to the energy wear and tear of viral infection, while HESN maintains it at normal levels (no significant changes were seen) and the increased levels of acetoacete in PLHIV-ART are the product of an energy compensation process of the PBMC.

We consider that glutation (GSH) could be related to the metabolomic profile found in HESN and PLHIV-ART. GSH is composed of glutamate, cysteine and glycine. In HESN and PLHIV-ART, glutamate was decreased, while glycine was increased in PLHIV-ART. It should be noted that cysteine cannot be determined by NMR spectroscopy in blood and cell samples, because its concentration is below the detection limits (Jung et al., 2010). GSH plays a crucial role in maintaining efficient mitochondrial functioning, and the levels are deficient in people with HIV (Nguyen et al., 2014). Acute induction of cellular GSH deficiency resulted in apoptosis and mitochondrial injury (Ghosh et al., 2005; Mastrocola et al., 2005), phenomena typical of HIV infection. A recent study demonstrated the relationship between GSH levels and mitochondrial function, muscle strength, insulin resistance, inflammation, and body fat. The study showed that providing N-acetylcysteine and glycine to HIV patients improved all these conditions (Kumar et al.,

2020). Finding two (glutamate and glycine) of the three metabolites that constitute GSH altered in PLHIV-ART and that glycine is altered only in this group, leads us to think that this metabolite may be associated with an intracellular imbalance due to the lack of GSH.

Finally, when analyzing the most altered metabolic pathways identified with the Metaboanalyst® pathway enrichment analysis, we highlight the metabolic pathway of phenylalanine, tyrosine and tryptophan biosynthesis, which was found impacted in both PLHIV-ART and HESN study groups. Tyrosine, phenylalanine and tryptophan are the three aromatic amino acids involved in protein synthesis. These metabolites mediate the transmission of nervous signals and quench reactive oxygen species in the brain (Parthasarathy et al., 2018). Changes in mood status can be observed in the very early stages of HIV-1 infection (Gold et al., 2014) and, notwithstanding ART, HIV-1-infected individuals may develop cognitive impairment (Nightingale et al., 2014). Changes in the metabolism of tryptophan and phenylalanine have been associated with HIV disease and both are precursors for neurotransmitter biosynthesis, providing a link to the development of disease-associated neurocognitive impairments (Gostner et al., 2015).

In the HESN group, tryptophan and phenylalanine levels were not found to be altered, only tyrosine levels. While, in PLHIV-ART, decreased levels of tryptophan were found compared to healthy controls, this event would explain the difference between the groups and the prognosis of the PLHIV-ART group. We believe that monitoring amino acid metabolism in HIV-1-infected patients during ART could be useful for tailoring personalized treatment regimens.

3.6. Conclusions

This research managed to identify differential metabolomic profiles in PBMC from PLHIV-ART patients and HESN individuals from serodiscordant couples. Our findings suggest that the immunological changes produced in individuals exposed and/or infected by HIV-1 can be quantifiable at the cellular level in the form of metabolite levels. At the same time, the metabolites identified as significant for the difference between groups can be proposed as biomarkers of treatment efficiency (PLHIV-ART) or protection factors in case of exposure (HESN).

We are aware of the limitations of the cross-sectional methodology, which did not allow us to observe the complete panorama of the evolution of the volunteers within each category. Carrying out a longitudinal study with this type of population would allow us to validate our results and contrast their variants over time. Likewise, to analyze other HESN groups, such as female sex

workers (FSWs), children born to HIV-infected mothers and men who have sex with men (MSM) to find similar or different profiles to our study groups, help us clarify the origins or factors that define a HESN. We additionally consider that analyzing cysteine in these groups of individuals allows us to clarify the relationship between exposure and infection by the virus through the lens of GSH.

Although PLHIV-ART is highly efficient in most of the population adhering to treatment, the impact generated by HIV-1 is evident. In our study group, the identified metabolites were related to marked immune activation, which was corroborated with the literature. It would be important to evaluate whether supplementation of metabolites that are decreased and control of intake of those that are increased improves cellular activation markers.

The natural resistance to infection exhibited by HESN is a phenomenon that must be constantly studied to find the factors that determine its appearance. We managed to identify metabolites that establish an anti-inflammatory profile and a state of immune quiescence, which would explain the resistance to the HIV infection.

3.7. Author Contributions

Conceptualization: León Gabriel Gómez-Archila, Martina Palomino-Schätzlein, Elkin Galeano.

Data curation: León Gabriel Gómez-Archila, Martina Palomino-Schätzlein, Elkin Galeano.

Formal analysis: León Gabriel Gómez-Archila, Martina Palomino-Schätzlein.

Funding acquisition: Martina Palomino-Schätzlein, Wildeman Zapata-Builes, Elkin Galeano.

Investigation: León Gabriel Gómez-Archila.

Methodology: León Gabriel Gómez-Archila, Martina Palomino-Schätzlein, Elkin Galeano.

Project administration: León Gabriel Gómez-Archila, Elkin Galeano, Wildeman Zapata-Builes.

Resources: Wildeman Zapata-Builes, Elkin Galeano.

Supervision: Elkin Galeano.

Validation: Martina Palomino-Schätzlein.

Visualization: León Gabriel Gómez-Archila, Martina Palomino-Schätzlein

Writing - original draft preparation: León Gabriel Gómez-Archila, Martina Palomino-Schätzlein, Wildeman Zapata-Builes, Elkin Galeano.

Writing - review & editing: León Gabriel Gómez-Archila, Martina Palomino-Schätzlein, Daniel S. Rincón-Tabares, Wildeman Zapata-Builes, Elkin Galeano.

3.8. References

- Alam MS, Costales MG, Cavanaugh C, Williams K. Extracellular adenosine generation in the regulation of pro-inflammatory responses and pathogen colonization. Biomolecules 2015; 5:775–92.
- Alarcón-Uribe S, Zapata-Builes W, Higuita-Gutiérrez LF. Resistencia natural a la infección por el VIH-1. Revisión sistemática de la literatura. Iatreia [Internet]. 13 de marzo de 2023 [citado 21 de febrero de 2024];37(1). Disponible en: https://revistas.udea.edu.co/index.php/iatreia/article/view/349513
- Barré-Sinoussi, F., Chermann, J. C., Rey, F., Nugeyre, M. T., Chamaret, S., Gruest, J., et al. (1983). Isolation of a T-lymphotropic retrovirus from a patient at risk for acquired immune deficiency syndrome (AIDS). Science 220 (4599), 868–871. doi:10.1126/science.6189183
- Bégaud E, Chartier L, Marechal V, Ipero J, Léal J, Versmisse P, Breton G, Fontanet A, Capoulade-Metay C, Fleury H, Barré-Sinoussi F, Scott-Algara D, Pancino G. Reduced CD4 T cell activation and in vitro susceptibility to HIV-1 infection in exposed uninfected Central Africans. Retrovirology. 2006 Jun 22;3:35. doi: 10.1186/1742-4690-3-35. PMID: 16792805; PMCID: PMC1524799.
- Bertini, I., Cacciatore, S., Jensen, B. V., Schou, J. V., Johansen, J. S., Kruhøffer, M., et al. (2012). Metabolomic NMR fingerprinting to identify and predict survival of patients with metastatic colorectal cancer. Cancer Res. 72 (1), 356–364. Available at:. doi:10.1158/0008-5472.CAN-11-1543
- Bour S, Schubert U, Strebel K. The human immunodeficiency virus type 1 Vpu protein specifically binds to the cytoplasmic domain of CD4: implications for the mechanism of degradation. J Virol. 1995 Mar;69(3):1510-20. doi: 10.1128/JVI.69.3.1510-1520.1995. PMID: 7853484; PMCID: PMC188742.
- Card CM, Ball TB, Fowke KR. Immune quiescence: a model of protection against HIV

infection. Retrovirology. 2013 Nov 20;10:141. doi: 10.1186/1742-4690-10-141. PMID: 24257114; PMCID: PMC3874678.

- Cai CW, Sereti I. Residual immune dysfunction under antiretroviral therapy. Semin Immunol 2021:101471.
- Card CM, Ball TB, Fowke KR. Immune quiescence: a model of protection against HIV infection. Retrovirology. 2013 Nov 20;10:141. doi: 10.1186/1742-4690-10-141. PMID: 24257114; PMCID: PMC3874678.
- Card CM, McLaren PJ, Wachihi C, Kimani J, Plummer FA, Fowke KR. Decreased immune activation in resistance to HIV-1 infection is associated with an elevated frequency of CD4(+)CD25(+)FOXP3(+) regulatory T cells. J Infect Dis. 2009;199:1318–1322. doi: 10.1086/597801.
- Coleman SH, Van Damme N, Day JR, Noviello CM, Hitchin D, Madrid R, Benichou S, Guatelli JC. Leucine-specific, functional interactions between human immunodeficiency virus type 1 Nef and adaptor protein complexes. J Virol. 2005 Feb;79(4):2066-78. doi: 10.1128/JVI.79.4.2066-2078.2005. PMID: 15681409; PMCID: PMC546596.
- DeHaan E, McGowan JP, Fine SM, et al. PEP to Prevent HIV Infection [Internet]. Baltimore (MD): Johns Hopkins University; 2022 Aug 11. Available from: https://www.ncbi.nlm.nih.gov/books/NBK562734/
- Elvstam O, Marrone G, Medstrand P, et al.. All-cause mortality and serious non-AIDS events in adults with low-level human immunodeficiency virus viremia during combination antiretroviral therapy: results from a Swedish Nationwide Observational Study. Clin Infect Dis 2021; 72:2079–86.
- Flanagan, J.L., Simmons, P.A., Vehige, J. et al. Role of carnitine in disease. Nutr Metab (Lond) 7, 30 (2010). https://doi.org/10.1186/1743-7075-7-30
- Flórez-Álvarez L, Blanquiceth Y, Ramírez K, Ossa-Giraldo AC, Velilla PA, Hernandez JC and Zapata W (2020) NK Cell Activity and CD57C/NKG2Chigh Phenotype Are Increased in Men Who Have Sex With Men at High Risk for HIV. Front. Immunol. 11:537044. doi: 10.3389/fimmu.2020.537044
- Gallo, R. C., Sarin, P. S., Gelmann, E. P., Robert-Guroff, M., Richardson, E., Kalyanaraman, V. S., et al. (1983). Isolation of human T-cell leukemia virus in acquired immune deficiency syndrome (AIDS). Science 220 (4599), 865–867. doi:10.1126/science.6601823
- Ghosh S., Pulinilkunnil T., Yuen G., Kewalramani G., An D., Qi D., Abrahani A., Rodrigues B. Cardiomyocyte apoptosis induced by short-term diabetes requires mitochondrial GSH

depletion. Am. J. Physiol. Heart Circ. Physiol. 2005;289:H768–H776. doi: 10.1152/ajpheart.00038.2005.

- Gold JA, Grill M, Peterson J, Pilcher C, Lee E, Hecht FM, Fuchs D, Yiannoutsos CT, Price RW, Robertson K, Spudich S. Longitudinal characterization of depression and mood states beginning in primary HIV infection. AIDS Behav. 2014 Jun;18(6):1124-32. doi: 10.1007/s10461-013-0688-5. PMID: 24385231.
- Gómez-Archila LG, Palomino-Schätzlein M, Zapata-Builes W, Galeano E (2021) Development of an optimized method for processing peripheral blood mononuclear cells for 1H-nuclear magnetic resonance-based metabolomic profiling. PLoS ONE 16(2): e0247668. https://doi.org/10.1371/journal.pone.0247668
- Gómez-Archila LG, Palomino-Schätzlein M, Zapata-Builes W, Rugeles MT., Galeano Elkin. Plasma metabolomics by nuclear magnetic resonance reveals biomarkers and metabolic pathways associated with the control of HIV-1 infection/progression. Frontiers in Molecular Biosciences. 10. 2023. https://www.frontiersin.org/articles/10.3389/fmolb.2023.1204273. DOI=10.3389/fmolb.2023.1204273. ISSN=2296-889X
- Gostner JM, Becker K, Kurz K, Fuchs D. Disturbed Amino Acid Metabolism in HIV: Association with Neuropsychiatric Symptoms. Front Psychiatry. 2015 Jul 14;6:97. doi: 10.3389/fpsyt.2015.00097. PMID: 26236243; PMCID: PMC4500866.
- Günthard HF, Saag MS, Benson CA, del Rio C, Eron JJ, Gallant JE, Hoy JF, Mugavero MJ, Sax PE, Thompson MA, Gandhi RT, Landovitz RJ, Smith DM, Jacobsen DM, Volberding PA. Antiretroviral Drugs for Treatment and Prevention of HIV Infection in Adults: 2016 Recommendations of the International Antiviral Society-USA Panel. JAMA. 2016 Jul 12;316(2):191-210. doi: 10.1001/jama.2016.8900. PMID: 27404187; PMCID: PMC5012643.
- Hatjiharissi E, Xu L, Santos DD, Hunter ZR, Ciccarelli BT, Verselis S, et al. Increased natural killer cell expression of CD16, augmented binding and ADCC activity to rituximab among individuals expressing the Fc{gamma}RIIIa-158 V/V and V/F polymorphism. Blood. 2007;110: 2561–2564. 10.1182/blood-2007-01-070656
- Hixson EA, Borker PV, Jackson EK, Macatangay BJ. The Adenosine Pathway and Human Immunodeficiency Virus-Associated Inflammation. Open Forum Infect Dis. 2021 Jul 24;8(9):ofab396. doi: 10.1093/ofid/ofab396. PMID: 34557556; PMCID: PMC8454523.
- Jung YY, Park Y, Jones DP, Ziegler TR, Vidakovic B. Self-similarity in NMR Spectra: An Application in Assessing the Level of Cysteine. J Data Sci. 2010 Jan 1;8(1):1-19. PMID:

21572901; PMCID: PMC3092712.

- Kim JS, Nam MH, An SSA, Lim CS, Hur DS, Chung C, et al. Comparison of the automated fluorescence microscopic viability test with the conventional and flow cytometry methods. J Clin Lab Anal. 2011 Jan 1;25(2):90–4. pmid:21437999
- Kumar P, Liu C, Suliburk JW, Minard CG, Muthupillai R, Chacko S, Hsu JW, Jahoor F, Sekhar RV. Supplementing Glycine and N-acetylcysteine (GlyNAC) in Aging HIV Patients Improves Oxidative Stress, Mitochondrial Dysfunction, Inflammation, Endothelial Dysfunction, Insulin Resistance, Genotoxicity, Strength, and Cognition: Results of an Open-Label Clinical Trial. Biomedicines. 2020 Sep 30;8(10):390. doi: 10.3390/biomedicines8100390. PMID: 33007928; PMCID: PMC7601820.
- Li, T., and Deng, P. (2016). Nuclear Magnetic Resonance technique in tumor metabolism. Genes Dis. 4 (1), 28–36. Available at:. doi:10.1016/j.gendis.2016.12.001
- Louis KS, Siegel AC. Cell Viability Analysis Using Trypan Blue: Manual and Automated Methods BT—Mammalian Cell Viability: Methods and Protocols. In: Stoddart MJ, editor. Totowa, NJ: Humana Press; 2011. p. 7–12.
- Mastrocola R., Restivo F., Vercellinatto I., Danni O., Brignardello E., Aragno M., Boccuzzi G. Oxidative and nitrosative stress in brain mitochondria of diabetic rats. J. Endocrinol. 2005;187:37–44. doi: 10.1677/joe.1.06269.
- Mazzoli S, Trabattoni D, Lo Caputo S, Piconi S, Blé C, Meacci F, Ruzzante S, Salvi A, Semplici F, Longhi R, Fusi ML, Tofani N, Biasin M, Villa ML, Mazzotta F, Clerici M. HIV-specific mucosal and cellular immunity in HIV-seronegative partners of HIV-seropositive individuals. Nat Med. 1997 Nov;3(11):1250-7. doi: 10.1038/nm1197-1250. PMID: 9359700.
- Miyazawa M, Lopalco L, Mazzotta F, Lo Caputo S, Veas F, Clerici M; ESN Study Group. The 'immunologic advantage' of HIV-exposed seronegative individuals. AIDS. 2009 Jan 14;23(2):161-75. doi: 10.1097/QAD.0b013e3283196a80. PMID: 19098485.
- Montrucchio C, De Nicolò A, D'Ettorre G, D'Ascenzo F, Lazzaro A, Tettoni M, D'Avolio A, Bonora S, Celani L, Di Perri G, Calcagno A. Serum Trimethylamine-N-oxide Concentrations in People Living with HIV and the Effect of Probiotic Supplementation. Int J Antimicrob Agents. 2020 Apr;55(4):105908. doi: 10.1016/j.ijantimicag.2020.105908. Epub 2020 Jan 25. PMID: 31991223.
- Moreno-Fernandez ME, Rueda CM, Rusie LK, Chougnet CA. Regulatory T cells control HIV replication in activated T cells through a cAMP-dependent mechanism. Blood. 2011;117:5372–5380. doi: 10.1182/blood-2010-12-323162.

- Moreno-Fernandez ME, Rueda CM, Velilla PA, Rugeles MT, Chougnet CA. CAMP during HIV infection: Friend or Foe? AIDS Res Hum Retroviruses. 2012;28:49–53. doi: 10.1089/aid.2011.0265.
- Munshi SU, Rewari BB, Bhavesh NS, Jameel S (2013) Nuclear Magnetic Resonance Based Profiling of Biofluids Reveals Metabolic Dysregulation in HIV-Infected Persons and Those on Anti-Retroviral Therapy. PLoS ONE 8(5): e64298. https://doi.org/10.1371/journal.pone.0064298
- Nguyen D., Hsu J.W., Jahoor F., Sekhar R.V. Effect of increasing glutathione with cysteine and glycine supplementation on mitochondrial fuel oxidation, insulin sensitivity, and body composition in older HIV-infected patients. J. Clin. Endocrinol. Metab. 2014;99:169–177. doi: 10.1210/jc.2013-2376.
- Nightingale S, Winston A, Letendre S, Michael BD, McArthur JC, Khoo S, Solomon T. Controversies in HIV-associated neurocognitive disorders. Lancet Neurol. 2014 Nov;13(11):1139-1151. doi: 10.1016/S1474-4422(14)70137-1. PMID: 25316020; PMCID: PMC4313542.
- Ossa-Giraldo AC, Blanquiceth Y, Flórez-Álvarez L, Contreras-Ramírez K, Rojas M, Hernandez JC, et al. (2022) Seronegative MSM at high risk of HIV-1 acquisition show an immune quiescent profile with a normal immune response against common antigens. PLoS ONE 17(12): e0277120. https://doi.org/10.1371/journal.pone.0277120
- Palomino-Schtzlein M, García H, Gutiérrez-Carcedo P, Pineda-Lucena A, Herance JR. Assessment of gold nanoparticles on human peripheral blood cells by metabolic profiling with 1H-NMR spectroscopy, a novel translational approach on a patient-specific basis. PLoS One. 2017;12(8):e0182985.
- Pan X, Baldauf HM, Keppler OT, Fackler OT. Restrictions to HIV-1 replication in resting CD4+ T lymphocytes. Cell Res. 2013 Jul;23(7):876-85. doi: 10.1038/cr.2013.74. Epub 2013 Jun 4. PMID: 23732522; PMCID: PMC3698640.
- Panther E, Corinti S, Idzko M, et al.. Adenosine affects expression of membrane molecules, cytokine and chemokine release, and the T-cell stimulatory capacity of human dendritic cells. Blood 2003; 101:3985–90.
- Paris, D., Maniscalco, M., and Motta, A. (2018). Nuclear magnetic resonance-based metabolomics in respiratory medicine. Eur. Respir. J. [Internet] 52 (4), 1801107. Available at:. doi:10.1183/13993003.01107-2018
- Parthasarathy A, Cross PJ, Dobson RCJ, Adams LE, Savka MA, Hudson AO. A Three-Ring Circus: Metabolism of the Three Proteogenic Aromatic Amino Acids and Their Role

in the Health of Plants and Animals. Front Mol Biosci. 2018 Apr 6;5:29. doi: 10.3389/fmolb.2018.00029. PMID: 29682508; PMCID: PMC5897657.

- Qiu S, Cai Y, Yao H, Lin C, Xie Y, Tang S, Zhang A. Small molecule metabolites: discovery of biomarkers and therapeutic targets. Signal Transduct Target Ther. 2023 Mar 20;8(1):132. doi: 10.1038/s41392-023-01399-3. PMID: 36941259; PMCID: PMC10026263.
- Rincón, D.S., Flórez-Álvarez, L., Taborda, N.A. et al. NK cells from Men Who Have Sex with Men at high risk for HIV-1 infection exhibit higher effector capacity. Sci Rep 13, 16766 (2023). https://doi.org/10.1038/s41598-023-44054-1
- Sankaranantham M. HIV - Is a cure possible? Indian J Sex Transm Dis AIDS. 2019 Jan-Jun;40(1):1-5. doi: 10.4103/ijstd.IJSTD_112_15. PMID: 31143852; PMCID: PMC6532483.
- Sitole, L. J., Tugizimana, F., and Meyer, D. (2019). Multi-platform metabonomics unravel amino acids as markers of HIV/combination antiretroviral therapy-induced oxidative stress. J. Pharm. Biomed. Anal. [Internet] 176, 112796. Available from. doi:10.1016/j.jpba.2019.112796
- Steiber A, Kerner J, Hoppel CL, Carnitine: a nutritional, biosynthetic, and functional perspective. Molecular Aspects of Medicine, Volume 25, Issues 5–6, 2004. Pages 455-473. ISSN 0098-2997, https://doi.org/10.1016/j.mam.2004.06.006. (https://www.sciencedirect.com/science/article/pii/S0098299704000512)
- Stranford SA, Skurnick J, Louria D, Osmond D, Chang SY, Sninsky J, Ferrari G, Weinhold K, Lindquist C, Levy JA. Lack of infection in HIV-exposed individuals is associated with a strong CD8(+) cell noncytotoxic anti-HIV response. Proc Natl Acad Sci U S A. 1999 Feb 2;96(3):1030-5. doi: 10.1073/pnas.96.3.1030. PMID: 9927688; PMCID: PMC15345.
- Strober W. Trypan Blue Exclusion Test of Cell Viability. Curr Protoc Immunol. 1997 Mar 1;21(1):A.3B.1–A.3B.2.
- Strober W. Trypan Blue Exclusion Test of Cell Viability. Curr Protoc Immunol. 2015 Nov 2;111:A3.B.1–A3.B.3. pmid:26529666
- Su RC, Plesniarski A, Ao Z, Kimani J, Sivro A, Jaoko W, Plummer FA, Yao X, Ball TB. Reducing IRF-1 to Levels Observed in HESN Subjects Limits HIV Replication, But Not the Extent of Host Immune Activation. Mol Ther Nucleic Acids. 2015 Oct 27;4(10):e259. doi: 10.1038/mtna.2015.29. PMID: 26506037; PMCID: PMC4881757.
- Sugden, S and Cohen, EA. Attacking the Supply Lines: HIV-1 Restricts Alanine Uptake to Prevent T Cell Activation, Cell Host & Microbe,Volume 18, Issue 5,2015, Pages 514-517, ISSN 1931-3128, https://doi.org/10.1016/j.chom.2015.10.017.

(https://www.sciencedirect.com/science/article/pii/S1931312815004278)

- Tarancon-Diez, L., Rodríguez-Gallego, E., Rull, A., Peraire, J., Viladés, C., Portilla, I., et al. (2019). Immunometabolism is a key factor for the persistent spontaneous elite control of HIV-1 infection. EBioMedicine 42, 86–96. Available at:. doi:10.1016/j.ebiom.2019.03.004
- R. Wang, C.P. Dillon, L.Z. Shi, S. Milasta, R. Carter, D. Finkelstein, L.L. McCormick, P. Fitzgerald, H. Chi, J. Munger, D.R. Green Immunity, 35 (2011), pp. 871-882
- Woodham AW, Skeate JG, Sanna AM, Taylor JR, Da Silva DM, Cannon PM, Kast WM. Human Immunodeficiency Virus Immune Cell Receptors, Coreceptors, and Cofactors: Implications for Prevention and Treatment. AIDS Patient Care STDS. 2016 Jul;30(7):291-306. doi: 10.1089/apc.2016.0100. PMID: 27410493; PMCID: PMC4948215.
- Wu, V.H., Nordin, J.M.L., Nguyen, S. et al. Profound phenotypic and epigenetic heterogeneity of the HIV-1-infected CD4+ T cell reservoir. Nat Immunol 24, 359–370 (2023). https://doi.org/10.1038/s41590-022-01371-3
- Zangerle R, Kurz K, Neurauter G, Kitchen M, Sarcletti M, Fuchs D. Increased blood phenylalanine to tyrosine ratio in HIV-1 infection and correction following effective antiretroviral therapy. Brain Behav Immun (2010) 24:403–8. doi:10.1016/j.bbi.2009.11.004
- Zhao NQ, Vendrame E, Ferreira AM, Seiler C, Ranganath T, Alary M, Labbé AC, Guédou F, Poudrier J, Holmes S, Roger M, Blish CA. Natural killer cell phenotype is altered in HIV-exposed seronegative women. PLoS One. 2020 Sep 1;15(9):e0238347. doi: 10.1371/journal.pone.0238347. PMID: 32870938; PMCID: PMC7462289.
- Zimmermann H. Extracellular metabolism of ATP and other nucleotides. Naunyn Schmiedebergs Arch Pharmacol 2000; 362:299–309.

CAPÍTULO 4:

Plasma metabolomics by Nuclear Magnetic Resonance reveals biomarkers and metabolic pathways associated with the control of HIV-1 infection/progression.
Frontiers in Molecular Biosciences, Vol 10, 17 pag, 2023

Plasma metabolomics by Nuclear Magnetic Resonance reveals biomarkers and metabolic pathways associated with the control of HIV-1 infection/progression.

4.1. Abstract

How the human body reacts to the exposure of HIV-1 is an important research goal. Frequently, HIV exposure leads to infection, but some individuals show natural resistance to this infection; they are known as HIV-1-exposed but seronegative (HESN). Others, although infected but without antiretroviral therapy, control HIV-1 replication and progression to AIDS; they are named controllers, maintaining low viral levels and an adequate count of CD4+ T lymphocytes. Biological mechanisms explaining these phenomena are not precise. In this context, metabolomics emerges as a method to find metabolites in response to pathophysiological stimuli, which can help to establish mechanisms of natural resistance to HIV-1 infection and its progression. We conducted a cross-sectional study including 30 HESN, 14 HIV-1 progressors, 14 controllers and 30 healthy controls. Plasma samples (directly and deproteinized) were analyzed through Nuclear Magnetic Resonance (NMR) metabolomics to find biomarkers and altered metabolic pathways. The metabolic profile analysis of progressors, controllers and HESN demonstrated significant differences with healthy controls when a discriminant analysis (PLS-DA) was applied. In the discriminant models, 13 metabolites associated with HESN, 14 with progressors and 12 with controllers were identified, which presented statistically significant mean differences with healthy controls. In progressors, the metabolites were related to high energy expenditure (creatinine), mood disorders (tyrosine) and immune activation (lipoproteins), phenomena typical of the natural course of the infection. In controllers, they were related to an inflammation-modulating profile (glutamate and pyruvate) and a better adaptive immune system response (acetate) associated with resistance to progression. In the HESN group, with anti-inflammatory (lactate and phosphocholine) and virucidal (lactate) effects which constitute a protective profile in the sexual transmission of HIV. Concerning the significant metabolites of each group, we identified 24 genes involved in HIV-1 replication or virus proteins that were all altered in progressors but only partially in controllers and HESN. In summary, our results indicate that exposure to HIV-1 in HESN, as well as infection in progressors and controllers, affects the metabolism of individuals and that this affectation can be determined using NMR metabolomics.

4.2. Introduction

Human immunodeficiency virus type 1 (HIV-1), the causal agent of the acquired immunodeficiency syndrome (AIDS) in humans (1,2), continues to be a serious public health problem, after nearly 40 years of research (3), generating considerable mortality among those infected, and an excessive cost for the health care system (4,5).

The progression of infection from the acute phase to advanced infection or AIDS is a very complex process, which takes approximately ten years in absence of treatment (6,7). Some individuals can naturally control HIV-1 replication, maintaining low viral load (VL) levels and an adequate count of CD4+ T lymphocytes, in the absence of antiretroviral treatment (ART) for at least one year (8,9). These individuals are known as controllers (elite or viremic) and exhibit specific resistance mechanisms to disease progression, including the presence of HLA alleles, HLA-B27 and HLA-B57 (10).

Likewise, researchers have tried to characterize the natural resistance to HIV-1 infection among people exposed to the virus, who remain seronegative, known as HIV-exposed seronegative (HESN) individuals (11,12). To date, only the homozygous *Δ32* mutation in the *CCR5* gene, the main entry coreceptor of the virus, has been consistently associated with host resistance to HIV-1 in less than 3% of resistant individuals (13,14). Other known genetic and immunologic factors involved in resistance to HIV-1 infection only partially explain this phenomenon (15,16), which means that further mechanisms remain unclear.

In this context, metabolomics understood as the objective identification and quantification of small molecules in biological fluids (17), might help to understand the biochemical state of an organism for discovering biomarkers. Through case-control studies of metabolites in plasma, urine, or cells, by quantitative measurement using nuclear magnetic resonance (NMR) spectroscopy, different pathophysiological states have been explained (18–20), suggesting that metabolomics could be a potential tool for prognosis, diagnosis, and monitoring the efficacy of treatment (21), including HIV-1 infection.

Studies of the HIV effects on metabolism during *in vitro* replication and infection in animal and human models have provided new insights and targets for biomarker development and therapy. To date, little is known about the metabolic profiles that generate resistance to infection or a differential response to AIDS and its progression.

In the current study, we hypothesize that differences in the phenotype of infected individuals with high or low viral loads and seronegative individuals continuously exposed to HIV-1 will result in a dissimilar metabolomic plasma profile. Therefore, we collected and analyzed plasma samples of age and sex-matched groups of progressors, controllers, HESN and healthy controls by proton Nuclear Magnetic Resonance Spectroscopy (^{1}H NMR). We aim to identify a specific metabolic fingerprint of each group and to obtain biomarkers related to HIV-1 progression and natural resistance, providing valuable information on the pathogenesis of HIV-1 infection.

4.3. Materials and Methods

4.3.1. Chemicals and materials

All solvents and reagents were analytical grade, sodium phosphate dibasic dihydrate, sodium azide, deuterium oxide, 3-(Trimethylsilyl) propionic-2,2,3,3-d_4 acid sodium salt (TSP-d_4) and 3-(Trimethylsilyl)-1-propanesulfonic acid-d_6 sodium salt (DSS-d_6) were supplied by Merck (Germany). The ultrapure water was obtained in a Milli-Q purification system of Merck Millipore. The Vivaspin® 500 3000K MWCO Centrifugal Concentrators were provided by Sartorius.

4.3.2. Human subjects

A retrospective cross-sectional study was developed using a defined database of volunteers to build case-control relationships. Plasma samples from 88 volunteers were evaluated distributed as follows:

- HESN: thirty individuals, from serodiscordant couples (couples in which one partner is HIV-positive and the other HIV-negative). HESN reported multiple unprotected sexual episodes for >2 years at the time of enrollment, with at least 5 episodes of at-risk intercourse within 6 months before study entry with an HIV positive partner with a detectable viral load (22). The median VL of the partner was 2,569 RNA copies/mL (interquartile range= 400–25,250 copies/mL) (23). From these individuals, 10 (35%) were ART-naïve [VL median (interquartile range)] [10,257 (718 - 23,188)]. Eight (25%) were ART-responders VL<400. Finally, 12 (40%) were ART-non-responders [35,806 (18,200 – 118,770)]. No Δ32-homozygous subjects were included.
- Controllers: fourteen, with 1 year of diagnosis of HIV-1 infection, and viral load less than 2000 copies / mL in the absence of Antiretroviral therapy (ART) and normal CD4+ T

lymphocyte count (24). The median diagnosis time was 46 months (range 12-168). The median VL was 211 copies/mL (range 20-1885), and the median CD4+ T cells count was 745 cells/uL (range 514-1367). Only 2 (14%) controllers showed the HLA-B*27 allele, and 3 (21%) controllers showed the HLA-B*57 allele.

- Chronic progressors: fourteen, with a CD4 + T lymphocyte count> 350 cells / µL and a viral load between 10,000 and 100,000 copies / mL without receiving ART (25). The median diagnosis time was 51 months (range 12-120). From these, ten individuals had between 1 to 5 years of infection, three reported 6 to 9 years, and one had ten years of infection. The median VL was 31552 copies/mL (range 11206-160405) and the median CD4+ T cells count was 443 cells/uL (range 267-819).
- PLHIV: people living with HIV. In this case it refers to a mix of controllers and progressors.
- Healthy controls: thirty, with negative serological tests for HIV-1 without risk behaviors.

This study was approved by the Bioethical Committee Universidad de Antioquia; and all the individuals signed informed consent prepared according to Colombian Legislation Resolution 008430/1993.

4.3.3. Processing of blood samples

The Blood sample was collected from all participants by using potassium-EDTA collection tubes. Then, it was centrifuged at 1000 x g for 5 min at 4ºC, and 2mL of plasma was stored at -80ºC until processing. Two methodologies were established to process the biofluid: a direct analysis and a deproteinization analysis.

For the direct analysis 300 µL of Buffer pH 7.4 (Na_2HPO_4 75 mM DSS 2.3 mM and NaN_3 0.04%) was added to a microcentrifuge tube (1.5 or 2 mL) and reserved. Then, the plasma sample was thawed, homogenized, and 300 µL transferred to the previously mentioned vial with buffer. The resulting solution was mixed and 550 µL transferred to a 5 mm NMR tube for analysis. Tubes were degassed for 3 min before capping.

In the case of deproteinization analysis, 300 µL of Buffer pH 7.4 (Na_2HPO_4 75 mM TSP 2.3 mM and NaN_3 0.04%) was added to a microcentrifuge tube (1.5 or 2 mL) and reserved. Then, the vial containing the sample was thawed, the plasma was homogenized, and 500 µL of plasma were taken to a Vivaspin 500 centrifugal filter (Previously pre-washed 5 times with Buffer pH 7.4). The sample was centrifuged at 12,000 gravities at 4 ° C for 60 minutes. 300 µL of the filtrate was brought to the microcentrifuge tube containing the 300 µL of Buffer pH 7.4 they were mixed with

a micropipette. Finally, 550 µL of the solution were taken and transferred to a 5 mm NMR tube for analysis. The tubes were degassed for 3 minutes before being capped.

4.3.4. ^{1}H-NMR experiments

The ^{1}H-NMR spectra of extracts were recorded at 300K by a Bruker AVANCE III 600.13 MHz spectrometer equipped with 5 mm triple-resonance z-gradient cryoprobe (Prodigy TCI 1H-13C/15N-2H). TopSpin version 3.6.2 (Bruker GmbH Karlsruhe Germany) was used for spectrometer control purposes. Carr-Purcell-Meiboom-Gill (CPMG) pulse sequence with water presaturation and spoil gradients (*cpmgpr1d* pulse sequence) for direct analysis (64k data points, spectral width 12019 Hz, dummy scans 8, 64 scans, loop for T2 filter 80, gain 80,6, delay time 4 sec, fixed echo time 0.0007 sec and the 90° pulse length was adjusted to about 10.40 µs). ^{1}H 1D Nuclear Overhauser Effect Spectroscopy (NOESY) NMR spectra with water presaturation and spoil gradients (*noesygppr1d* pulse sequence) was used for analysis of deproteinization samples Spectra were acquired with 128 scans, 64k data points, spectral width of 7211 Hz, and relaxation delay of 20 s (dummy scans 4, gain 203, and the 90° pulse length was adjusted to about 10.42 µs)

Total Correlation Spectroscopy (TOCSY) and multiplicity Heteronuclear Single Quantum Correlation (HSQC) were performed on representative samples with 256–512 t1 increments 32–96 transients and a relaxation delay of 1.5 s. The TOCSY spectra were recorded by a standard MLEV-17 pulse sequence with mixing times (spin-lock) of 65 ms.

4.3.5. Data analysis and statistics

NMR spectra processing: ^{1}H-NMR spectra were transformed with a 0.5 line-broadening and manually baseline- and phase-corrected with Topspin 3.6.4. NMR signals of DSS-d6 (for direct analysis) or TSP-d_4 (for deproteinization analysis) were referenced to 0.0 ppm. For metabolite identification purposes the ^{1}H and chemical shift values and multiplicity of signals were compared with the reference data from the Chenomx software (Chenomx NMR Suite 8.4 Chenomx Inc. Edmonton Canada) in combination with spectral databases Human Metabolome Database, and the Biological Magnetic Resonance Bank and several literature reports (26,27). Optimal integration regions were defined for each metabolite to select signals without overlapping. Integration was performed with MestreNova 14 (Mestrelab Research SL Santiago de Compostela Spain) by manually integrating of the previously identified signals. With these regions an

integration matrix (Integral Regions) was built which was later applied to the 88 acquired spectra and a matrix of integrals was built for all the spectra (Integral series). This matrix of integrals was normalized by the sum of the total signals of the spectrum using Excel (Microsoft USA).

Multivariate and univariate analysis of Metabolomic Profiles: The previously normalized matrix of integrals was processed using MetaboAnalyst 5.0. First a principal component analysis (PCA) was performed which allowed finding groups of samples with a similar metabolic pattern and/or segmenting those with a different metabolome.

Then five case-control relationships were established: healthy controls versus progressors; healthy controls versus controller; healthy controls versus PLHIV (progressors and controllers); healthy controls versus HESN, and controllers versus progressors. These relationships were evaluated by Partial Least Squares Discriminant Analysis (PLS-DA) which links two data matrices and improves the separation between different groups of samples. The quality of the PLS-DA was evaluated, and a permutation test was carried out to calculate the goodness of fit (R2) and the predictive capacity (Q2) of the randomly generated models. An analysis of the results of the PLS-DA statistic (VIP scores) was performed and the metabolites that contributed significantly to the separation of the groups were identified. Variables with a VIP score greater than 1.0 were considered significant for the model.

Finally, the selected variables were subjected to a Univariate analysis using a difference of means test (Wilcoxon Test). For tests with a p value less than 0.05 (p<0.05) a statistically significant difference between the means (mean or median as appropriate) was assumed for the variable evaluated. In the case of obtaining more than one significant signal for a given metabolite, we selected the signal with less overlapping for graphical representation.

4.3.6. Gene Analysis

Analysis of associated genes was carried out with the metabolites that were statistically significant after univariate analysis. For this, the web interface of MetaboAnalyst 5.0 [14] was used. Metabolites were introduced in the *Network Explorer* section of the platform and the *Metabolite-Gene-Disease Interaction Network analysis* was carried out, which provides a global view of potential functional relationships between metabolites, connected genes, and target diseases. The network integrates gene-metabolite, metabolite-disease, and gene-disease interaction networks.

The genes identified through the previous analysis were filtered through a comparison process with the National Center for Biotechnology Information (NCBI) gene database of the U.S. National

Library of Medicine, excluding genes unrelated to HIV-1. Additionally, to perform a more specific analysis, genes that were not related to two or more groups and/or metabolites were excluded.

Then, we proceeded to perform an individual analysis of the selected genes through a review in the NCBI gene database. Looking specifically at the section on HIV-1 interactions, we filter further into the subcategories *Replication interactions* (human proteins shown to be required for HIV-1 infectivity and replication) and *Protein interactions* (proteins that have been shown to interact with proteins from HIV-1).

4.4. Results

4.4.1. Human subjects

Figure 4.1 shows the main characteristics of the five case-control relationships analyzed in the study. Out of the 88 available volunteers, a selection was made to generate groups balanced by gender and age. A summarized table of all individuals can be found in **Supplementary Table 1 (Anexo 8)**.

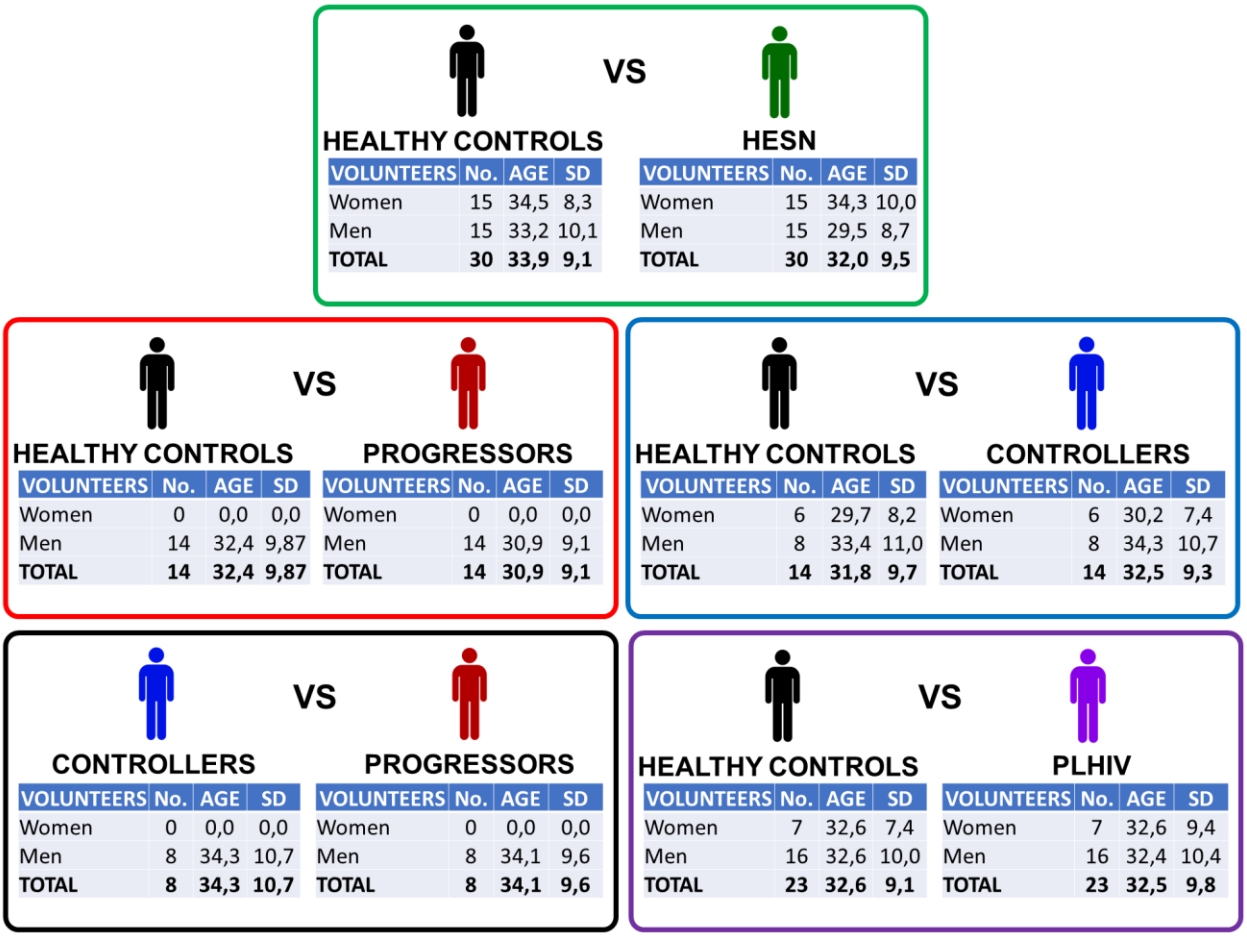

FIGURE 4.1. Case-control relationships. Detail of each of the five relationships built to analyze plasma samples in a direct and filtered way. To know the details of each of the volunteers who participated in the study, see **Supplementary Table 1 (Anexo 8)**. Exclusion criteria: Individuals with hemoglobin ≤8.0 g/dl; neutrophil count ≤1,000/mm3; receiving some immunosuppressive treatment; pregnant or lactating women; cancer or with an active infection or disease requiring hospitalization. Age reported as the sample mean. SD: standard deviation.

To compare HESN with healthy individuals, we achieved a completely gender-balanced comparison, with 15 women and 15 men in each group. Also, in the case of controllers, the number of women and men was similar in both groups. In the case of joining controllers and progressors (PLHIV), we built up groups with a higher number of men than women, but that was still gender-matched between patients and controls.

4.4.2. Analysis of metabolic plasma profiles

^{1}H NMR metabolomics analysis was performed on intact and filtered plasma samples, to identify the highest possible number of compounds. During the spectral analysis process, it was possible to identify fifty-five metabolites in the direct plasma samples: two alcohols, twenty-one amino acids, fourteen lipid-related signals, sixteen organic acids, one purine derivative, and one sugar. In the filtered plasma samples, forty-five metabolites were identified: two alcohols, twenty amino acids, two lipid-related signals, eighteen organic acids, two derived from purine and one from sugar. It should be noted that three metabolites that were not observed in direct plasma could be detected in filtered plasma samples: two organic acids (2-hydroxybutyrate and 3-Hydroxyisovalerate) and one purine derivative (Inosine). In **Supplementary Figure 1 (Anexo 14)** and **Supplementary Figure 2 (Anexo 15)** a model NMR spectrum can be seen with the relative assignment for direct and filtered Plasma respectively. Furthermore, the quantification of small metabolites was more accurate in the filtered samples due to the absence of overlapping with broad lipoprotein samples. It should be noted that the lipoproteins evaluated in the unfiltered samples complement the metabolomic analysis of the plasma samples from the volunteers. To know the details of the metabolites identified in the plasma samples, see **Supplementary Table 2 (Anexo 9)**.

After assignment, normalized integration tables were obtained of all spectra **(Supplementary Table 3) (Anexo 10)** and analyzed by multivariate analysis.

4.4.3. Multivariate analysis of plasma metabolomic profiles

Initially, a principal component analysis (PCA) was performed with all 88 samples to get a general overview. The result is shown in Figure 4.2, which corresponds to the PCA score plots of direct plasma samples and filtered plasma samples. In this unsupervised analysis, we detected a clustering between samples belonging to the same group (healthy control, controller, HESN or progressor). This grouping was more evident for direct plasma samples, which could indicate that lipoproteins play a key role in the differentiation of the groups. HESN samples seem to have the highest dispersion. PCAs were also performed for the five established case-control relationships, which can be seen in **Supplementary Figure 3 (Anexo 16)**.

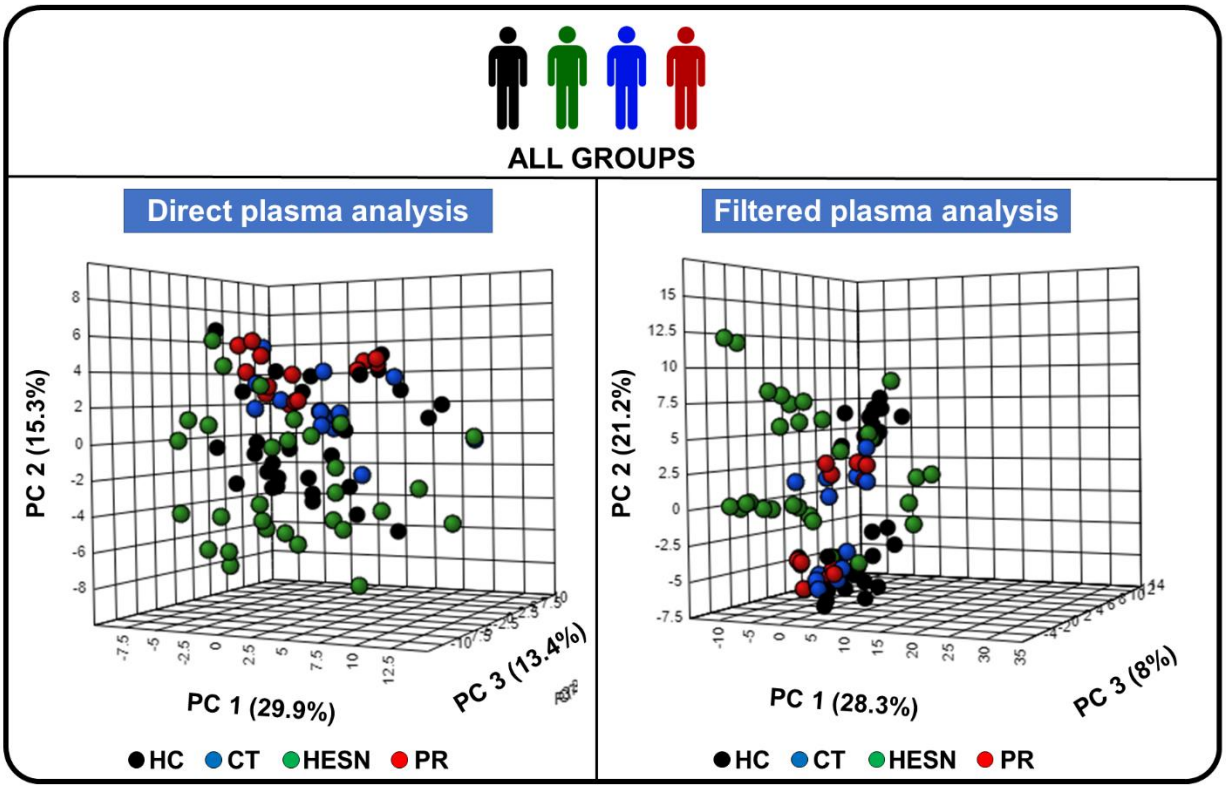

FIGURE 4.2. Principal component analysis (PCA) of the study groups. 3D score plot charts of the PCA analysis of all study volunteers, on the left side the analysis with direct plasma and on the right side with filtered plasma. PC: Principal component, HC: Healthy control, CT: controller, HESN: HIV-exposed seronegative, PR: Progressor. Each of the three axes of the graph represents a principal component. The values that each of the axes takes is related to the fact that there is a score value for each observation (row) in the data set; so, there is score values for the first component, another for the second component, and one for the third. The score value for an observation, say the first component, is the distance from the origin, along the direction (load vector) of the first component, to the point where that observation projects onto the direction vector.

In addition, to observe specific metabolic differences between our five case-control relationships, a pair-wise Partial Least Squares Discriminant Analysis (PLS-DA) was performed (see Figure 4.3).

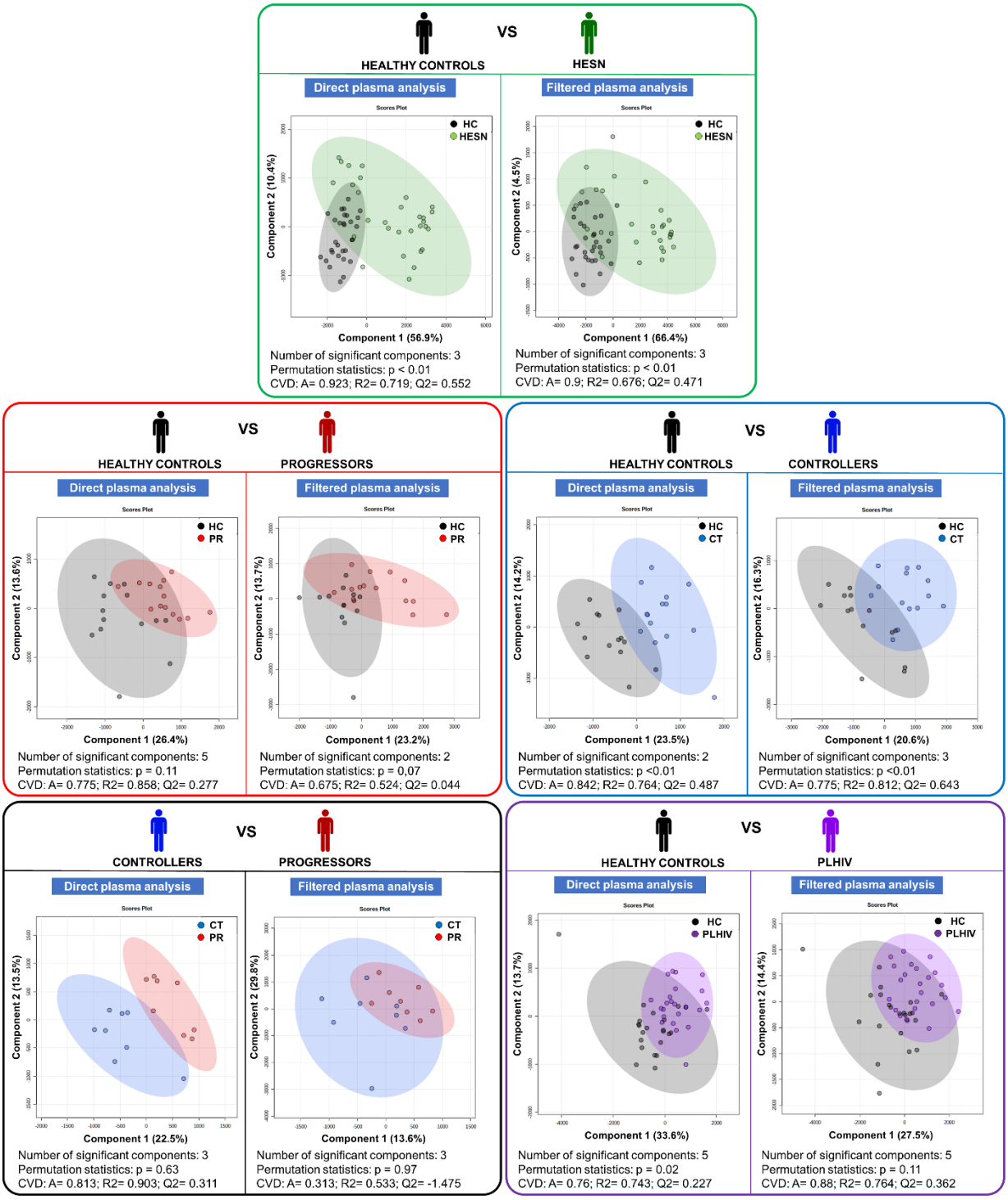

FIGURE 4.3. Partial Least Squares Discriminant Analysis (PLS-DA). Score plot charts of the PLS-DA of the five case-control relationships established; on the left side, the analysis with direct plasma and on the right side with filtered plasma (in each colored box). HC: Healthy control, CT: controller, HESN: HIV-exposed seronegative, PR: Progressor. CVD: Cross-validation details, A: Accuracy, R2: goodness of fit, Q2:

predictive capacity. Healthy controls in black, HESN in green, Progressors in red, Controllers in blue and PLHIV in purple.

Statistically significant PLS-DA models were obtained comparing HESN and controllers with healthy controls. Models between healthy controls and progressors and healthy controls versus PLHIV were statistically significant. The analysis of the PLS-DA statistics through the VIP score allowed reducing the number of relevant variables (metabolites) to be analyzed as follows:

- Healthy controls versus HESN: 27 in direct plasma (DP) and 26 in filtered plasma (FP).
- Healthy controls versus progressors: 47 in DP and 33 in FP.
- Healthy controls versus controllers: 35 in DP and 38 in FP.
- Healthy controls versus PLHIV (progressors and controllers): 39 in DP and 36 in FP.
- Controllers versus progressors: 45 in DP and 39 in FP.

For the details of the PLS-DA statistics see **Supplementary Table 4 (Anexo 11)**.

4.4.4. Univariate analysis of plasma metabolomic profiles

The metabolites relevant for PLS discriminant modeling were further submitted to univariate statistical analysis to identify significant changes in each case-control comparison. The detail of the mean difference analysis (Wilcoxon Test) can be seen in **Supplementary Table 5 (Anexo 12)**.

For the Healthy controls versus HESN comparison, 21 signals (variables) were identified with a significant variation, 13 associated with the FP. These signals are associated with 13 metabolites: 6 lipid-related signals (Low density lipoprotein aliphatic chain, Low density lipoprotein (CH3), very low-density lipoprotein (CH3), Lipids CH2C=C, lipids: (-n(CH3)3 and VDL (aliphatic chain)), 3 amino acids (Serine, alanine and phosphocholine), 2 organic acids (3-Hydroxybutyrate and Lactate), 1 alcohol (Myo inositol) and 1 sugar (Glucose). Only the lactate was increased in HESN, the rest of the metabolites were decreased compared to healthy controls.

In healthy controls versus progressors comparison, 28 signals were identified, 19 associated with DP. These signals correspond to 14 metabolites: 8 amino acids (Creatine, creatinine, Glutamine, Methionine, Serine, Alanine, Tyrosine and Valine), 4 lipid-related signals (Lipid: CH2CH2O, VLDL, Lipids CH2C=C, VDL-2 (aliphatic chain) and very low-density lipoprotein (CH3)), 1 alcohol (Myo

inositol) and 1 sugar (Glucose). The metabolites of the lipid-related signals, Serine, Alanine and Tyrosine, are decreased.

While for the comparison healthy controls versus controllers 24 signals were identified (equal amount of each matrix), which were associated with 12 metabolites: 5 amino acids (Glutamine, Glutamate, Methionine, Serine and Valine), 3 lipid-related signals (Low density lipoprotein (CH3), very low-density lipoprotein (CH3) and lipids: (-n(CH3)3), 3 organic acids (3-Hydroxybutyrate, Acetate and Pyruvate) and 1 sugar (Glucose).

Figure 4.4 shows a quantitative comparison of the most representative metabolites that change between healthy controls and HESN, progressor and controller groups.

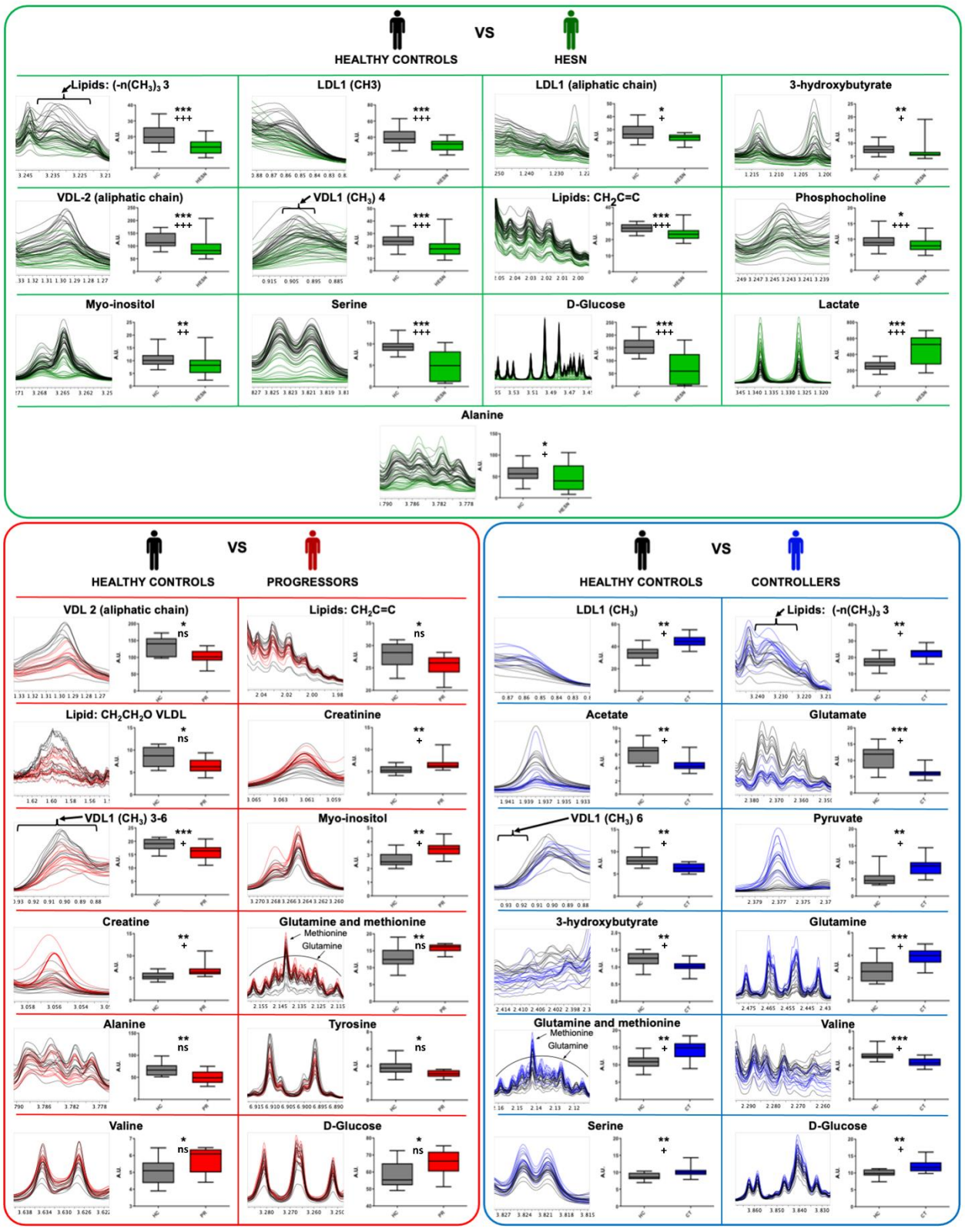
HEALTHY CONTROLS
VS
HESN
Lipids: (-n(CH3)3 3
LDL1 (CH3)
LDL1 (aliphatic chain)
3-hydroxybutyrate
VDL-2 (aliphatic chain)
VDL1 (CH3) 4
Lipids: CH2C=C
Phosphocholine
Myo-inositol
Serine
D-Glucose
Lactate
Alanine
HEALTHY CONTROLS
VS
PROGRESSORS
VDL 2 (aliphatic chain)
Lipids: CH2C=C
Lipid: CH2CH2O VLDL
Creatinine
VDL1 (CH3) 3-6
Myo-inositol
Creatine
Glutamine and methionine
Methionine
Glutamine
Alanine
Tyrosine
Valine
D-Glucose
HEALTHY CONTROLS
VS
CONTROLLERS
LDL1 (CH3)
Lipids: (-n(CH3)3 3
Acetate
Glutamate
VDL1 (CH3) 6
Pyruvate
3-hydroxybutyrate
Glutamine
Glutamine and methionine
Methionine
Glutamine
Valine
Serine
D-Glucose

FIGURE 4.4. Metabolites that explain the difference between the groups. Results of the Wilcoxon test for the significant variables (metabolites) for each proposed PLS-DA model. In the panel (A) (main green box), the comparison of healthy controls and HESN, in the panel (B) (main red box) the comparison between healthy controls and progressives, and in the panel (C) (main blue box) the comparison between healthy controls and controllers. Within each small individual box: on the left the region of the spectrum (metabolite signal) ^{1}H-NMR superimposed of all the samples analyzed in each comparison, on the right side the box-and-whisker plot for the normalized concentration and the statistical significance of each test. *: p-value < 0.05, **: p-value < 0.01 and ***: p-value < 0.001. +: False Discovery Rate (FDR) < 0.05, + +: FDR <0.01, + + +: FDR <0.001 and ns: FDR >0.05. Healthy controls in black, HESN in green, progressors in red, and the controllers in blue.

The comparisons of healthy controls versus PLHIV and controllers versus progressors can be seen in **Supplementary Figure 4 (Anexo 17)**.

4.5. Discussion

4.5.1. All three study groups show a specific metabolic profile

PCA and the PLS-DA analysis demonstrated significant differences between the controllers, progressors, and HESN study groups versus healthy controls. In contrast, only weak models were obtained comparing controllers and progressors, which may be due to the low sample number in this case (n=8). Differences were related to specific metabolites present in different concentrations between the groups as demonstrated by univariate analysis (Wilcoxon Test). For each case-control comparison, a list of metabolites with altered levels were established. Figure 4.5 provides an overview of all the important metabolites in the different comparisons.

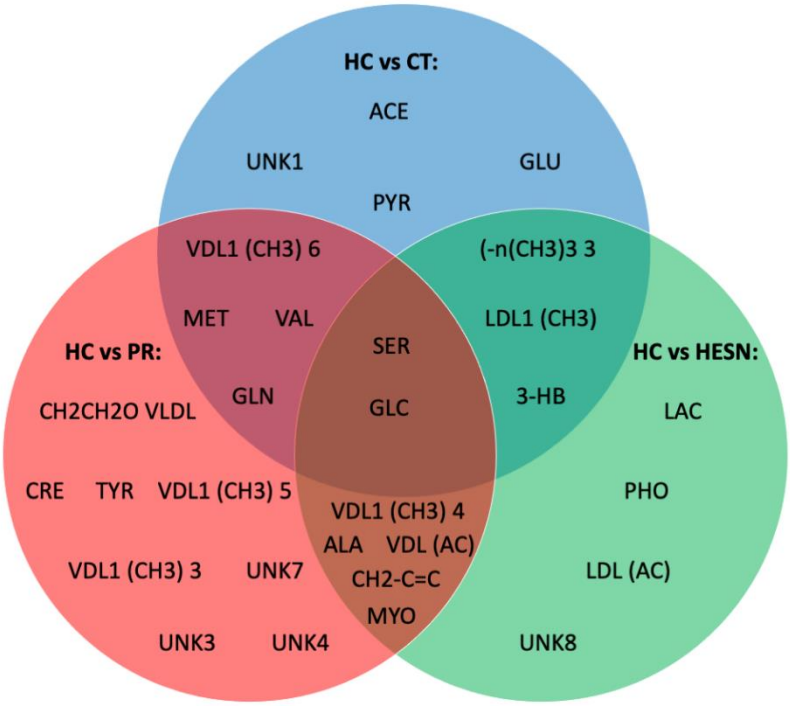

FIGURE 4.5. Venn diagram of metabolites that explain differences among groups. Set Analysis showing the metabolites related to differences similarities among the metabolomic profiles of controllers, progressors and HESN. In the main part of each set the metabolites related only to one study group and in the intercepts the metabolites related to two or more groups (central intercept). CT: controllers (In blue color set), HESN: HIV-exposed seronegative (In green color set), PR: Progressors (In red color set). HC: Healthy controls, 3-HB: 3-Hydroxybutyrate, ACE: Acetate, ALA: Alanine, CRE: Creatine, Cre: Creatinine, Glc: d-Glucose, GLN: Glutamine, GLU: Glutamate, LAC: Lactate, LDL1 (CH3): Low density lipoprotein (CH3), LDL (AC): Low density lipoprotein aliphatic chain, MET: Methionine, MYO: Myo-inositol, PHO: Phosphocholine, PYR: Pyruvate, SER: Serine, TYR: Tyrosine, UNK: Unknown, VAL: Valine, VDL (AC): VDL-2 (aliphatic chain), VDL1 (CH3): Very low-density lipoprotein (CH3), (-n (CH3)3: Lipids (-n (CH3)3, CH2CH2O VLDL: Lipid: CH2CH2O VLDL, CH2-C=C: Lipids CH2C = C.

We observed that the disease altered the metabolomics blood profile of progressors, showing the highest number of relevant variables compared to healthy controls in the PLS-DA (47 in DP and 33 in FP), and the highest number of differentiated metabolites (14) in the univariate analysis. The impact on controllers was lower (35 variables in DP and 38 in FP, 12 relevant metabolites), while

HESNs are the group with the lowest number of relevant variables in the PLS-DA (27 in DP and 26 in FP) and 13 differentiated metabolites. The progression of HIV induces the massive elimination of CD4+ T lymphocytes and alterations in various components of the immune system (28), which would explain the difference in the metabolic profiles of the progressors compared to controllers and HESN. Since the controllers resist the progression to AIDS, maintaining low levels of viral load and an adequate count of CD4+ T lymphocytes (8,9), it is directly reflected in a lesser impairment of their metabolism. Likewise, identifying of a differential metabolomic profile in HESNs allows us to affirm that the natural resistance of the host to HIV-1 is associated with a differential phenotype. Detailed analysis of the metabolomics changes (positive or negative variation) between the groups, as shown in Figure 4.6, allowed establishing differential (a) and comparative profiles (b) for each of the case-control comparisons.

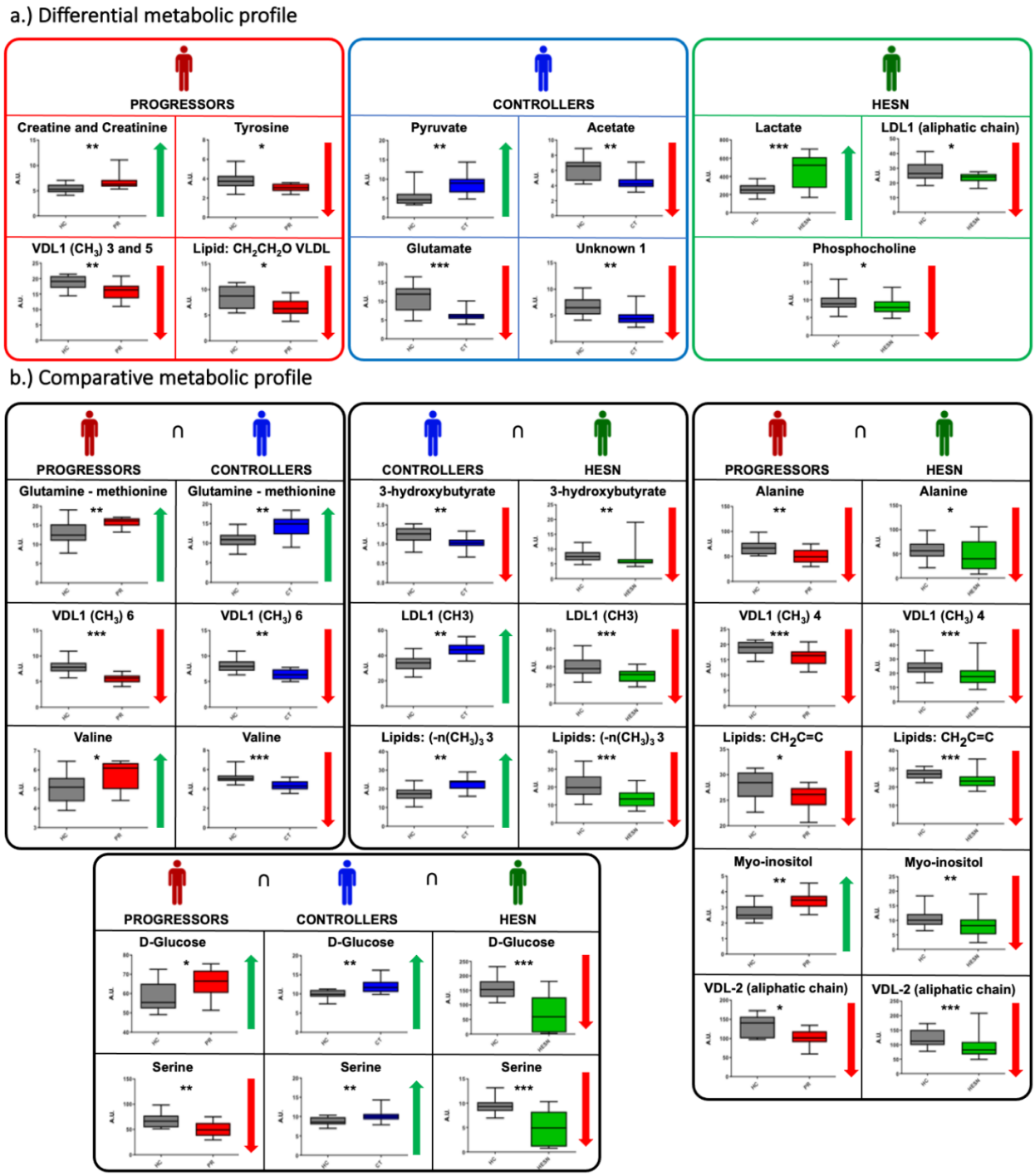

FIGURE 4.6. Specific and related metabolites in the study groups. (A) Differential metabolic profile: Metabolites that only exhibit a statistically significant mean difference compared to healthy controls in a study group, (B) Comparative metabolic profile: Metabolites exhibiting a statistically significant mean difference compared to healthy controls in two or more study groups. Variation: ↓ (Smaller area or relative concentration in the reference method) ↑ (Bigger area or relative concentration in the reference method). The box-and-whisker plot for the normalized concentration and the statistical significance of each test. *: p-

value < 0.05, **: p-value < 0.01 and ***: p-value < 0.001. +: False Discovery Rate (FDR) < 0.05, + +: FDR <0.01, + + +: FDR <0.001 and ns: FDR >0.05. Healthy controls in gray, HESN in green, progressors in red, and the controllers in blue.

Alterations associated to progressors: Progressors stand out for the variation of specific lipoproteins and creatine/creatinine and tyrosine, while changes in glutamate, pyruvate and acetate seem to be specific for controllers. On the other hand, alterations in lactate, phosphocholine and VDL are characteristic of HESN.

Concerning the comparative analysis (Figure 4.6b), it is worth mentioning that glucose and serine change in all three case-control comparisons, although these changes do not always have the same sign. It is also noteworthy that progressors and HESN have five metabolic changes in common, four of which have the same sign.

Differentially, it was possible to identify an increase in the expression of creatine-creatinine in progressors; creatine is found in muscles (29). Altered creatine-creatinine values have been previously found in HIV positive patients (30) and are related to the prolonged period of high energy expenditure (31) and cachexia (32).

Likewise, tyrosine was decreased in the HIV progressors group. Tyrosine is a precursor of catecholamines (adrenaline, dopamine and noradrenaline) whose altered metabolism is related to mood disorders (36). An increased phenylalanine/tyrosine ratio is common in patients with HIV-1 infection and is related to immune activation (39). Previous NMR studies identified tyrosine downregulation in untreated HIV-infected patients (30). This change was not observed in HIV controllers, which allows us to state that low tyrosine levels are a biomarker of HIV infection progression.

One factor associated with HIV progression is the response of immune cells (41). Immune cells undergo energetic and structural remodeling following immune activation. It generates metabolic changes associated with increased energy and biosynthetic demands as viral load increases and the immune system responds (42). This metabolic changes , including lipid homeostasis, since mitochondria plays a key role in the biosynthesis of phospholipids for membranes, as well as in the catabolism of fatty acids (46). Unsurprisingly, phospholipid alterations are a common finding in the metabolic profiles of HIV-infected individuals.

A comparison of the commonly altered metabolites in controllers and progressors showed that valine is differentially regulated between both groups; it increased in progressors and decreased in controllers compared to healthy controls. A recent study show a significant increase in Valine levels in TEC before the loss of control compared to PEC, therefore, valine was defined as the main differentiating factor between the studied groups (62). That is, elevated valine levels could be a potential biomarker for the prediction of virological progression in controllers and progressors.

Alterations associated to controllers: L-glutamic acid and pyruvate are differentially altered in controllers; these metabolites modulate latent HIV reactivation and/or macrophage inflammation *in vitro* (57). A previous study demonstrated that glutamic acid was elevated in Persistent Elite Controllers (PEC) compared to Transient HIV Elite Controllers (TEC) (62), suggesting that glutamate metabolism is associated with a delay in the recovery time from HIV.

Likewise, in controllers, acetate is differentially decreased. This metabolite is transiently released into the circulation in response to systemic bacterial infection, as a resistance mechanism of the host's adaptive immune system. (63)(64)(65). The virus-associated mechanism may be related to the group of HIV controllers, where downregulation of acetate concentration would slow down the lipogenesis.

Alterations associated to HESN: In all groups (controllers, progressors and HESN) evaluated, changes in the lipid profile were observed. However, HESNs showed variations in response compared to controllers and progressors; all significant changes were downward. It highlights the Low-density lipoproteins (LDL) signals that are decreased in HESN and increased in the other groups. LDLs are considered proinflammatory lipid species (48) and associated with immune activation in HIV-infected persons (49). Other NMR metabolomics studies support our findings on altered lipid metabolism in HIV-infected people (30,50–54). We did not identify previous studies that used NMR metabolomics to characterize HESNs as done in this study; however, a previous study that included 32 HESN individuals demonstrated that immune status secondary to HIV exposure influences the plasma efflux capacity of HDL cholesterol, which is buffered in HESN (55).

Likewise, glucose was altered in all groups. It is decreased in HESN and increased in the other groups. Early steps of virus replication are moderately affected by the ability of the target cell to perform glycolysis at the time of infection. Similarly, virion production in cultures containing

galactose was reduced by 20% to 60% compared to the amount produced in glucose-containing cultures (56). That suggests that high glucose availability in the body is associated with infection process and virus replication, which do not occur in HESN.

The HESN group showed higher lactate expression compared to healthy controls, lactate has anti-inflammatory effects modeling the production of interleukins and other proinflammatory molecules (66) (67). This suggests a protective role of lactate in the sexual transmission of HIV.

Phosphocholine was found significantly decreased in the HESN group. Phosphocholine shown to be able to suppress immune response in human placenta (68), initiate phagocytic immune recognition (69) and is an intermediate in the synthesis of phosphatidylcholine in tissues (70). Phosphatidylcholine has anti-inflammatory effects(71). The low concentration of phosphocholine in HESN could be related to the production of phosphatidylcholine that would reduce the inflammation of the colon and rectum that occurs in anal intercourse, a common means of HIV exposure in HESN.

It should be noted that cell activation and inflammation have been reported to enhance infection. (72–74). The metabolites identified in HESN, and the metabolic and signaling pathways associated with these metabolites, may contribute to the reduction of inflammation and cell activation. Inflammation increases the risk of contracting HIV by causing the activation of HIV target cells (CD4+ T cells), increasing their susceptibility to HIV infection (75). Inflammation also leads to increased recruitment of these activated target CD4+ T cells at the site of HIV exposure (76).

A specific comparison of progressors and HESN revealed that Myo-inositol was elevated in progressors and decreased in HESN. Myo-inositol is a marker of glial reactivity, gliosis and neuroinflammation (77). Previously, it was found to be elevated in different brain regions by Magnetic Resonance Spectroscopy (MRS) studies of HIV-infected patients with cognitive impairment (78–81). A previous NMR study on CSF found that impairments in late recall and motor function were associated with higher levels of myo-inositol (33). Alterations in myo-inositol levels were also identified in human mouthwashes (34) and brain tissue of HIV-infected rodents (82). All these findings, including those presented in our research, suggest that elevated levels of myo-inositol promote HIV progression in infected people and resistance to infection in HESN.

4.5.2. HIV-related genes associated with significant metabolites

In addition to the altered metabolic pathways, we also wanted to study the genes that were related to these pathways, whose expression could be altered. An analysis of the genes associated to HIV-1 that were related to the metabolites responsible for the difference between the study groups and the healthy controls **(**See **Supplementary Table 6) (Anexo 13)**, revealed that patients living with HIV (Controllers and progressors) had the highest number of genes involved in their infectious status (231 and 185 genes versus 78 for HESN). (Figure 4.7) affected by the expression or differential regulation of the metabolites. A total of 341 genes.

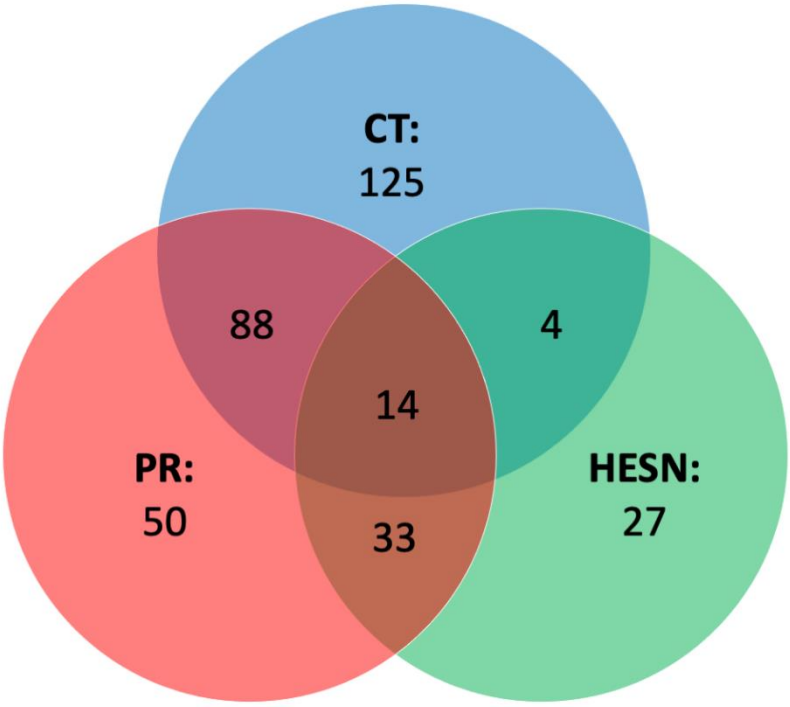

FIGURE 4.7. Venn diagram of HIV-related genes. Genes identified by Metabolite-Gene-Disease Interaction Network analysis and filtered through the NCBI gene database as related to HIV-1. In the main part of each set, the genes are related only to one study group and in the intercepts, the genes are related to two or more groups (central intercept). CT: controllers (In blue color set), HESN: HIV-exposed seronegative (In green color set), PR: Progressors (In red color set).

We further obtained a more reduce list of genes by filtering only those found in two or more study groups or related to two or more metabolite (Table 4.1). From these, 21 genes were specifically related to replications interactions (Table 4.2). The table also summarizes how the alteration of these genes has been previously related to HIV.

Table 4.1. HIV-related genes that were associated with two or more study groups and/or metabolites.

Gene	PR	CT	HESN
GLUD2	ALA↓ GLN↑	GLU↓ GLN↑	ALA↓
DNAJB1 PABPN1 FOXP2	ALA↓ GLN↑	GLN↑	ALA↓
LDHA LDHB LDHC	CRE↑ Cre↑ ALA↓	GLU↓ PYR↑	ALA↓ LAC↑
MDH2	ALA↓	GLU↓ PYR↑	ALA↓
PKLR PKM	ALA↓ CRE↑	PYR↑	ALA↓ LAC↑
SLC38A2 SLC38A1	ALA↓ GLN↑ MET↑		ALA↓
GPT2	ALA↓ Cre↑	GLU↓ PYR↑	ALA↓
SLC16A10	ALA↓ GLN↑ MET↑ TYR↓ VAL↑		ALA↓
ARG2	CRE↑ VAL↑	GLU↓ VAL↓	N/A
SERPINC1 CAD CREBBP F13A1 MTOR HTT HIP1 DNAJA1 HSPA1A HSPA4 HSPB1 KCNN3 PML PPP2R2B MAPK8 PSMD2 ATXN2 TAF4 TGM4 TGM1 TGM3 UBA52 SUMO1 UFD1 VCP VEGFA NCOA3 HAP1 TGM5 HDAC6 DNAJB6 STUB1 BAIAP2 TARDBP UBQLN2 ASRGL1 RBM17 TGM7 TMEM37 TGM6.	GLN↑		
BDNF CREB1 GAPDH GART GRIN2B IMPDH2 JUN MAPT MSN PFAS ALDH18A1 QARS1 SPTBN TGM2 NME6	GLN↑	GLU↓ GLN↑	
CASP3	GLN↑ VAL↑	GLU↓ GLN↑ VAL↓	
CAT	CRE↑ MET↑ TYR↓	GLU↓ MET↑	
COMT	VAL↑	GLU↓ VAL↓	
DARS1 EPRS1 GLUL KARS1 RARS1 AIMP2 AIMP1 EEF1E1 LARS1	GLN↑ MET↑	GLU↓ GLN↑ MET↑	
DLD	VAL↑	GLU↓ PYR↑ VAL↓	
F2	Cre↑	GLU↓	
FMO3 HBB MAT2A MSRA MTR MTRR MYH9 SMUG1	MET↑		

GAD1 SOD1	MET↑	GLU↓ MET↑	
IARS1	GLN↑ MET↑ VAL↑	GLU↓ GLN↑ MET↑ VAL↓	
IGF1 OAT PFKM	CRE↑	GLU↓	
MARS1	Cre↑ GLN↑ MET↑	GLU↓ GLN↑ MET↑	
TH	TYR↓	GLU↓	
MAP3K14	Cre↑ GLN↑	GLN↑	
ALB	Cre↑ TYR↓	N/A	PHO↓
BGLAP	Cre↑		LAC↑
FOXL2 FTL HMOX1 HOXA13 LYZ PIN1 PPIA SRSF1 SLC7A5 KYNU	ALA↓		ALA↓
CD79A CRP	Cre↑		PHO↓
DNMT1 FCN2 GCK B4GALT1 HK2 IFNB1 LGALS3 PYGL SGCB B4GALT2 SIGLEC5 H6PD SIGLEC7 CD207 GBA2 GXYLT1	Glc↑		Glc↓
F3	Cre↑ Glc↑		Glc↓
GYPA	CRE↑ Glc↑		Glc↓
FOS	N/A	GLU↓	LAC↑
OXCT1		3 HB↓	
PLA2G1B		GLU↓	PHO↓
LDHD		PYR↑	LAC↑
ALPI MPO	Cre↑ TYR↓	N/A	N/A
GAA CRNKL1 PIK3C2A	CRE↑ Cre↑		

CT: controllers, HESN: HIV-exposed seronegative, PR: Progressors, N/A: Not Applicable. Variation: ↓ (Smaller area or relative concentration in the reference method) ↑ (Bigger area or relative concentration in the reference method). 3-HB: 3-Hydroxybutyrate, ALA: Alanine, CRE: Creatine, Cre: Creatinine, Glc: D-Glucose, GLN: Glutamine, GLU: Glutamate, LAC: Lactate, MET: Methionine, PHO: Phosphocholine, PYR: Pyruvate, TYR: Tyrosine, VAL: Valine.

Table 4.2. List of genes differentially expressed in the study groups and associated with replication and protein interactions with HIV-1.

Description	Progressors	Controllers	HESN	Replication and/or protein interactions with HIV-1
DnaJ heat shock protein	ALA↓ - GLN↑	GLN↑	ALA↓	Knockdown of DnaJ inhibits HIV-1 replication in HeLa-derived TZM-bl cells (83), while an increase in

family (Hsp40) member B1				gene expression is relevant for Tat recruitment in HIV-infected cells (97). Hsp40 protein is required for HIV-1 Nef-mediated enhancement of viral gene expression and replication (98), and that members of this family of interferon-inducible proteins should be considered within its anti-HIV function (99).
Pyruvate kinase L/R	ALA↓ - CRE↑	PYR↑	ALA↓ - LAC↑	*PKLR* has shown a regulatory role in HIV replication in HeLa P4/R5 cells (84).
solute carrier family 38 member 2	ALA↓ - GLN↑ - MET↑	GLU↓ - GLN↑ - MET↑	ALA↓	Down-regulation of *SLC38A1* and *SLC38A2* is associated with HIV interference with immunometabolism in activated primary human CD4+ T cells (85). This gene uses alanine as an endogenous substrate for T cell mitogenesis (85).
solute carrier family 38 member 1	ALA↓ - GLN↑ - MET↑	GLU↓ - GLN↑ - MET↑	ALA↓	
Glutamic--pyruvic transaminase 2	ALA↓ Cre↑	GLU↓ PYR↑	ALA↓	Knockdown has been shown to inhibit early stages of HIV-1 replication in an *in vitro* model (86).
Caspase-3	GLN↑ VAL↑	GLU↓ GLN↑ VAL↓	N/A	Is related to HIV-associated dementia (HAD) (87)(104).
Coagulation factor II thrombin	Cre↑	GLU↓		Encodes the protein prothrombin (108). Knockdown of *F2* has previously been suggested to have a regulatory role in HIV replication (84). Thrombin was shown to activate gp120/gp41 of HIV-1, enhances virus-cell fusion (110), and enhance the gp160-mediated fusion of HIV-1 with R5 tropism (111).
Glyceraldehyde-3-phosphate dehydrogenase	GLN↑	GLU↓ GLN↑		Negatively regulates HIV-1 infection by directly interacting with *Gag* and *Gag-Pol* (88).
Glutamate ionotropic receptor NMDA type subunit 2B	GLN↑	GLU↓ GLN↑		*GRIN2B* deletion inhibits HIV-1 replication in HeLa P4/R5 cells (84), this inhibition is related to HIV-gp120 and Tat upregulating *GRIN2B* (120,121).
Lysyl-trna synthetase 1	GLN↑ MET↑	GLU↓ GLN↑ MET↑		Knockdown inhibited the initial stages of HIV-1 replication *in vitro*(86).
Methionyl-trna synthetase 1	Cre↑ GLN↑ MET↑	GLU↓ GLN↑ MET↑		Knockdown inhibited HIV-1 replication (89).

Moesin	GLN↑	GLU↓ GLN↑		Knockdown inhibited HIV-1 replication (89).
Phosphofructo kinase muscle	CRE↑	GLU↓		Knockdown inhibited the initial stages of HIV-1 replication *in vitro*(86).
Mitogen-activated protein kinase 14	Cre↑ GLN↑	GLN↑		MAP kinases (MAPK) have been associated with HIV proteins such as *gp120* (124), *Nef* (125), *Tat* (126) and *Vpr* (127), which generate a strong activation of these enzymes.
Aminoacyl trna synthetase complex interacting multifunctional protein 1	GLN↑ MET↑	GLU↓ GLN↑ MET↑		Knockdown inhibited HIV-1 replication (89).
Leucyl-trna synthetase 1	GLN↑ MET↑	GLU↓ GLN↑ MET↑		Knockdown of DnaJ inhibits HIV-1 replication in HeLa-derived TZM-bl cells (83)
Ficolin 2	Glc↑	N/A	Glc↓	Ficolin-2 binds to HIV-1 *gp120* and blocks viral infection (90).
Glucokinase	Glc↑		Glc↓	Knockdown inhibited HIV-1 replication in HeLa-derived TZM-bl cells (83).
Interferon beta 1	Glc↑		Glc↓	Interferon-beta, encoded by *IFNB1* gene, has antiviral, antibacterial and anticancer properties (130). HIV-1 replication upregulates the expression of *IFNB1* gene (91).
Galectin 3	Glc↑		Glc↓	In HIV infection, deletion of *LGALS3* by shRNA was shown to inhibit HIV-1 production *in vitro* (92). Furthermore, it promotes HIV-1 budding through association with Alix and Gag p6 (92).
Sialic acid binding Ig like lectin 5	Glc↑		Glc↓	Siglec-5 associated with divergent outcomes of HIV-1 infection in human and chimpanzee CD4 T cells (93).
Phospholipase A2 group IB	N/A	GLU↓	PHO↓	This gene was involved in CD4 anergy and CD4 lymphopenia in HIV-infected patients (94).
Myeloperoxidase	Cre↑ TYR↓	N/A	N/A	Knockdown of MPO inhibits HIV-1 replication in HeLa P4/R5 cells (84).
Crooked neck pre-mrna splicing factor 1	CRE↑ Cre↑			CRNKL1 was identified as a highly Selective Regulator of Intron-Retaining HIV-1 and Cellular mRNAs (95).

CT: controllers, HESN: HIV-exposed seronegative, PR: Progressors, N/A: Not Applicable. Variation: ↓ (Smaller area or relative concentration in the reference method) ↑ (Bigger area or relative concentration in

the reference method). 3-HB: 3-Hydroxybutyrate, ALA: Alanine, CRE: Creatine, Cre: Creatinine, Glc: D-Glucose, GLN: Glutamine, GLU: Glutamate, LAC: Lactate, MET: Methionine, PHO: Phosphocholine, PYR: Pyruvate, TYR: Tyrosine, VAL: Valine.

Among the genes listed in Table 2, five are related to the three study groups (progressors, controllers and HESN): *DnaJ heat shock protein family (Hsp40) member B1,* Pyruvate kinase liver and red blood cell (*PKLR*) gene, Solute carrier gene family *SLC38A1* and *SLC38A2*, and glutamic-pyruvic transaminase 2 (*GPT2*).

High pyruvate expression in controllers may be associated with elevated PKLR function, whereas in HESN, high lactate expression that is associated with reduced pyruvate would explain a differential gene response in these two groups. *SLC38A1* and *SLC38A2* uses alanine as an endogenous substrate for T cell mitogenesis (85). This metabolite is markedly down regulated in HESN and progressors, but not in controllers, which instead have a low concentration of GLU. In contrast to the HESN, progressors and controllers increase GLN and MET metabolites.

GPT2 encodes a mitochondrial alanine transaminase, a pyridoxal enzyme that catalyzes the reversible transamination between alanine and 2-oxoglutarate to generate pyruvate and glutamate (101). The differential regulations of pyruvate and glutamate in Controllers may be related to a differential expression of this gene and low rates of virus replication.

On the other hand, when the association between HIV progressors and controllers was analyzed, eleven genes (*CASP3* gene, coagulation factor II thrombin gene (*F2*), Glyceraldehyde-3-phosphate dehydrogenase (*GAPDH*), Glutamate ionotropic receptor NMDA type subunit 2B (*GRIN2B*), Mitogen-activated protein kinase 14 (*MAP3K14*) gene, Lysyl-trna synthetase 1 (*KARS*), Phosphofructokinase muscle (*PFKM*), Methionyl-tRNA synthetase 1 (*MARS*) Moesin (*MSN*), Aminoacyl tRNA synthetase complex interacting multifunctional protein 1 (*AIMP1*),) were identified expressed in both groups, but related to different metabolites or opposite metabolite concentration changes (See Table 2).

Between progressors and controllers there are two differences in terms of the associated metabolites: the expression of valine (elevated in progressors and decreased in controllers) and the expression of glutamate that is exclusively decreased in controllers. For this reason, glutamate is then the most important metabolite in the difference between progressors and controllers. Glutamate causes neuronal cell death by apoptosis at high concentrations (105,106) and glutamate-induced apoptotic cell death was associated with caspase-3 gene regulation (107). It

could then be stated that low concentrations of glutamate in Controllers may be related to a neuroprotective profile and regulation of apoptosis in HIV infection.

The relationship between prothrombin and/or thrombin with glutamate has been previously determined (112,113). Thus, the differential expression of glutamate in controllers may be related to an optimized cell proliferation mediated by *F2* that participates in resistance to HIV progression.

There is a relationship between glutamate and *GAPDH* shown previously (116), so, it can be inferred that the differential levels observed in controllers can promote the downregulation of the infection.

Creatinine was only found to be altered in progressors. It has been demonstrated that dietary supplementation with creatinine generates a decrease in MAPK expression (122); this could occur in progressors with high creatinine levels. MAP kinases (MAPK) are involved in cellular processes such as development, proliferation, differentiation, and transcription regulation (123).

Furthermore, in our study we were able to identify five genes that were associated with progressors and HESN: *Ficolin 2* (*FCN2*), *Glucokinase* (*GCK*), *Interferon-beta 1* (*IFNB1*), *Galectin 3* (*LGALS3*), and *Sialic acid binding Ig like lectin 5* (*SIGLEC5*) (See Table 2). All five genes are associated with D-Glucose regulation in study groups. In the progressors, D-Glucose is upregulated and downregulated in the HESNs group. Glucokinase is a type IV isozyme found exclusively in the liver. It is highly specific, only uses D-glucose as a substrate (129); it is encoded by the GCK gene, and its knockdown inhibited HIV-1 replication in HeLa-derived TZM-bl cells (83). The low concentration of D-Glucose in HESNs may be related to this phenomenon.

It was possible to identify a gene that is related to controllers and HESN, phospholipase A2 group IB gene *(PLA2G1B)*. Recently, this gene was involved in CD4 anergy and CD4 lymphopenia in HIV-infected patients (94). This gene could potentially be differentially expressed between controllers and HESN. It is enough to identify that HESN present a decreased concentration of PHO, a metabolite directly related to *PLA2G1B*.

Finally, within the replication interactions, two progressor-specific genes associated with increased expression of CRE and Cre were identified: Myeloperoxidase (MPO) and Crooked neck pre-mRNA splicing factor 1 (CRNKL1).

4.6. Conclusions

This study presents differential metabolic profile for controllers, progressors and HESN individuals. Thus, the resistance to HIV-1 progression is associated with changes in the individual's metabolome, represented in the form of metabolites, that could provide biomarkers of the infectious status of PLHIV, and it will be key to determine the factors that control the infection. Based on our results, we propose tyrosine, glutamate, and valine as biomarkers of progression in HIV infection in progressors and controllers.

It should be noted that the variation in the viral load during progression could affect the metabolomic profile of these individuals. Therefore, conducting a longitudinal study with this population help to resolve this issue. However, according to the HIV “test and treat” guidelines, it is challenging to recruit HIV-positive individuals without receiving ART; therefore, evaluations spanning continuous years of suppressive or not suppressive ART compared with our cohort can help to elucidate the impact of the ART in the metabolomic profile.

Likewise, our study visualized that natural resistance to HIV-1 infection in HESN individuals is associated with a specific metabolic fingerprint, described here for the first time according to our research. We consider LDL, glucose, lactate and Phosphocholine plausible biomarkers of natural resistance to HIV infection in HESN. However, additional studies should be carried out with other HESN groups: female sex workers (FSWs), children born to HIV infected mothers and men who have sex with men (MSM). These analyses allow us to compare and contrast our results, to determine if the metabolites are repeated in the different groups or if there are other phenotypes associated with HIV resistance.

The specific biomarkers for each group were associated with genes and proteins related to HIV-1, therefore, differential expression among groups could potentially explain the characteristics of each group. Finally, we consider that proteomic, transcriptomic and genomic analyzes should be carried out to have a more comprehensive look at the progression and the natural resistance to HIV-1 infection.

4.7. Conflict of Interest

The authors declare that the research was conducted in the absence of any commercial or financial relationships that could be construed as a potential conflict of interest.

4.8. Author Contributions

Conceptualization: LGGA, MPS, EG.

Data curation: LGGA, MPS and EG.

Formal analysis: LGGA and MPS.

Funding acquisition: MPS, WZB and EG.

Investigation: LGGA.

Methodology: LGGA, MPS and EG.

Project administration: EG.

Resources: WZB, EG and MTR.

Supervision: EG.

Validation: LGGA and MPS.

Visualization: LGGA and MPS.

Writing original draft preparation: LGGA, MPS, WZB and EG.

Writing review & editing: LGGA, MPS, WZB and MTR.

4.9. Funding

The authors acknowledge the Comité para el Desarrollo de la Investigación (CODI) of the University of Antioquia https://www.udea.edu.co for the financial support of this work. The funder had no role in study design, data collection and analysis, decision to publish, or preparation of the manuscript.

4.10. References

1. Barré-Sinoussi F, Chermann JC, Rey F, Nugeyre MT, Chamaret S, Gruest J, et al. Isolation

of a T-lymphotropic retrovirus from a patient at risk for acquired immune deficiency syndrome (AIDS). Science. 1983 May;220(4599):868–71.

2. Gallo RC, Sarin PS, Gelmann EP, Robert-Guroff M, Richardson E, Kalyanaraman VS, et al. Isolation of human T-cell leukemia virus in acquired immune deficiency syndrome (AIDS). Science. 1983 May;220(4599):865–7.

3. ONUSIDA, Comunicaciones y Promoción Mundial. HOJA INFORMATIVA 2021. Estadísticas mundiales sobre el VIH. 2021;1–7. Available from: https://www.unaids.org/sites/default/files/media_asset/UNAIDS_FactSheet_es.pdf

4. Frank TD, Carter A, Jahagirdar D, Biehl MH, Douwes-Schultz D, Larson SL, et al. Global, regional, and national incidence, prevalence, and mortality of HIV, 1980-2017, and forecasts to 2030, for 195 countries and territories: a systematic analysis for the Global Burden of Diseases, Injuries, and Risk Factors Study 2017. Lancet HIV [Internet]. 2019 Dec 1;6(12):e831–59. Available from: https://doi.org/10.1016/S2352-3018(19)30196-1

5. Roth GA, Abate D, Abate KH, Abay SM, Abbafati C, Abbasi N, et al. Global, regional, and national age-sex-specific mortality for 282 causes of death in 195 countries and territories, 1980-2017: a systematic analysis for the Global Burden of Disease Study 2017. Lancet [Internet]. 2018 Nov 10;392(10159):1736–88. Available from: https://doi.org/10.1016/S0140-6736(18)32203-7

6. Vergis EN, Mellors JW. Natural history of HIV-1 infection. Infect Dis Clin North Am. 2000 Dec;14(4):809–25, v–vi.

7. Kumar P. Long term non-progressor (LTNP) HIV infection. Indian J Med Res [Internet]. 2013 Sep;138(3):291–3. Available from: https://pubmed.ncbi.nlm.nih.gov/24135172

8. Walker BD. Elite control of HIV Infection: implications for vaccines and treatment. Top HIV Med. 2007;15(4):134–6.

9. Cao Y, Qin L, Zhang L, Safrit J, Ho DD. Virologic and immunologic characterization of long-term survivors of human immunodeficiency virus type 1 infection. N Engl J Med. 1995 Jan;332(4):201–8.

10. Gonzalo-Gil E, Ikediobi U, Sutton RE. Mechanisms of Virologic Control and Clinical Characteristics of HIV+ Elite/Viremic Controllers. Yale J Biol Med [Internet]. 2017 Jun 23;90(2):245–59. Available from: https://pubmed.ncbi.nlm.nih.gov/28656011

11. Meyers AFA, Fowke KR. International symposium on natural immunity to HIV: a gathering of the HIV-exposed seronegative clan. Vol. 202 Suppl, The Journal of infectious diseases. United States; 2010. p. S327-8.

12. Young JM, Turpin JA, Musib R, Sharma OK. Outcomes of a National Institute of Allergy and Infectious Diseases Workshop on understanding HIV-exposed but seronegative individuals. Vol. 27, AIDS research and human retroviruses. 2011. p. 737–43.

13. Huang Y, Paxton WA, Wolinsky SM, Neumann AU, Zhang L, He T, et al. The role of a mutant CCR5 allele in HIV-1 transmission and disease progression. Nat Med. 1996 Nov;2(11):1240–3.

14. Ding J, Liu Y, Lai Y. Knowledge From London and Berlin: Finding Threads to a Functional HIV Cure [Internet]. Vol. 12, Frontiers in Immunology . 2021. Available from: https://www.frontiersin.org/articles/10.3389/fimmu.2021.688747

15. Lederman MM, Alter G, Daskalakis DC, Rodriguez B, Sieg SF, Hardy G, et al. Determinants of protection among HIV-exposed seronegative persons: an overview. J Infect Dis. 2010 Nov;202 Suppl(Suppl 3):S333-8.

16. Taborda-Vanegas N, Zapata W, Rugeles MT. Genetic and Immunological Factors Involved in Natural Resistance to HIV-1 Infection. Open Virol J [Internet]. 2011/05/11. 2011;5:35–43. Available from: https://pubmed.ncbi.nlm.nih.gov/21660188

17. Nicholson JK, Lindon JC, Holmes E. “Metabonomics”: understanding the metabolic responses of living systems to pathophysiological stimuli via multivariate statistical analysis of biological NMR spectroscopic data. Xenobiotica. 1999 Nov;29(11):1181–9.

18. Bertini I, Cacciatore S, Jensen B V, Schou J V, Johansen JS, Kruhøffer M, et al. Metabolomic NMR Fingerprinting to Identify and Predict Survival of Patients with Metastatic Colorectal Cancer. Cancer Res [Internet]. 2012 Jan 1;72(1):356 LP – 364. Available from: http://cancerres.aacrjournals.org/content/72/1/356.abstract

19. Li T, Deng P. Nuclear Magnetic Resonance technique in tumor metabolism. Genes Dis [Internet]. 2016 Dec 13;4(1):28–36. Available from: https://pubmed.ncbi.nlm.nih.gov/30258906

20. Paris D, Maniscalco M, Motta A. Nuclear magnetic resonance-based metabolomics in respiratory medicine. Eur Respir J [Internet]. 2018 Oct 1;52(4):1801107. Available from:

http://erj.ersjournals.com/content/52/4/1801107.abstract

21. Puchades-Carrasco L, Pineda-Lucena A. Metabolomics in pharmaceutical research and development. Curr Opin Biotechnol [Internet]. 2015;35:73–7. Available from: http://dx.doi.org/10.1016/j.copbio.2015.04.004

22. Zapata W, Rodriguez B, Weber J, Estrada H, Quiñones-Mateu ME, Zimermman PA, et al. Increased levels of human beta-defensins mRNA in sexually HIV-1 exposed but uninfected individuals. Curr HIV Res. 2008 Nov;6(6):531–8.

23. Aguilar-Jiménez W, Zapata W, Caruz A, Rugeles MT. High Transcript Levels of Vitamin D Receptor Are Correlated with Higher mRNA Expression of Human Beta Defensins and IL-10 in Mucosa of HIV-1-Exposed Seronegative Individuals. PLoS One [Internet]. 2013 Dec 5;8(12):e82717. Available from: https://doi.org/10.1371/journal.pone.0082717

24. Pereyra F, Addo MM, Kaufmann DE, Liu Y, Miura T, Rathod A, et al. Genetic and immunologic heterogeneity among persons who control HIV infection in the absence of therapy. J Infect Dis. 2008 Feb;197(4):563–71.

25. Taborda NA, González SM, Alvarez CM, Correa LA, Montoya CJ, Rugeles MT. Higher Frequency of NK and CD4+ T-Cells in Mucosa and Potent Cytotoxic Response in HIV Controllers. PLoS One [Internet]. 2015 Aug 20;10(8):e0136292. Available from: https://doi.org/10.1371/journal.pone.0136292

26. Wishart DS, Feunang YD, Marcu A, Guo AC, Liang K, Vázquez-Fresno R, et al. HMDB 4.0: the human metabolome database for 2018. Nucleic Acids Res [Internet]. 2018 Jan 4;46(D1):D608–17. Available from: https://pubmed.ncbi.nlm.nih.gov/29140435

27. Ulrich EL, Akutsu H, Doreleijers JF, Harano Y, Ioannidis YE, Lin J, et al. BioMagResBank. Nucleic Acids Res [Internet]. 2007 Nov 4;36(suppl_1):D402–8. Available from: https://doi.org/10.1093/nar/gkm957

28. Brenchley JM, Price DA, Douek DC. HIV disease: fallout from a mucosal catastrophe? Nat Immunol. 2006 Mar;7(3):235–9.

29. Kreider RB, Stout JR. Creatine in Health and Disease. Vol. 13, Nutrients . 2021.

30. Sitole LJ, Tugizimana F, Meyer D. Multi-platform metabonomics unravel amino acids as markers of HIV/combination antiretroviral therapy-induced oxidative stress. J Pharm Biomed Anal [Internet]. 2019;176:112796. Available from:

https://doi.org/10.1016/j.jpba.2019.112796

31. Kosmiski L. Energy expenditure in HIV infection. Am J Clin Nutr [Internet]. 2011/11/16. 2011 Dec;94(6):1677S-1682S. Available from: https://pubmed.ncbi.nlm.nih.gov/22089443

32. Von Roenn JH, Roth EL, Craig R. HIV-Related Cachexia: Potential Mechanisms and Treatment. Oncology [Internet]. 1992;49(suppl 2(Suppl. 2):50–4. Available from: https://www.karger.com/DOI/10.1159/000227129

33. Dickens AM, Anthony DC, Deutsch R, Mielke MM, Claridge TDW, Grant I, et al. Cerebrospinal fluid metabolomics implicate bioenergetic adaptation as a neural mechanism regulating shifts in cognitive states of HIV-infected patients. Aids. 2015;29(5):559–69.

34. Ghannoum MA, Mukherjee PK, Jurevic RJ, Retuerto M, Brown RE, Sikaroodi M, et al. Metabolomics reveals differential levels of oral metabolites in HIV-infected patients: Toward novel diagnostic targets. Omi A J Integr Biol. 2013;17(1):5–15.

35. Fisher MJ, Dickson AJ, Pogson CI. The role of insulin in the modulation of glucagon-dependent control of phenylalanine hydroxylation in isolated liver cells. Biochem J [Internet]. 1987 Mar 15;242(3):655–60. Available from: https://pubmed.ncbi.nlm.nih.gov/3036097

36. Hasler G, Fromm S, Carlson PJ, Luckenbaugh DA, Waldeck T, Geraci M, et al. Neural response to catecholamine depletion in unmedicated subjects with major depressive disorder in remission and healthy subjects. Arch Gen Psychiatry [Internet]. 2008 May;65(5):521–31. Available from: https://pubmed.ncbi.nlm.nih.gov/18458204

37. Shintaku H. Disorders of tetrahydrobiopterin metabolism and their treatment. Curr Drug Metab. 2002 Apr;3(2):123–31.

38. Stein DJ. Depression, anhedonia, and psychomotor symptoms: the role of dopaminergic neurocircuitry. CNS Spectr. 2008 Jul;13(7):561–5.

39. Zangerle R, Kurz K, Neurauter G, Kitchen M, Sarcletti M, Fuchs D. Increased blood phenylalanine to tyrosine ratio in HIV-1 infection and correction following effective antiretroviral therapy. Brain Behav Immun [Internet]. 2010;24(3):403–8. Available from: https://www.sciencedirect.com/science/article/pii/S0889159109005157

40. Meyer D, Sitole L. Raman Spectroscopy-Based Metabonomics of HIV-Infected Sera Detects Amino Acid and Glutathione Changes. Curr Metabolomics. 2015 Mar 28;03:1.

41. Shi Y, Su J, Chen R, Wei W, Yuan Z, Chen X, et al. The Role of Innate Immunity in Natural Elite Controllers of HIV-1 Infection. Front Immunol [Internet]. 2022;13. Available from: https://www.frontiersin.org/article/10.3389/fimmu.2022.780922

42. González Plaza JJ, Hulak N, Kausova G, Zhumadilov Z, Akilzhanova A. Role of metabolism during viral infections, and crosstalk with the innate immune system. Intractable Rare Dis Res. 2016;5(2):90–6.

43. Pinti M, Nasi M, Gibellini L, Roat E, De Biasi S, Bertoncelli L, et al. The Role of Mitochondria in HIV Infection and Its Treatment. J Exp Clin Med [Internet]. 2010;2(4):145–55. Available from: https://www.sciencedirect.com/science/article/pii/S1878331710600241

44. Nunnari J, Suomalainen A. Mitochondria: In Sickness and in Health. Cell [Internet]. 2012;148(6):1145–59. Available from: https://www.sciencedirect.com/science/article/pii/S0092867412002358

45. Hulgan T, Gerschenson M. HIV and mitochondria: more than just drug toxicity. J Infect Dis [Internet]. 2012/04/03. 2012 Jun 15;205(12):1769–71. Available from: https://pubmed.ncbi.nlm.nih.gov/22476715

46. Tilokani L, Nagashima S, Paupe V, Prudent J. Mitochondrial dynamics: overview of molecular mechanisms. Garone C, Minczuk M, editors. Essays Biochem [Internet]. 2018 Jul 20;62(3):341–60. Available from: https://doi.org/10.1042/EBC20170104

47. O'Donnell VB, Rossjohn J, Wakelam MJO. Phospholipid signaling in innate immune cells. J Clin Invest [Internet]. 2019;128(7):2670–9. Available from: https://doi.org/10.1172/JCI97944

48. Brennan E, Kantharidis P, Cooper ME, Godson C. Pro-resolving lipid mediators: regulators of inflammation, metabolism and kidney function. Nat Rev Nephrol [Internet]. 2021;17(11):725–39. Available from: https://doi.org/10.1038/s41581-021-00454-y

49. Funderburg NT, Mehta NN. Lipid Abnormalities and Inflammation in HIV Inflection. Curr HIV/AIDS Rep [Internet]. 2016;13(4):218–25. Available from: https://doi.org/10.1007/s11904-016-0321-0

50. Hewer R, Vorster J, Steffens FE, Meyer D. Applying biofluid 1H NMR-based metabonomic techniques to distinguish between HIV-1 positive/AIDS patients on antiretroviral treatment and HIV-1 negative individuals. J Pharm Biomed Anal. 2006;41(4):1442–6.

51. Philippeos C, Steffens FE, Meyer D. Comparative 1H NMR-based metabonomic analysis of HIV-1 sera. J Biomol NMR. 2009;44(3):127–37.

52. Riddler SA, Li X, Otvos J, Post W, Palella F, Kingsley L, et al. Antiretroviral therapy is associated with an atherogenic lipoprotein phenotype among HIV-1-infected men in the multicenter AIDS cohort study. J Acquir Immune Defic Syndr. 2008;48(3):281–8.

53. Swanson B, Sha BE, Keithley JK, Fogg L, Nerad J, Novak RM, et al. Lipoprotein particle profiles by nuclear magnetic resonance spectroscopy in medically underserved HIV-infected persons. J Clin Lipidol. 2009;3(6):379–84.

54. Rodríguez-Gallego E, Gómez J, Domingo P, Ferrando-Martínez S, Peraire J, Viladés C, et al. Circulating metabolomic profile can predict dyslipidemia in HIV patients undergoing antiretroviral therapy. Atherosclerosis [Internet]. 2018;273:28–36. Available from: https://doi.org/10.1016/j.atherosclerosis.2018.04.008

55. Tort O, Escribà T, Egaña-Gorroño L, de Lazzari E, Cofan M, Fernandez E, et al. Cholesterol efflux responds to viral load and CD4 counts in HIV+ patients and is dampened in HIV exposed. J Lipid Res [Internet]. 2018/09/13. 2018 Nov;59(11):2108–15. Available from: https://pubmed.ncbi.nlm.nih.gov/30213800

56. Hegedus A, Kavanagh Williamson M, Huthoff H. HIV-1 pathogenicity and virion production are dependent on the metabolic phenotype of activated CD4+ T cells. Retrovirology [Internet]. 2014 Nov 25;11:98. Available from: https://pubmed.ncbi.nlm.nih.gov/25421745

57. Giron L, Palmer C, Liu Q, Yin X, Papasavvas E, Sharaf R, et al. Non-invasive plasma glycomic and metabolic biomarkers of post-treatment control of HIV. Nat Commun. 2021 Jun 29;12:3922.

58. Kornberg MD, Bhargava P, Kim PM, Putluri V, Snowman AM, Putluri N, et al. Dimethyl fumarate targets GAPDH and aerobic glycolysis to modulate immunity. Science. 2018 Apr;360(6387):449–53.

59. Pålsson-McDermott EM, O'Neill LAJ. Targeting immunometabolism as an anti-inflammatory strategy. Cell Res. 2020 Apr;30(4):300–14.

60. Palsson-McDermott EM, Curtis AM, Goel G, Lauterbach MAR, Sheedy FJ, Gleeson LE, et al. Pyruvate kinase M2 regulates Hif-1α activity and IL-1β induction and is a critical determinant of the warburg effect in LPS-activated macrophages. Cell Metab. 2015

Jan;21(1):65–80.

61. Peng M, Yin N, Chhangawala S, Xu K, Leslie CS, Li MO. Aerobic glycolysis promotes T helper 1 cell differentiation through an epigenetic mechanism. Science. 2016 Oct;354(6311):481–4.

62. Tarancon-Diez L, Rodríguez-Gallego E, Rull A, Peraire J, Viladés C, Portilla I, et al. Immunometabolism is a key factor for the persistent spontaneous elite control of HIV-1 infection. EBioMedicine [Internet]. 2019/03/14. 2019 Apr;42:86–96. Available from: https://pubmed.ncbi.nlm.nih.gov/30879922

63. Bose S, Ramesh V, Locasale JW. Acetate Metabolism in Physiology, Cancer, and Beyond. Trends Cell Biol [Internet]. 2019/05/31. 2019 Sep;29(9):695–703. Available from: https://pubmed.ncbi.nlm.nih.gov/31160120

64. Balmer ML, Ma EH, Bantug GR, Grählert J, Pfister S, Glatter T, et al. Memory CD8(+) T Cells Require Increased Concentrations of Acetate Induced by Stress for Optimal Function. Immunity. 2016 Jun;44(6):1312–24.

65. Vysochan A, Sengupta A, Weljie AM, Alwine JC, Yu Y. ACSS2-mediated acetyl-CoA synthesis from acetate is necessary for human cytomegalovirus infection. Proc Natl Acad Sci U S A. 2017 Feb;114(8):E1528–35.

66. Hearps AC, Tyssen D, Srbinovski D, Bayigga L, Diaz DJD, Aldunate M, et al. Vaginal lactic acid elicits an anti-inflammatory response from human cervicovaginal epithelial cells and inhibits production of pro-inflammatory mediators associated with HIV acquisition. Mucosal Immunol [Internet]. 2017;10(6):1480–90. Available from: https://doi.org/10.1038/mi.2017.27

67. Aldunate M, Tyssen D, Johnson A, Zakir T, Sonza S, Moench T, et al. Vaginal concentrations of lactic acid potently inactivate HIV. J Antimicrob Chemother [Internet]. 2013 Sep 1;68(9):2015–25. Available from: https://doi.org/10.1093/jac/dkt156

68. Lovell TM, Woods RJ, Butlin DJ, Brayley KJ, Manyonda IT, Jarvis J, et al. Identification of a novel mammalian post-translational modification, phosphocholine, on placental secretory polypeptides. J Mol Endocrinol [Internet]. 2007;39(3):189–98. Available from: https://jme.bioscientifica.com/view/journals/jme/39/3/0390189.xml

69. Thompson D, Pepys MB, Wood SP. The physiological structure of human C-reactive

protein and its complex with phosphocholine. Structure [Internet]. 1999 Feb 15;7(2):169–77. Available from: https://doi.org/10.1016/S0969-2126(99)80023-9

70. El-Bacha T, Torres AG. Phospholipids: Physiology. In: Caballero B, Finglas PM, Toldrá FBT-E of F and H, editors. Oxford: Academic Press; 2016. p. 352–9. Available from: https://www.sciencedirect.com/science/article/pii/B9780123849472005407

71. Treede I, Braun A, Sparla R, Kühnel M, Giese T, Turner JR, et al. Anti-inflammatory effects of phosphatidylcholine. J Biol Chem [Internet]. 2007/07/18. 2007 Sep 14;282(37):27155–64. Available from: https://pubmed.ncbi.nlm.nih.gov/17636253

72. Masson L, Passmore J-AS, Liebenberg LJ, Werner L, Baxter C, Arnold KB, et al. Genital inflammation and the risk of HIV acquisition in women. Clin Infect Dis [Internet]. 2015/04/21. 2015 Jul 15;61(2):260–9. Available from: https://pubmed.ncbi.nlm.nih.gov/25900168

73. Liebenberg LJP, Masson L, Arnold KB, Mckinnon LR, Werner L, Proctor E, et al. Genital-Systemic Chemokine Gradients and the Risk of HIV Acquisition in Women. J Acquir Immune Defic Syndr [Internet]. 2017 Mar 1;74(3):318–25. Available from: https://pubmed.ncbi.nlm.nih.gov/28187085

74. Wall KM, Kilembe W, Vwalika B, Haddad LB, Hunter E, Lakhi S, et al. Risk of heterosexual HIV transmission attributable to sexually transmitted infections and non-specific genital inflammation in Zambian discordant couples, 1994-2012. Int J Epidemiol [Internet]. 2017 Oct 1;46(5):1593–606. Available from: https://pubmed.ncbi.nlm.nih.gov/28402442

75. Koning FA, Otto SA, Hazenberg MD, Dekker L, Prins M, Miedema F, et al. Low-level CD4+ T cell activation is associated with low susceptibility to HIV-1 infection. J Immunol. 2005 Nov;175(9):6117–22.

76. Arnold KB, Burgener A, Birse K, Romas L, Dunphy LJ, Shahabi K, et al. Increased levels of inflammatory cytokines in the female reproductive tract are associated with altered expression of proteases, mucosal barrier proteins, and an influx of HIV-susceptible target cells. Mucosal Immunol. 2016 Jan;9(1):194–205.

77. Bertran-Cobo C, Wedderburn CJ, Robertson FC, Subramoney S, Narr KL, Joshi SH, et al. A Neurometabolic Pattern of Elevated Myo-Inositol in Children Who Are HIV-Exposed and Uninfected: A South African Birth Cohort Study [Internet]. Vol. 13, Frontiers in Immunology . 2022. Available from: https://www.frontiersin.org/article/10.3389/fimmu.2022.800273

78. Cohen RA, Harezlak J, Gongvatana A, Buchthal S, Schifitto G, Clark U, et al. Cerebral metabolite abnormalities in human immunodeficiency virus are associated with cortical and subcortical volumes. J Neurovirol. 2010 Nov;16(6):435–44.

79. Cysique LA, Moffat K, Moore DM, Lane TA, Davies NWS, Carr A, et al. HIV, vascular and aging injuries in the brain of clinically stable HIV-infected adults: a (1)H MRS study. PLoS One. 2013;8(4):e61738.

80. Chang L, Lee PL, Yiannoutsos CT, Ernst T, Marra CM, Richards T, et al. A multicenter in vivo proton-MRS study of HIV-associated dementia and its relationship to age. Neuroimage. 2004 Dec;23(4):1336–47.

81. Cassol E, Misra V, Holman A, Kamat A, Morgello S, Gabuzda D. Plasma metabolomics identifies lipid abnormalities linked to markers of inflammation, microbial translocation, and hepatic function in HIV patients receiving protease inhibitors. BMC Infect Dis. 2013 May;13:203.

82. Epstein AA, Narayanasamy P, Dash PK, High R, Bathena SPR, Gorantla S, et al. Combinatorial assessments of brain tissue metabolomics and histopathology in rodent models of human immunodeficiency virus infection. J Neuroimmune Pharmacol. 2013;8(5):1224–38.

83. Brass AL, Dykxhoorn DM, Benita Y, Yan N, Engelman A, Xavier RJ, et al. Identification of host proteins required for HIV infection through a functional genomic screen. Science. 2008 Feb;319(5865):921–6.

84. Zhou H, Xu M, Huang Q, Gates AT, Zhang XD, Castle JC, et al. Genome-scale RNAi screen for host factors required for HIV replication. Cell Host Microbe. 2008 Nov;4(5):495–504.

85. Matheson NJ, Sumner J, Wals K, Rapiteanu R, Weekes MP, Vigan R, et al. Cell Surface Proteomic Map of HIV Infection Reveals Antagonism of Amino Acid Metabolism by Vpu and Nef. Cell Host Microbe [Internet]. 2015;18(4):409–23. Available from: http://dx.doi.org/10.1016/j.chom.2015.09.003

86. König R, Zhou Y, Elleder D, Diamond TL, Bonamy GMC, Irelan JT, et al. Global analysis of host-pathogen interactions that regulate early-stage HIV-1 replication. Cell. 2008 Oct;135(1):49–60.

87. Yndart A, Kaushik A, Agudelo M, Raymond A, Atluri VS, Saxena SK, et al. Investigation of

Neuropathogenesis in HIV-1 Clade B and C Infection Associated with IL-33 and ST2 Regulation. ACS Chem Neurosci. 2015 Sep;6(9):1600–12.

88. Kishimoto N, Onitsuka A, Kido K, Takamune N, Shoji S, Misumi S. Glyceraldehyde 3-phosphate dehydrogenase negatively regulates human immunodeficiency virus type 1 infection. Retrovirology. 2012 Dec;9:107.

89. Yeung ML, Houzet L, Yedavalli VSRK, Jeang K-T. A genome-wide short hairpin RNA screening of jurkat T-cells for human proteins contributing to productive HIV-1 replication. J Biol Chem. 2009 Jul;284(29):19463–73.

90. Luo F, Chen T, Liu J, Shen X, Zhao Y, Yang R, et al. Ficolin-2 binds to HIV-1 gp120 and blocks viral infection. Virol Sin. 2016 Oct;31(5):406–14.

91. Czubala MA, Finsterbusch K, Ivory MO, Mitchell JP, Ahmed Z, Shimauchi T, et al. TGFβ Induces a SAMHD1-Independent Post-Entry Restriction to HIV-1 Infection of Human Epithelial Langerhans Cells. J Invest Dermatol. 2016 Oct;136(10):1981–9.

92. Wang S-F, Tsao C-H, Lin Y-T, Hsu DK, Chiang M-L, Lo C-H, et al. Galectin-3 promotes HIV-1 budding via association with Alix and Gag p6. Glycobiology. 2014 Nov;24(11):1022–35.

93. Soto PC, Karris MY, Spina CA, Richman DD, Varki A. Cell-intrinsic mechanism involving Siglec-5 associated with divergent outcomes of HIV-1 infection in human and chimpanzee CD4 T cells. J Mol Med (Berl). 2013 Feb;91(2):261–70.

94. Pothlichet J, Rose T, Bugault F, Jeammet L, Meola A, Haouz A, et al. PLA2G1B is involved in CD4 anergy and CD4 lymphopenia in HIV-infected patients. J Clin Invest. 2020 Jun;130(6):2872–87.

95. Xiao H, Wyler E, Milek M, Grewe B, Kirchner P, Ekici A, et al. CRNKL1 Is a Highly Selective Regulator of Intron-Retaining HIV-1 and Cellular mRNAs. MBio. 2021 Jan;12(1).

96. Takashima K, Oshiumi H, Matsumoto M, Seya T. DNAJB1/HSP40 Suppresses Melanoma Differentiation-Associated Gene 5-Mitochondrial Antiviral Signaling Protein Function in Conjunction with HSP70. J Innate Immun. 2018;10(1):44–55.

97. Dhamija N, Choudhary D, Ladha JS, Pillai B, Mitra D. Tat predominantly associates with host promoter elements in HIV-1-infected T-cells - regulatory basis of transcriptional repression of c-Rel. FEBS J. 2015 Feb;282(3):595–610.

98. Kumar M, Mitra D. Heat shock protein 40 is necessary for human immunodeficiency virus-1 Nef-mediated enhancement of viral gene expression and replication. J Biol Chem. 2005 Dec;280(48):40041–50.

99. Urano E, Morikawa Y, Komano J. Novel role of HSP40/DNAJ in the regulation of HIV-1 replication. J Acquir Immune Defic Syndr. 2013 Oct;64(2):154–62.

100. van Wijk R, Huizinga EG, van Wesel ACW, van Oirschot BA, Hadders MA, van Solinge WW. Fifteen novel mutations in PKLR associated with pyruvate kinase (PK) deficiency: structural implications of amino acid substitutions in PK. Hum Mutat. 2009 Mar;30(3):446–53.

101. Qing O, Tojo N, Ozan B, M. DS, Chendong Y, Michael S, et al. Mutations in mitochondrial enzyme GPT2 cause metabolic dysfunction and neurological disease with developmental and progressive features. Proc Natl Acad Sci [Internet]. 2016 Sep 20;113(38):E5598–607. Available from: https://doi.org/10.1073/pnas.1609221113

102. Kohlmeier M. Alanine. In: Kohlmeier MBT-NM, editor. Food Science and Technology [Internet]. London: Academic Press; 2003. p. 308–14. Available from: https://www.sciencedirect.com/science/article/pii/B9780124177628500508

103. Garden GA, Budd SL, Tsai E, Hanson L, Kaul M, D'Emilia DM, et al. Caspase cascades in human immunodeficiency virus-associated neurodegeneration. J Neurosci [Internet]. 2002 May 15;22(10):4015–24. Available from: https://pubmed.ncbi.nlm.nih.gov/12019321

104. Zhou L, Saksena NK. HIV associated neurocognitive disorders. Vol. 5, Infectious Disease Reports . 2013.

105. Froissard P, Duval D. Cytotoxic effects of glutamic acid on PC12 cells. Neurochem Int. 1994 May;24(5):485–93.

106. Behl C, Widmann M, Trapp T, Holsboer F. 17-beta estradiol protects neurons from oxidative stress-induced cell death in vitro. Biochem Biophys Res Commun. 1995 Nov;216(2):473–82.

107. Zhang Y, Bhavnani BR. Glutamate-induced apoptosis in neuronal cells is mediated via caspase-dependent and independent mechanisms involving calpain and caspase-3 proteases as well as apoptosis inducing factor (AIF) and this process is inhibited by equine estrogens. BMC Neurosci [Internet]. 2006;7(1):49. Available from:

https://doi.org/10.1186/1471-2202-7-49

108. Smolkin MB, Perrotta PL. Chapter 18 - Molecular Diagnostics for Coagulopathies. In: Coleman WB, Tsongalis GJBT-DMP, editors. Academic Press; 2017. p. 221–33. Available from: https://www.sciencedirect.com/science/article/pii/B9780128008867000182

109. Rennert H, DeSimone RA. Chapter 153 - Molecular Testing for Factor V Leiden and Prothrombin Gene Mutations in Inherited Thrombophilia. In: Shaz BH, Hillyer CD, Reyes Gil MBT-TM and H (Third E, editors. Elsevier; 2019. p. 903–6. Available from: https://www.sciencedirect.com/science/article/pii/B9780128137260001537

110. Cheng D-C, Zhong G-C, Su J-X, Liu Y-H, Li Y, Wang J-Y, et al. A sensitive HIV-1 envelope induced fusion assay identifies fusion enhancement of thrombin. Biochem Biophys Res Commun. 2010 Jan;391(4):1780–4.

111. Ling H, Xiao P, Usami O, Hattori T. Thrombin activates envelope glycoproteins of HIV type 1 and enhances fusion. Microbes Infect. 2004 Apr;6(5):414–20.

112. Hoogland G, Bos IWM, Kupper F, van Willigen G, Spierenburg HA, van Nieuwenhuizen O, et al. Thrombin-stimulated glutamate uptake in human platelets is predominantly mediated by the glial glutamate transporter EAAT2. Neurochem Int [Internet]. 2005;47(7):499–506. Available from: https://www.sciencedirect.com/science/article/pii/S0197018605001737

113. Chinnaraj M, Planer W, Pozzi N. Structure of Coagulation Factor II: Molecular Mechanism of Thrombin Generation and Development of Next-Generation Anticoagulants [Internet]. Vol. 5, Frontiers in Medicine . 2018. Available from: https://www.frontiersin.org/article/10.3389/fmed.2018.00281

114. White MR, Garcin ED. D-Glyceraldehyde-3-Phosphate Dehydrogenase Structure and Function BT - Macromolecular Protein Complexes: Structure and Function. In: Harris JR, Marles-Wright J, editors. Cham: Springer International Publishing; 2017. p. 413–53. Available from: https://doi.org/10.1007/978-3-319-46503-6_15

115. Mansur NR, Meyer-Siegler K, Wurzer JC, Sirover MA. Cell cycle regulation of the glyceraldehyde3phosphate dehydrogenaseluracil DNA glycosylase gene in normal human cells. Nucleic Acids Res [Internet]. 1993 Feb 25;21(4):993–8. Available from: https://doi.org/10.1093/nar/21.4.993

116. Ikemoto A, Bole DG, Ueda T. Glycolysis and Glutamate Accumulation into Synaptic

Vesicles: ROLE OF GLYCERALDEHYDE PHOSPHATE DEHYDROGENASE AND 3-PHOSPHOGLYCERATE KINASE *. J Biol Chem [Internet]. 2003 Feb 21;278(8):5929–40. Available from: https://doi.org/10.1074/jbc.M211617200

117. Hu C, Chen W, Myers SJ, Yuan H, Traynelis SF. Human GRIN2B variants in neurodevelopmental disorders. J Pharmacol Sci [Internet]. 2016;132(2):115–21. Available from: https://www.sciencedirect.com/science/article/pii/S1347861316301335

118. Li D, He L. Association study between the NMDA receptor 2B subunit gene (GRIN2B) and schizophrenia: A HuGE review and meta-analysis. Genet Med [Internet]. 2007;9(1):4–8. Available from: https://doi.org/10.1097/01.gim.0000250507.96760.4b

119. Endele S, Rosenberger G, Geider K, Popp B, Tamer C, Stefanova I, et al. Mutations in GRIN2A and GRIN2B encoding regulatory subunits of NMDA receptors cause variable neurodevelopmental phenotypes. Nat Genet [Internet]. 2010;42(11):1021–6. Available from: https://doi.org/10.1038/ng.677

120. Che X, He F, Deng Y, Xu S, Fan X, Gu P, et al. HIV-1 Tat-mediated apoptosis in human blood-retinal barrier-associated cells. PLoS One. 2014;9(4):e95420.

121. Xiong W, Xie J, Liu J, Xiong H. [HIV-1gp120 injures neurons by alteration of neuronal expressions of NR2B and PSD-95]. Xi bao yu fen zi mian yi xue za zhi = Chinese J Cell Mol Immunol. 2014 Feb;30(2):139–42.

122. Alves CRR, Ferreira JC, de Siqueira-Filho MA, Carvalho CR, Lancha AH, Gualano B. Creatine-induced glucose uptake in type 2 diabetes: a role for AMPK-α? Amino Acids [Internet]. 2012;43(4):1803–7. Available from: https://doi.org/10.1007/s00726-012-1246-6

123. Plotnikov A, Zehorai E, Procaccia S, Seger R. The MAPK cascades: Signaling components, nuclear roles and mechanisms of nuclear translocation. Biochim Biophys Acta - Mol Cell Res [Internet]. 2011;1813(9):1619–33. Available from: https://www.sciencedirect.com/science/article/pii/S0167488910003228

124. Jin C, Li J, Cheng L, Liu F, Wu N. Gp120 binding with DC-SIGN induces reactivation of HIV-1 provirus via the NF-κB signaling pathway. Acta Biochim Biophys Sin (Shanghai). 2016 Mar;48(3):275–81.

125. Hashimoto M, Nasser H, Chihara T, Suzu S. Macropinocytosis and TAK1 mediate anti-inflammatory to pro-inflammatory macrophage differentiation by HIV-1 Nef. Cell Death Dis.

2014 May;5(5):e1267.

126. Planès R, Ben Haij N, Leghmari K, Serrero M, BenMohamed L, Bahraoui E. HIV-1 Tat Protein Activates both the MyD88 and TRIF Pathways To Induce Tumor Necrosis Factor Alpha and Interleukin-10 in Human Monocytes. J Virol. 2016 Jul;90(13):5886–98.

127. Hoshino S, Konishi M, Mori M, Shimura M, Nishitani C, Kuroki Y, et al. HIV-1 Vpr induces TLR4/MyD88-mediated IL-6 production and reactivates viral production from latency. J Leukoc Biol. 2010 Jun;87(6):1133–43.

128. Thomsen T, Schlosser A, Holmskov U, Sorensen GL. Ficolins and FIBCD1: Soluble and membrane bound pattern recognition molecules with acetyl group selectivity. Mol Immunol [Internet]. 2011;48(4):369–81. Available from: https://www.sciencedirect.com/science/article/pii/S0161589010005808

129. Sanchez Caballero L, Gorgogietas V, Arroyo MN, Igoillo-Esteve M. Chapter Three - Molecular mechanisms of β-cell dysfunction and death in monogenic forms of diabetes. In: Santin I, Galluzzi LBT-IR of C and MB, editors. Pancreatic ß-Cell Biology in Health and Disease [Internet]. Academic Press; 2021. p. 139–256. Available from: https://www.sciencedirect.com/science/article/pii/S1937644821000101

130. Graber JJ, Dhib-Jalbut S. Interferons. In: Aminoff MJ, Daroff RBBT-E of the NS (Second E, editors. Oxford: Academic Press; 2014. p. 718–23. Available from: https://www.sciencedirect.com/science/article/pii/B9780123851574001822

131. Soper A, Kimura I, Nagaoka S, Konno Y, Yamamoto K, Koyanagi Y, et al. Type I Interferon Responses by HIV-1 Infection: Association with Disease Progression and Control. Front Immunol [Internet]. 2018 Jan 15;8:1823. Available from: https://pubmed.ncbi.nlm.nih.gov/29379496

132. Machmach K, Leal M, Gras C, Viciana P, Genebat M, Franco E, et al. Plasmacytoid dendritic cells reduce HIV production in elite controllers. J Virol. 2012 Apr;86(8):4245–52.

133. Sivro A, Su R-C, Plummer FA, Ball TB. Interferon responses in HIV infection: from protection to disease. AIDS Rev. 2014;16(1):43–51.

134. Nangia-Makker P, Nakahara S, Hogan V, Raz A. Galectin-3 in apoptosis, a novel therapeutic target. J Bioenerg Biomembr [Internet]. 2007 Feb;39(1):79–84. Available from: https://pubmed.ncbi.nlm.nih.gov/17318396

135. Sato S, St-Pierre C, Bhaumik P, Nieminen J. Galectins in innate immunity: dual functions of host soluble beta-galactoside-binding lectins as damage-associated molecular patterns (DAMPs) and as receptors for pathogen-associated molecular patterns (PAMPs). Immunol Rev. 2009 Jul;230(1):172–87.

136. Perillo NL, Marcus ME, Baum LG. Galectins: versatile modulators of cell adhesion, cell proliferation, and cell death. J Mol Med (Berl). 1998 May;76(6):402–12.

137. Hsu DK, Chen H-Y, Liu F-T. Galectin-3 regulates T-cell functions. Immunol Rev [Internet]. 2009 Jul 1;230(1):114–27. Available from: https://doi.org/10.1111/j.1600-065X.2009.00798.x

138. Leslie CC. Cytosolic phospholipase A2: physiological function and role in disease. J Lipid Res [Internet]. 2015;56(8):1386–402. Available from: https://www.sciencedirect.com/science/article/pii/S0022227520355188

139. Klebanoff SJ, Rosen H. The role of myeloperoxidase in the microbicidal activity of polymorphonuclear leukocytes. Ciba Found Symp. 1978 Jun;(65):263–84.

CAPÍTULO 5:

Conclusiones y recomendaciones

5.1 Conclusiones

5.1.1 Conclusiones relacionadas con el objetivo específico 1: Desarrollar un protocolo optimizado para la determinación del perfil metabolómico de muestras de CMSP de voluntarios mediante RMN.

La ejecución del estudio presentado por medio de esta tesis, permitió dar respuesta a los objetivos planteados en la propuesta de investigación. Se desarrolló y estandarizó un nuevo método de procesamiento de CMSP para perfiles metabolómicos mediante espectroscopia de RMN. Este nuevo método, permite la obtención de datos de alta calidad, sólidos y reproducibles a partir de la mitad de CMSP reportada anteriormente necesaria para analizar este tipo de células a través de RMN. Este método, combina ultrasonido de alta intensidad y filtración desproteinizante, y se caracteriza por una mínima manipulación de la muestra (todo el proceso se puede realizar en el mismo vial) y un menor tiempo de procesamiento (6 h vs. 16 h que se demora el método tradicional).

5.1.2 Conclusiones relacionadas con el objetivo específico 2: Construir matrices metabolómicas para el plasma sanguíneo y las CMSP que permitan comparar los grupos de individuos del estudio.

En CMSP, se lograron identificar perfiles metabolómicos diferenciales en PLHIV-TAR y HESN. Se encontró un perfil metabólico diferencial para controladores, progresores e individuos HESN en muestras de plasma sanguíneo. Es decir que, la resistencia a la infección o a la progresión del VIH-1 está asociada a cambios en el metaboloma del individuo, los cuales están representados en forma de metabolitos, que podrían proporcionar biomarcadores de resistencia o de pronóstico de las personas que viven con el VIH-1.

5.1.3 Conclusiones relacionadas con los objetivos específicos 3 y 4: Determinar, mediante análisis multivariado dependiente e interdependiente, los metabolitos que se puedan identificar como biomarcadores diferenciadores de los grupos del estudio. 4. Proponer las rutas metabólicas que ayuden a explicar las diferencias metabolómicas que se encuentren entre los grupos del estudio.

Se propone como biomarcadores de eficacia del tratamiento (TAR) a niveles disminuidos de: carnitina (62,2% respecto a los controles sanos), fenilalanina (76,1% respecto a los controles sanos), sarcosina (66,3% respecto a los controles sanos) y trimetilamina N-oxido (90,7% respecto a los controles sanos). El impacto que genera el VIH-1 es evidente a pesar de la respuesta positiva a la TAR, dado que, en el grupo PLHIV-ART, los metabolitos identificados se relacionaron también con una marcada activación inmune.

Como factor de protección en caso de exposición (HESN) se propone como biomarcadores en CMSP niveles disminuidos de alanina (52% respecto a los controles sanos), AMP (60% respecto a los controles sanos), inosina (65,5% respecto a los controles sanos) y valina (37,6% respecto a los controles sanos). Metabolitos relacionados con un perfil antiinflamatorio (AMP e inosina) y un estado de quiescencia inmune (alanina) en las CMSP, lo que explicaría la resistencia natural a la infección de estos individuos.

En plasma, la tirosina (con un nivel 19,5% por debajo en progresores en relación a los controles sanos), el glutamato (con un nivel 42,7% por debajo en controladores en relación a los controles sanos) y la valina (Elevada un 13,8% en progresores respecto a los niveles de los controles sanos y disminuida un 15,6% en controladores respecto a los niveles de los controles sanos) son potenciales biomarcadores de progresión de la infección por el VIH-1 en progresores y controladores. Un infectado con bajos niveles de tirosina y elevados de valina, potencialmente progresará más rápido a SIDA que un infectado con niveles disminuidos de valina y glutamato, el cual mostraría un perfil de controlador.

La resistencia natural a la infección por el VIH-1 en individuos HESN está asociada con una huella metabólica específica, que no había sido previamente descrita. Esta huella está compuesta por un nivel elevado de lactato (80% respecto a los controles sanos), y niveles disminuidos de fosfocolina (13,8% por debajo de los controles sanos) y mioinositol (23,3% por debajo de los controles sanos). Estos metabolitos podrían ser biomarcadores en plasma de resistencia natural a la infección por el VIH en HESN.

Los biomarcadores específicos de cada grupo se asociaron con genes y proteínas relacionadas con el VIH-1 a través de MetaboAnalyst®, obteniendo una lista de genes conectados a los biomarcadores y al VIH-1. Ejemplo, el gen *Caspasa-3,* relacionado con la demencia asociada al VIH-1, se asoció con controladores (niveles de valina y glutamato disminuidos) y progresores (niveles de valina elevados). El gen de trombina del factor II de coagulación (*F2*), con un rol

regulatorio en la replicación del VIH-1, se asoció con progresores (niveles disminuidos de creatinina) y controladores (niveles disminuidos de glutamato).

El glutamato es el metabolito más importante en la diferencia entre progresores y controladores, las bajas concentraciones de glutamato en controladores pueden estar relacionadas con un perfil neuroprotector y regulación de la apoptosis en la infección por VIH. Así mismo, la expresión diferencial de glutamato en controladores podría estar relacionada con una proliferación celular optimizada mediada por *F2* que participa en la resistencia a la progresión del VIH.

Se identificó el gen de la fosfolipasa A2 del grupo IB (*PLA2G1B*) relacionado con controladores (niveles disminuidos de glutamato) y HESN (niveles disminuidos de fosfocolina); este gen está involucrado en la anergia de linfocitos T CD4+ y linfopenia de linfocitos T CD4+ en personas infectadas por el VIH-1. La inducción de anergia y linfopenia propia de la infección por VIH-1, pueden ser claves para entender los dos fenómenos más importantes que busca explicar este estudio: la resistencia a la infección y a la progresión del VIH-1.

Finalmente, dentro del estudio del VIH, este estudio propone que cambios en los niveles de ciertos metabolitos en las personas que se exponen y/o infectan con VIH-1 pueden predecir el pronóstico de su condición médica o estatus infeccioso. Queda entonces demostrado que el metabolismo juega un papel preponderante en la salud humana y la respuesta a las infecciones.

5.2 Recomendaciones

Se espera que el método desarrollado genere nuevas vías para la aplicación de perfiles metabolómicos de CMSP basados en ^{1}H-RMN para el seguimiento, diagnóstico y tratamiento de enfermedades. Especialmente, nuevas investigaciones deberían abordar este enfoque de procesamiento de CMSP para el estudio del metabolismo de otras enfermedades infecciosas u otras condiciones médicas que afecten a este importante componente del sistema inmune. Se podría entonces, usar el método desarrollado para el estudio de CMSP en infecciones bacterianas, parasitarias y virales diferentes al VIH-1. Estos estudios permitirían determinar cuáles son las afecciones metabólicas que a nivel celular se presentan por estas enfermedades. También cabe resaltar que, nuestro protocolo puede ser ajustado para llevar a cabo el estudio de otras células del cuerpo humano diferentes a las CMSP, como hepatocitos, nefronas, hematocritos, entre otras. Lo que abre un horizonte amplio en la investigación de enfermedades y condiciones médicas que afectan a las células de cuerpo humano usando metabolómica por RMN.

Dada la relación de la disminución en la concentración relativa identificada de ciertos metabolitos en los grupos de estudio, sería importante evaluar si la suplementación de los metabolitos disminuidos y el control de la ingesta de los aumentados mejora los marcadores de activación celular.

Además, es necesario complementar y corroborar estos resultados mediante el análisis de otras cohortes de HESN como las trabajadoras sexuales, niños nacidos de madres infectadas por el VIH-1 y hombres que tienen sexo con hombres, para determinar si los metabolitos se repiten en los diferentes grupos o si existen otros fenotipos asociados a la resistencia al VIH-1.

Según este estudio, existe una relación directa entre el porcentaje de linfocitos T CD4+ y el perfil metabólico de las CMSP en individuos con VIH-1. Podría ser interesante estudiar si la variación del porcentaje de linfocitos T CD4+ durante la progresión de la enfermedad afecta también el perfil metabólico de estos individuos. Por tanto, la realización de un estudio longitudinal con esta población ayudaría a resolver esta cuestión. Sin embargo, según las directrices de “prueba y tratamiento” del VIH-1, resulta complicado reclutar personas VIH-1 positivas sin recibir TAR; por lo tanto, las evaluaciones que abarcan años continuos de TAR supresor o no supresor en comparación con nuestra cohorte pueden ayudar a dilucidar el impacto del TAR en el perfil metabolómico.

Con base en los resultados del análisis de genes realizados en este estudio, consideramos que se deberían realizar análisis proteómicos, transcriptómicos y genómicos para tener una visión más completa de la progresión y la resistencia natural a la infección por VIH-1.

Anexo 1

Artículo 1, Capítulo 2

PLOS ONE

RESEARCH ARTICLE

Development of an optimized method for processing peripheral blood mononuclear cells for ^{1}H-nuclear magnetic resonance-based metabolomic profiling

León Gabriel Gómez-Archila[1☯*], Martina Palomino-Schätzlein[2☯*], Wildeman Zapata-Builes[3,4], Elkin Galeano[1☯]

1 Grupo de Investigación en Sustancias Bioactivas, Facultad de Ciencias Farmacéuticas y Alimentarias, Universidad de Antioquia (UdeA), Medellín, Colombia, 2 Servicio de RMN, Centro de Investigación Príncipe Felipe, Valencia, Spain, 3 Grupo Inmunovirología, Facultad de Medicina, Universidad de Antioquia (UdeA), Medellín, Colombia, 4 Grupo Infettare, Facultad de Medicina, Universidad Cooperativa de Colombia, Medellín, Colombia

☯ These authors contributed equally to this work.
* lgabriel.gomez@udea.edu.co (LGGA); mpalomino@cipf.es (MPS)

Citation: Gómez-Archila LG, Palomino-Schätzlein M, Zapata-Builes W, Galeano E (2021) Development of an optimized method for processing peripheral blood mononuclear cells for ^{1}H-nuclear magnetic resonance-based metabolomic profiling. PLoS ONE 16(2): e0247668. https://doi.org/10.1371/journal.pone.0247668

Editor: Oscar Millet, CIC bioGUNE, SPAIN

Received: May 20, 2020

Accepted: February 11, 2021

Published: February 25, 2021

Peer Review History: PLOS recognizes the benefits of transparency in the peer review process; therefore, we enable the publication of all of the content of peer review and author responses alongside final, published articles. The editorial history of this article is available here: https://doi.org/10.1371/journal.pone.0247668

Data Availability Statement: All relevant data are within the paper and its Supporting Information files.

Abstract

Human peripheral blood mononuclear cells (PBMCs) are part of the innate and adaptive immune system, and form a critical interface between both systems. Studying the metabolic profile of PBMC could provide valuable information about the response to pathogens, toxins or cancer, the detection of drug toxicity, in drug discovery and cell replacement therapy. The primary purpose of this study was to develop an improved processing method for PBMCs metabolomic profiling with nuclear magnetic resonance (NMR) spectroscopy. To this end, an experimental design was applied to develop an alternative method to process PBMCs at low concentrations. The design included the isolation of PBMCs from the whole blood of four different volunteers, of whom 27 cell samples were processed by two different techniques for quenching and extraction of metabolites: a traditional one using organic solvents and an alternative one employing a high-intensity ultrasound probe, the latter with a variation that includes the use of deproteinizing filters. Finally, all the samples were characterized by ^{1}H-NMR and the metabolomic profiles were compared by the method. As a result, two new methods for PBMCs processing, called Ultrasound Method (UM) and Ultrasound and Ultrafiltration Method (UUM), are described and compared to the Folch Method (FM), which is the standard protocol for extracting metabolites from cell samples. We found that UM and UUM were superior to FM in terms of sensitivity, processing time, spectrum quality, amount of identifiable, quantifiable metabolites and reproducibility.

Introduction

A peripheral blood mononuclear cell (PBMC) is any blood cell with a round nucleus, such as lymphocyte, monocyte or macrophage [1]. PBMC are composed of three types of cells:

Anexo 2

Tablas suplementarias 1 y 2, Artículo 1, Capítulo 2
DOCUMENTO ANEXO EN ARCHIVO EN FORMATO PDF

Anexo 3

Figuras suplementarias 1 a 7, Artículo 1, Capítulo 2

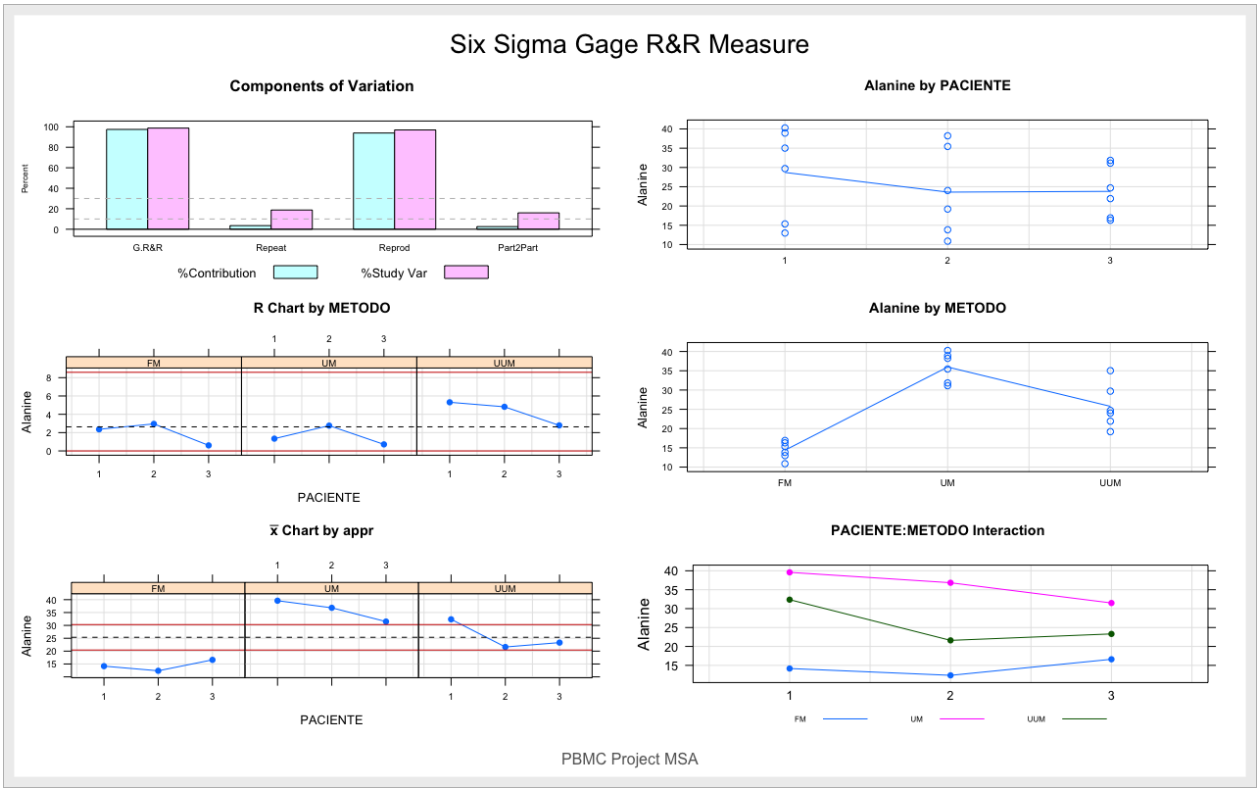

S1 Figure. Six Sigma Gage R&R Measure for alanine. Comparative repeatability and reproducibility analysis between FM, UM and UUM, for the normalized concentration of Alanine.

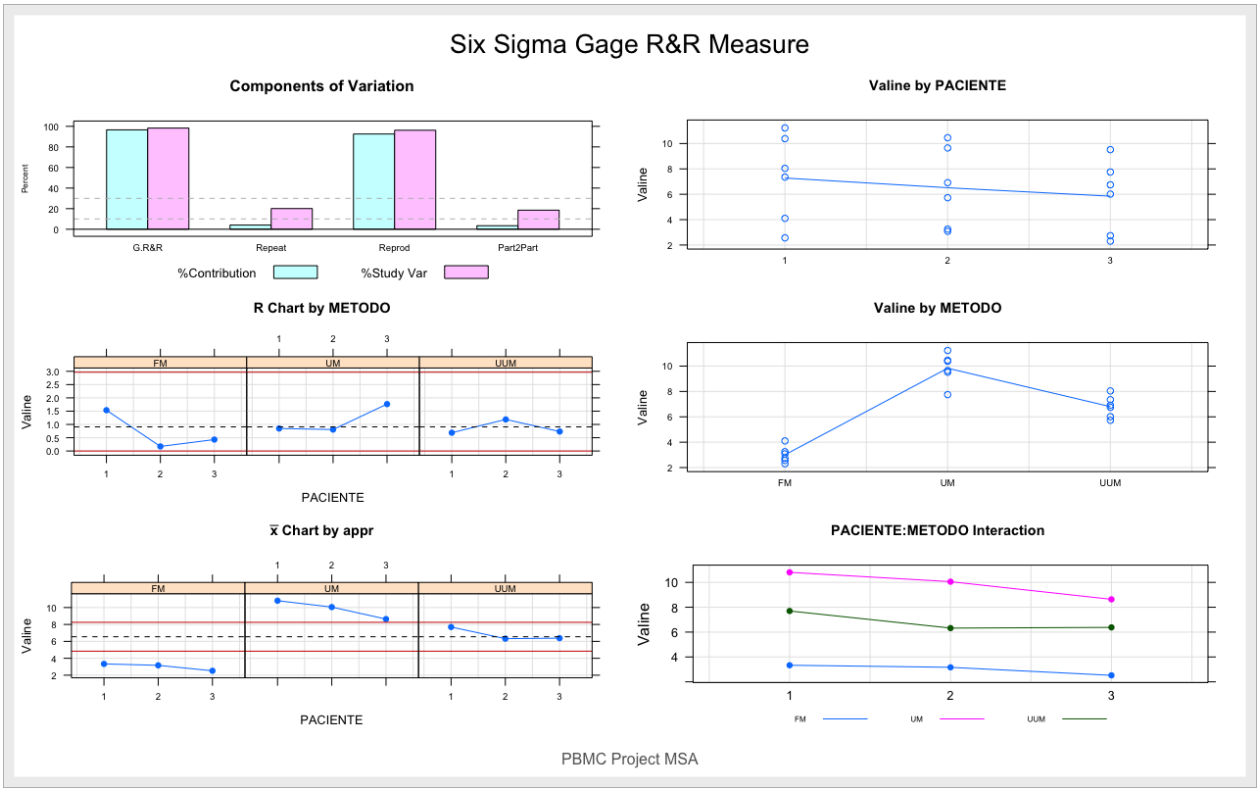

S2 Figure. Six Sigma Gage R&R Measure for valine. Comparative repeatability and reproducibility analysis between FM, UM and UUM, for the normalized concentration of valine.

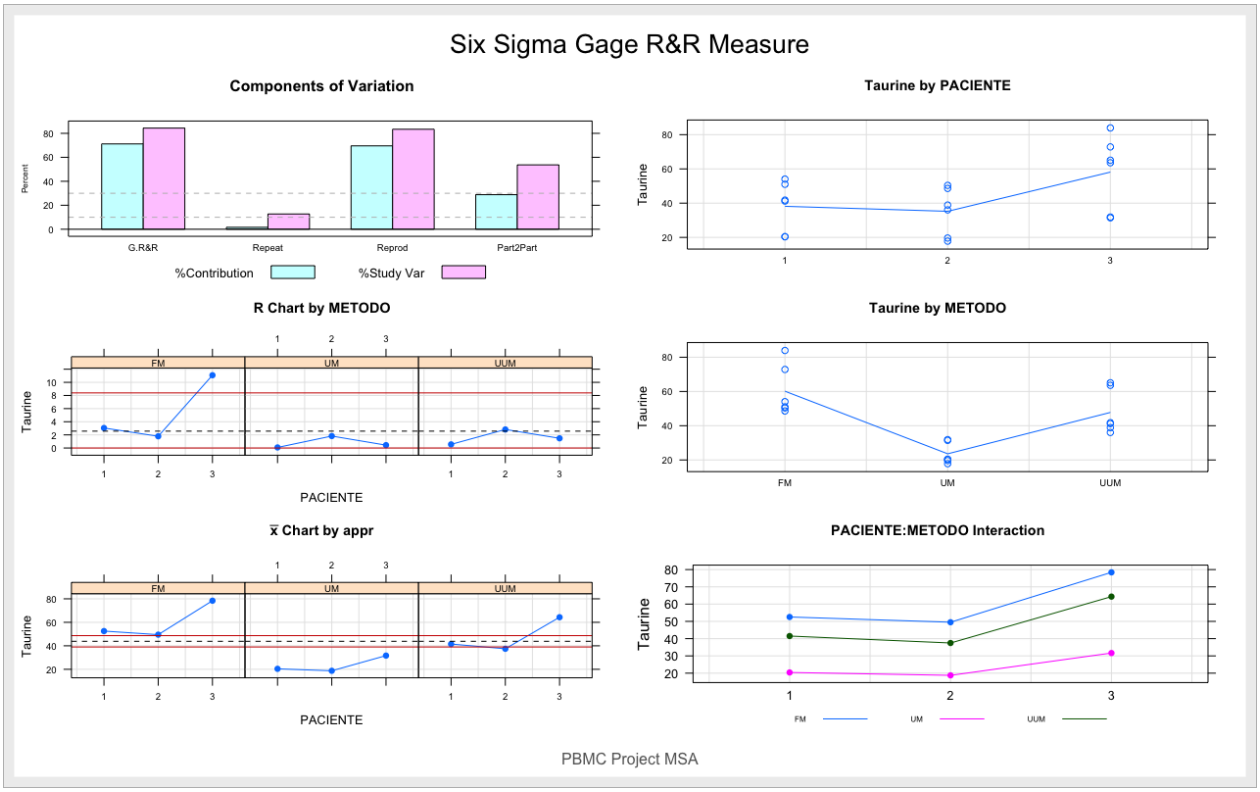

S3 Figure. Six Sigma Gage R&R Measure for taurine. Comparative repeatability and reproducibility analysis between FM, UM and UUM, for the normalized concentration of taurine.

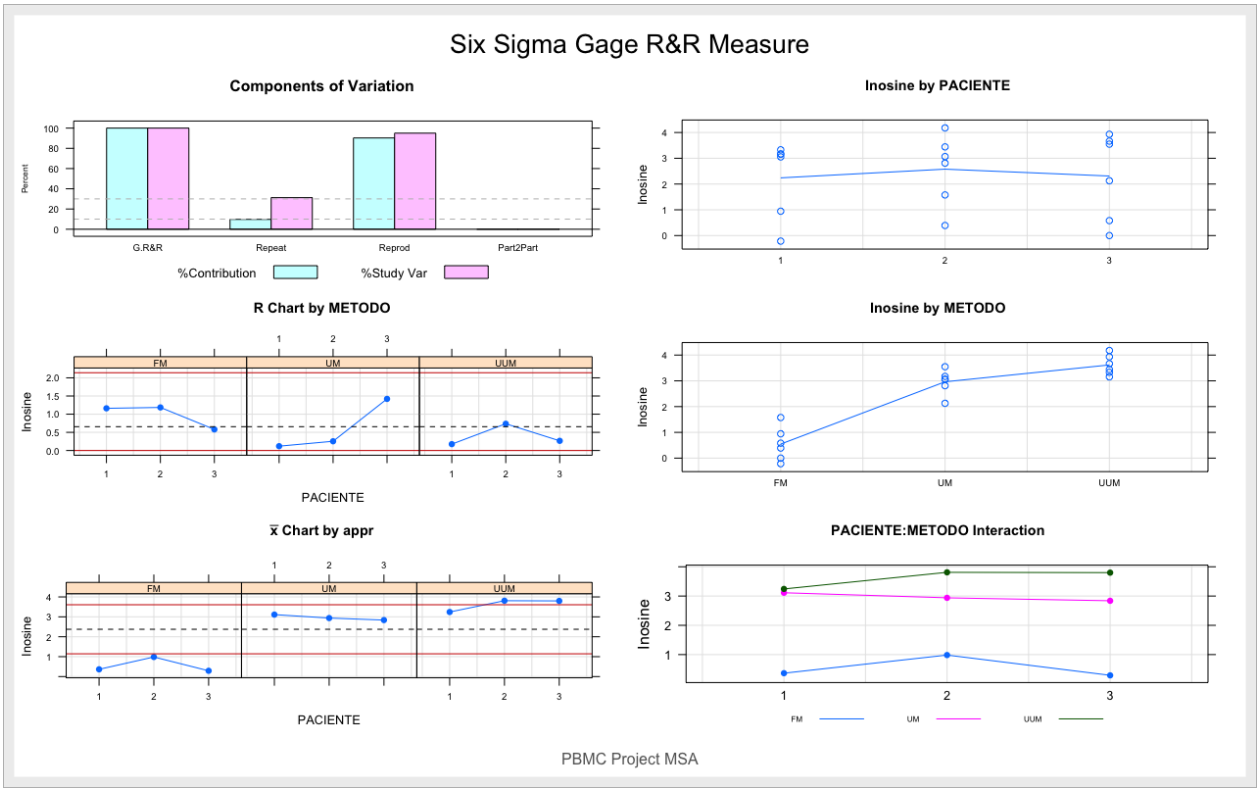

S4 Figure. Six Sigma Gage R&R Measure for inosine. Comparative repeatability and reproducibility analysis between FM, UM and UUM, for the normalized concentration of inosine.

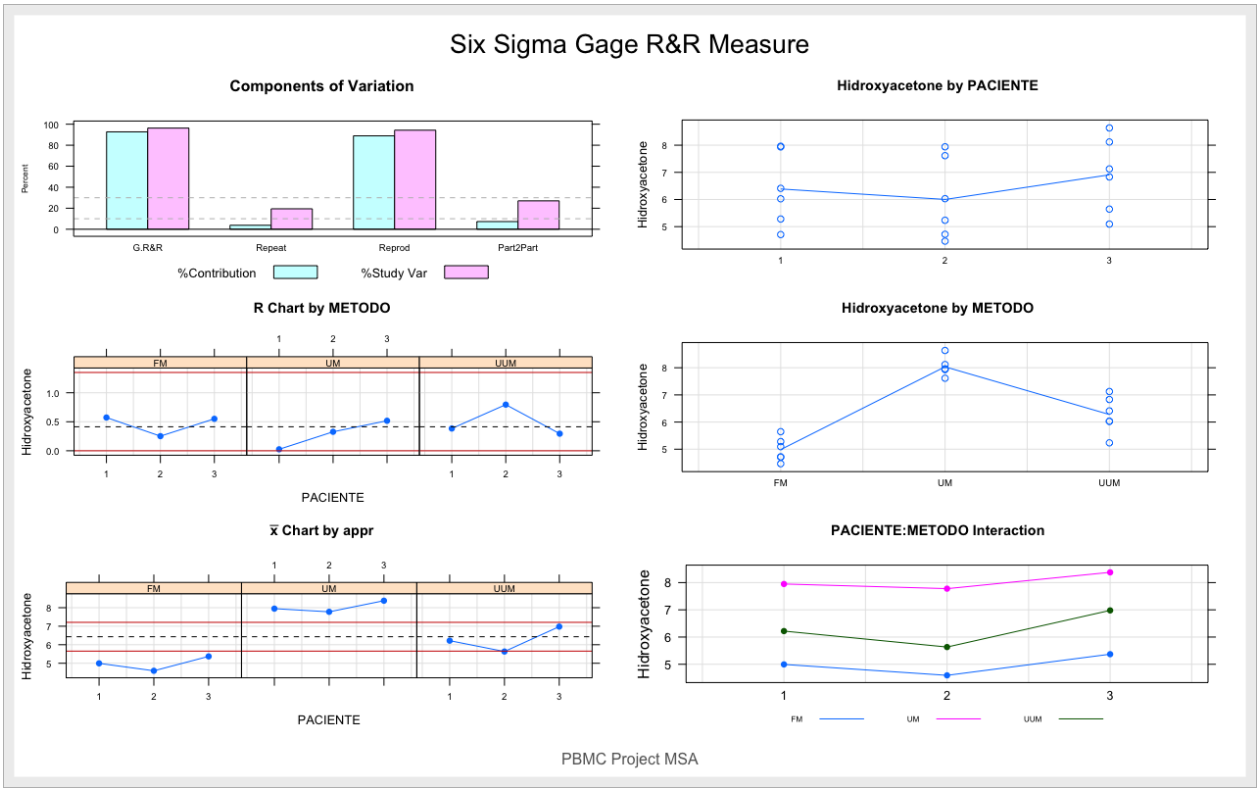

S5 Figure. Six Sigma Gage R&R Measure for Hidroxyacetone. Comparative repeatability and reproducibility analysis between FM, UM and UUM, for the normalized concentration of Hidroxyacetone.

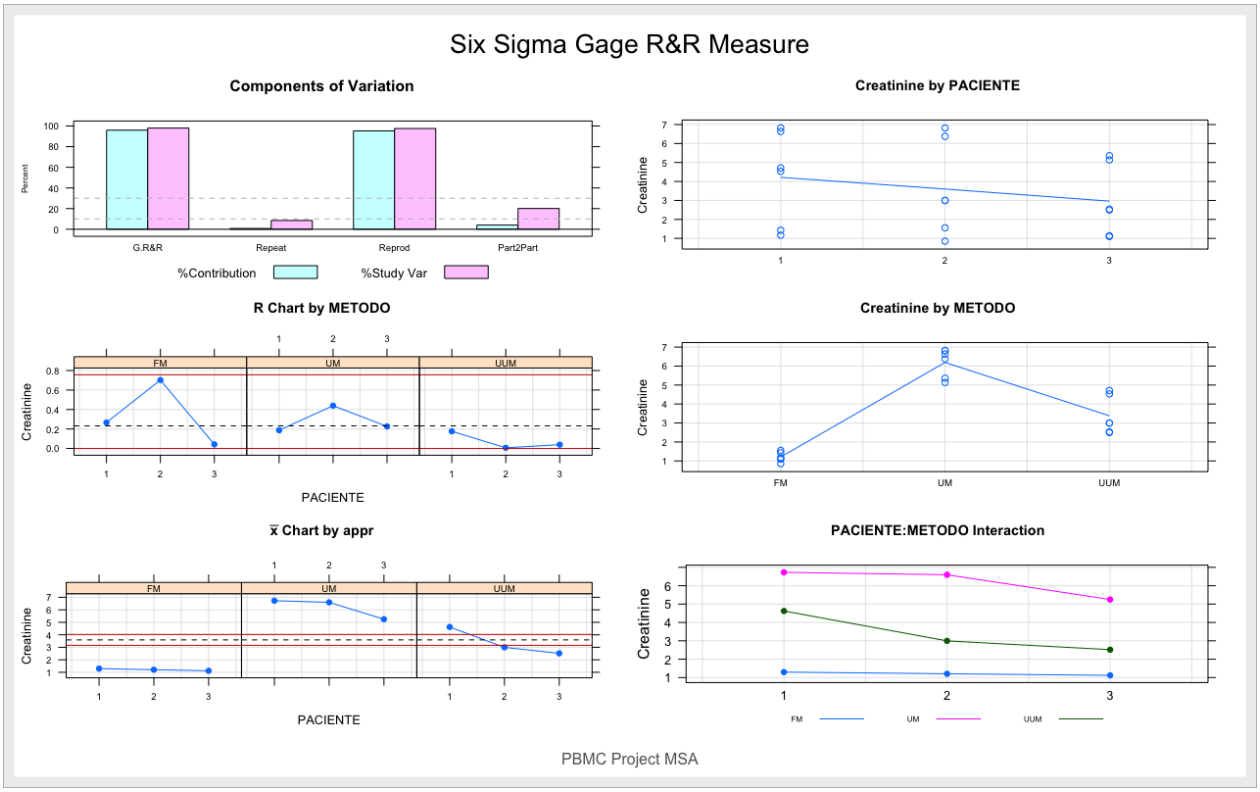

S6 Figure. Six Sigma Gage R&R Measure for Creatinine. Comparative repeatability and reproducibility analysis between FM, UM and UUM, for the normalized concentration of Creatinine.

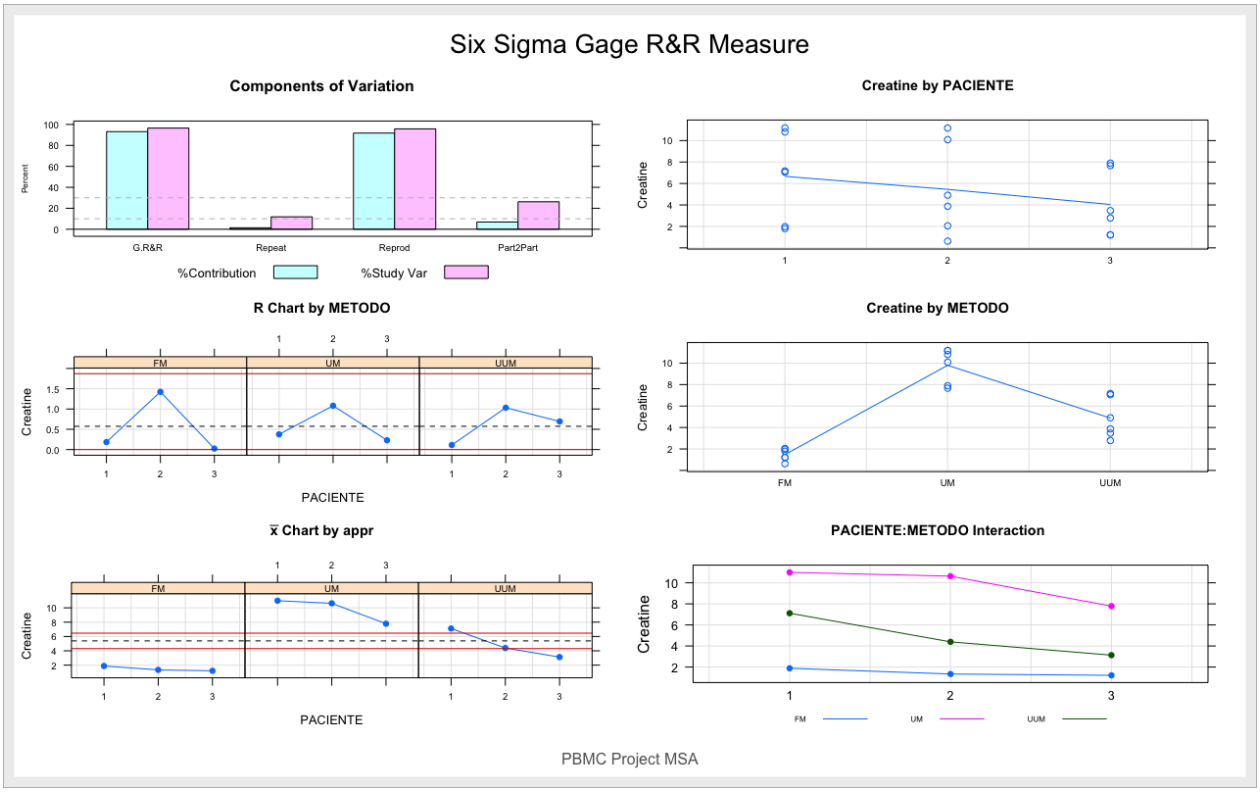

S7 Figure. Six Sigma Gage R&R Measure for creatine. Comparative repeatability and reproducibility analysis between FM, UM and UUM, for the normalized concentration of creatine.

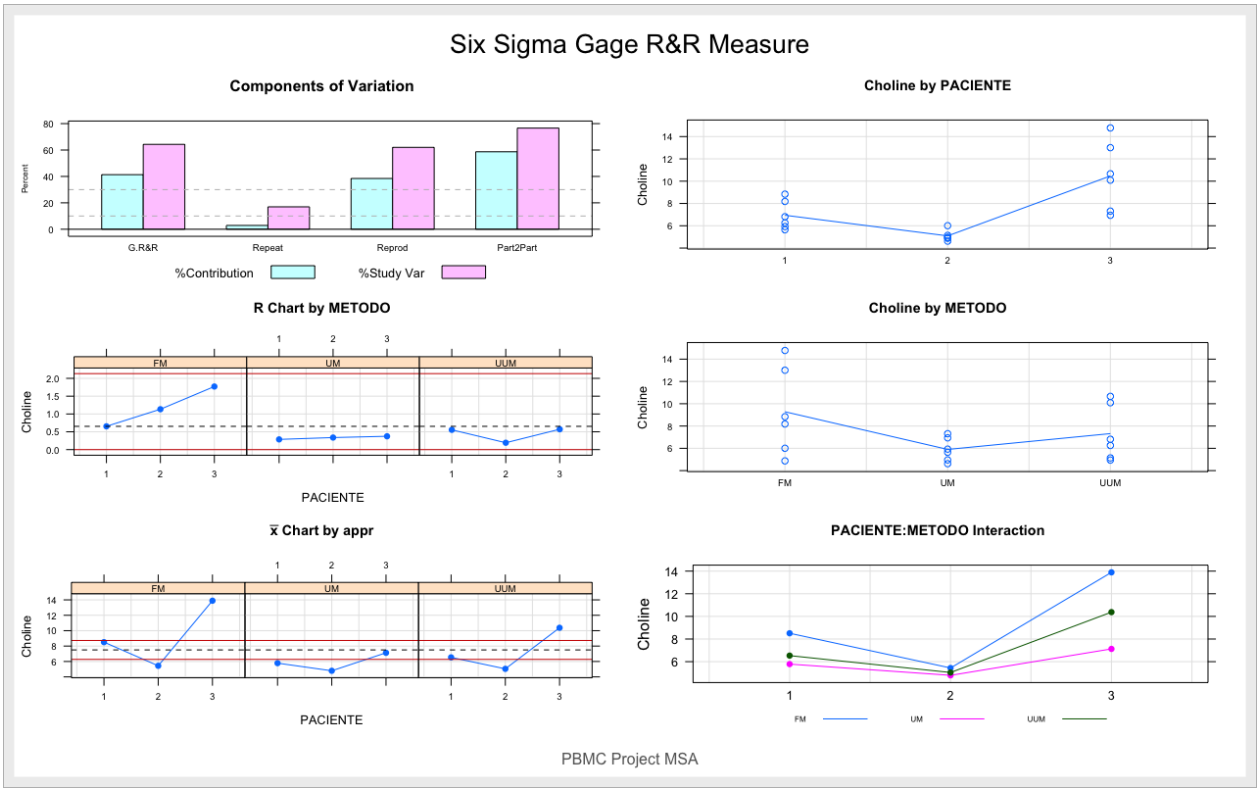

S8 Figure. Six Sigma Gage R&R Measure for choline. Comparative repeatability and reproducibility analysis between FM, UM and UUM, for the normalized concentration of choline.

Anexo 4

Tabla suplementaria 1, Artículo 2, Capítulo 3

Signal assignment in ^{1}H-NMR spectrum of PBMC samples

Type	H's	Metabolite	ppm 1	ppm 2
s		TSP	0,0428	-0,0466
t	3	2-hydroxybutyrate	0,9229	0,8599
-	-	Unknown 1	0,9354	0,9247
t	3	Isoleucine	0,9479	0,9359
t	6	Leucine	0,9799	0,9503
d	3	Valine	1,0016	0,9799
d	3	Isoleucine	1,0248	1,0016
d	3	Valine	1,058	1,0337
-	-	Unknown 2	1,1007	1,0649
t	3	Ethanol	1,2478	1,1354
s	6	3-Hidroxyisovalerate	1,2576	1,2508
-	-	Unknown 3	1,3109	1,2737
d	3	Lactate	1,3503	1,3136
d	3	Alanine	1,5001	1,4645
m	2	2-hydroxybutyrate	1,6294	1,5908
m	2	2-hydroxybutyrate	1,6653	1,6299
m	2	Lysine	1,7974	1,6768
-	-	Unknown 4	1,8234	1,8096
-	-	Unknown 5	1,8582	1,8434
m	2	Lysine	1,9177	1,8747
s	3	Acetate	1,9285	1,9179
m	2	Glutamate	2,098	1,996
m	2	Glutamine	2,1356	2,1114
s	3	Hidroxyacetone	2,1498	2,1359
m	5	Methionine	2,1929	2,1506
s	-	Unknown 6	2,2326	2,2234
s	-	Unknown 7	2,2398	2,233
s	3	Acetoacetate	2,2706	2,258
m	1	Valine	2,2989	2,271
s	3	Methylacetoacetate	2,34	2,3302
-	-	Unknown 8	2,3522	2,3404

m	2	Glutamate	2,3651	2,3523
s	4	Succinate	2,3723	2,3652
s	3	Pyruvate	2,3801	2,3724
-	-	Unknown 9	2,4117	2,4035
-	-	Unknown 10	2,4674	2,4335
m	2	Glutamine	2,4983	2,4674
m	2	GSH+GSSG	2,5612	2,5522
d	2	Citrate	2,5952	2,5224
d	2	Citrate	2,6434	2,6285
t	2	Methionine	2,663	2,6435
-	-	Unknown 11	2,673	2,6631
m	1	Aspartate	2,7038	2,6726
s	3	Sarcosine	2,7196	2,7089
-	-	Unknown 12	2,7377	2,7293
m	1	Aspartate	2,8541	2,7938
s	9	Trimethylamine	2,8792	2,8591
dd	2	GSH+GSSG	2,9859	2,9316
-	-	Unknown 13	3,0261	3,0147
s	3	Creatine	3,0391	3,0263
s	3	Creatinine	3,0539	3,0392
s	2	Malonate	3,1376	3,1285
m	1	Phenylalanine	3,1671	3,1378
s	9	Choline	3,2082	3,1984
s	9	O-Phosphocoline	3,2143	3,2082
s	9	Trimethylamine N-oxide	3,2245	3,2146
s	9	Carnitine	3,2343	3,2247
s	9	Betaine	3,2416	3,2342
t	2	Taurine	3,2803	3,2419
m	1	Phenylalanine	3,3122	3,2904
s	3	Methanol	3,377	3,3531
t	2	Taurine	3,4458	3,4102
-	-	Unknown 14	3,5415	3,5165
m	4	Glycerol	3,5685	3,5438
s	2	Glycine	3,5908	3,5687
d	1	Treonine	3,5976	3,5909
d	1	Valine	3,6236	3,6086

-	-	Unknown 15	3,6347	3,6244
m	4	Glycerol	3,664	3,6399
q	2	Ethanol	3,6888	3,664
-	-	Unknown 16	3,7264	3,7027
-	-	Unknown 17	3,7405	3,7346
m	1	Glutamate	3,7671	3,7415
dd + q	1	Serine + Alanine	3,818	3,7665
dd	1	Methionine	3,8593	3,8349
s	2	Betaine	3,8892	3,8839
-	-	Unknown 18	3,9138	3,8929
s	2	Creatine	3,9218	3,9141
dd	1	Tyrosine	3,9759	3,9389
m	2	Serine	4,0051	3,9761
s	2	Creatinine	4,0133	4,0054
m	2	Choline	4,0423	4,0356
-	-	Unknown 19	4,052	4,0427
-	-	Unknown 20	4,0608	4,0528
-	-	Unknown 21	4,0881	4,0611
-	-	Unknown 22	4,0972	4,0906
q	1	Lactate	4,118	4,0972
q	1	Lactate	4,1289	4,1184
q	1	Lactate	4,1407	4,1291
-	-	Unknown 23	4,1519	4,1423
m	1	Treonine	4,2436	4,1836
-	-	Unknown 24	4,2759	4,2442
-	-	Unknown 25	5,6375	5,6064
d	1	Inosine	6,1597	6,1248
d	2	Tyrosine	6,9311	6,8779
dd	1	Xanthurenate	7,1227	7,0595
d	2	Tyrosine	7,2147	7,1804
d	1	Phenylalanine	7,3525	7,2973
d	1	Phenylalanine	7,4036	7,3753
t	1	Phenylalanine	7,4547	7,4125
-	-	Unknown	7,5018	7,4604
s	1	Xanthine	7,8583	7,8134

s	2	GTP	8,0456	8,0185
s	1	Inosine	8,2025	8,1871
s	1	Inosine	8,2305	8,2049
s	1	AMP	8,2851	8,2598
s	1	Oxypurinol	8,3917	8,3745
s	1	Formiate	8,4729	8,4426
s	1	AMP	8,6282	8,5897

Anexo 5

Tabla suplementaria 2, Artículo 2, Capítulo 3
DOCUMENTO ANEXO EN ARCHIVO EN FORMATO PDF

Anexo 6

Tabla suplementaria 3, Artículo 2, Capítulo 3
DOCUMENTO ANEXO EN ARCHIVO EN FORMATO EXCEL

Anexo 7

Artículo 3, Capítulo 4

frontiers | Frontiers in Molecular Biosciences

TYPE Original Research
PUBLISHED 29 June 2023
DOI 10.3389/fmolb.2023.1204273

OPEN ACCESS

EDITED BY
Martin Aran,
IBBA-CONICET Leloir Institute Foundation, Argentina

REVIEWED BY
Sakshi Arora,
Children's Hospital of Philadelphia, United States
Gaia Meoni,
University of Florence, Italy

*CORRESPONDENCE
León Gabriel Gómez-Archila,
lgabriel.gomez@udea.edu.co
Martina Palomino-Schätzlein,
mpalomino@protoqsar.com

RECEIVED 12 April 2023
ACCEPTED 16 June 2023
PUBLISHED 29 June 2023

CITATION
Gómez-Archila LG, Palomino-Schätzlein M, Zapata-Builes W, Rugeles MT and Galeano E (2023) Plasma metabolomics by nuclear magnetic resonance reveals biomarkers and metabolic pathways associated with the control of HIV-1 infection/progression. *Front. Mol. Biosci.* 10:1204273. doi: 10.3389/fmolb.2023.1204273

Plasma metabolomics by nuclear magnetic resonance reveals biomarkers and metabolic pathways associated with the control of HIV-1 infection/progression

León Gabriel Gómez-Archila[1,2]*, Martina Palomino-Schätzlein[3]*, Wilderman Zapata-Builes[4,5], María T. Rugeles[4] and Elkin Galeano[1]

[1]Grupo de Investigación en Sustancias Bioactivas, Facultad de Ciencias Farmacéuticas y Alimentarias, Universidad de Antioquia (UdeA), Medellín, Colombia, [2]Grupo de Investigación en Ciencias Farmacéuticas ICIF-CES, Facultad de Ciencias y Biotecnología, Universidad CES, Medellín, Colombia, [3]Servicio de RMN, Centro de Investigación Príncipe Felipe, Valencia, España, [4]Grupo Inmunovirología, Facultad de Medicina, Universidad de Antioquia (UdeA), Medellín, Colombia, [5]Grupo Infettare, Facultad de Medicina, Universidad Cooperativa de Colombia, Medellín, Colombia

How the human body reacts to the exposure of HIV-1 is an important research goal. Frequently, HIV exposure leads to infection, but some individuals show natural resistance to this infection; they are known as HIV-1-exposed but seronegative (HESN). Others, although infected but without antiretroviral therapy, control HIV-1 replication and progression to AIDS; they are named controllers, maintaining low viral levels and an adequate count of CD4+ T lymphocytes. Biological mechanisms explaining these phenomena are not precise. In this context, metabolomics emerges as a method to find metabolites in response to pathophysiological stimuli, which can help to establish mechanisms of natural resistance to HIV-1 infection and its progression. We conducted a cross-sectional study including 30 HESN, 14 HIV-1 progressors, 14 controllers and 30 healthy controls. Plasma samples (directly and deproteinized) were analyzed through Nuclear Magnetic Resonance (NMR) metabolomics to find biomarkers and altered metabolic pathways. The metabolic profile analysis of progressors, controllers and HESN demonstrated significant differences with healthy controls when a discriminant analysis (PLS-DA) was applied. In the discriminant models, 13 metabolites associated with HESN, 14 with progressors and 12 with controllers were identified, which presented statistically significant mean differences with healthy controls. In progressors, the metabolites were related to high energy expenditure (creatinine), mood disorders (tyrosine) and immune activation (lipoproteins), phenomena typical of the natural course of the infection. In controllers, they were related to an inflammation-modulating profile (glutamate and pyruvate) and a better adaptive immune system response (acetate) associated with resistance to progression. In the HESN group, with anti-inflammatory (lactate and phosphocholine) and virucidal (lactate) effects which constitute a protective profile in the sexual transmission of HIV. Concerning the significant metabolites of each group, we identified 24 genes involved in HIV-1 replication or virus proteins that were all altered in progressors but only partially in controllers and HESN. In summary, our results indicate that exposure to HIV-1 in

Anexo 8

Tabla suplementaria 1, Artículo 3, Capítulo 4

Supplementary Table 1. Characteristics of the study volunteers: Healthy control versus HESN

SAMPLE	COD	GROUP	SEX	AGE		SAMPLE	COD	GROUP	SEX	AGE
PF5	2	Healthy control	F	28		**PF1**	34	HESN	M	
PF8	7	Healthy control	F	32		**PF4**	53	HESN	F	37
PF12	8	Healthy control	F	25		**PF7**	79	HESN	F	29
PF15	12	Healthy control	F	40		**PF10**	236	HESN	F	38
PF18	13	Healthy control	F	45		**PF17**	238	HESN	M	24
PF24	16	Healthy control	F	47		**PF20**	240	HESN	M	25
PF27	25	Healthy control	F	26		**PF23**	242	HESN	F	25
PF30	26	Healthy control	F	32		**PF26**	245	HESN	M	34
PF34	27	Healthy control	F	45		**PF29**	278	HESN	M	31
PF37	28	Healthy control	F	38		**PF32**	284	HESN	M	22
PF40	33	Healthy control	M	22		**PF36**	285	HESN	M	22
PF43	34	Healthy control	M	24		**PF39**	294	HESN	M	31
PF46	35	Healthy control	M	25		**PF42**	302	HESN	M	22
PF49	39	Healthy control	M	24		**PF45**	303	HESN	F	33

PF52	51	Healthy control	M	50		**PF48**	313	HESN	F	50
PF62	H-01	Healthy control	F	38		**PF51**	336	HESN	M	17
PF65	H-02	Healthy control	F	43		**PF54**	338	HESN	M	29
PF68	H-03	Healthy control	F	32		**PF58**	342	HESN	F	39
PF71	H-05	Healthy control	M	45		**PF61**	346	HESN	M	27
PF74	H-08	Healthy control	M	48		**PF64**	349	HESN	M	46
PF78	H-09	Healthy control	M	30		**PF67**	350	HESN	F	26
PF81	H-11	Healthy control	M	45		**PF70**	353	HESN	M	39
PF84	H-12	Healthy control	M	38		**PF76**	357	HESN	F	26
PF87	H-17	Healthy control	F	22		**PF89**	375	HESN	F	47
PF90	H-19	Healthy control	M	31		**PF92**	376	HESN	F	24
PF93	H-33	Healthy control	F	25		**PF95**	377	HESN	M	44
PF96	H-34	Healthy control	M	25		**PF98**	378	HESN	F	40
PF103	H-46	Healthy control	M	30		**PF102**	379	HESN	F	17
PF106	H-47	Healthy control	M	39		**PF105**	380	HESN	F	34
PF109	H-48	Healthy control	M	22		**PF108**	381	HESN	F	50

Supplementary Table 1. Characteristics of the study volunteers: Healthy control versus PLHIV

SAMPLE	COD	GROUP	SEX	AGE		SAMPLE	COD	GROUP	SEX	AGE	Viral Load	LT CD4+ (%)	LT CD4 + (cel)
PF2	1	Healthy control	F	32		**PF3**	C-13	Controller	F	21	162	29,63 %	996
PF5	2	Healthy control	F	28		**PF9**	C-21	Controller	M	29	286	36,78 %	1367
PF12	8	Healthy control	F	25		**PF16**	C-23	Controller	F	39	412	31,05 %	635
PF15	12	Healthy control	F	40		**PF25**	C-24	Controller	F	25	37	30,49 %	936
PF18	13	Healthy control	F	45		**PF31**	C-25	Controller	F	37	20	25,04 %	731
PF27	25	Healthy control	F	26		**PF47**	C-28	Controller	F	25	1464	24,45 %	722
PF30	26	Healthy control	F	32		**PF53**	C-31	Controller	M	38	1383	27,10 %	514
PF40	33	Healthy control	M	22		**PF60**	C-38	Controller	M	49	1885	27,90 %	759
PF43	34	Healthy control	M	24		**PF69**	C-40	Controller	M	45	64	29,50 %	647
PF46	35	Healthy control	M	25		**PF75**	C-41	Controller	M	20	20	37,48 %	769

PF49	39	Healthy control	M	24		**PF82**	C-44	Controller	M	24	162	29,69%	789
PF52	51	Healthy control	M	50		**PF97**	S-35	Controller	F	34	2928	21,00%	819
PF56	57	Healthy control	M	24		**PF6**	S-14	Progressor	M	50	4600	21,69%	669
PF71	H-05	Healthy control	M	45		**PF13**	S-20	Progressor	M	27	21200	18,05%	434
PF74	H-08	Healthy control	M	48		**PF19**	S-22	Progressor	M	39	18500	16,20%	267
PF78	H-09	Healthy control	M	30		**PF28**	C-04	Progressor	M	44	35500	27,56%	706
PF81	H-11	Healthy control	M	45		**PF50**	S-32	Progressor	M	32	23637	24,98%	557
PF84	H-12	Healthy control	M	38		**PF57**	C-06	Progressor	M	29	4700	36,40%	790
PF90	H-19	Healthy control	M	31		**PF63**	C-10	Progressor	F	47	5270	26,63%	755
PF96	H-34	Healthy control	M	25		**PF72**	S-37	Progressor	M	26	63715	22,80%	359
PF103	H-46	Healthy control	M	30		**PF79**	S-39	Progressor	M	27	44016	16,10%	306
PF106	H-47	Healthy control	M	39		**PF85**	S-42	Progressor	M	19	160405	16,48%	328

PF109	H-48	Healthy control	M	22		**PF94**	S-43	Progressor	M	21	28801	22,65%	633

Supplementary Table 1. Characteristics of the study volunteers: Healthy control versus Controllers

SAMPLE	**COD**	**GROUP**	**SEX**	**AGE**		**SAMPLE**	**COD**	**GROUP**	**SEX**	**AGE**	**Viral Load**	**LT CD4+ (%)**	**LT CD4 + (cel)**
PF5	2	Healthy control	F	28		**PF3**	C-13	Controller	F	21	162	29,63%	996
PF8	7	Healthy control	F	32		**PF9**	C-21	Controller	M	29	286	36,78%	1367
PF12	8	Healthy control	F	25		**PF16**	C-23	Controller	F	39	412	31,05%	635
PF27	25	Healthy control	F	26		**PF25**	C-24	Controller	F	25	37	30,49%	936
PF34	27	Healthy control	F	45		**PF31**	C-25	Controller	F	37	20	25,04%	731
PF40	33	Healthy control	M	22		**PF38**	C-26	Controller	M	27	1885	0,279	759
PF43	34	Healthy control	M	24		**PF47**	C-28	Controller	F	25	1464	24,45%	722
PF46	35	Healthy control	M	25		**PF53**	C-31	Controller	M	38	1383	27,10%	514

PF49	39	Healthy control	M	24		**PF60**	C-38	Controller	M	49	1885	27,90 %	759
PF52	51	Healthy control	M	50		**PF69**	C-40	Controller	M	45	64	29,50 %	647
PF71	H-05	Healthy control	M	45		**PF75**	C-41	Controller	M	20	20	37,48 %	769
PF84	H-12	Healthy control	M	38		**PF82**	C-44	Controller	M	24	162	29,69 %	789
PF87	H-17	Healthy control	F	22		**PF91**	C-27	Controller	M	42	11206	0,317	818
PF106	H-47	Healthy control	M	39		**PF97**	S-35	Controller	F	34	2928	21,00 %	819

Supplementary Table 1. Characteristics of the study volunteers: Healthy control versus Progressors

SAMPLE	**COD**	**GROUP**	**SEX**	**AGE**		**SAMPLE**	**COD**	**GROUP**	**SEX**	**AGE**	**Viral Load**	**LT CD4+ (%)**	**LT CD4 + (cel)**
PF40	33	Healthy control	M	22		**PF6**	S-14	Progressor	M	50	4600	21,69 %	669
PF43	34	Healthy control	M	24		**PF13**	S-20	Progressor	M	27	21200	18,05 %	434
PF46	35	Healthy control	M	25		**PF19**	S-22	Progressor	M	39	18500	16,20 %	267

PF49	39	Healthy control	M	24		**PF28**	C-04	Progressor	M	44	35500	27,56%	706
PF52	51	Healthy control	M	50		**PF35**	S-29	Progressor	M	25	16656	34,84%	372
PF71	H-05	Healthy control	M	45		**PF50**	S-32	Progressor	M	32	23637	24,98%	557
PF74	H-08	Healthy control	M	48		**PF57**	C-06	Progressor	M	29	4700	36,40%	790
PF78	H-09	Healthy control	M	30		**PF72**	S-37	Progressor	M	26	63715	22,80%	359
PF84	H-12	Healthy control	M	38		**PF79**	S-39	Progressor	M	27	44016	16,10%	306
PF90	H-19	Healthy control	M	31		**PF85**	S-42	Progressor	M	19	160405	16,48%	328
PF96	H-34	Healthy control	M	25		**PF94**	S-43	Progressor	M	21	28801	22,65%	633
PF103	H-46	Healthy control	M	30		**PF101**	S-45	Progressor	M	23	47245	22,73%	443
PF106	H-47	Healthy control	M	39		**PF104**	C-49	Progressor	M	30	17630	22,00%	
PF109	H-48	Healthy control	M	22		**PF107**	S-50	Progressor	M	40	31552	17,80%	344

Supplementary Table 1. Characteristics of the study volunteers: Controllers versus Progressors

SAMPLE	COD	GROUP	SEX	AGE	Viral Load	LT CD4+ (%)	LT CD4+ (cel)		SAMPLE	COD	GROUP	SEX	AGE	Viral Load	LT CD4+ (%)	LT CD4+ (cel)
PF9	C-21	Controller	M	29	286	36,78 %	1367		**PF6**	S-14	Progressor	M	50	4600	21,69%	669
PF38	C-26	Controller	M	27	1885	0,279	759		**PF28**	C-04	Progressor	M	44	35500	27,56%	706
PF53	C-31	Controller	M	38	1383	27,10 %	514		**PF35**	S-29	Progressor	M	25	16656	34,84%	372
PF60	C-38	Controller	M	49	1885	27,90 %	759		**PF50**	S-32	Progressor	M	32	23637	24,98%	557
PF69	C-40	Controller	M	45	64	29,50 %	647		**PF57**	C-06	Progressor	M	29	4700	36,40%	790
PF75	C-41	Controller	M	20	20	37,48 %	769		**PF101**	S-45	Progressor	M	23	47245	22,73%	443
PF82	C-44	Controller	M	24	162	29,69 %	789		**PF104**	C-49	Progressor	M	30	17630	22,00%	
PF91	C-27	Controller	M	42	11206	0,317	818		**PF107**	S-50	Progressor	M	40	31552	17,80%	344

Anexo 9

Tabla suplementaria 2, Artículo 3, Capítulo 4

Direct Plasma metabolites

Metabolite	Compound Type
2-oxoglutarate	Organic acid
2-oxoisovalerate	Organic acid
3-hydroxybutyrate	Organic acid
Acetate	Organic acid
Acetoacetate	Organic acid
Alanine	Amino acid
Albuminlysil	Lipid
Arginine	Amino acid
Asparagine	Amino acid
Aspartate	Organic acid
Choline	Organic acid
Citrate	Organic acid
Citrulline	Amino acid
Creatine	Amino acid
Creatinine	Amino acid
D-Glucose	Sugar
Dimethylamine	Organic acid
Dimethylglycine	Amino acid
Ethanol	Alcohol
Formiate	Organic acid
Glutamate	Organic acid
Glutamine	Amino acid
Glycerol	Lipid
Glycerol of lipids	Lipid
Glycine	Amino acid

Histidine	Amino acid
Hypoxanthine	Purine
Isobutyrate	Organic acid
Isoleucine	Amino acid
Lactate	Organic acid
LDL1 CH3-VDL1 -CH3	Lipid
LDL1 aliphatic chain	Lipid
Leucine	Amino acid
Lipid CH2CH2O-VLDL	Lipid
Lipids CH-CH	Lipid
Lipids CH-CHCH2CH-CH	Lipid
Lipids CH2-C-C	Lipid
Lipids CH2-CO	Lipid
Lipids n-CH3-3	Lipid
Liporoteins	Lipid
Lysine	Amino acid
Methionine	Amino acid
Myo inositol	Alcohol
N-acetyl groups in proteins	Lipid
N-acetylcysteine	Amino acid
Phenylalanine	Amino acid
Phosphocholine	Amino acid
Pyruvate	Organic acid
Serine	Amino acid
Succinate	Organic acid
Threonine	Amino acid
Tyrosine	Amino acid
Valine	Amino acid
VDL-2 aliphatic chain	Lipid
Xanthurenate	Organic acid

Filtered plasma metabolites

Metabolite	Compound Type
2-hydroxybutyrate	Organic acid
2-oxoglutarate	Organic acid
2-oxoisovalerate	Organic acid
3-Hidroxyisovalerate	Organic acid
3-hydroxybutyrate	Organic acid
Acetate	Organic acid
Acetoacetate	Organic acid
Alanine	Amino acid
Arginine	Amino acid
Asparagine	Amino acid
Aspartate	Organic acid
Choline	Organic acid
Citrate	Organic acid
Citrulline	Amino acid
Creatine	Amino acid
Creatinine	Amino acid
D-Glucose	Sugar
Dimethylamine	Organic acid
Dimethylglycine	Amino acid
Ethanol	Alcohol
Formiate	Organic acid
Glutamate	Organic acid
Glutamine	Amino acid
Glycerol	Lipid
Glycerol of lipids	Lipid
Glycine	Amino acid
Histidine	Amino acid
Hypoxanthine	Purine
Inosine	Purine
Isobutyrate	Organic acid

Isoleucine	Amino acid
Lactate	Organic acid
Leucine	Amino acid
Lysine	Amino acid
Methionine	Amino acid
Myo inositol	Alcohol
Phenylalanine	Amino acid
Phosphocholine	Amino acid
Pyruvate	Organic acid
Serine	Amino acid
Succinate	Organic acid
Threonine	Amino acid
Tyrosine	Amino acid
Valine	Amino acid
Xanthurenate	Organic acid

Anexo 10

Tabla suplementaria 3 Artículo 3, Capítulo 4

DOCUMENTO ANEXO EN ARCHIVO EN FORMATO EXCEL

Anexo 11

Tabla suplementaria 4, Artículo 3, Capítulo 4
DOCUMENTO ANEXO EN ARCHIVO EN FORMATO EXCEL

Anexo 12

Tabla suplementaria 5, Artículo 3, Capítulo 4
DOCUMENTO ANEXO EN ARCHIVO EN FORMATO EXCEL

Anexo 13

Tabla suplementaria 6, Artículo 3, Capítulo 4
DOCUMENTO ANEXO EN ARCHIVO EN FORMATO PDF

Anexo 14

Figura suplementaria 1, Artículo 3, Capítulo 4

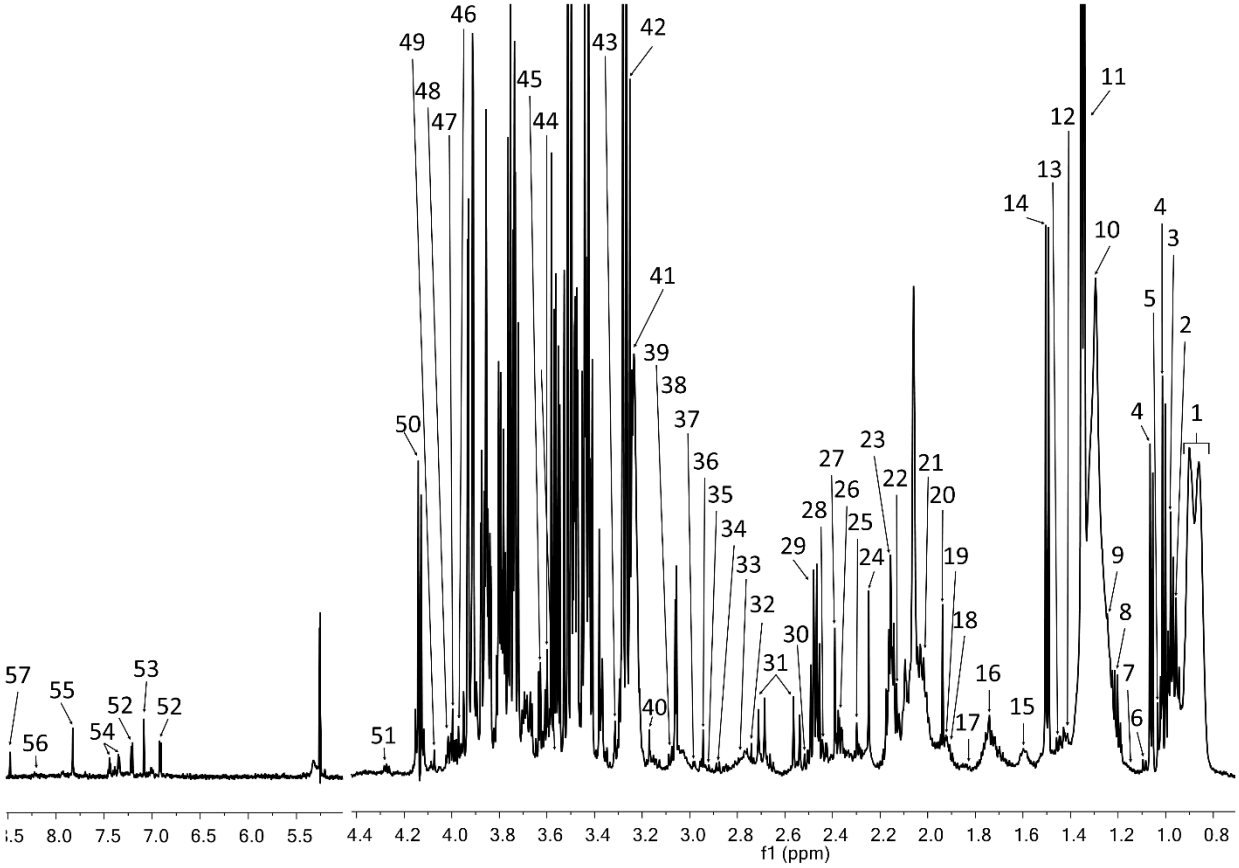

Supplementary Figure 1. Assignment of direct plasma spectrum signals

Anexo 15

Figura suplementaria 2, Artículo 3, Capítulo 4

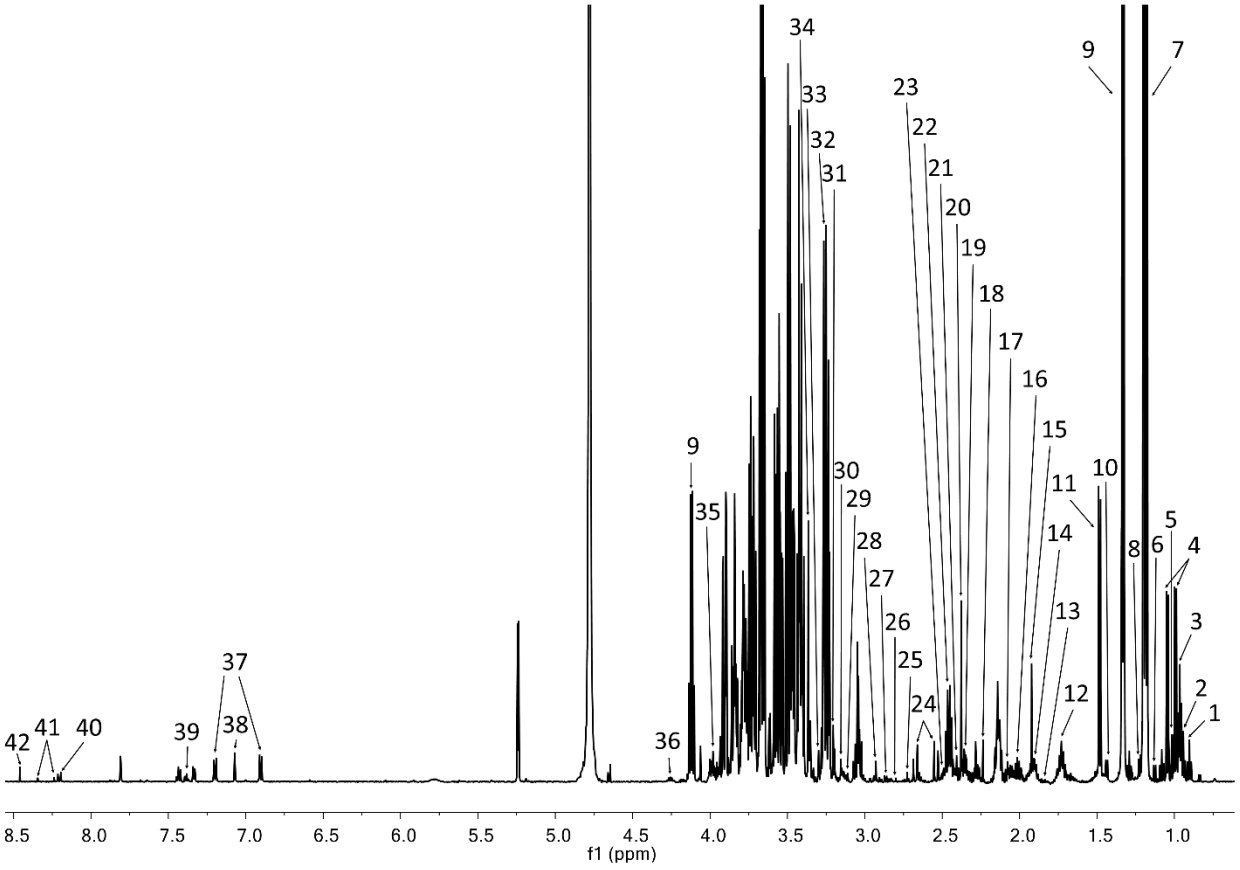

Supplementary Figure 2. Assignment of filtered plasma spectrum signals

Anexo 16

Figura suplementaria 3, Artículo 3, Capítulo 4

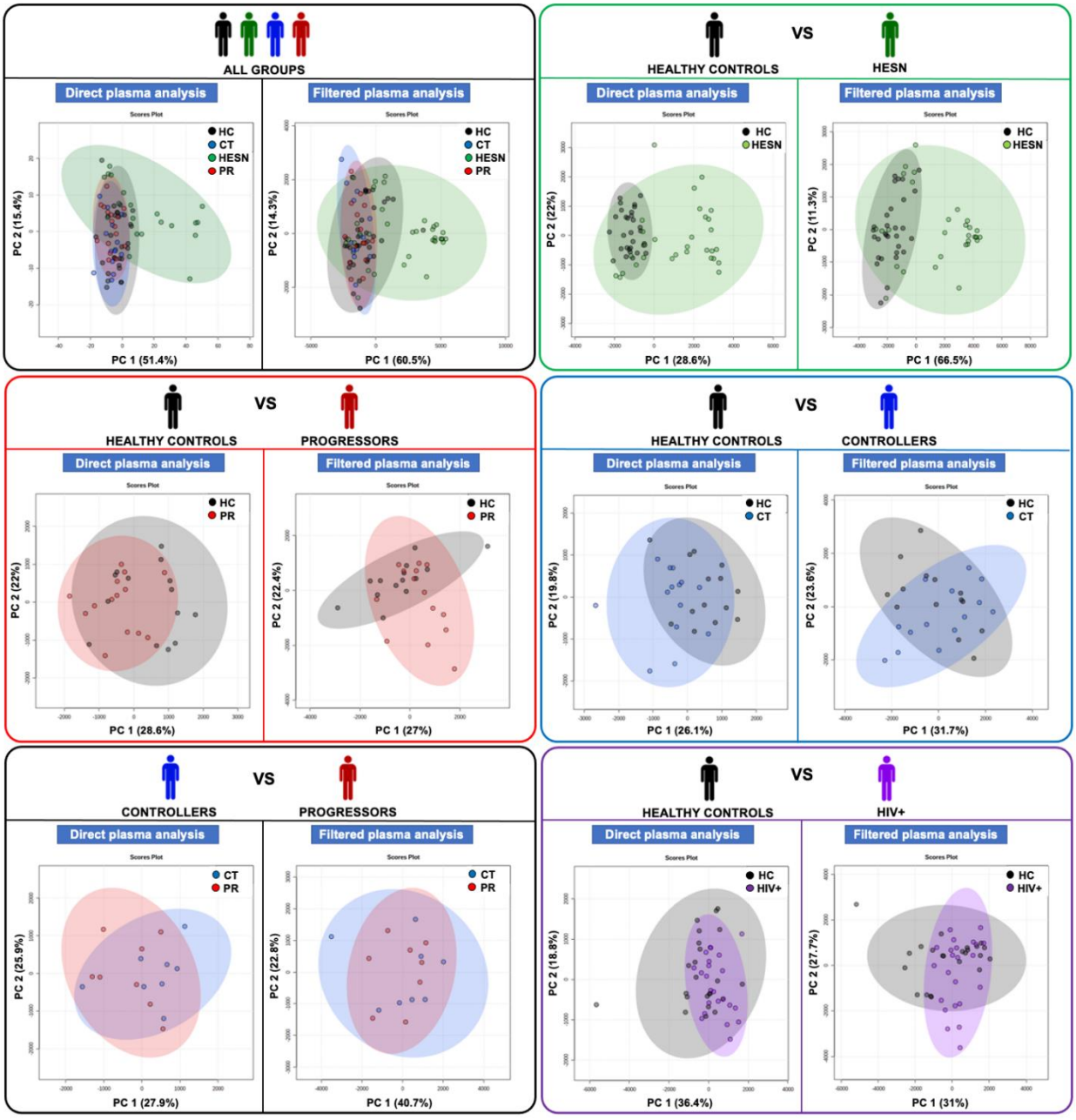

Supplementary Figure 3. Principal component analysis (PCA) of the study groups. 2D score plot charts of the PCA analysis of all study volunteers, on the left side the analysis with direct plasma and on the right side with filtered plasma. PC: Principal component, HC: Healthy control, CT: controller, HESN: HIV-exposed seronegative, PR: Progressor.

Anexo 17

Figura suplementaria 4, Artículo 3, Capítulo 4

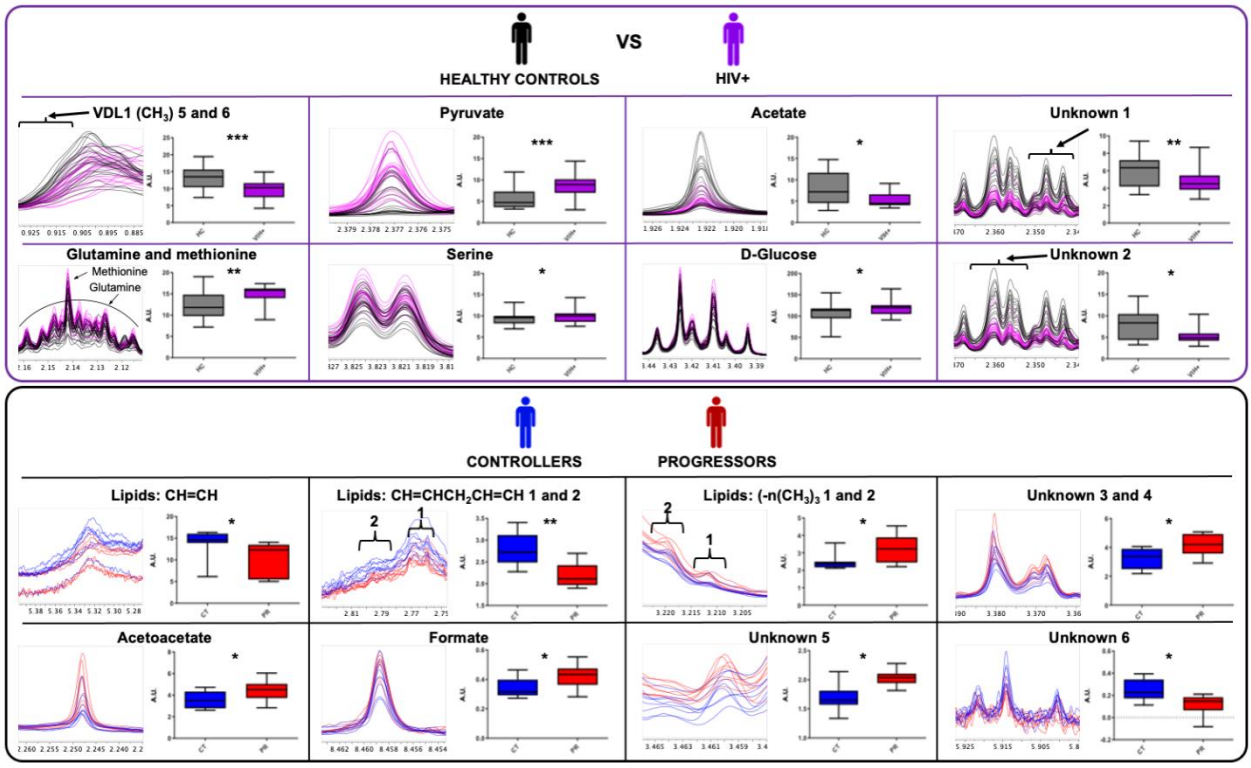

Supplementary Figure 4. Metabolites that explain the difference between the groups. Results of the Wilcoxon test for the significant variables (metabolites) for each proposed PLS-DA model.